



If you have discovered material in AURA which is unlawful e.g. breaches copyright, (either yours or that of a third party) or any other law, including but not limited to those relating to patent, trademark, confidentiality, data protection, obscenity, defamation, libel, then please read our [Takedown Policy](#) and [contact the service](#) immediately

INVESTIGATIONS INTO VISUAL HYPERACUITY

David MacVeigh

Doctor of Philosophy

THE UNIVERSITY OF ASTON IN BIRMINGHAM

September 1991

This copy of the thesis has been supplied on condition that anyone who consults it is understood to recognise that its copyright rests with its author and that no quotation from the thesis and no information derived from it may be published without the author's prior, written consent.

The University of Aston in Birmingham

Investigations into visual hyperacuity

David MacVeigh

Doctor of Philosophy

1991

Abstract

Visual hyperacuties are a group of thresholds whose values surpass that expected by the anatomical and optical constraints of the eye. There are many variables which affect hyperacuties of which this thesis considers the following..

1. The effect of contrast on displacement detection and bisection acuity. It is proposed that spatial summation may account for the different response of these two hyperacuties compared with the contrast response of vernier acuity.
2. The effect of references on displacement detection. These were shown to greatly enhance performance when present. Their effect was, however, dependent upon the temporal characteristics of the displacement.
3. The effect of spatial frequency on vernier acuity. Evidence from this experiment suggests that vernier performance can be explained on the basis of the output of orientationally selective spatial frequency filters.
4. Evidence for a weighting function for visual location using random dot clusters. The weighting attached to different parts of the retinal light distribution was found to alter non-linearly with increasing offset from the geometric center of the cluster. A relationship between dot density and peak amplitude of the weighting function was found.
5. Spatial scaling of vernier acuity in the peripheral field. With careful choice of a technique which did not allow separation and eccentricity to co-vary it was found possible to scale vernier acuity both for two lines and two separated dots.
6. The effect of increasing age on hyperacuity. No change in vernier acuity with age was found which contrasted with displacement detection and bisection acuity both of which showed a significant decline with increasing age.

Keywords: Hyperacuity; contrast; spatio-temporal parameters; eccentricity; age.

This thesis is dedicated to my wife, Jane-Anne,
and son, Stuart David Charles.

I wish to take the opportunity of acknowledging the assistance and patience of all those who have aided me in completing this work.

Firstly, to my supervisor, Dr. David Whitaker, who has shown great enthusiasm and dedication to the successful completion of this project.

My thanks are also due to

Dr. David Elliott, for assistance with several areas of the work

Mr. Derek Barnes and Professor Graham Harding, who both strongly supported my original application to carry out this research and have continued to provide encouragement throughout.

Miss Jennifer Pooler, who has provided invaluable secretarial assistance with the production of this thesis

and also to

The University of Aston

for provision of the facilities and finance which allowed me to undertake this research.

Chapters and sections		53
		53
1	General introduction	19
1.1	Introduction	19
1.2	Detection of an object	20
1.3	Relative localisation	23
1.4	Resolution	29
2	Spatial configurations for hyperacuity	34
2.1	Introduction	34
2.2	Vernier acuity	34
2.2.1	The effect of line length on vernier acuity	37
2.2.2	Separation	37
2.2.3	Stimulus motion	39
2.2.4	Interference effects	39
2.2.5	Practice effects	40
2.3	Bisection acuity	41
2.3.1	The effect of separation on bisection acuity	43
2.3.2	Line length	46
2.3.3	Interfering stimuli	47
2.4	Displacement detection	48
2.4.1	Effect of references on displacement thresholds	49
2.4.2	Duration of presentation	49
2.4.3	Temporal frequency	50
2.4.4	Luminance	52
2.4.5	Spatial frequency	53

2.5	Other hyperacuity configurations	53
2.5.1	Orientation discrimination	53
2.5.2	Spatial Interval detection	55
2.5.3	Spatial frequency discrimination	56
3	Models of hyperacuity detection	58
3.1	Introduction	58
3.2	Local-sign models	58
3.3	Channel models	68
3.3.1	Geisler (1984)	69
3.3.2	Carlson and Klopfenstein (1985)	70
3.3.3	Klein and Levi (1985)	71
3.3.4	Wilson (1986)	72
3.3.5	Morgan and Regan (1987)	79
3.3.6	Paradiso (1988)	81
3.3.7	Channel models, the final answer?	82
3.4	Can single cell responses determine hyperacuity?	83
3.5	Parallel pathways and their relationship to hyperacuity	85
4	Psychophysics	89
4.1	Introduction	89
4.2	The sensory threshold	89
4.3	Classical psychophysical methods	89
4.3.1	The method of adjustment	89
4.3.2	The method of limits	91
4.3.3	The method of constant stimuli	91
4.3.4	Criterion dependency	91

4.4	Forced choice measurements	92
4.5	The staircase routine	93
4.6	The Up and Down Transformed Rule (UDTR)	97
4.7	The Parameter Estimation by Sequential Testing method (PEST)	98
4.7.1	PEST modifications	100
4.8	Bias	101
4.9	Conclusion	102
5	Equipment	103
5.1	Introduction	103
5.2	The RM Nimbus AX	103
5.2.1	Stimulus generation	103
5.2.2	The experimental environment	107
5.3	The VENUS stimulator	108
6	Hyperacuity and contrast	111
6.1	Introduction	111
6.1.1	Vernier acuity and contrast	111
6.1.2	The effect of contrast on other hyperacuities	113
6.2	Methods	114
6.2.1	Stimulus configurations	114
6.2.2	Observations	115
6.3	Results	115
6.4	Discussion	118

6.5	Conclusion	124
7	Displacement detection and reference features	126
7.1	Introduction	126
7.1.1	The Movement analysing system (MAS)	126
7.1.2	The Displacement analysing system (DAS)	128
7.1.3	The effect of references	129
7.2	Methods	131
7.3	Experiment 1, the "no reference" condition	134
7.4	Experiment 2, non simultaneous reference presentation	135
7.5	Experiment 3, continuous reference presentation	138
7.6	Discussion	142
7.6.1	Movement detection in the presence of references	142
7.6.2	Movement detection without references	143
7.7	Conclusion	145
8	Spatial frequency and vernier acuity	146
8.1	Introduction	146
8.2	Method	148
8.3	Results	152
8.3.1	Experiment 1	152
8.3.2	Experiment 2	157
8.4	Discussion	160
8.5	Conclusion	162

9	Weighting functions for visual location	164
9.1	Introduction	164
9.2	Method	166
9.3	Experiment 1	167
9.3.1	Stimulus configurations	167
9.3.2	Results	170
9.4	Experiment 2	172
9.4.1	Stimulus configuration	172
9.4.2	Results	172
9.5	Experiment 3	174
9.5.1	Stimulus configuration	174
9.5.2	Results	174
9.6	Experiment 4	176
9.6.1	Stimulus configuration	176
9.6.2	Results	176
9.7	Discussion	182
10	Spatial scaling of vernier acuity	184
10.1	Introduction	184
10.2	Cortical magnification	184
10.2.1	Direct estimates of M	184
10.2.2	Indirect estimates of M	188
10.2.3	Psychophysical estimates	189
10.2.4	Stimulus scaling	190
10.3	Method	192

10.4	Results	194
10.4.1	Line stimuli	194
10.4.2	Dot stimuli	201
10.4.3	Separation and eccentricity	206
10.5	Discussion	208
10.5.1	A comparison of results	208
10.5.2	A plea for standardised methodology	214
11	Hyperacuity and age	216
11.1	Introduction	216
11.1.1	Changes in visual acuity with age	216
11.1.2	Changes in CSF with age	216
11.1.3	Changes in other visual functions with age	220
11.1.4	Changes in hyperacuity with age	221
11.1.5	Optical or neural factors in visual decline with ageing?	223
11.2	Method	225
11.3	Results	227
11.3.1	Acuity results	227
11.3.2	Bias results	230
11.4	Discussion	231
12	Conclusion and further studies	234
12.1	Summary of experiment conclusions	234
12.1.1	Contrast	234
12.1.2	Displacement thresholds and references	234
12.1.3	Spatial frequency and separation	235
12.1.4	Weighting function	236
12.1.5	Eccentricity	236
12.1.6	Age	236

12.2	General conclusion	237
12.3	Further studies	238
12.3.1	Use of strongly orientated interfering stimuli	238
12.3.2	Spatial scaling as a clinical tool	242
	List of publications, presentations and abstracts	245
	List of references	248

List of Tables

1.01	Detection threshold as a function of background light intensity	22
1.02	$\Delta L/L$ as a function of the angular subtense of a wire	22
3.01	Features of the channels used in the Wilson model (1986)	73
4.01	Estimation of various points on the psychometric function using different response sequences	97
5.01	The minimum thresholds obtainable using the Nimbus AX microcomputer.	107
6.01	Exponent values found by investigators into the effect of contrast on vernier acuity	112
6.02	Exponents, relating thresholds with line length at different contrast levels, found in this study	118
10.01	Values of M_o found by various investigators	187

List of figures

1.01	Retinal luminance profiles for wires of different thicknesses and for two background luminance levels	21
1.02	Vernier acuity for abutting and separated lines compared	24
1.03	Line and point spread functions related to photoreceptor spacing	26
1.04	A possible scheme for spatial interpolation	27
1.05	Resolution and localisation compared	28
1.06	Sinusoidal gratings used by Campbell and Green (1965)	30
1.07	Contrast sensitivity as found by Campbell and Green (1965)	31
1.08	Grating resolution limit imposed by photoreceptor spacing	32
2.01	Examples of vernier acuity configurations	35
2.02	Vernier thresholds as a function of line length	37
2.03	Vernier thresholds as a function of dot separation	38
2.04	The effect of exposure duration on vernier thresholds	40
2.05	The effect of flanking lines on vernier thresholds	41
2.06	Examples of bisection acuity configurations	42
2.07	Bisection thresholds as a function of feature separation (Andrews and Miller, 1978)	43
2.08	Bisection thresholds as a function of feature separation (Westheimer and McKee, 1979)	44
2.09	Examples of the stimuli used by Klein and Levi (1985) to investigate bisection thresholds and separation	44
2.10	Bisection thresholds as a function of feature separation (Klein and Levi, 1985)	45
2.11	$\Delta s/s$ as a function of mean separation (Burbeck, 1987)	46
2.12	Stimulus used by Klein and Levi (1985) to investigate the effect of flanking lines on bisection acuity	47
2.13	Examples of types of movement used in experimental situations	50
2.14	Displacement thresholds as a function of temporal frequency	51
2.15	Waveforms used in oscillatory displacement experiments	52
2.16	Orientation recognition threshold as a function of line length	55
2.17	Spatial interval threshold as a function of separation	56

3.01	Photoreceptor response to a vernier stimulus	59
3.02	Model to perform vernier task using line spread functions proposed by Sullivan <i>et al</i> (1972)	61
3.03	Features of the retinal light distribution which could be used in assigning location, as suggested by Watt and Morgan (1983a)	62
3.04	Stimulus configuration used by Watt and Morgan (1983a) in their third experiment	64
3.05	Vernier thresholds as a function of luminance ratio found by Watt and Morgan (1983a)	65
3.06	Stimulus configuration used by Watt and Morgan (1983a) in their fourth experiment	65
3.07	Vernier thresholds as a function of luminance ratio found by Watt and Morgan (1983a)	66
3.08	Examples of the use of a primitive code proposed by Watt and Morgan (1985)	68
3.09	Receptive field layouts suggested by Wilson (1986)	74
3.10	Change in response to an offset by high and low spatial frequency filters.	75
3.11	Response to two dots with different separations of variously orientated fields	75
3.12	Filter response to lines of different separations	77
3.13a	Coincidence detector model of Morgan and Regan (1987)	80
3.13b	The above models response to a vernier offset	81
3.14	Simplified diagram of the Magno- and parvocellular pathway connections	86
4.01	The response of an organism to a stimulus	90
4.02	The effect of criterion dependency on threshold estimation	92
4.03	The psychometric function obtained in a two-alternate forced choice technique	93
4.04	An example of a staircase routine	94
4.05	The effect of using too large a step size on the accuracy of the threshold estimate	95
4.06	An example of two interleaved staircases	96

5.01	A photograph of the Nimbus AX microcomputer	105
5.02	A schematic of the experimental set up when using the Nimbus AX microcomputer	106
5.03	A photograph of the VENUS stimulator	109
5.04	A schematic of the experimental set up when using the VENUS stimulator	110
6.01	Vernier thresholds plotted against contrast	111
6.02	Displacement thresholds plotted against contrast (previous studies)	113
6.03	Displacement thresholds plotted against line length	116
6.04	Bisection thresholds plotted against line length	117
6.05	Displacement thresholds plotted against contrast (this study)	119
6.06	Bisection thresholds plotted against contrast	120
6.07	Contrast response of magno- and parvocellular neurones	122
7.01	A movement detection model proposed by Barlow and Levick (1965)	127
7.02	The effect of references on displacement thresholds for different durations of movement (previous studies)	130
7.03	The effect of reference proximity on displacement thresholds	131
7.04	The different types of movement used in experimental situations	132
7.05	Displacement thresholds plotted against duration of movement for unreferenced motion	134
7.06	Displacement thresholds plotted against duration of movement with temporal separation of references	136
7.07	Displacement thresholds plotted against duration of movement for referenced movement	140
8.01	Photograph of grating stimuli used in experiment 1	149
8.02	Photograph of grating stimuli used in experiment 2	151
8.03	Vernier thresholds plotted as a function of spatial frequency	153
8.04	Comparison of results from this study with previous reports	154
8.05	Vernier thresholds as a function of spatial frequency. The best fitting curve used to estimate the optimum spatial frequency.	154

8.06	Cycle width plotted as a function of grating separation for optimum and cut-off spatial frequencies	155
8.07	Vernier thresholds plotted as a function of grating separation	156
8.08	Vernier thresholds plotted as a function of spatial frequency for grating strip stimuli	158
8.09	Sensitivity ratio plotted as a function of spatial frequency	159
9.01	Stimulus configurations used in the experiments	169
9.02a	Vernier bias plotted as a function of cluster size	171
9.02b	Vernier acuity plotted as a function of cluster size	171
9.03	Net bias plotted as a function of weighting dot offset for standard cluster size	173
9.04a	Net bias plotted as a function of weighting dot offset for different cluster separations	175
9.04b	Vernier acuity plotted as a function of weighting dot offset for different cluster separations	175
9.05	Net bias plotted as a function of weighting dot offset for smaller cluster size	177
9.06	Net bias plotted as a function of weighting dot offset for larger cluster size	178
9.07	Net bias plotted as a function of weighting dot offset for increased dot number	179
9.08	Net bias plotted as a function of weighting dot offset for lower dot number	180
9.09	Peak amplitude of the weighting function plotted as a function of dot density	181
10.01	A schematic of the method proposed by Watson (1987) to estimate local spatial scale	191
10.02	Vernier thresholds plotted as a function of line length at different eccentricities	196
10.03	A graphical definition of E_2	197
10.04	Vernier thresholds as a proportion of line length plotted as a function of line length at different eccentricities	198
10.05	Calculated scaling factor plotted as a function of eccentricity	199

10.06	Vernier thresholds as a proportion of line length plotted as a function of scaled line length at different eccentricities	200
10.07	Vernier thresholds plotted as a function of gap size at different eccentricities for two dot stimuli	202
10.08	Vernier thresholds as a proportion of gap size plotted as a function of gap size at different eccentricities	203
10.09	Calculated scaling factor plotted as a function of eccentricity	204
10.10	Vernier thresholds as a proportion of gap size plotted as a function of scaled gap size at different eccentricities	205
10.11	A graphical definition of E_2 for iso-eccentric arc data	208
10.12	Vernier thresholds plotted as a function of gap size at different eccentricities for iso-eccentric two dot stimuli	209
10.13	Vernier thresholds as a proportion of gap size plotted as a function of gap size at different eccentricities for iso-eccentric two dot stimuli	210
10.14	Calculated scaling factor plotted as a function of eccentricity	211
10.15	Vernier thresholds as a proportion of gap size plotted as a function of scaled gap size at different eccentricities for iso-eccentric two dot stimuli	212
11.01	Examples of changes in contrast sensitivity with age	217
11.02	Vernier acuity plotted as a function of age (Odom <i>et al.</i> 1989)	221
11.03	Vernier acuity plotted as a function of age (Lakshminarayanan <i>et al.</i> 1991)	222
11.04	Displacement detection thresholds plotted as a function of age (Elliott <i>et al.</i> 1989)	222
11.05	Visual acuity plotted as a function of age	228
11.06	Displacement detection thresholds plotted as a function of age	228
11.07	Bisection acuity plotted as a function of age	229
11.08	Vernier acuity plotted as a function of age	229
11.09a	Absolute vernier bias plotted as a function of age	230
11.09b	Absolute bisection bias plotted as a function of age	230

12.01	Stimuli used by Morgan <i>et al.</i> (1990) in an investigation into the effect of perturbing features on two dot vernier acuity	238
12.02	Stimulus configuration used to investigate interference with orientationally tuned filters	240
12.03	Net vernier bias plotted as a function of the orientation of the perturbing line	241
12.04	Vernier acuity plotted as a function of the orientation of the perturbing line	241
12.05	Displacement thresholds obtained by Fitzke <i>et al.</i> (1987) for three classes of subject; normal, ocular hypertensive and POAG	243

Chapter 1: General introduction

1.1 Introduction

The eye, the organ of sight, allows us to view a constantly changing picture of the outside world. It is a picture which encompasses a huge range of brightness, exquisite nuances of color and shading and a vast complexity of detail. In order to process this we need to break down the information into at most 2 million bits of information, the number of nerve fibers available between the two retinae and the brain, and then reconstitute it to form the picture we see. As an optical system the eye is far from perfect. It suffers from many aberrations and inefficiencies which combine to produce a blurred and jittery image which no photographer would accept from his camera. Despite this the eye has the capacity, under the right circumstances, to detect a few photons, to recognise as different two wavelengths separated by a few nanometers, to detect objects which subtend fractions of a second of arc and to locate the relative position of two objects to within a few seconds of arc. How can this optically poor image, of necessity coarsely sampled, be analysed to reconstruct such a good representation of the outside world, and what mechanisms operate within the visual system to allow this remarkable feat to occur?

To seek an answer to these questions in their entirety would require a work far beyond this remit. Instead, this thesis will concentrate on the last mentioned of the eyes abilities, the relative localisation of objects within the visual field.

Spatial visual thresholds can be broadly divided into three categories which, in ascending order of their minimum magnitudes, are.....

- a. **Detection**, or the minimum perceptible size of an object;
- b. **Relative localisation**, or the position of one object relative to others within the visual field;
- c. **Resolution**, or the ability to recognise two objects as being separate.

1.2 Detection of an object

Detection requires no more than the ability to isolate the object signal from the background noise. Consider, for example, the ability to see a star; the angle subtended by it at the eye is infinitesimally small and visibility depends only on whether the difference in luminance between the star and the sky exceeds the luminance differential threshold of the eye. Hence during daylight the star is invisible because the sky is too bright while during the night, when the sky is much darker, the star is visible.

Whilst one normally expresses detection in terms of light energy it is, under certain circumstances, possible to consider detection in spatial terms. Let us take a more down to earth example where spatial considerations as well as the luminance difference is important. If we now consider the visibility of a dark wire against a uniform bright background we again find that detection requires that the luminance differential between the retinal image of the dark wire and the background is suprathreshold (*Figure 1.01*). In essence, the variation in retinal illumination (ΔL) has to exceed the luminance differential threshold (ΔL_{thresh}). Hecht and Mintz (1939) showed that the minimum angle that a wire needs to subtend at the eye in order to be detected is just 0.55 second of arc, a remarkably fine line! This represents the angular subtense of the line at the eye of the observer, and is the usual method of expressing spatial dimensions. The actual threshold value varies as a function of illumination and pupil size, and a background light intensity of over 30 millilamberts with a pupil diameter of 3 mm was necessary to obtain such a very low threshold. They then calculated that detection is possible when the light intensity distribution in the diffracted retinal image has a dip in its value of less than 1%.

Hecht and Mintz investigated the ability to detect a thin wire viewed against a diffuse evenly illuminated background and varied its physical thickness between 12 μm and 8 mm. They carried out three series of runs in all and *Table 1.01* shows the results from their third series. It is clear that as the light intensity falls the detection threshold (defined as the angular subtense of the wire) grows rapidly.

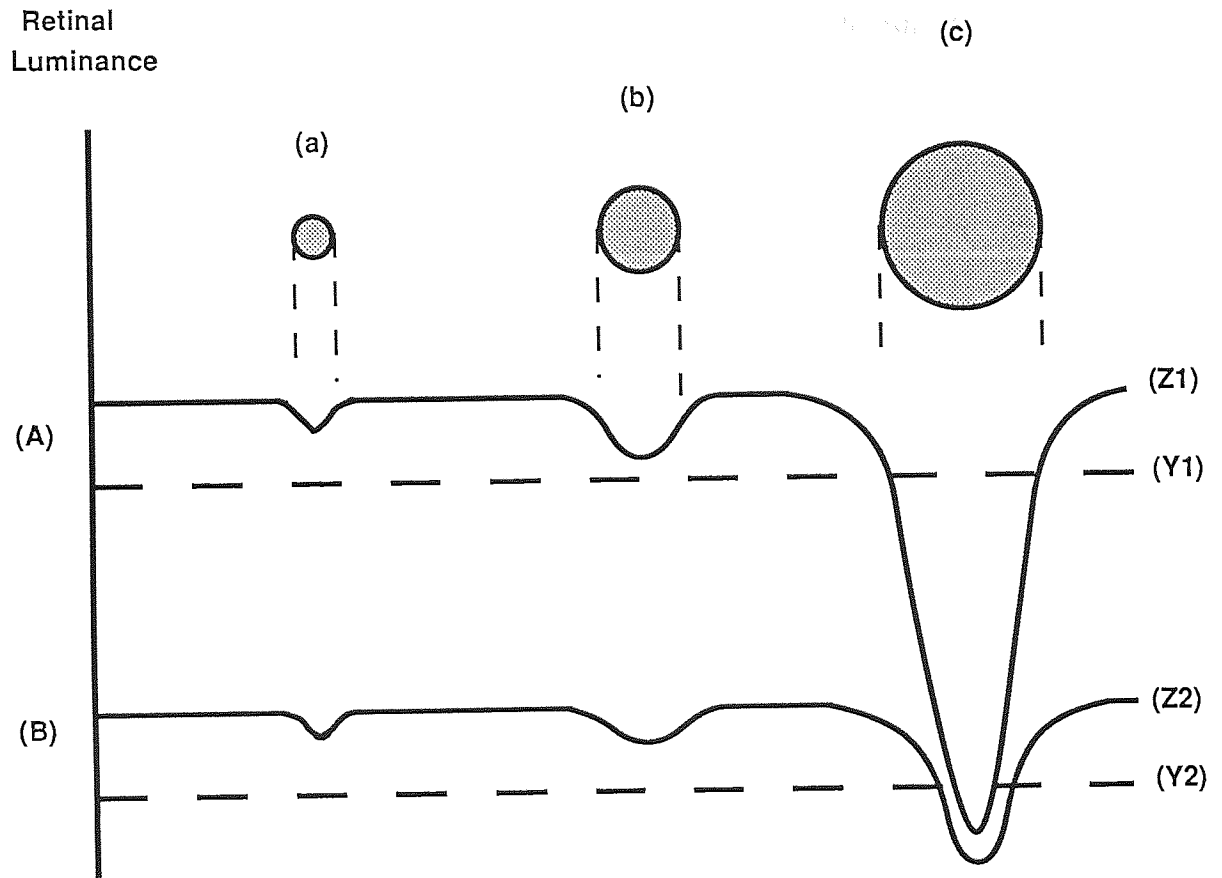


Figure 1.01: A plot of the retinal luminance profiles (line Z1 and Z2) for three wires of different thicknesses (a, b and c) and for two levels of background luminance (A and B). The horizontal dashed lines (Y1 and Y2) indicate the threshold at each background luminance value. In other words the dips in the retinal luminance profiles (ΔL) must be deep enough to reach this line if threshold is to be attained. ($Z - Y$) is, therefore, equivalent to the luminance differential threshold (ΔL_{thresh}). Wire (a) will not be seen in either condition as the difference in luminance between it and the background does not exceed threshold. Wire (b), which is somewhat thicker than (a), lies near to threshold in condition "A" and may or may not be visible. A decrease in illumination, as in "B", will cause it to fall below threshold and it will therefore be invisible. The retinal luminance profile of the thickest wire (c) clearly exceeds threshold under both condition "A" and condition "B". There should be no difficulty in detecting this wire under either background luminance level.

Table 1.01:

Background light intensity (millilamberts)	Detection threshold (seconds of arc)
30.2	0.55
7.0	0.60
3.0	0.75
0.06	4.25
0.02	7.50
5.0×10^{-3}	20.00
3.0×10^{-4}	60.00
2.6×10^{-5}	250.00
6.0×10^{-6}	750.00

The retinal light distribution was computed using a technique described by Rayleigh (1903) and it was found that for the highest background light intensity the $\Delta L/L$ values for different angular sizes of the wires were as shown in *Table 1.02*.

Table 1.02:

Angular subtense (seconds of arc)	$\Delta L/L$
0.55	0.95%
4.1	12.00%
6.8	19.00%
35.5	75.00%

The two tables show clearly that even the simple detection of an object, when the object is not self-luminous, is not an easy problem. However, in comparison to other spatial thresholds this detection limit is, under optimum conditions, exquisitely small. The detection of small

luminance differences will be alluded to later as it can intrude upon the process of relative localisation and lead to controversy regarding the mechanism responsible for observed visual performance.

1.3 Relative localisation

The second spatial threshold measure, relative localisation, is the one upon which this thesis concentrates. Threshold values do not fall as low as those of detection but are usually less than those of resolution. While threshold values in this range have been demonstrated for many years (Wulfing, 1892; Stratton, 1902) only relatively recently have they been grouped together under the generic term "hyperacuties" (Westheimer, 1975). Under optimal conditions one can obtain threshold values between 4 and 10 seconds of arc and there are many stimulus configurations which can give rise to such thresholds including vernier acuity, bisection acuity, displacement detection, spatial interval detection, stereoacuity, spatial frequency discrimination and orientation discrimination.

It should be noted that there is some confusion about the exact definition of a hyperacuity. Westheimer originally used the magnitude of the threshold as the definition and hence any stimulus configuration giving rise to these sort of threshold levels could be classed as a hyperacuity. The difficulty arises in deciding whether the threshold value or the underlying mechanism of determining threshold should govern the definition. Take, for example, vernier acuity; a typical stimulus consists of two vertical abutting straight lines placed end to end with one offset relative to the other. Threshold values for detecting the horizontal offset of as little as 6 seconds of arc can easily be obtained (*Figure 1.02*) (Westheimer and McKee, 1977a). If, however, a large vertical gap is introduced between the inner ends of the two lines the threshold values are much worse. With a sufficiently large separation, thresholds can fall to well over 30 seconds of arc. Do we classify this second configuration as a hyperacuity or not? On the basis of threshold size the answer has to be no. On the other hand, the same visual process underlies performance in both conditions.

To further confuse the situation consider a vernier target viewed in the peripheral visual field. At 10 degrees eccentricity even an abutting stimulus will give threshold values greater than 30 seconds of arc. However, at this eccentricity the resolution ability of the eye has also declined (to about 25% of its foveal value; Westheimer, 1979), and so this vernier threshold value still remains considerably better than resolution thresholds at the same point.

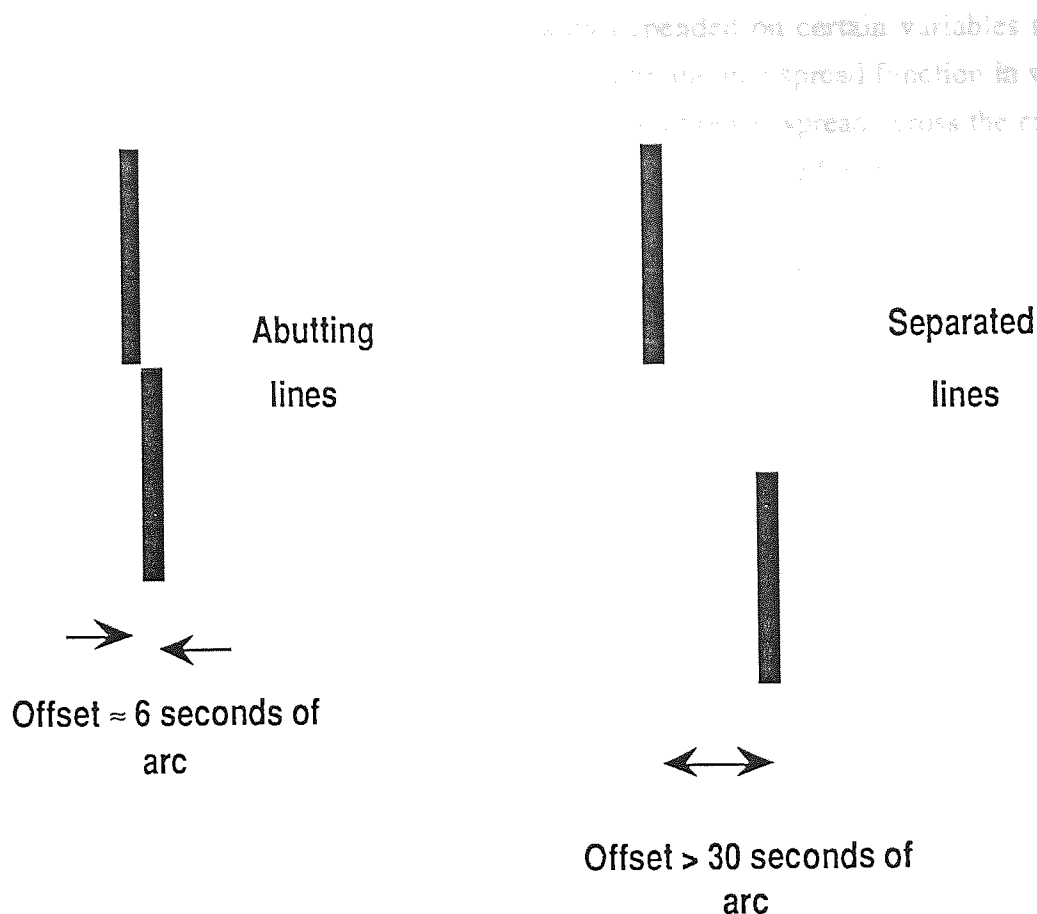


Figure 1.02: The left hand figure shows a typical vernier stimulus consisting of two abutting lines. Threshold values for the minimum detectable offset as low as 6 seconds of arc are commonly obtained from such a configuration. The right hand figure shows the effect of introducing a vertical separation between the ends of the lines. Depending on the magnitude of the separation threshold values may then greatly exceed the 30 seconds of arc commonly taken to be the limit of resolution.

In view of the difficulty in precise definition as outlined above, the alternative title of pattern acuity has been suggested for stimulus configurations that can give rise to hyperacuity thresholds (Howard, 1982). In this thesis, however, I will use the term hyperacuity to define those spatial configurations where the threshold is determined using a relative localisation mechanism even when the absolute threshold value may be higher than the 30 seconds of arc limit for resolution.

Hyperacuity tasks differ from simple detection tasks in that two or more features are localised relative to one another. It appears at first sight curious, but in order to perform localisation tasks with hyperacuity precision it is necessary for the retinal image to be blurred. Fortunately, the optics of the eye are such that a sharply defined object gives rise to a somewhat blurred retinal image. Campbell and Gubisch (1966) carried out an investigation to

consider this and found that the optical quality depended on certain variables including defocus and pupil size. This situation is described by the line spread function in which the width of the image of a thin line under optimum conditions is spread across the retina such that its line spread function has a half width (*i.e.* the width of the function at half its height) of about one minute of arc and will thus cover several photoreceptors (Westheimer and Campbell, 1962). The same effect occurs for a point source which will be blurred in all directions to give a circular blur circle on the retina, the point spread function, which again covers several photoreceptors along any diameter.

If the line or point spread function of the stimulus were to fall entirely within the diameter of one photoreceptor it would be impossible to allocate its position with an accuracy less than the diameter of that photoreceptor, about 30 seconds of arc. However, with the blurring occasioned by the eye's optics, all the information regarding position is contained within the group of photoreceptors covered by the line or point spread function and interpolation between these photoreceptors, which occurs at a higher level of neural processing, allows fine relative localisation to take place (*Figure 1.03*) (Fahle and Poggio, 1981; Hirsch and Hylton, 1982; Snyder, 1982).

The exact location of the site of this interpolation is still unclear but Barlow (1979) has put forward cortical layer IVc as a possible site, in view of the extreme density of the granule cells within this layer. There are 30 to 100 granule cells for each terminating optic radiation fiber per unit area. If this is expressed along a straight line it allows each incoming fiber to diverge by a factor of 5 to 10 (Hubel and Wiesel, 1972). This ability to reconstitute the visual image to a much finer grain would certainly be sufficient to explain hyperacuity performance. Fahle and Poggio (1981) give a simple example of how this interpolation could be carried out (*Figure 1.04*) although they admit that in reality the process would be more complex. However, it can be argued that such an explicit representation of the visual image is not essential to explain hyperacuity performance. Indeed, there are many models which propose an implied representation of the stimulus in order to carry out hyperacuity tasks (Carlson and Klopfenstein, 1985; Klein and Levi, 1985; Wilson, 1986; Paradiso, 1988). These, and other models of hyperacuity performance will be reviewed in chapter 3.

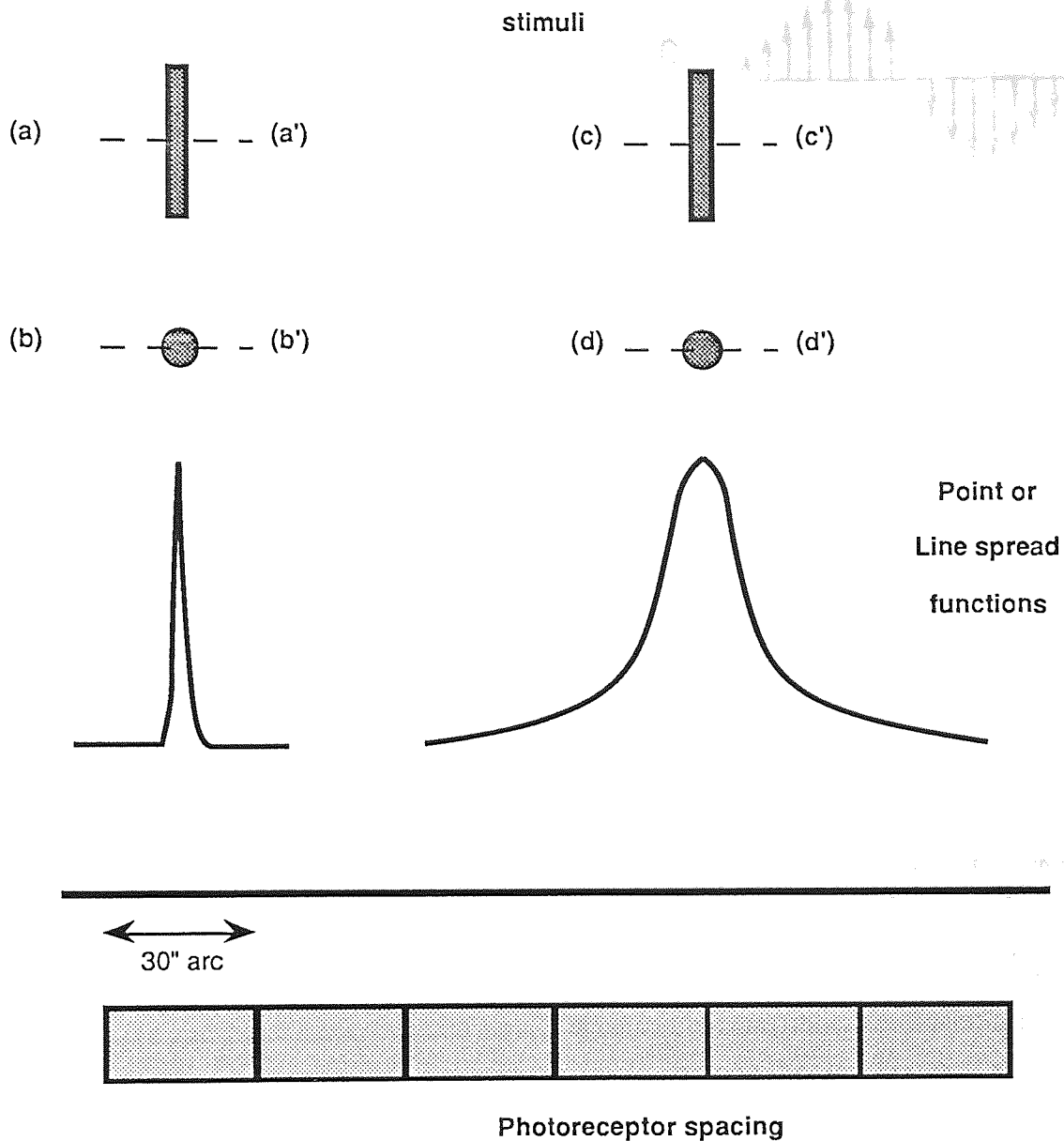


Figure 1.03: The left hand stimuli have a hypothetical point or line spread function, measured along (a - a') or (b - b'), which is so fine that it falls entirely within the boundary of one photoreceptor. The accuracy with which the line or point can be positioned is therefore limited to the size of that receptor, approximately 30 seconds of arc. The right hand stimuli have a point or line spread function, measured along (c - c') or (d - d'), which spreads over a number of photoreceptors. Interpolation, as described in the text, allows the responses of these photoreceptors to be pooled thus enabling location to be assessed to a much finer accuracy than is possible from a single photoreceptor.

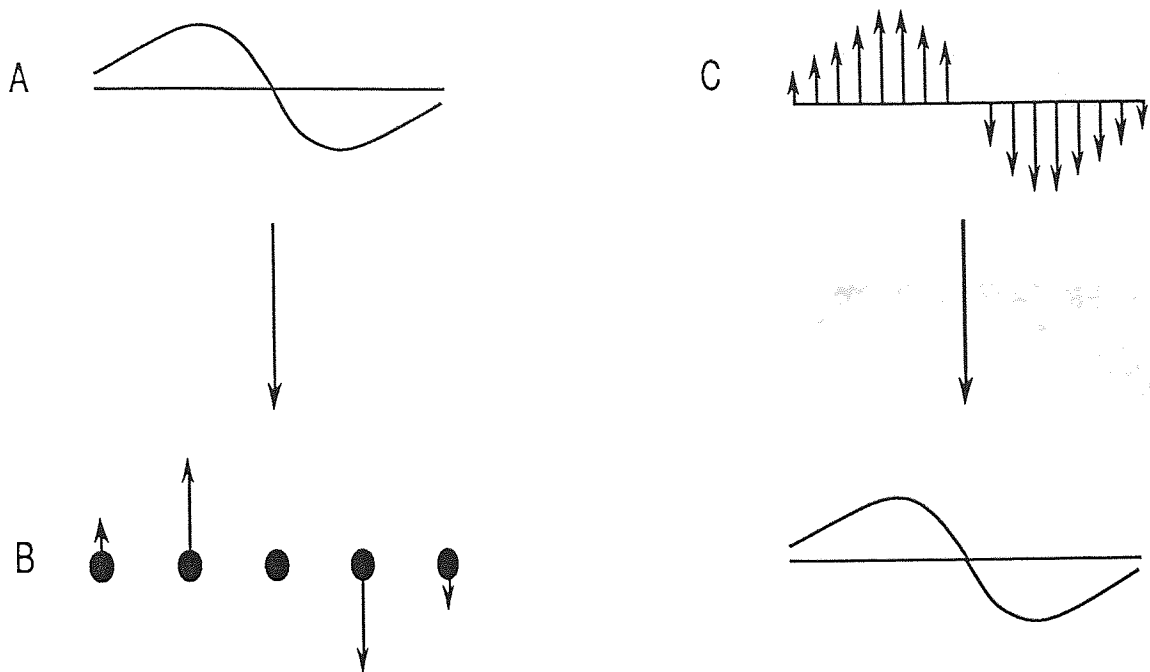


Figure 1.04: A simple scheme for spatial interpolation suggested by Fahle and Poggio (1981). The input pattern (A) is sampled by an array of cells (B). Sampling theory requires that in order to fully represent the original pattern sampling must take place at intervals not more than $1/2F_{\max}$, where F_{\max} is the highest spatial frequency contained within the original function (Bracewell, 1978). In the eye, which is limited to an F_{\max} value of approximately 60 cycles per degree, this requires sampling every 30 seconds of arc which corresponds closely to the foveal cone separation. The interpolation is shown at (C) where the original pattern is reproduced by a finer interpolation grid of cells. This is carried out by convolving the output of the cells at (B) with a weighting function $\{\sin \pi x / \pi x\}$. If one considers only the position of the arrow points in (C) it can be seen that this interpolation is analogous to the fitting of a continuous curve through a series of discrete data points.

We have seen that blurring of the retinal image is a prerequisite for hyperacuity. Given this fact it is not altogether surprising that certain hyperacuity tasks show considerable resistance to excess optical blur caused by, for example, cataracts and other media opacities (Stigmar, 1971; Williams, Enoch and Essock, 1984; Whitaker and Buckingham, 1987; Whitaker and Elliott, 1989) (*Figure 1.05*).

These investigations have all shown that the relative localisation task is essentially independent of blur over a considerable range. This is completely different from resolution where relatively small amounts of blur cause a marked reduction in performance (Campbell and Green, 1965; Westheimer, 1979).

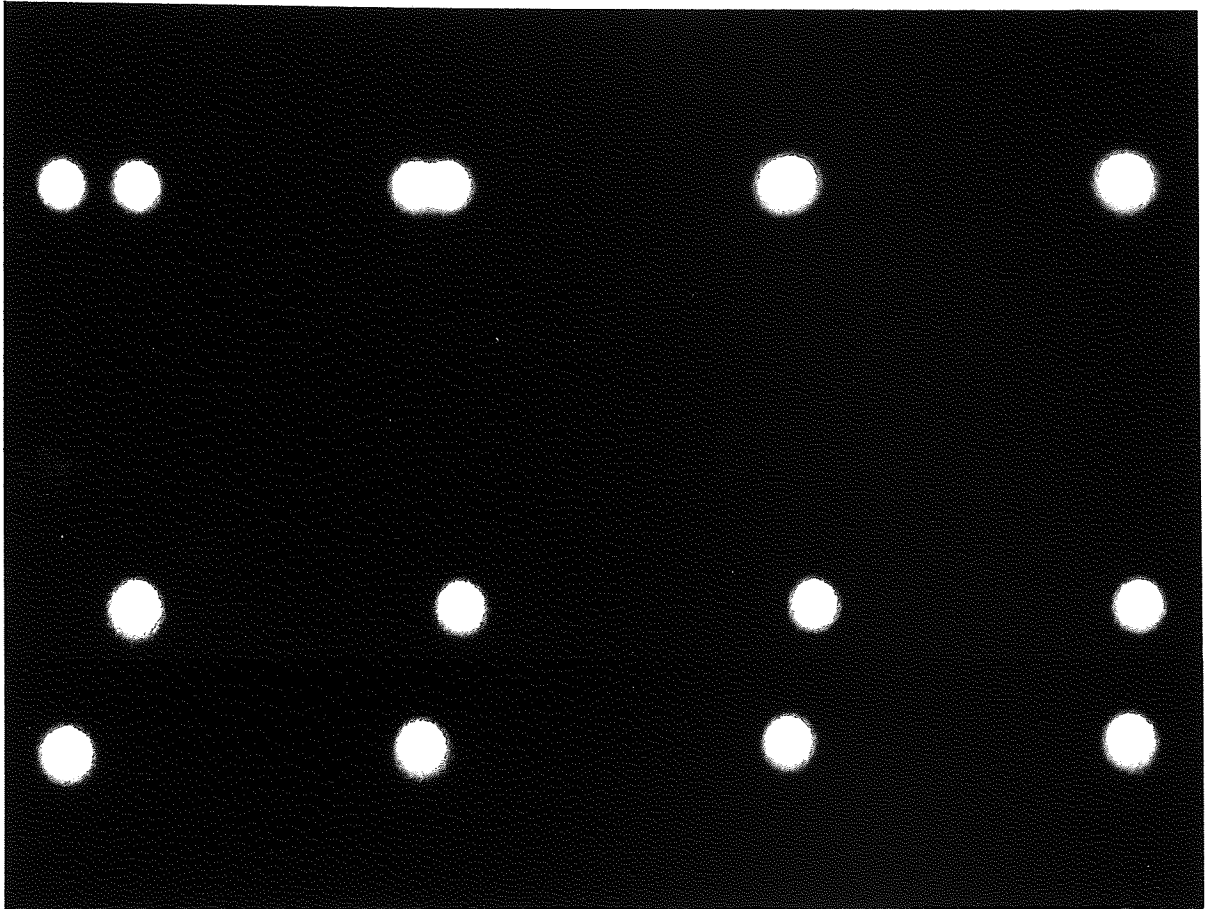


Figure 1.05: A comparison of resolution (top row) and localisation (bottom row). In order for resolution to take place the two lights must be seen as separate. Localisation, on the other hand, only requires that the horizontal offset of the upper light relative to the lower can be determined. It is clear that localisation remains possible long after resolution fails.

1.4: Resolution

The third group of thresholds, resolution, yields higher minimum values than the other two and is the acuity most commonly used, in the form of letter charts, to assess visual performance.

Campbell and Green (1965) used an interference fringe technique which allowed the resolving ability of the retina to be estimated without modification by the optics of the eye. They also compared this result with that obtained after transmission through the eye's optics. The stimulus was a sinusoidal grating of the form shown in *Figure 1.06*. Contrast was defined by the Michelson equation

$$L_{\max} - L_{\min} / L_{\max} + L_{\min}$$

In order for resolution to occur at a particular spatial frequency the amplitude (A) of the grating, which determines contrast, has to exceed a threshold value determined by the noise in the system. The optimum resolution of the neural system can then be defined as the highest spatial frequency that can just be detected with a retinal image of 100% contrast. Using the interference fringe technique Campbell and Green (1965) found that the highest spatial frequency which was resolvable at the retina was approximately 60 cycles per degree. This, usually known as the cut-off frequency, is a measure of the resolution ability of the retina after elimination of the optical effects of the eye's refracting components and media. If the optics of the eye are included certain other factors influence the result including defocus and pupil size. Defocus reduces the amplitude (A) of a sinusoidal contrast grating thus lowering the cut-off spatial frequency. Visual acuity is also reduced by increasing the pupil size, since optical aberrations become greater. Taking account of these items Campbell and Green showed that the cut-off frequency, for an optimum combination of the two factors, is reduced from about 60 to 50 cycles per degree (*Figure 1.07*).

In fact it was shown that, under optimal conditions, it is possible for the performance of the eye to closely approach the performance of an ideal diffraction limited optical system (Campbell and Green, 1965).

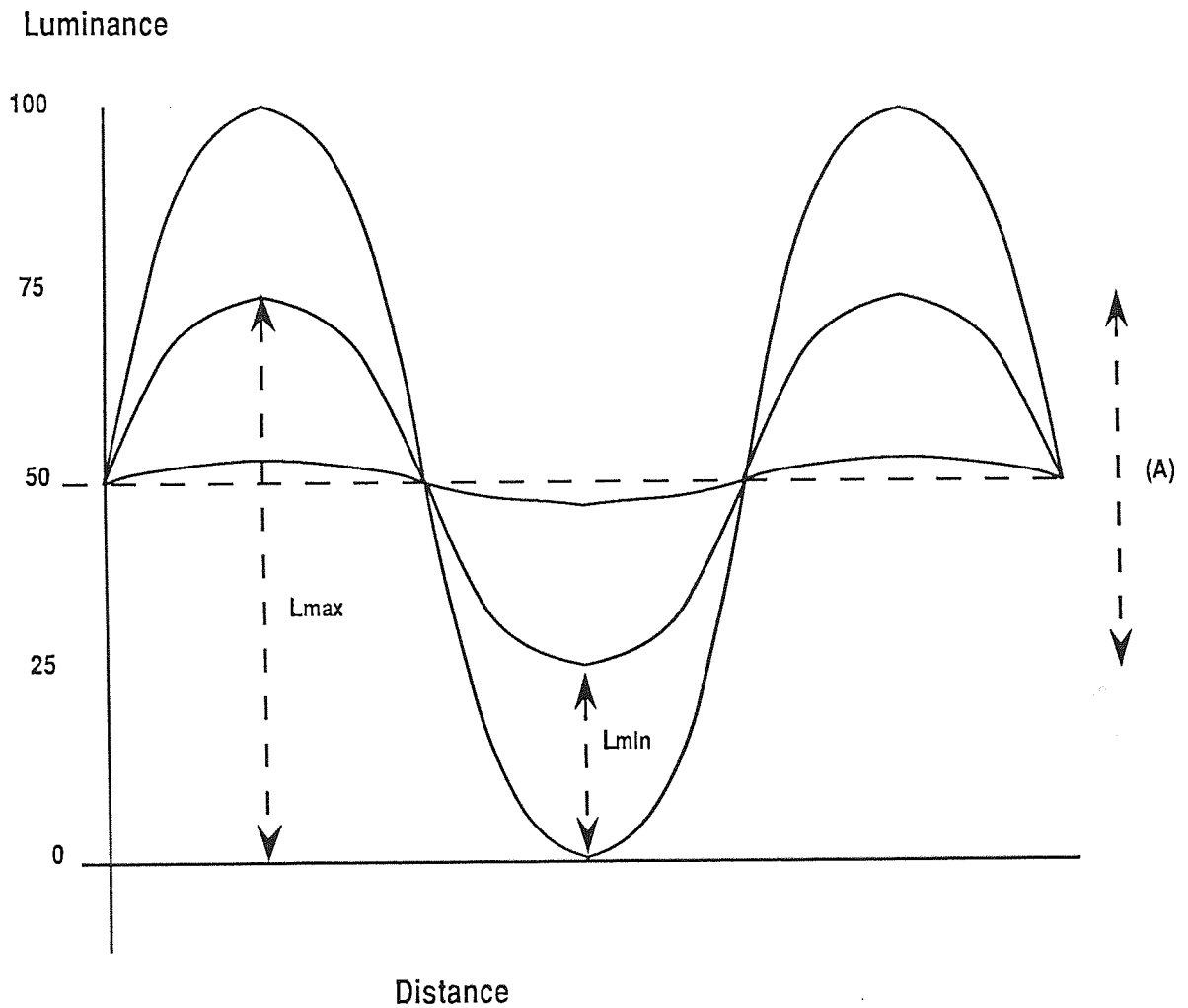


Figure 1.06: The sinusoidal contrast grating used by Campbell and Green (1965) in their experiments on visual resolution. The three curves represent contrast levels of 100%, 50% and 5%. It should be noted that the mean luminance of all three gratings remains constant but as contrast is lowered the amplitude of the sinusoidal grating (A) reduces. The spatial frequency mentioned in the text is the reciprocal of the angular distance between successive maxima in the sinusoidal intensity distribution. The definition of contrast is also discussed in the text.

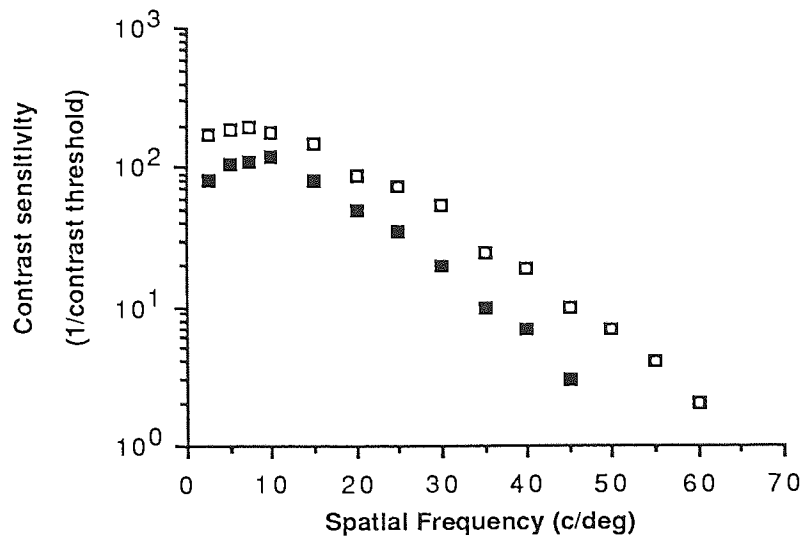


Figure 1.07: The results of Campbell and Green (1965) showing contrast sensitivity both with the optics of the eye bypassed (open squares) and including the effects of transmission through the eye's optics (filled squares). The results are discussed in the text.

Snyder and Miller (1977) thought it logical to assume that the resolution of a sinusoidal contrast grating would occur if there were a photoreceptor at each peak and trough. Using sampling theory they were able to calculate the theoretical diameter of a foveal cone necessary to meet this requirement. This diameter, for a hexagonal photoreceptor array as found in the human fovea, can be calculated using the formula...

$$\Delta P = W / D \times \sqrt{3}$$

where ΔP is the receptor diameter, W the wavelength of the incident light and D the pupil diameter (*Figure 1.08*). This estimate is very close to the well known Rayleigh criterion for two point resolution;

$$\Delta P = 0.61 \times W / D$$

Sinusoidal grating of 60 cycles per degree

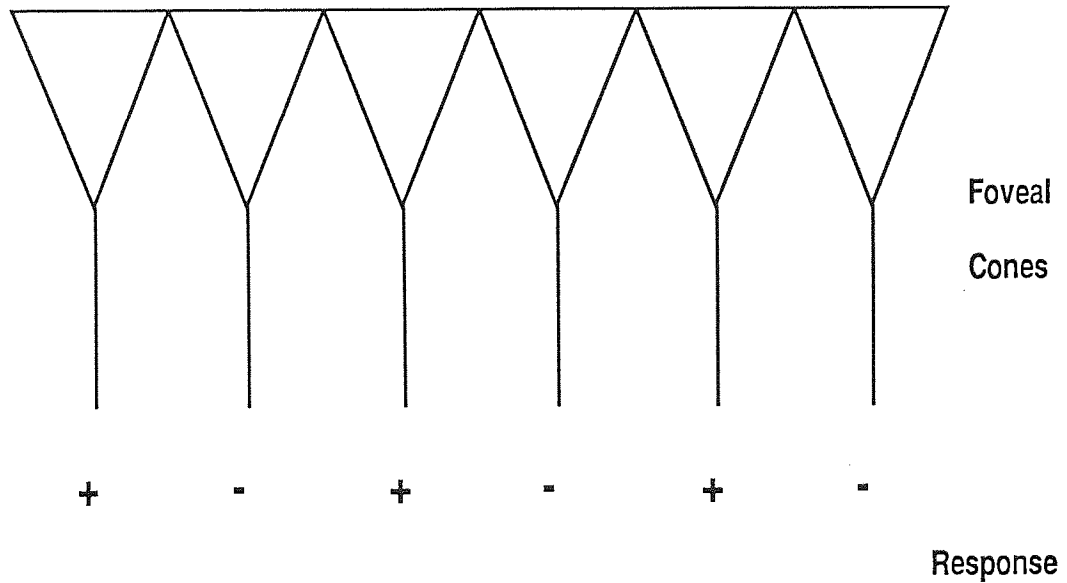
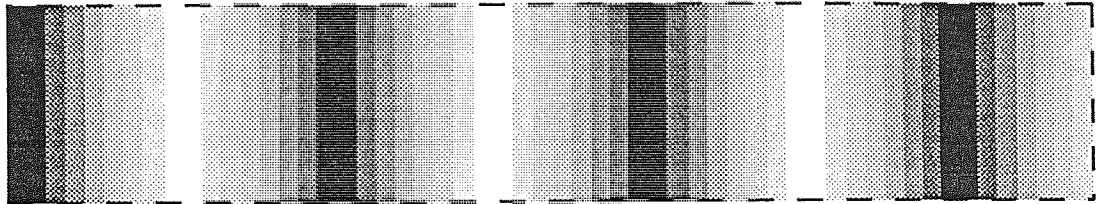


Figure 1.08: The response of foveal receptors to a sinusoidal grating at the eye's limiting spatial frequency of 60 cycles per degree. The minimum diameter of the receptors required to respond to such a grating corresponds closely to the actual size of foveal cones as measured *in vitro*.

Snyder and Miller (1977) went on to show that the foveal cone diameter thus estimated gives the highest signal to photon noise ratio. This is based on optimising the conflicting requirements of a large receptor diameter to capture more photons and a small receptor diameter to increase the modulation at the photoreceptor level. In order to resolve gratings close to the theoretical limit high luminance values are required. However, given a high enough luminance it is possible to resolve gratings at a spatial frequency 96% of the theoretical limit given by ΔP . It has been shown that the quality of the retinal image is optimal with a pupil diameter of 2.4 mm (Campbell and Gubisch, 1966) and the eye's photopic sensitivity is maximal for light of wavelength 555 nm (Le Grand, 1972). Using these figures one obtains an estimate of the angular receptor diameter of approximately 27 seconds of arc. This should, therefore, correspond to the observed resolution limit in man.

Several studies have looked at actual foveal photoreceptor size both in monkeys (Hirsch and Hylton, 1984) and in humans (Østerberg, 1935; Hirsch and Curcio, 1989) and have found cone diameters between 2 and 3 μm . If one assumes a foveal receptor diameter of about 2.5 μm this again leads to a theoretical resolution limit at the fovea of approximately 27 seconds of arc. The calculation of this value follows from the optics of the eye; if a foveal cone 2.5 μm in diameter is projected into space through the nodal points of the eye it subtends an angle of 27 seconds of arc. We now have two values for resolution; one theoretical based on optical considerations and the other anatomical. The fact that these two values are in such good agreement is not surprising since any major difference would simply imply a degree of redundancy in the system. It also has to be said that the theoretical estimates are based on a regular retinal mosaic which is not always found to be the case (Hirsch and Curcio, 1989). The effect of this irregularity is that the best resolution thresholds obtained are usually somewhat greater than the theoretical ideal. Hirsch and Curcio reviewed several previous studies on human resolution thresholds and found that the spatial frequencies corresponding to the best threshold values varied between 30 and 60 cycles per degree with a mean value of 44. In angular measure this limits resolution to between 30 and 60 seconds of arc with a mean of 41. Laboratory measurements of visual acuity show that it is possible for some observers to reach very close to the theoretical limit for resolution: the majority, however, fall some way below this.

Chapter 2: Spatial configurations for hyperacuity.

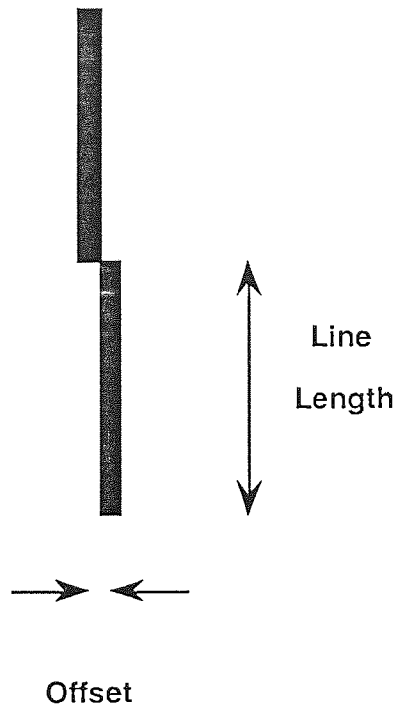
2.1: Introduction

As was mentioned in chapter 1 there are many spatial configurations which can produce threshold values in the hyperacuity range. The important factor which links them is the need to localise two or more points relative to each other in order to successfully perform the task. This chapter will deal with those configurations which are used in this thesis together with a review of their chief characteristics which have been investigated to date. In addition, certain other hyperacuity configurations not directly dealt with in the present experiments will be described.

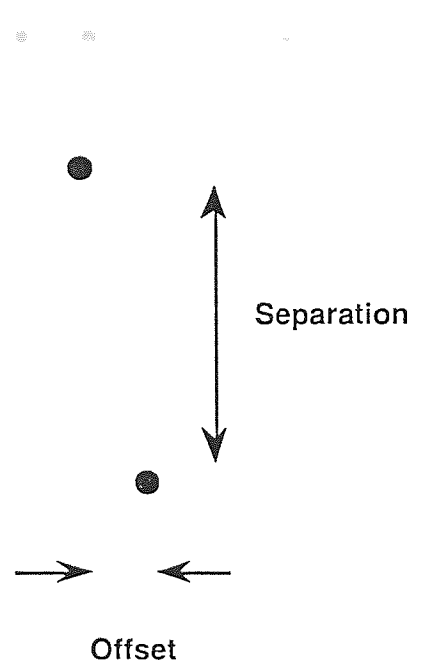
2.2: Vernier Acuity

The most frequently cited of the hyperacuity paradigms is vernier acuity, named after the inventor of the scale which bears his name, Pierre Vernier (1580 - 1637). In the traditional form it involves aligning two vertical lines placed end to end. The vernier threshold is defined as the smallest horizontal offset which can be detected and its value is frequently found to be as little as 6 seconds of arc (Westheimer and McKee, 1977a). However, the vernier stimulus is not restricted to lines; thresholds in the hyperacuity range have been obtained from a variety of different spatial configurations including separated dots (Ludvigh, 1953; Sullivan, Oatley and Sutherland, 1972; Westheimer and McKee, 1977a), a line and chevron (Westheimer and McKee, 1977a), gaps in two parallel lines (Westheimer and McKee, 1977a), clusters of random dots (Ward, Casco and Watt, 1985; Whitaker and Walker, 1988) and sinusoidal gratings (Bradley and Skottun, 1987; Funakawa, 1989; Whitaker and MacVeigh, 1991) (*Figure 2.01*). All have one common feature; the spatial dimensions of the stimulus are critical. The components must be of a certain length, or have a certain separation or a combination of both in order to achieve hyperacuity performance (see Westheimer and McKee, 1977a). The dependence of vernier thresholds on a variety of stimulus dimensions has been investigated and the following are a selection which highlight the main features.

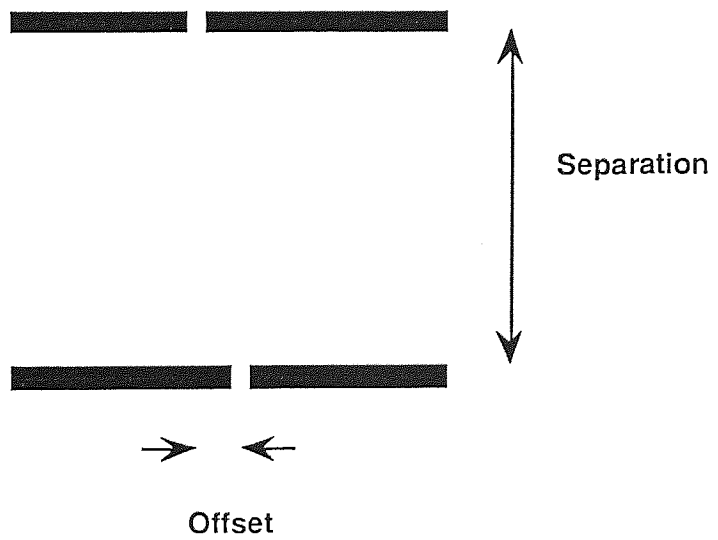
a)



b)



c)



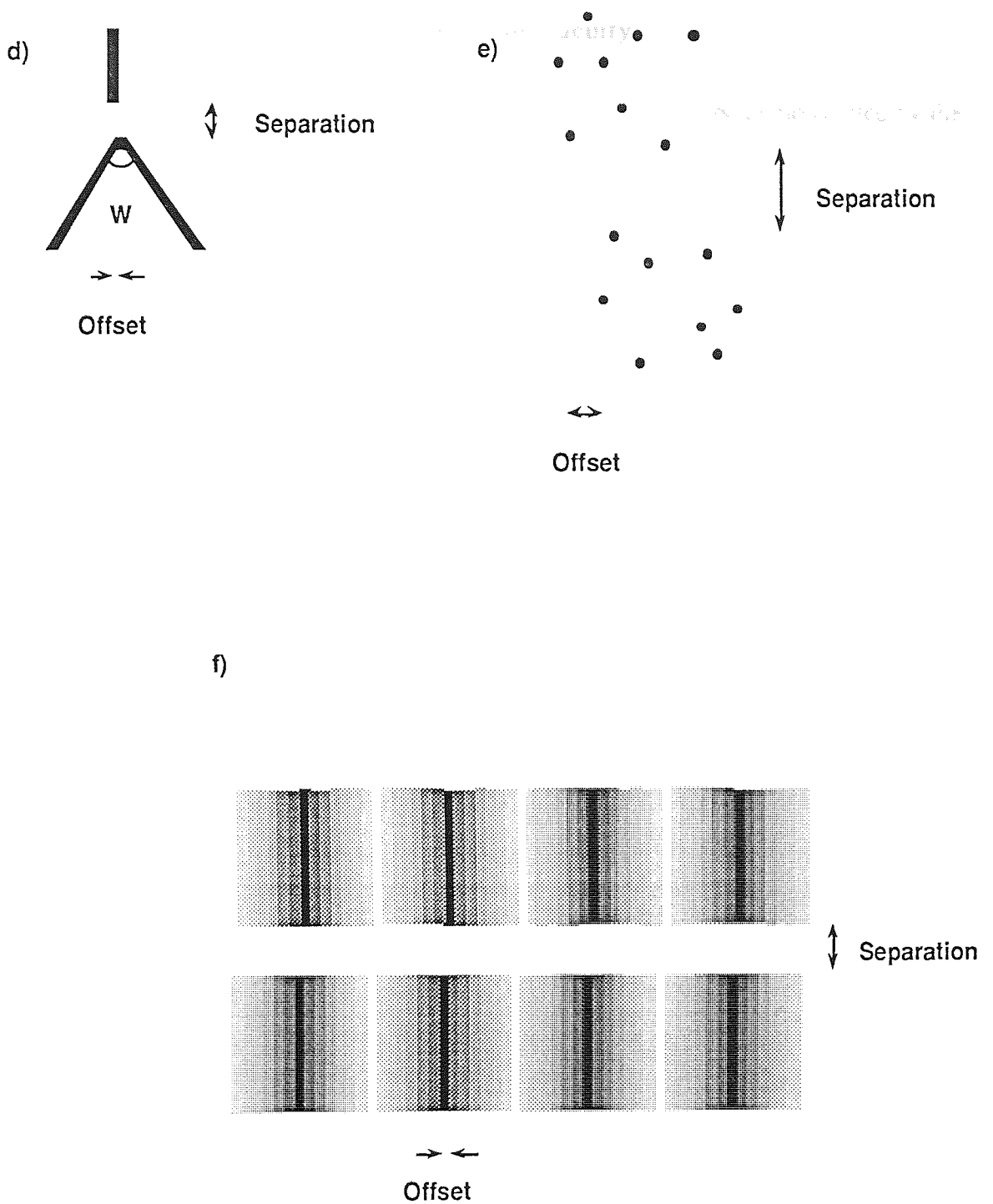


Figure 2.01: A selection of vernier acuity stimulus configurations. **a.** the traditional two abutting lines. **b.** two separated dots. **c.** two parallel lines containing a small gap. **d.** a chevron whose component lines subtend an angle (W) and a line. **e.** two separated random dot clusters. **f.** two sinusoidal gratings, these are shown as separated although the task is often performed with the gratings abutting. In all cases the offset to be detected is marked. The dependence of threshold values on the various stimulus parameters is discussed in the text.

2.2.1: The effect of line length on vernier acuity

there was a separation between
 thresholds increased sharply

The relationship between vernier thresholds and line length was first demonstrated by French (1920) who found no further improvement in vernier thresholds once line length reached between 4 and 12 minutes of arc. Sullivan *et al.* (1972) repeated this experiment and found, for abutting lines, that thresholds reached a minimum for line lengths around 3 minutes of arc and that there was no further improvement in thresholds above this value. The same relationship between line length and vernier threshold has also been shown by Andrews, Butcher and Buckley (1973) and Westheimer and McKee (1977a). It is clear from these reports that line length is not a critical feature provided it exceeds a modest value (*Figure 2.02*).

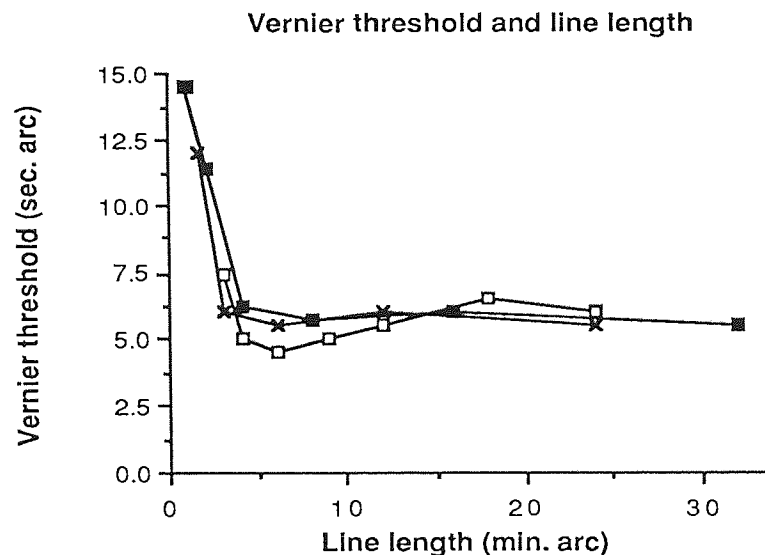


Figure 2.02: Vernier thresholds plotted as a function of line length from three studies. Crosses represent the average of two observers from Sullivan *et al.* (1972); open squares are the average of two observers from Andrews *et al.* (1973) and filled squares the subject SM from Westheimer and McKee (1977a). The independence of thresholds to changes in line length over about 5 minutes of arc is clearly apparent.

2.2.2: Separation

With a small gap (1.5 minutes of arc) introduced between the inner ends of the lines, Sullivan *et al.* (1972) found no effect of line length on vernier threshold. The small gap had the effect of making the two parameters independent over the whole range investigated (1.5 to 22 minutes of arc). Westheimer and McKee (1977a) showed that, for two dots, minimum

thresholds (around 6 seconds of arc) were obtained when there was a separation between them of about 4 minutes of arc. For separations less than this thresholds increased sharply whilst with greater separations there was a more gradual increase in threshold values. These results had previously been reported by Ludvigh (1953) (using a slightly different three dot arrangement where alignment is between the center dot and the imaginary line joining the outer two) and Sullivan *et al.* (1972). Both of these reports indicated that thresholds worsened with increasing separation (*Figure 2.03*). The fact that vernier thresholds are well below those predictable by the anatomical limitations of the retina had been described by Wulffing (1892) using line targets. This discovery was used by Hering (1899) to develop his "local-sign" model. Briefly he argued that each receptor stimulated by the line produced a "local-sign", these were then averaged together along the length of the line to give it a precise location. The location of each of the two lines could then be compared in order to determine whether there was any offset between them. An ability to obtain hyperacuity thresholds with two dots is clearly incompatible with the "local-sign" model in the original form mentioned earlier, but, as will be shown in chapter 3, it has provided support for alternative "local-sign" models using specific feature location (Watt and Morgan, 1983a).

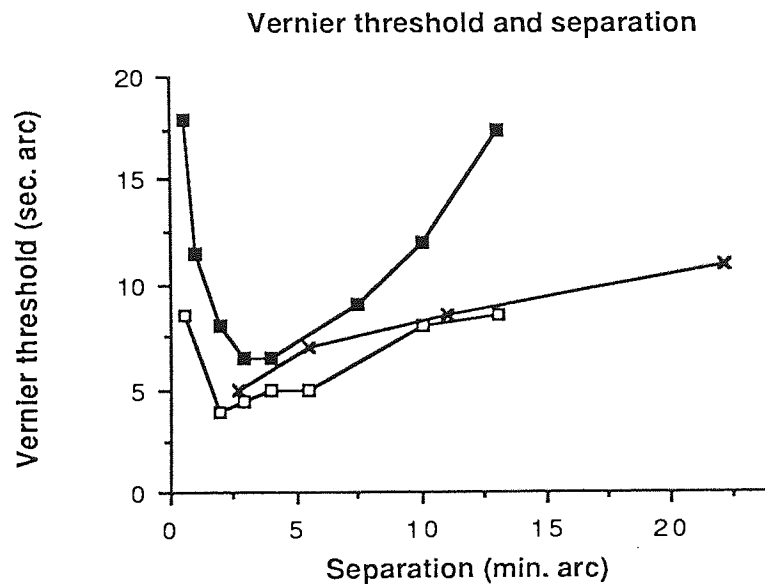


Figure 2.03: Vernier thresholds plotted as a function of separation for two dot targets. The crosses are averaged results of the three observers used by Sullivan *et al.* (1972); the open squares are for subject SM and the filled squares for subject LK as reported in Westheimer and McKee (1977a). It is clear that minimum thresholds occur for separations around 2 to 5 minutes of arc with an increase in thresholds away from this separation.

2.2.3: Stimulus motion

Using two-line stimuli, Westheimer and McKee (1975) showed that thresholds were not affected by movement of the stimulus across the retina at up to 3.5 degrees per second. However, Funakawa (1989) has shown that this may have been due to the broad Fourier spectrum of the line targets. He used vertical sinusoidal gratings to restrict the spatial frequency content of the stimuli and showed a clear relationship between target velocity and thresholds. This relationship, however, depended on two factors - velocity and spatial frequency. Thus, for low spatial frequency targets (0.8 cycles per degree), threshold values were independent of velocity whilst for a spatial frequency of 10 cycles per degree there was a sharp deterioration in threshold values as velocity increased from 0 to 4 degrees per second.

2.2.4: Interference effects

Westheimer and Hauske (1975) investigated both temporal and spatial interference effects on vernier acuity. They found that so long as the two elements of the stimulus were presented together an exposure duration of as little as 50 msec was enough to obtain hyperacuity thresholds around 6 seconds of arc. Such short exposure durations did, however, make thresholds susceptible to temporal interference from competing stimuli presented after the vernier stimulus although not to competitive stimuli presented before the vernier stimulus. This temporal interference was not found when the stimulus was presented for greater than 250 msec. Finally, they showed that non-simultaneous presentation of the two components of the vernier stimulus caused a substantial rise in thresholds; a gap between presentation of the two components of only 50 msec caused a threefold increase in thresholds (*Figure 2.04*). In the spatial domain they used supernumerary features positioned close to the stimulus - in this case horizontal and vertical lines. With them they mapped a flanking band in which the presence of a competing stimulus had a deleterious effect on thresholds. This effect peaked around 3 to 5 minutes of arc from the vernier stimulus (*Figure 2.05*). Badcock and Westheimer (1985) also investigated the effect of flanking lines on vernier performance. They found that if induced shift of the mean location of the lower target line (analogous to bias or the subjective position of alignment, see chapter 4) is plotted as a function of flank separation the flanking band has two components. Within about 4 minutes of arc of the stimulus the interfering lines attracted the target line while above this separation they repelled it. Morgan, Ward and Hole (1990) also used supernumerary features, on this occasion extra

dots placed in the interval between the main stimulus dots. They found that these noise dots had no effect on threshold values except when placed very close to the stimulus dots. This result has important implications for models of vernier performance which involve a single spatial filter encompassing both vernier elements.

2.2.5: Practice effects

It has been shown (McKee and Westheimer, 1978) that vernier thresholds are improved markedly with practice. Their subjects performed 18 blocks of trials with 120 to 150 responses in each. They showed that this training, amounting to some 2,500 trials, produced on average a 40% improvement in thresholds. Fendick and Westheimer (1983) confirmed this finding in a similar study.

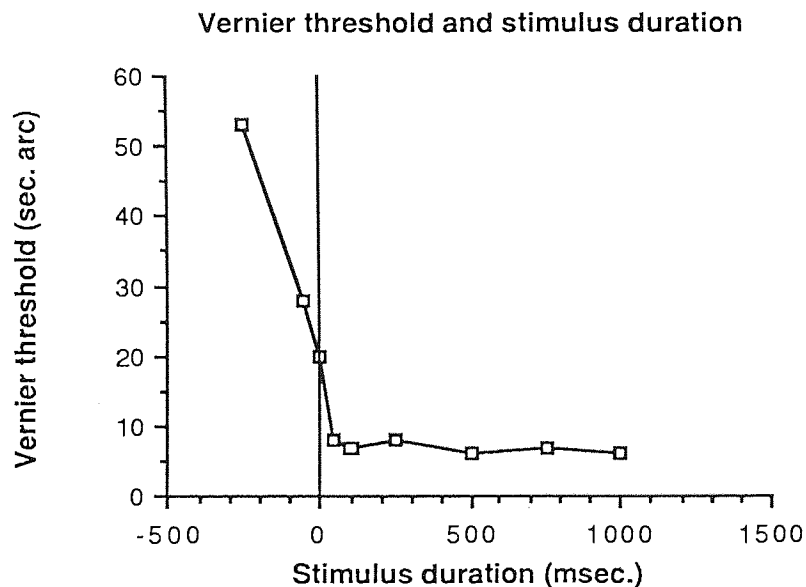


Figure 2.04: The effect of exposure duration on vernier thresholds. Negative values denote the gap between presentation of the two stimulus features, positive values the period of simultaneous presentation. It is clear that optimal thresholds can be obtained with very short exposure durations while even very short gaps cause a marked deterioration in threshold values (from Westheimer and Hauske, 1975).

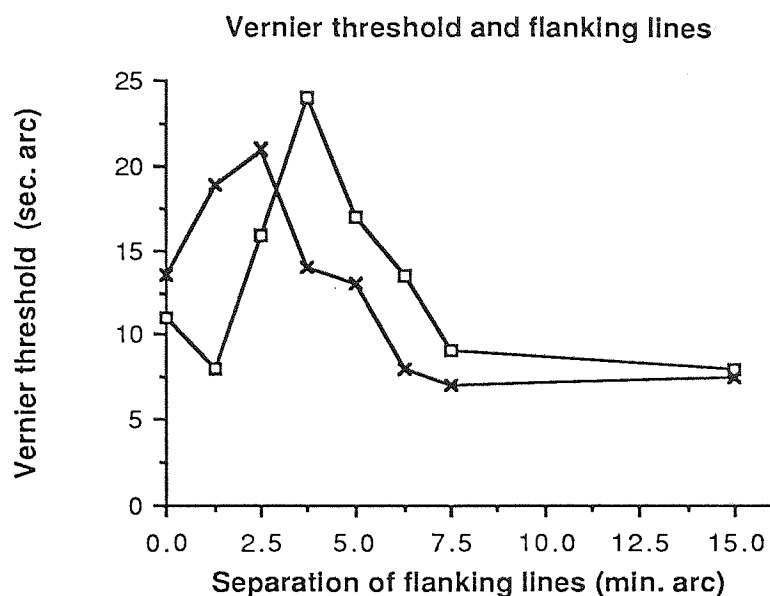


Figure 2.05: The effect of flanking lines on vernier thresholds. The open squares are for vertical flanking lines, the crosses for horizontal flanking lines. Separation is the distance between the inner ends of the lines and the mean position of the vernier stimulus. The presence of a zone of reduced performance centered around 3 to 5 minutes of arc from the stimulus position is clearly shown (from Westheimer and Hauske, 1975).

As can be seen, the effect of manipulating the spatial and temporal features of vernier acuity stimuli has been well investigated over the years and the variation in thresholds as these parameters are varied has been extensively documented. There are other stimulus features which need to be discussed but I will consider them in more detail in later chapters. These include the effect of contrast (chapter 6), spatial frequency (chapter 8) and eccentric viewing (chapter 10).

2.3: Bisection acuity

The usual bisection acuity task tests the ability to judge whether the central bar in a set of three is closer to one or other of the outer bars. Such an interval can, however, be defined equally well by the length of a line, by a circle or other regular shape as well as the usual three bars (*Figure 2.06*).

The task could be performed in one of two possible ways. The first is by locating the exact center of the interval between the two outer bars and then making a decision as to which side of this the central bar is lying, the inferred center. An alternative approach is, however, possible; the two gaps between the bars can be compared sequentially and the decision as to

which is larger than the other will then solve the bisection problem. In effect the bisection task can be looked on as a spatial interval detection task with simultaneous presentation of the two intervals. Burbeck and Yap (1990a) investigated the spatial and temporal limitations in both bisection and spatial interval detection tasks. They compared thresholds obtained when the three lines were presented simultaneously and also when the two intervals were presented sequentially. The center bar was maintained at the same position throughout, in order to act as a fixation marker, while the outer bars were varied to produce the stimuli. It was found that for short exposure durations (33 msec) the spatial interval detection thresholds were lower while the opposite was the case at longer exposure durations (500 msec). They suggested that the task was carried out by a separation discriminator which, for the short exposure durations, was unable to simultaneously process the bisection task because the time available was insufficient. As exposure durations were increased bisection thresholds improved faster than spatial interval detection thresholds. The results support the premise that the bisection task is performed by carrying out sequential comparison of the two spatial intervals rather than the alternate inferred center method.

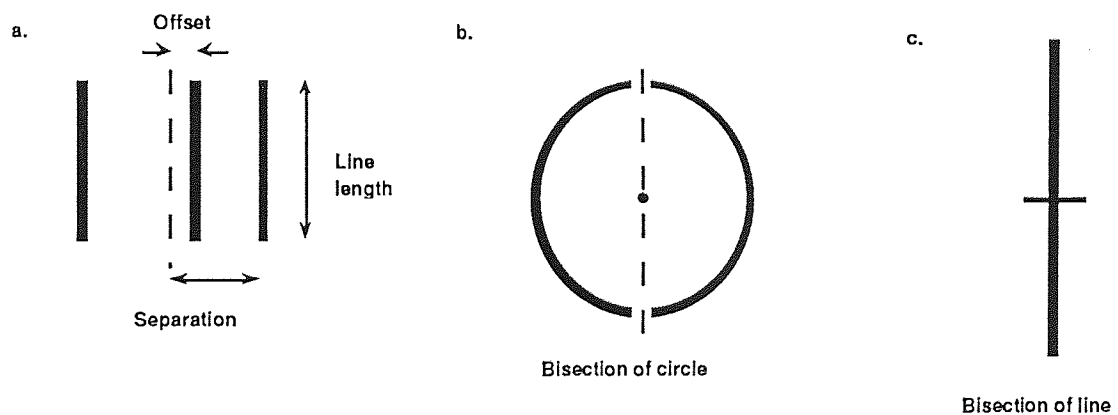


Figure 2.06: A selection of configurations for bisection tasks. a): the usual task with three bars, where separation is defined as the mean distance from the outer bars to the center bar. Offset is the distance of the center bar from the geometric center. b): bisection of a circle, the task is to estimate the geometric center of the circle. c): bisection of a line, the task is to estimate the exact mid-point of the line.

2.3.1: The effect of separation on bisection acuity

Andrews and Miller (1978), Westheimer and McKee (1979) and Klein and Levi (1985) have all investigated the effect on thresholds of changing the separation between the bars. Interestingly they have all concentrated on a different range of separations and taken together they cover the range from 0.8 to 164 minutes of arc. The definition of separation needs to be established. The nature of the task is such that the center bar must have a different separation from each of the outer bars if an offset is present. Therefore, the separations referred to in this section will be taken to be half the separation of the inner edges of the two outer bars. It follows that the median line of the center bar defines this position when no offset is present.

Andrews and Miller (1978) looked at the effect of varying the separation in the range 20.5 to 164 minutes of arc and found that as separation increased thresholds deteriorated from 24 to 190 seconds of arc (*Figure 2.07*).

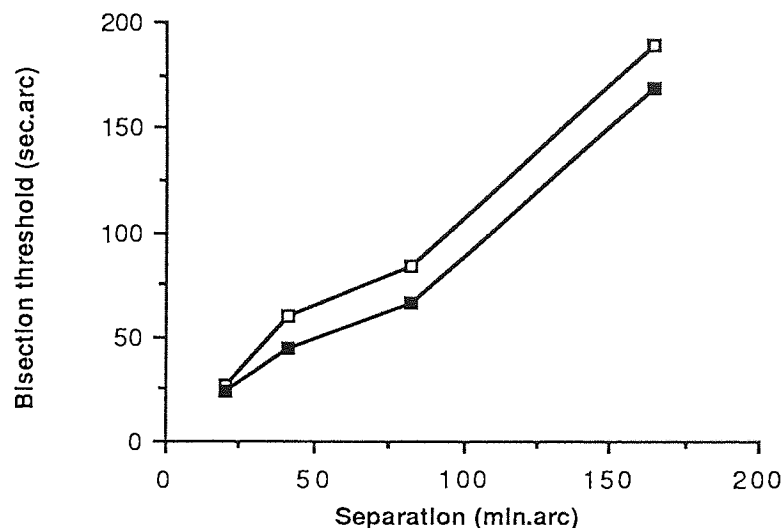


Figure 2.07: Bisection thresholds plotted against separation for the two observers, DPA (open squares) and DTM (filled squares), used by Andrews and Miller (1978). Note the linearity of the relationship between the two parameters.

Westheimer and McKee (1979) examined the range of separations from 3 to 21 minutes of arc and again found an approximately linear relationship between thresholds and separation (Figure 2.08).

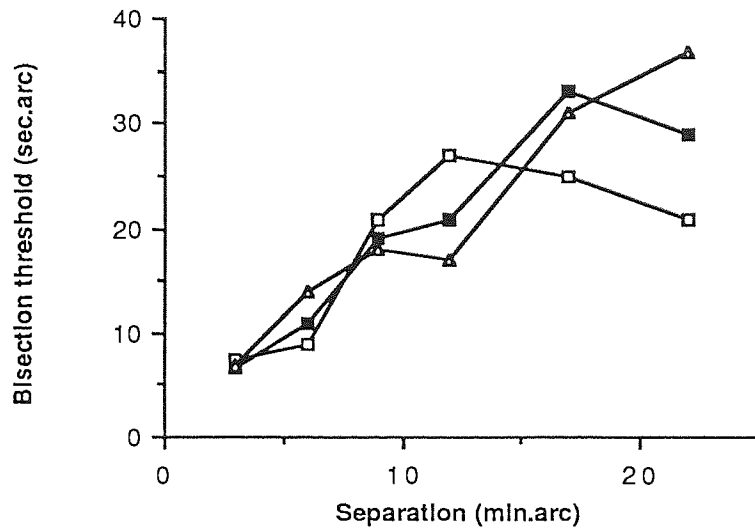


Figure 2.08: Bisection thresholds plotted against separation from Westheimer and McKee (1979). Three observers were used, GW (open squares), JW (filled squares) and SM (open triangles). Again there is a reasonable linear proportionality between the two parameters.

The investigation by Klein and Levi (1985) covered the range of separations between 0.8 and 10 minutes of arc. They performed the experiment both with and without an overlap between the central and outer lines and found two differing results (Figure 2.09).

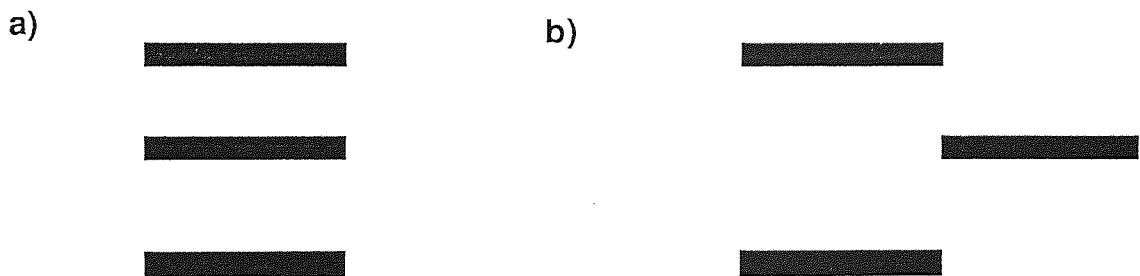


Figure 2.09: The stimulus used by Klein and Levi (1985). In (a) the three bars overlap and in this configuration luminance clues become important for very small separations. In (b) there is no overlap between the three bars and the luminance clue does not occur.

Without an overlap thresholds were generally higher and, as with the other investigators, showed an approximate straight line relationship between thresholds and separation. In the presence of an overlap, however, Klein and Levi found that their results showed a marked departure from linearity as separation was reduced (*Figure 2.10*). They admit that below 2.5 minutes of arc separation there was a strong luminance clue which helped in the decision regarding the offset of the center bar. If the three bars are very close together they blur into each other and in these circumstances, using bright bars, there will be a luminance peak in the direction of the offset of the central bar and a corresponding trough in the other direction. Indeed, it can be argued that the threshold values obtained at very small separations owe more to detection acuity than to localisation acuity and that the results below the 2.5 minutes separation do not reflect the action of a relative localisation mechanism. The authors agree that this may be the case and this point will be returned to when discussing one of the models described in chapter 3.

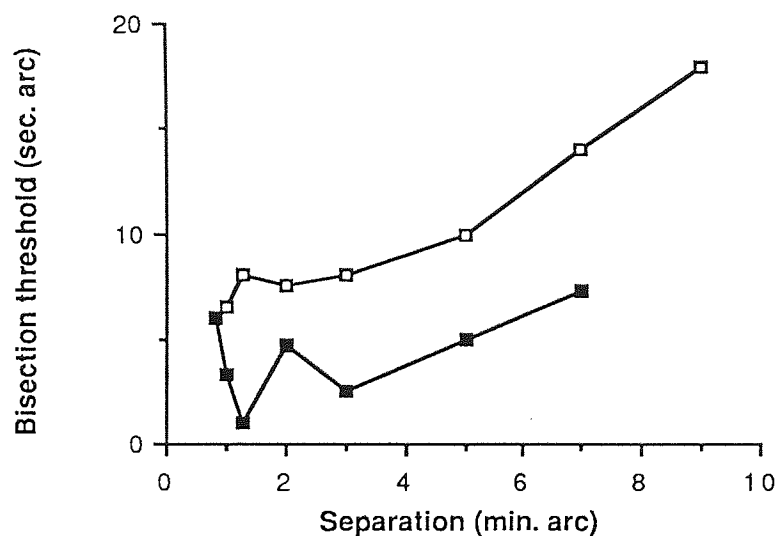


Figure 2.10: Bisection thresholds as a function of separation. This graph covers the range from 1 to 10 minutes of arc separation. The two lines show results both with an overlap between the three lines (filled squares) and without an overlap (open squares). Note how the overlap, which introduces a luminance clue, produces a kink in the function for separations around 1-2 minutes of arc (from Klein and Levi, 1985).

The relationship between separation and bisection thresholds shows a striking linearity which indicates proportionality between the two parameters. This reflects the operation of Weber's Law. The law, as applied to the judgment of relative position, states that the localisation

threshold (Δs) will scale with the separation of the stimulus features (s) such that $\Delta s/s$ is a constant. This proportionality has been well documented for many years; it was demonstrated as long ago as 1858, using a three line bisection task, by Volkman (1863). Over a range of separations he found that $\Delta s/s$ was indeed approximately constant. This same experiment was repeated by Burbeck (1987) and as can be seen in *Figure 2.11*, for separations greater than 5 minutes of arc, the same constancy applies. The value of the Weber constant varies between different experimenters. Westheimer and McKee (1978) and Burbeck (1987) both found a value of about 2.25% but Andrews and Miller (1978) and Klein and Levi (1985) find a lower value of around 1.67%. This variability is probably due to differences in stimulus parameters (size, luminance, contrast etc.) and psychophysical technique.

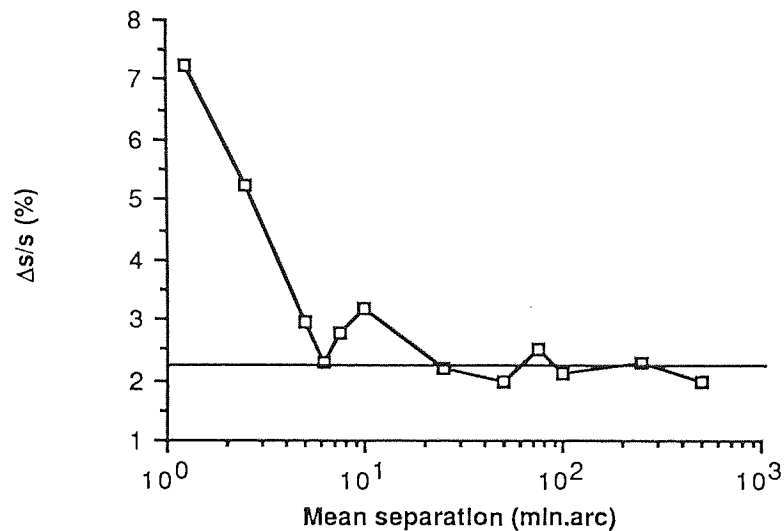


Figure 2.11: A plot of mean separation against $\Delta s/s$ from the data of Burbeck (1987). The graph clearly shows that once the separation exceeds a few minutes of arc the value of the localisation threshold expressed as a percentage of mean separation is indeed approximately constant. The straight line shows the value of the Weber fraction obtained, about 2.25%.

2.3.2: Line length

Andrews and Miller (1978) showed that bisection thresholds were independent of line length below 30 minutes of arc. For longer line lengths, however, they found that thresholds improved with increasing length. This result is somewhat curious as it would tend to contradict findings which have found independence of threshold and line length for other

hyperacuity configurations (see section 2.2.1). Given the experimental set up, with separations of the components set at 82 minutes of arc, the improvement they found may well be due to an artefact introduced by peripheral retinal locations. Klein and Levi (1985) also investigated this parameter and found that for a fixed separation of 3 minutes of arc there was little effect on thresholds for lines between 1.3 and 32 minutes of arc long. With a closer separation they did find an improvement with increasing line length but admit that this is again due to the greater luminance clue obtained with the longer lines.

2.3.3: Interfering stimuli

The effect of flanking lines placed outside the stimulus was also considered in Klein and Levi's 1985 paper. The flanking lines were placed at various separations outside the stimulus bars and the experiment was carried out for a selection of inner bar separations (*Figure 2.12*).

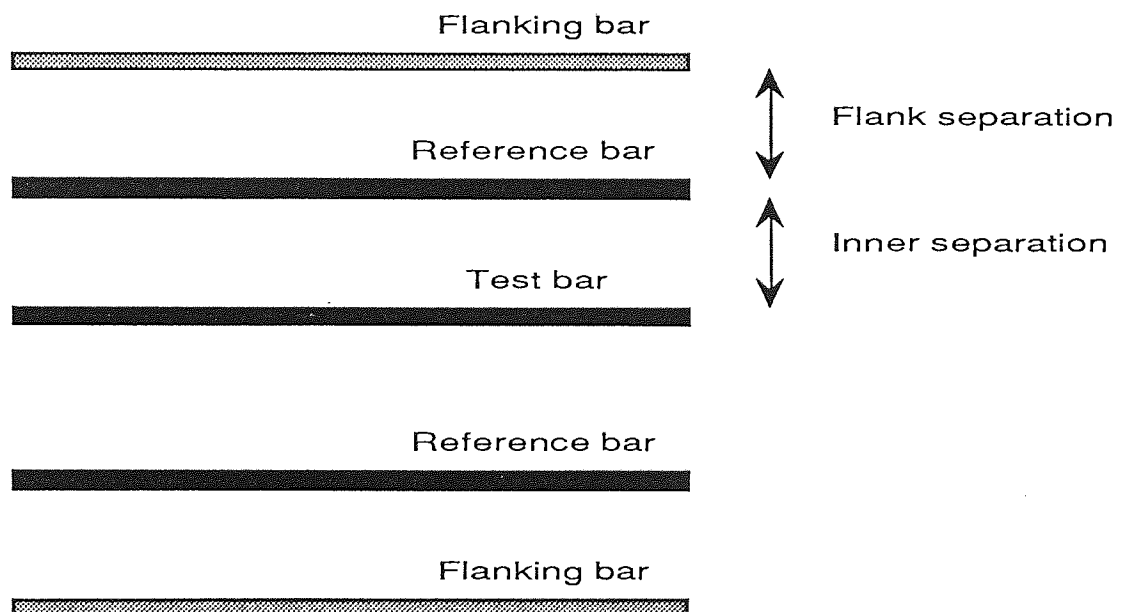


Figure 2.12: The bisection stimulus used by Klein and Levi (1985) to investigate the effect on thresholds of flanking lines. The results are discussed in the text.

With a fixed inner separation of 1.3 minutes of arc the lowest threshold values occurred when the flanking lines were 1.2 minutes of arc outside the outer bars. If the stimulus separation was altered, however, they found that the flanking lines had no effect on

thresholds for inner separations over 2 minutes of arc. Below this value there were marked effects but again due chiefly to the luminance clue rather than a relative localisation mechanism.

Because of the problems associated with bisection acuity, especially the introduction of a luminance clue, it requires some care in choosing the stimulus parameters if meaningful results are to be obtained. This thesis will investigate the effect of contrast on bisection thresholds (chapter 6) and will also use a bisection stimulus in an investigation of the effect of age on hyperacuties (chapter 11).

2.4: Displacement detection

Displacement detection can be considered to be a hyperacuity, since in certain circumstances thresholds as low as 5 to 10 seconds of arc are obtainable. Displacements are, however, different from the other hyperacuties because of the involvement of a temporal factor which adds an extra dimension to the task. It is also important to draw a distinction between displacement detection and movement detection which are thought to have different underlying mechanisms. §

A useful concept, which highlights this dichotomy, has been proposed by Bonnet (1977, 1982, 1984) in order to distinguish between the detection of movement directly in terms of its velocity, the movement analysing system (MAS), and the inference of movement by change in position, the displacement analysing system (DAS). Clearly, movement usually occurs in the presence of other objects in the visual field, i.e. *relative movement*. In such conditions movement could be either directly detected or inferred by the change in position against the references. It is, therefore, possible for the MAS or the DAS to operate. In certain situations, however, there are no references available, i.e. *absolute movement*, and in such a case movement would have to be directly detected and the MAS would then appear to be the only system available.

Bonnet proposes that the two systems will predominate under their preferred conditions but with a considerable overlap in which both systems operate. Thus the MAS should operate optimally for continuous movement at medium to high velocities and the presence of

§ Especially as it is also possible to create an illusion of movement using displacement. This involves the brief sequential presentation of two points of light in the peripheral field and has been named the "fine-grain movement illusion" (Thorson, Lange and Biederman-Thorson, 1969). The resultant illusion is that of a single dot moving linearly over an extended range, which can be up to 30 times the separation of the two retinal points (Foster, Thorson, McIlwain and Biederman-Thorson, 1981).

references, he argues, should be relatively unimportant. The DAS on the other hand logically needs some reference against which relative location can be compared. In the simplest form it is supposed that the position of the object is simply remembered across time, thus a form of motion with a stationary period at the beginning and end would represent the best stimulus. The presence of information which further improves relative localisation, in the form of nearby references, enhances operation of the DAS and should result in lower threshold values.

2.4.1: Effect of references on displacement thresholds

The effect of references on displacement thresholds will be considered at length in chapter 7. It is clear that references do tend to reduce displacement thresholds when present. However, there is some disagreement about the stimulus conditions where this holds true. Leibowitz (1955) and Bonnet (1984) found that references only improved thresholds for long durations of movement. On the other hand, Johnson and Scobey (1982) and Whitaker and MacVeigh (1990) found that references improved thresholds for all durations. In the absence of references there is considerable evidence that displacement thresholds are determined by a constant velocity prediction, at least for durations of movement above about 100 msec (Leibowitz, 1955; Johnson and Scobey, 1980; Whitaker and MacVeigh, 1990).

2.4.2: Duration of presentation

Various types of movement which have been used experimentally are shown in *Figure 2.13*. The relationship between the three parameters, time (T), distance (D) and velocity (V) is given by the simple formula $V = D / T$. For unreferenced continuous motion and stop-go-stop movement it has been shown that there is a marked dependence of thresholds on velocity (Leibowitz, 1955; Henderson, 1971; Johnson and Scobey, 1980; Bonnet, 1984; Whitaker and MacVeigh, 1990). This reflects the dependence of the MAS on velocity in order to function optimally. In the presence of references this relationship no longer always holds and under certain conditions displacement thresholds can show an independence of velocity (Johnson and Scobey, 1980; Whitaker and MacVeigh, 1990).

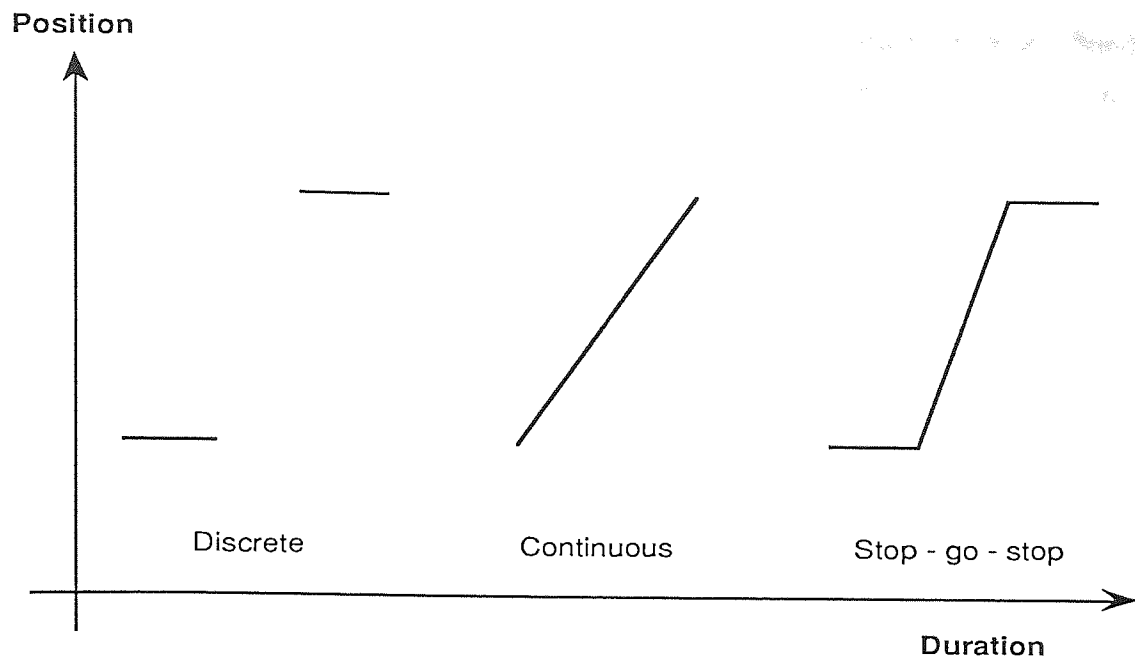


Figure 2.13: Representation of the three types of movement commonly used in experimental situations. Discrete movement involves the stimulus appearing in one position for a period then disappearing and after a time interval reappearing at a new position. Continuous movement involves the stimulus appearing, immediately moving at a constant velocity to a new position and then disappearing. For stop - go - stop movement the stimulus appears and remains stationary for a time, it then moves at a constant velocity to a second position and then remains there for another time interval until it disappears.

2.4.3: Temporal frequency

As well as investigating unidirectional displacement, it is possible to measure displacement thresholds for stimuli which undergo oscillatory movement. In these circumstances the relevant parameter is temporal frequency, measured in oscillations per second or Hertz (Hz). Tyler and Torres (1972) found that thresholds showed a strong dependence on temporal frequency for sinusoidally oscillating unreferenced motion. The introduction of references reduced thresholds but only for frequencies below 10 Hz. For referenced movement they obtained a low-pass threshold against temporal frequency function while without references this became band-pass. Tyler and Torres suggested that the results pointed towards two components mediating foveal sensitivity. The first operates at low frequencies and is affected by the presence of a reference; the second operates at high frequencies and is insensitive to the presence of references. Nakayama and Tyler (1981) investigated this idea with two types of stimuli. The first used a random dot pattern which lacked position clues and therefore required direct detection of motion. The second was a sinusoidally modulated straight line, this stimulus contained strong position clues and was not expected to isolate a movement

detection mechanism. They found that their motion sensitive system showed a band pass function whilst their position sensitive stimulus was low pass. These results were confirmed by Wright and Johnston (1985) and Buckingham and Whitaker (1986).

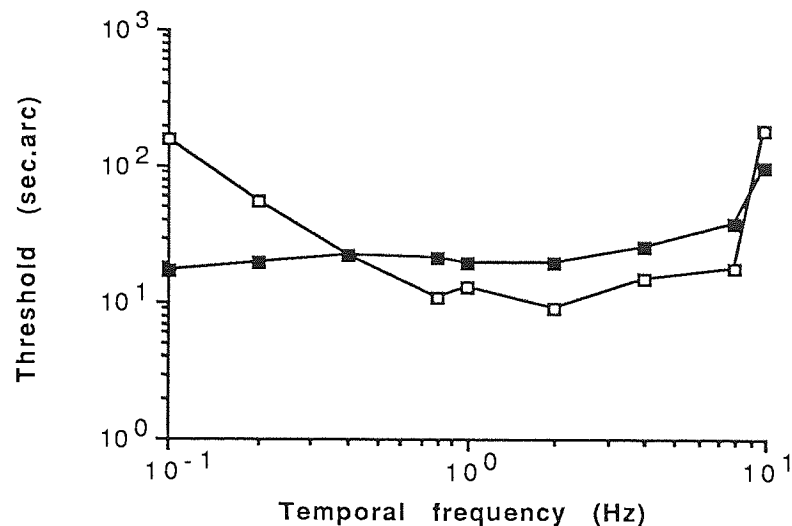


Figure 2.14: Displacement thresholds plotted against temporal frequency for a random dot pattern stimulus (open squares) and a sinusoidally modulated line stimulus (filled squares). The random dot pattern is poor in position information and can be compared with an unreferenced displacement. The line stimulus, on the other hand, is rich in positional information and equates with a referenced displacement. (from Nakayama and Tyler, 1981)

Buckingham and Whitaker (1986) also found that the waveform had an effect on the threshold values obtained. The three types of waveform shown in *Figure 2.15* were compared. The lowest thresholds were obtained from the square waveform. This outcome may be expected either because the velocity of the moving component is greatest or because this waveform remains at the extremities of its movement phase for the longest time.

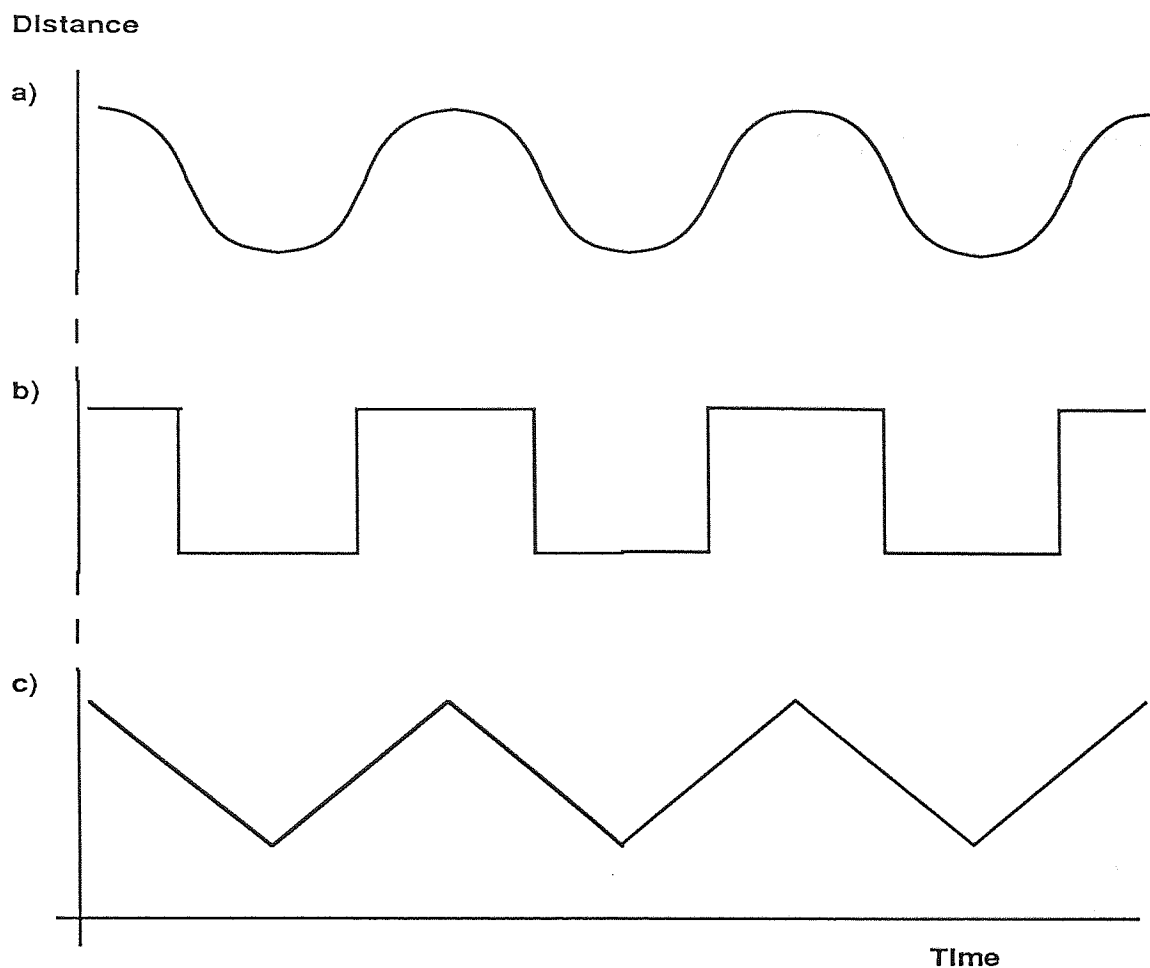


Figure 2.15: Three waveforms often used in oscillatory displacement experiments. a) is a sinusoidal oscillation; b) is a square wave which can be compared with a stop-go-stop unidirectional displacement; c) is a triangular wave equivalent to a continuous unidirectional displacement.

2.4.4: Luminance

Henderson (1971) found that displacement thresholds remained largely unaffected by changes in luminance and only at very low luminance levels did thresholds increase. Johnson and Scobey (1980) also investigated this relationship and found essentially the same independence of the two parameters for foveal conditions. In the periphery, however, they noted that luminance had a strong effect on displacement thresholds up to 4 log units above increment threshold. Elliott, Whitaker and Thompson (1989) used neutral density filters to attenuate stimulus luminance. Using a stimulus of 500 cd m^{-2} they found that up to 1.5 log unit attenuation there was little effect on displacement thresholds. Only for their 2 log unit attenuation did the effect become significant.

2.4.5: Spatial Frequency

Using oscillating gratings, studies have shown that spatial frequency has little effect on displacement thresholds over a considerable range. Westheimer (1978) showed independence of thresholds upon spatial frequency between 3 and 25 cycles per degree. Wright and Johnston found similar independence for oscillatory displacement between 2 and 24 cycles per degree while Buckingham and Whitaker (1986) found independence between 2 and 30 cycles per degree. However, Buckingham and Whitaker showed that this held only at low and medium temporal frequencies of oscillation (between 1 and 10 Hz). At high temporal frequencies (30 Hz) there was a marked worsening of thresholds as spatial frequency increased.

As the thesis is investigating the mechanism underlying relative localisation it is clear that Bonnet's DAS is the one of greatest interest. The choice of the stimuli used in experiments dealing with displacement detection thresholds has therefore been made with regard to the findings outlined here in order to minimise those variables not under consideration. I will endeavour to show that in the presence of references displacement detection can be considered a hyperacuity as it uses the same relative localisation mechanism as the static hyperacuities. These experiments, described later, will investigate the variations in displacement detection thresholds at different contrast levels (chapter 6) and the effect of both spatial and temporal reference proximity (chapter 7). In addition, the effect of changes in displacement thresholds with age will be considered (chapter 11).

2.5: Other hyperacuity configurations

While the three spatial configurations mentioned above are those used in this thesis there are other configurations which give minimum threshold values within the hyperacuity range.

2.5.1: Orientation discrimination

It has been proposed that vernier acuity can be considered as an alteration in the perceived orientation of the stimulus as a whole (Andrews, 1967; Sullivan *et al.* 1972). This in turn has led to the suggestion that the known orientation tuning of cortical cells may have a role to play in determining vernier acuity (Wilson, 1986). Several studies have shown that

orientation acuity is a function of line length. Andrews (1967) and Andrews *et al.* (1973) both obtained similar results from their experiments, with optimal threshold values for line lengths around 10 minutes of arc. Their stimulus consisted of two lines and the subjects had to decide whether the two lines were parallel or not. Thresholds were defined as the smallest offset of the endpoints of one of the lines when they were first recognised as not being parallel. Westheimer (1981) reported results in which subjects had to determine whether a line presented foveally was tilted to the left or the right. It was found that orientation recognition was dependent on line length in broadly similar fashion to vernier acuity (*Figure 2.16*). It has also been shown that flanking lines placed alongside the stimulus line cause thresholds to deteriorate in a band centered 2 minutes of arc on either side (Westheimer, Shimamura and McKee, 1976). This is very similar to the flanking bands mapped around the vernier stimulus by Westheimer and Hauske (1975) and Badcock and Westheimer (1985). Whilst orientation tuned cells are known to exist in the visual cortex (Hubel and Wiesel 1968), Westheimer (1981) suggests that a word of caution is required. The orientation half widths of cortical cells are usually around 5 degrees which appears far too large to explain the threshold values obtained above. However, Bradley, Skottun, Ohzawa, Sclar and Freeman (1985) found cortical cells in the cat which were sufficiently finely tuned to explain observed psychophysical results. They do point out, though, that the cell is also stimulated by other features of the visual environment and it would be very difficult to extract the orientation feature from this background noise. Summation amongst different neurons each with their own orientation tuning functions may allow the relevant signal to be extracted. (Andrews *et al.* 1973; Sullivan *et al.* 1972; Bradley *et al.* 1985; Parker and Hawken, 1985; Wilson 1986). In addition, Paradiso (1988) points out that if the cell with the finest tuning were the sole arbiter of performance the responses from all the less sensitive cells would have to be ignored which would clearly be a wasteful process. Heeley and Buchanan-Smith (1990) also determined orientation recognition for stimuli comprising either sinusoidal gratings, an edge or a line. Stimuli were presented at various orientations and the subject had to decide whether they were tilted to the left or the right. All the stimuli produced similar threshold values, around 0.6 degrees angle of rotation, from which it was concluded that the spatial frequency content of the stimulus was not important.

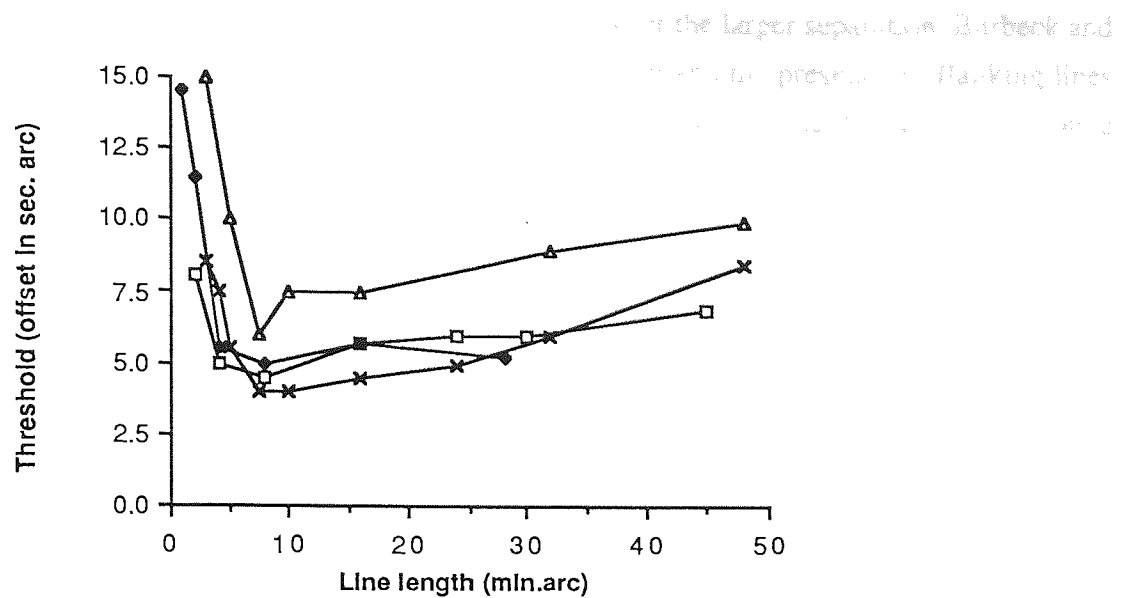


Figure 2.16: A comparison of threshold (defined as the horizontal offset of the ends of the two lines) for an orientation recognition task. The crosses are from Andrews (1967), the open triangles from Andrews *et al.* (1973) and the open squares from Westheimer (1981). The filled diamonds are the vernier thresholds from Westheimer and McKee (1977a) as a comparison. The results are discussed in the text.

2.5.2: Spatial Interval detection

Spatial Interval detection involves the comparison of two demarcated intervals in order to decide which is the larger of the two. The intervals can be presented sequentially with a temporal delay between the two presentations, simultaneously or sequentially with no delay between the presentations. Threshold values under this last condition were found to be about 6 seconds of arc and were essentially independent of separation of the two lines (Westheimer, 1979). This last type has clear similarities to the detection of an instantaneous displacement in the presence of references.

Figure 2.17 shows the results of experiments which considered the first two conditions mentioned above. It is clear that thresholds, for both conditions, are dependent on separation. In addition, the introduction of a temporal delay between the two presentations (in this case 500 msec) causes a marked increase in threshold values.

Morgan and Regan (1987) studied the effect of varying contrast on a spatial interval detection task at two separations. They showed that contrast, which was varied between about 10 and 75%, had no effect on threshold values. They also found, for all but the lowest contrast, the

same effect of separation, with higher threshold values for the larger separation. Burbeck and Yap (1990b) investigated the effect of exposure duration and the presence of flanking lines on spatial interval detection thresholds. With no flanking lines present there was complete independence of threshold values and exposure duration. In the presence of flanking lines, however, threshold values deteriorated considerably as exposure duration was reduced below about 500 msec.

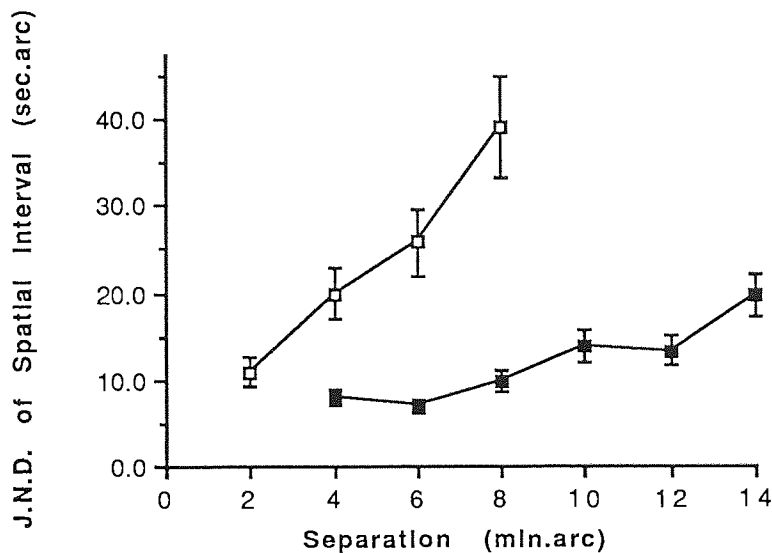


Figure 2.17: Just noticeable difference (J. N. D.) of Spatial Interval plotted against feature separation for sequential presentation of the two stimuli with a 500 msec delay between the presentations (open squares) and simultaneous presentation of the two stimuli (filled squares). The results are discussed in the text (From Westheimer, 1979).

2.5.3: Spatial frequency discrimination

Spatial frequency discrimination is a measure of the ability to determine whether two sequentially presented sinusoidal gratings differ in spatial frequency. Hirsch and Hylton (1982, 1985) carried out a series of experiments which attempted to measure spatial frequency discrimination and the stimulus features which might influence it. They found a Weber relationship between the just noticeable difference in spatial frequency (Δf) and the reference frequency (f) for the range of frequencies which they investigated (between 0.3 and 16 cycles per degree). In addition, it was shown that the $\Delta f/f$ function was independent of the

field size so long as there were at least two successive peaks visible. From this they concluded that spatial frequency discrimination can be looked on as another form of spatial interval detection task. As with orientation, individual cells have been found in the cortex of monkeys (Parker and Hawken, 1985) and cats (Bradley *et al.* 1985) which are sufficiently sensitive to changes in spatial frequency to explain observed performance. However, for the same reason as orientation, the use of such cells to perform spatial frequency discrimination would be liable to contamination by the other factors causing the cell to respond. It is more likely that responses from several neurons, in this case tuned to differing spatial frequencies, are used to isolate the required signal.

Chapter 3: Models of hyperacuity detection

3.1: Introduction

There are many models which attempt to explain the phenomenon of hyperacuity. Broadly they can be divided into two groups, those based on "local-signs" and those based on "channels". As with many areas of research there is some controversy regarding the application and design of the models. However, care is needed in addressing the correctness or otherwise of some of the objections. In particular, certain of the arguments used against the channel models do not negate their application to hyperacuity but would, correctly, dispute their application to large scale relative localisation. This chapter will describe those models which attempt to explain the mechanism by which relative localisation with hyperacuity precision may be obtained.

3.2: Local-sign models

The local-sign models have within them the common thread that some feature of the stimulus is used to allocate a unique position to it. These positions are then located relative to each other in order for any disparity to be extracted. It is a testimony to the strength of the idea that it has held, in its overall theme, for nearly a century although, it has to be said, the details have been the subject of considerable revision.

The original theory, which attempted to provide an explanation for those visual tasks yielding thresholds far lower than that expected by anatomical limitations, dates back to the turn of the century. Wulffing (1892) showed that vernier tasks could be performed with an accuracy far better than that predicted by the retinal photoreceptor spacing. It was proposed by Hering (1899) that each photoreceptor stimulated by the line was allocated a "local-sign". In essence, the position of each photoreceptor on the retina was projected out into visual space and any object stimulating that photoreceptor was then allocated that position or local-sign. The local-sign could, therefore, be considered as the signal emanating from the photoreceptor. Clearly, for a spatially extended object, there would be many stimulated photoreceptors and averaging together of all their individual local-signs, along the length of the stimulus for a line object, would enable the location to be estimated more accurately than would be possible using a single photoreceptor (*Figure 3.01*).

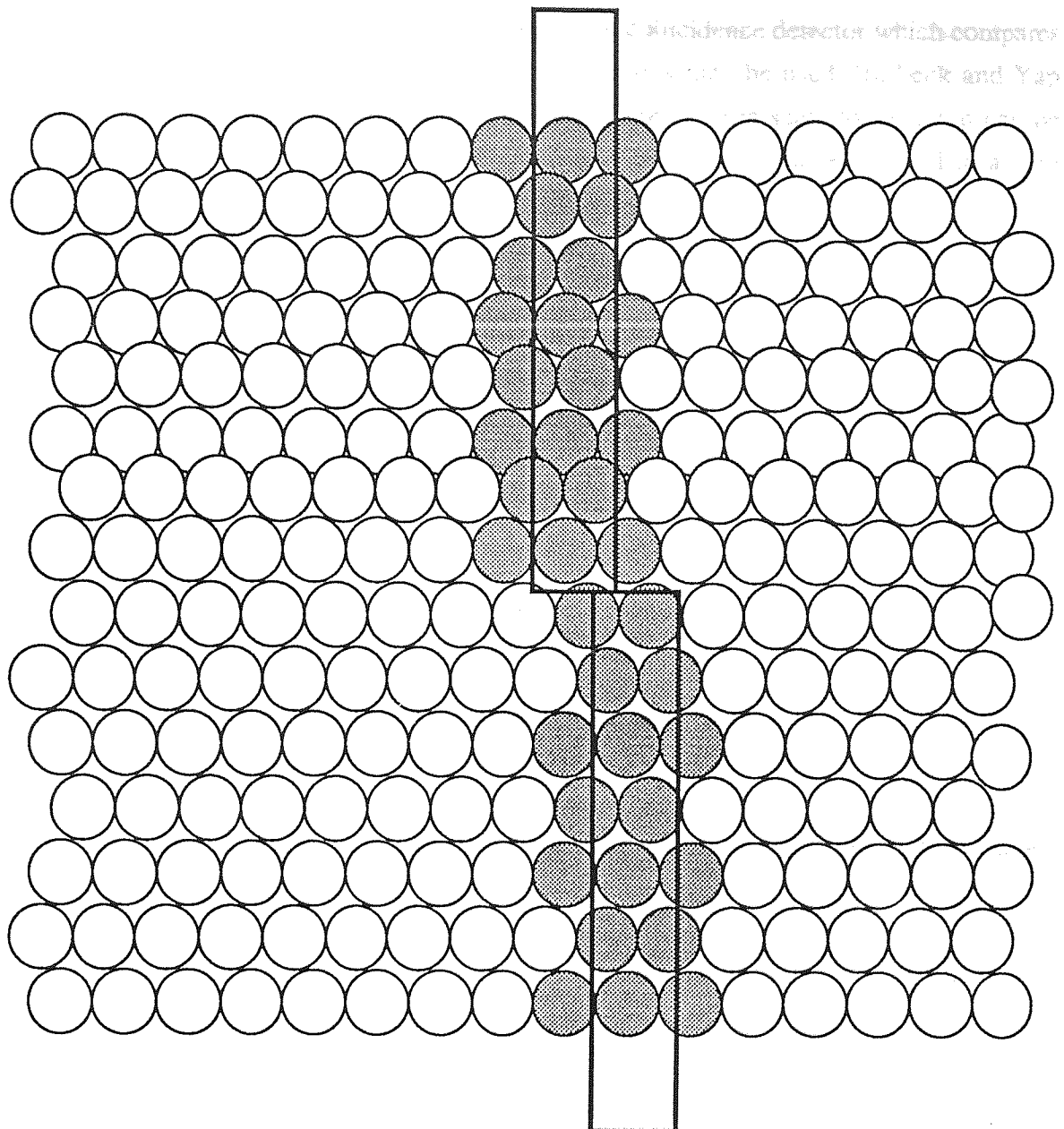


Figure 3.01: The response of photoreceptors to a vernier type stimulus, for simplicity the receptors are shown as circular. The stimulus consists of two bars (open rectangles) with a small offset. These stimulate the shaded photoreceptors each of which has a unique local-sign. In the model the averaged location of these local-signs assigns position to the bars.

As a prediction of the mechanism underlying hyperacuity this is only the first stage. A second comparative stage is required where these two locations can be compared relative to each other and any difference extracted. The mechanism by which this comparison is carried out has been the subject of much speculation. Morgan and Regan (1987), whose

idea will be discussed later, suggested that a form of coincidence detector which compares the output of receptive fields at paired retinal locations may be used. Burbeck and Yap (1990b) also proposed that a mechanism exists whereby large scale localisation can be undertaken. They suggested that a size and position indicator was employed to assign location. The outputs of these indicators were then used to determine relative localisation. This suggestion had previously been made by Paradiso, Carney and Freeman (1989) although they made no suggestion as to what the "local-sign" feature might be.

The local sign model as described held sway until the findings of Ludvigh (1953), Sullivan *et al.* (1972) and Westheimer and McKee (1977a) that vernier tasks can be performed with the same accuracy for two dots as for two lines *provided* that there is a small gap between them. As was stated in chapter 2, vernier thresholds as low as 5 to 6 seconds of arc can be obtained using two dot stimuli. This result requires some form of pooling amongst receptor responses (see chapter 1) which would be difficult to obtain by averaging along the length of a single dot! In addition, the theory implies that the accuracy should be better for longer lines, where logically the greater number of stimulated photoreceptors would allow more accurate localisation to take place. Unfortunately, this has also been shown not to be the case (French, 1920; Westheimer and McKee, 1977a). In order to overcome these difficulties an alternative local-sign was proposed by Sullivan *et al.* (1972) who suggested that comparison of the point spread functions of the two dots could provide sufficient information to allow relative localisation to the required accuracy. *Figure 3.02* illustrates their proposal. The line spread functions of the two stimulus elements are compared and any difference between them used to extract information regarding an offset. This is somewhat simplistic but it serves to show that extraction of information at right angles to the stimulus (*i.e.* orthoaxial) can be used. The figures show the response of each photoreceptor as a percentage of the maximum possible. Sullivan *et al.* were not sure what difference between the two retinal luminance profiles would be required in order to detect an offset but expressed the view that the percentage difference they calculated should certainly be sufficient. In short, they proposed that the averaging was performed at right angles to the line, *i.e.* in the direction of the offset, not along it.

This idea has since been taken up and refined, in particular by Watt and Morgan (1983a). They used a vernier type stimulus and, following from the work of Watt and Andrews (1982) who had argued that a mechanism exists which extracts information orthoaxial to the stimulus feature, set out to find which feature of the retinal image could assign a

position tag to the stimulus. In terms of the proposal put forward by Sullivan *et al.* (1972) they were attempting to answer the question; What is the feature of the retinal luminance profile which carries the signal allocating location?

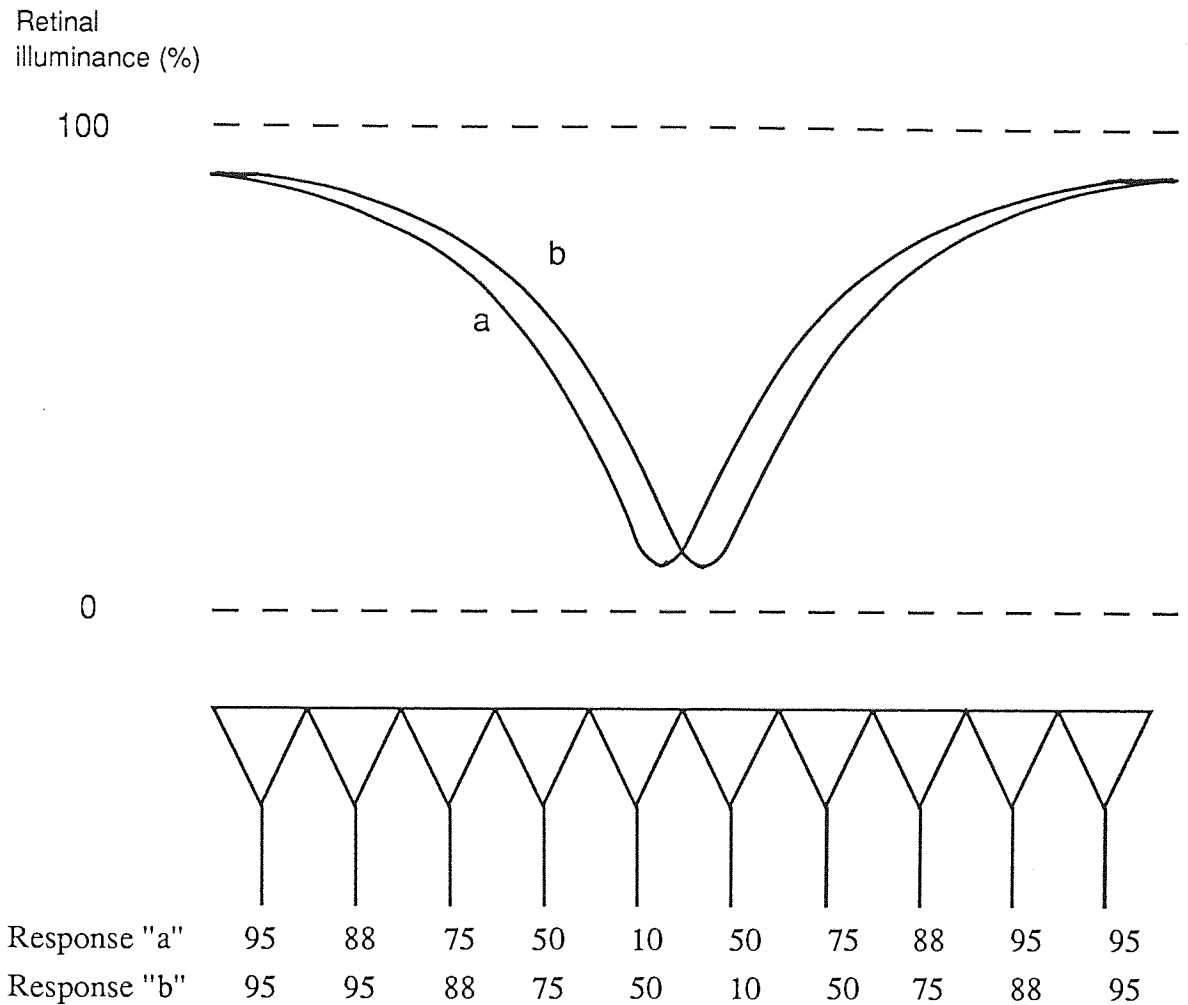


Figure 3.02: A model suggested by Sullivan *et al.* (1972) in which the line spread functions of the two stimulus features are compared. The line spread functions (in this case for dark lines on a bright background), expressed in terms of retinal luminance profiles, are shown at the top. The receptors are shown in the center and their outputs, expressed as a percentage of their maximum output, are listed at the bottom.

The chief problem in answering the question lay in the fact that there was no conclusive proof that the visual system did in fact average over the retinal luminance profile in order to extract a position. Watt and Morgan suggested that there was, however, some evidence that this might be so. They cited the work done by Westheimer and Hauske (1975), using

spatial interference, and Westheimer and McKee (1977b), using a stimulus whereby the internal light distribution could be altered without distorting the physical limits of the stimulus, as indicating that the visual system integrated the information from a region of visual space in order to perform the required task.

Watt and Morgan (1983a) postulated that the feature of the retinal light distribution used to assign location to an object could, sensibly, be one of four.

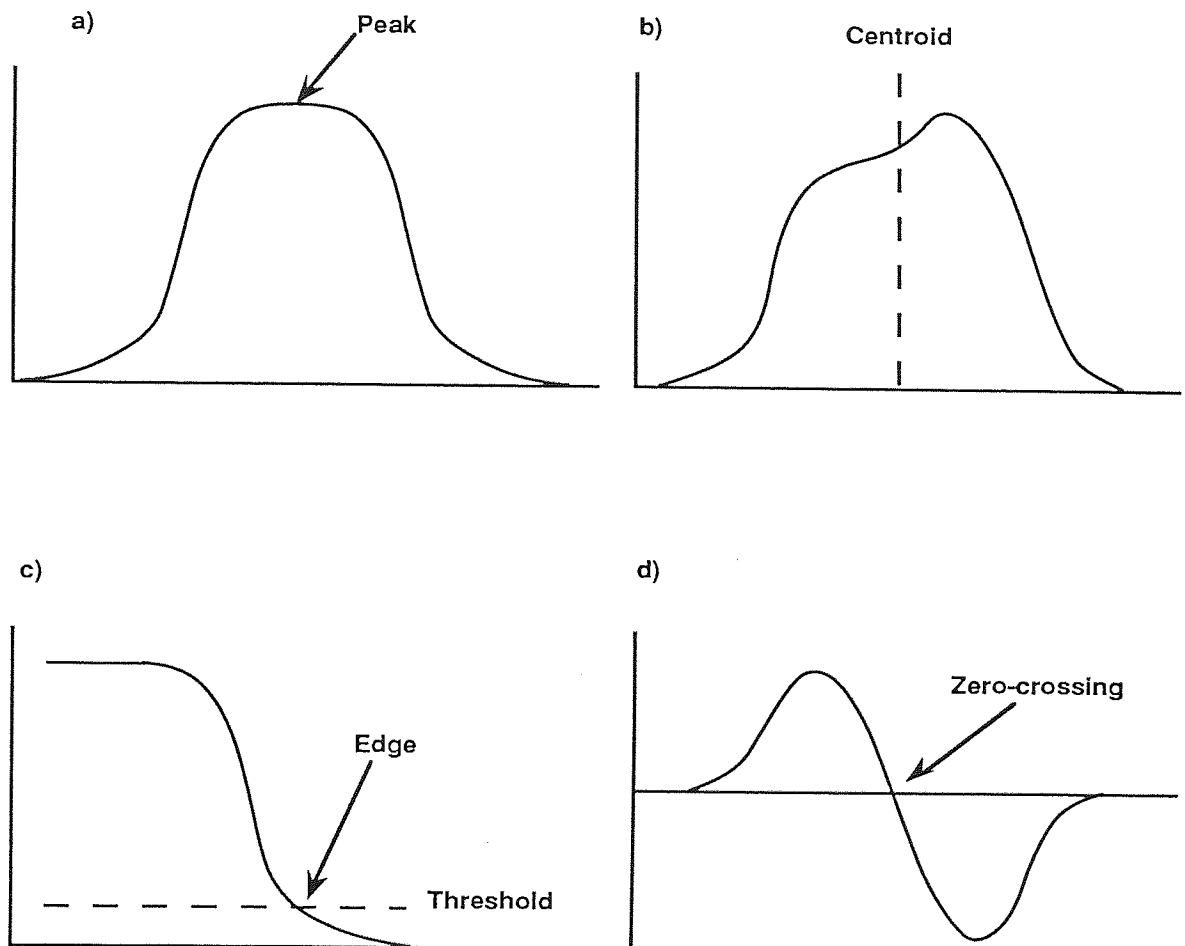


Figure 3.03: The features of the retinal light distribution of a stimulus which could be used in assigning location to the stimulus. (a) is the peak, defined as the point where the retinal light distribution reaches a maximum value. (b) is the centroid, defined as the arithmetic mean of the retinal light distribution. (c) a threshold edge, which is defined as the point where the retinal light distribution exceeds a threshold value dependent on the background light intensity. (d) the retinal light distribution convolved with the second derivative of a Gaussian (as described by Marr and Hildreth, 1980).

- a. **Peak:** the location is defined as the point where the retinal light distribution is a maximum (*Figure 3.03a*).
- b. **Mean:** the location is defined as the point equivalent to the mean value of the retinal light distribution. This is analogous to the center of gravity of a solid object and has been given the term "centroid" (*Figure 3.03b*) (Westheimer and McKee, 1977b).
- c. **Edge:** defined as the point where the retinal light distribution exceeds some threshold value dependent on the background illumination (*Figure 3.03c*).
- d. **Zero-crossings** as suggested by Marr and Hildreth (1980) to represent edges in the original retinal image (*Figure 3.03d*). They proposed that the retinal image (I) was convolved with a Gaussian operator (G) which has the effect of smoothing the retinal image and is expressed as $G * I$. Intensity changes (contours) in the original image are then located by zero-crossings in the second derivative of this function, $D^2(G * I)$ (*see figure 3.03d*). While this model suggests one possible feature which could be employed in assigning location it was felt to be relatively expensive in terms of computation. In order to reduce the amount of computation it was proposed by Marr and Hildreth that a Laplacian operator, which is independent of orientation, could be used. This convolution, with a two-dimensional differential operator instead of the one-dimensional Gaussian, would have zero-crossings which would not only detect the intensity change but also its orientation.

The first experiment performed by Watt and Morgan (1983a) involved a stimulus consisting of two bars one above the other. One of the bars was single while the other consisted of two bars with a small horizontal separation between them. The paired bars were either of equal luminance or had one bright (luminance L_b) and one dimmer (luminance L_d) bar the relationship between them being defined by the luminance ratio (L_b/L_d) {note that the total luminance of the paired bar always equalled the luminance of the single bar }. The task was to discern which of the two bars was the paired one. The second experiment used only the paired bar. This time the task involved detecting whether the dimmer bar was left or right of the brighter.

For experiment one the threshold values obtained were always better than that predicted by the theoretical resolution ability of the subject. In the second experiment the thresholds

were always worse than the theoretical resolution ability. Clearly, in experiment one the task was performed by use of a relative width judgment whilst in the second the two bars had to be resolved before their individual luminance profiles could be separated. Therefore, the first conclusion to be drawn was that if the two bars were not resolved then the visual system assigned a uniform luminance profile to the stimulus. If the bars were resolved then the individual luminance of the two bars was respected.

A third experiment was performed using a vernier task with an unusual stimulus configuration (*Figure 3.04*). Thresholds were always lower than in experiment 1, with minimum values around 6 seconds of arc being obtained. In addition, they used a control stimulus of two bars, both single, in a standard vernier configuration. They then went on to calculate the position of the four possible features which could be used to assign location. In order to be acceptable, the calculated magnitude of the offset cue supplied by the feature under consideration had to equal the control condition for all luminance values. *Figure 3.05*

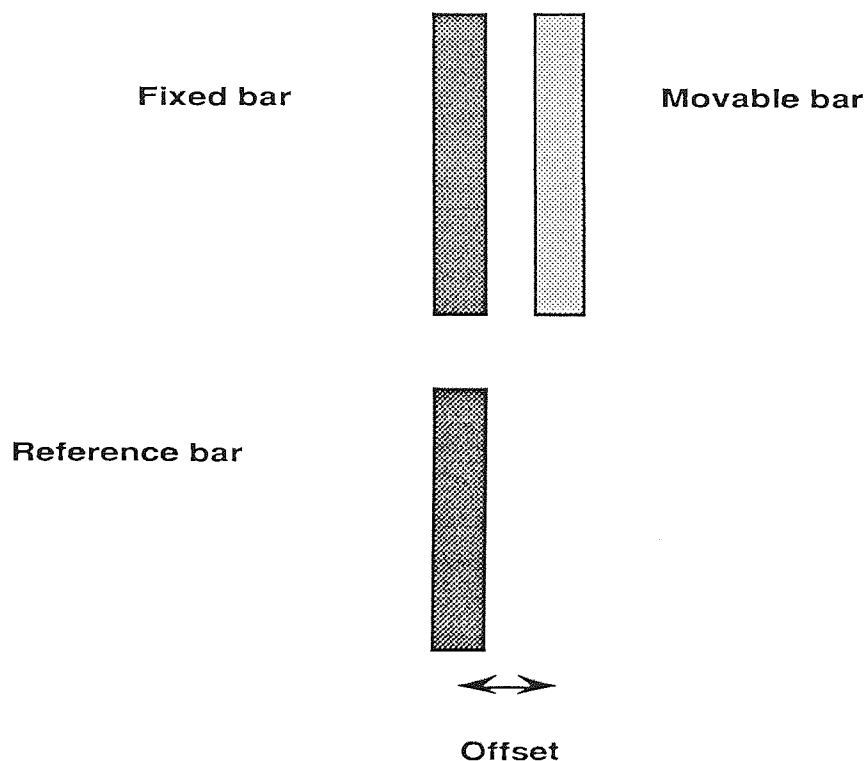


Figure 3.04: The stimulus configuration used by Watt and Morgan (1983a) in their third experiment. The lower single bar has a luminance ($L_b + L_d$) and is aligned directly below the brighter of the upper bar pair. The dimmer bar was offset, either right or left, the observers task being to decide in which direction the offset lay.

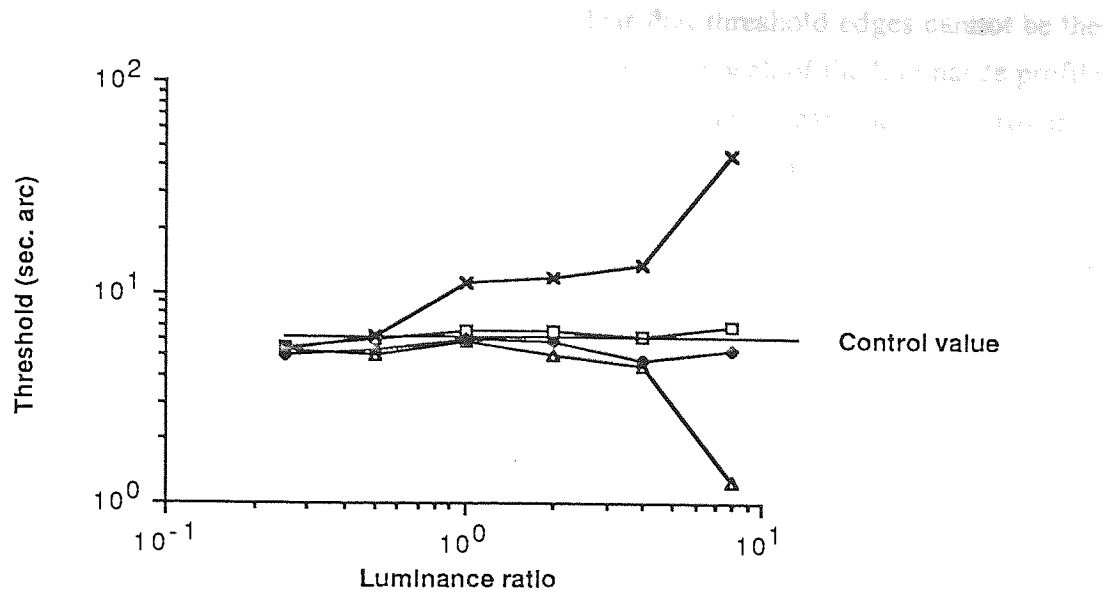


Figure 3.05: A comparison of the control result (horizontal line) to the four possible stimulus features which could logically assign location to the object. Open triangles indicate the peak of the RLD, open squares the centroid, filled diamonds the zero-crossings and crosses the threshold edge. The results are discussed in the text.

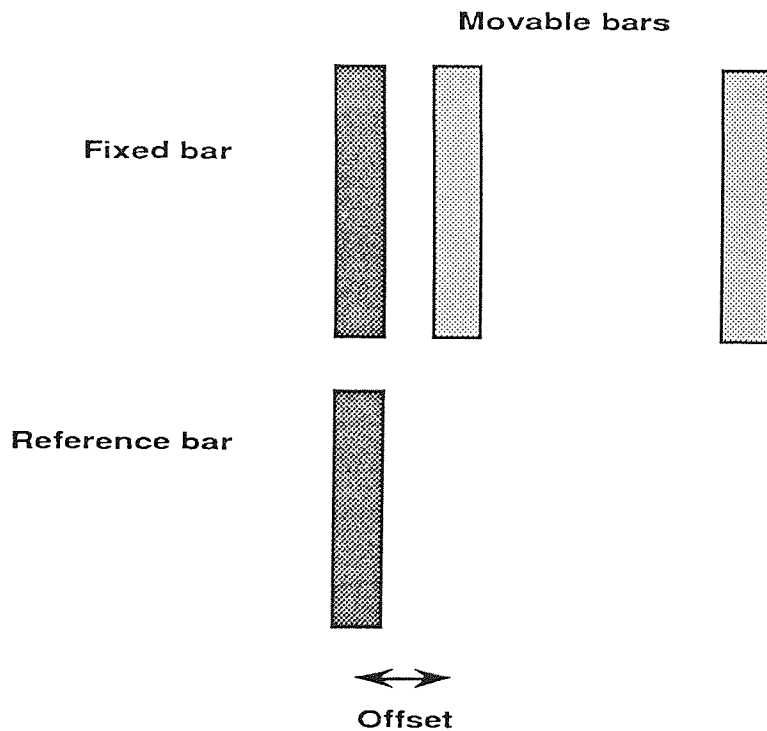


Figure 3.06: The stimulus configuration used in Watt and Morgan's (1983a) fourth experiment. This time the upper stimulus feature consisted of three bars. The brightest aligned exactly above the lower single bar (luminance of the lower bar was $L_b + 2 * L_d$) the two dimmer bars were both offset to the same side, either right or left. The outer bar was positioned four times as far from the fixed bar as the inner, offset was defined as the distance between the inner movable bar and the fixed bar.

shows how they compare and it is immediately clear that threshold edges cannot be the feature employed. There is also a question mark against the peak of the luminance profile given the marked departure at the highest luminance ratio. The mean and zero-crossings both closely follow the predicted value over the whole range investigated.

In order to gain more information, Watt and Morgan used a fourth experiment in which the luminance profile became more asymmetric (*Figure 3.06*). Again, threshold values are well below those obtained in experiment one, the lowest being around 4 seconds of arc. The magnitude of the offset cue provided by the remaining three possible features of the luminance profile was again calculated and compared with the control value from experiment three (*Figure 3.07*). This time, clearly, the peak of the luminance profile does not meet the requirements but again the mean and zero-crossings closely follow the predicted value.

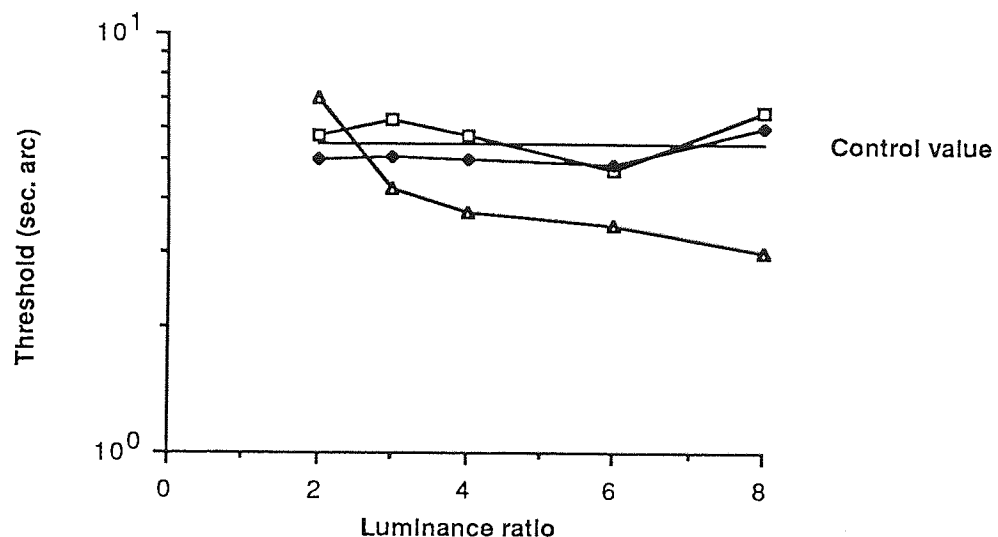


Figure 3.07: The results of the peak of the RLD (open triangles), the centroid (open squares) and the zero-crossings (filled diamonds) compared to the control value. This time the peak value is clearly unacceptable.

Watt and Morgan's experiments, therefore, showed that neither the peak nor threshold edge of the retinal luminance profile were used to attribute location. However, they were unable to distinguish clearly between the other two possibilities and on the grounds of parsimony backed the detection of zero-crossings in the second derivative of the retinal light distribution as the feature employed in assigning location.

Watt and Morgan (1985) then went on to develop this idea into a model in which a primitive code was extracted from the stimulus to assign location. This attempted to overcome the difficulty of reconciling the fact that blurred edges are harder to locate than sharp edges, a result which is not easily explained by the use of zero-crossings. In addition, the presence of several edges close together causes distortions in the filter output which leads to errors in the representation of the edges. The model, called MIRAGE, used the averaged output from filters covering a range of spatial scales to locate zero-bounded distribution of activity in the filtered retinal image to encode the stimulus and provide a basis for later processing. The zero-crossings in the filter response were used to generate the zero-bounded response distribution [RESP]. In addition, regions of inactivity in the luminance profile [ZVSP] were also plotted and the combination of these two primitives allowed the representation of bars and edges to be made. Three rules were needed to combine the primitives; a *null* rule where a single [ZVSP] indicates a luminance plateau; an *edge* rule where a [RESP] with a [ZVSP] on only one side is interpreted as a boundary; a *bar* rule where a [RESP] with a [ZVSP] on both sides or on neither side indicates a dark or light bar. *Figure 3.08* shows how these combinations enable an edge and a bright bar to be represented.

While Watt and Morgan's work showed that the extraction of zero-crossings could be used to assign location there is evidence that the centroid of the retinal light distribution may also be used. In particular Westheimer and McKee (1977b) and Whitaker and Walker (1988) both found that by altering the internal light distribution of the stimulus without altering its physical limits it was possible to alter perceived alignment. The zero-crossing model based on luminance discontinuities would not directly predict this.

The situation at present, therefore, is that it has been shown that averaging along the length of the stimulus cannot explain the phenomenon of hyperacuity in all conditions. The extraction of some tag from the retinal light distribution in a direction orthoaxial to the stimulus feature does, however, appear to meet this requirement. Chapter 6 of this thesis, however, will show that summation along the length of the stimulus feature is vital under certain conditions while chapter 9 will consider further the role of the centroid as the feature assigning location.

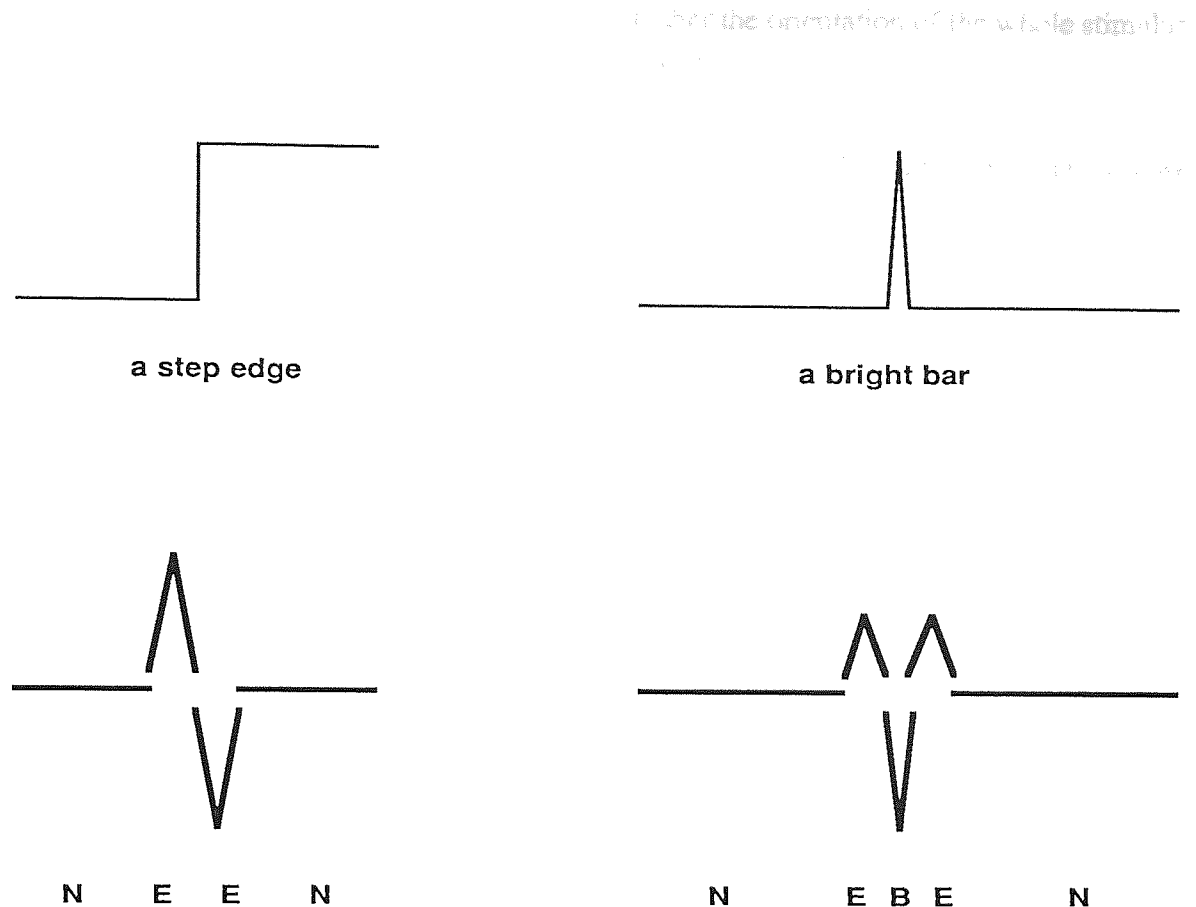


Figure 3.08: The primitive code used by Watt and Morgan (1985). At the top the luminance profile of the two features to be encoded, a step edge and a bright bar. Below this are the primitive responses, the horizontal line represents a [ZVSP] and the chevrons a [RESP]. The chevrons indicate the mass (proportional to the amplitude), the standard deviation (proportional to the base width) and the centroid (indicated by the position of the apex) of the filter responses. At the bottom the letters indicate which of the three combination rules is being employed, N indicates the null response, E the edge rule and B the bar rule.

3.3: Channel models

The underlying basis of the "local-sign" models is that the location of the stimulus features is made explicit and these positions are then compared by a secondary process in order to assign relative location. Channel models, a term coined by Burbeck (1987), differ in that they use an implied representation of the stimulus and perform the relative localisation of the individual features without reference to their absolute location. As an example of this, Andrews (1967) suggested that, under certain conditions, the vernier task could be simplified to detection of the orientation of the whole stimulus. If this is correct then it immediately removes the need to make the position of the stimulus features explicit. All that

is required to perform the task is to determine whether the orientation of the whole stimulus deviates from some standard, for example the vertical.

The channel models are based on the finding that individual cells within the striate cortex are tuned to particular spatial frequencies and orientations. DeValois, Albrecht and Thorell (1982) investigated the spatial frequency tuning of cells in the cortex of the macaque monkey.

Their data shows that for bandwidths there is little to choose between the X and Y cells with a median around 1.4 to 1.5 octaves. There are however a significant percentage of cells with a broad tuning characteristic (>2.6 octaves). With regard to peak spatial frequency (the channel models use filters tuned to particular spatial frequencies) the cell's peak sensitivities cover a wide range from 0.5 to 16 cycles per degree. In addition there are a small number of foveal cells tuned to higher spatial frequencies and a small number of parafoveal cells tuned to lower spatial frequencies. Y cells are generally tuned to higher spatial frequencies than X cells.

There are also two interesting correlations. First, a statistically significant correlation was found between spatial frequency and orientation bandwidths, with cells narrowly tuned for spatial frequency also being narrowly tuned to orientation and vice-versa. Secondly, those cells tuned to higher spatial frequencies tended to have narrower bandwidths than those tuned to low spatial frequencies. Finally, the results also support the idea that cells are arranged in hypercolumns (Hubel and Wiesel, 1974) in which all orientations and spatial frequencies between approximately 0.5 and 16 cycles per degree are represented. Models have been devised based on these findings which attempt to explain hyperacuity performance in terms of the response of filters tuned to different orientations, spatial frequencies and phase.

3.3.1: Geisler (1984)

Geisler (1984) attempted to devise an ideal observer against which he could compare human experimental data. In turn these differences would be expected to shed light on the underlying processes operating in the real observer. His model had the following features:

a). The line spread function for a 2 mm diameter pupil was calculated based on those reported by Campbell and Gubisch (1966; *figure 10*) with the curve approximated by the

sum of two Gaussian functions.

b). He used a receptor array based on a hexagonal matrix (after Miller, 1979) with receptors separated by 0.6 minutes of arc. (*It should be noted that this is slightly larger than anatomical findings in humans.*)

c). Finally he used statistical calculations, taking account of the chief anatomical, optical and physiological variables affecting the visual system, to estimate the response characteristics of the retinal receptors to a given stimulus.

He compared his predicted results to data on spatial interval detection (Westheimer, 1979) and vernier acuity (Westheimer and McKee, 1977a). It was concluded that real observers could, under the right circumstances, closely approach the ideal performance levels calculated using his model. The differences were put down to a combination of noise in the system and his chosen receptive field shape, which was a mathematical ideal and as such unlikely to be exactly duplicated in practice. He stressed that positional uncertainty, due to eye movements and unsteady fixation, would tend to reduce the performance of the human observer. However, if the visual system detects changes in the output of filters, without requiring the location of the stimulus to be made explicit, this would substantially reduce the problem. His model, while comparing the locations of the stimulus features, does so without the need to know their absolute locations and as such can be placed between true local-sign and channel models.

3.3.2: Carlson and Klopfenstein (1985)

An early, relatively simple channel model was suggested by Carlson and Klopfenstein (1985). They used a bank of spatial frequency filters each tuned to a particular frequency with a bandwidth of 1 octave. If one compares this value, which applies for channels with a spatial frequency peak over 1.5 cycles per degree, with those found by DeValois *et al.* (1982) it is clear that it may well be an underestimate.

Within each channel they had two noise sources. The first was the intrinsic noise from within the visual system due to the normal resting discharge of the neurons, eye movements etc. The second was a function describing external noise (that is noise due to

the stimulus signal) which grew in proportion to the strength of the signal within the channel.

There then followed a non-linearity, which was needed to explain basic contrast detection experiments carried out by Carlson and Cohen (1980), a smoothing stage and finally a detection stage which determined the likelihood of detecting a signal change in the most sensitive channel. This last feature specifically excluded probability summation over channels and thus restricted the model to a single channel system. By applying the model to the spatial interval discrimination results of Westheimer and McKee (1977a) they found good agreement apart from slightly higher optimum threshold values. The relationship between separation and threshold was correctly predicted. Finally, they showed that high spatial frequencies were not needed to perform hyperacuity tasks and that performance should be insensitive to contrast at suprathreshold contrast levels.

3.3.3: Klein and Levi (1985)

Klein and Levi (1985) used results from a series of bisection task experiments to show that combining the outputs of spatial filters could explain hyperacuity. Essentially, spatial discrimination tasks were carried out by concentrating on a particular feature of the stimulus and analysis was then based on the output of a continuum of spatial frequency filters at different locations. These filter outputs were then combined to produce a "viewprint", analogous to a voiceprint in audition. By simultaneously conveying spatial frequency and spatial information this allowed judgment of size and position to be made. Their model used several mathematical procedures in order to compute the "viewprint".

a). Receptive field shape was defined by a Cauchy function which was shown to more closely match observed receptive field sensitivity profiles than the DOG function. The Cauchy function can be adjusted to give a large range of bandwidths but for the purposes of the model these were restricted to 1.5 and 2 octaves. They further felt that this function had the advantages that the filters existed as matched pairs and their shape was consistent with psychophysical estimates of the CSF.

b). Since the sensitivity of the mechanism could not be greater than the CSF the latter was defined by Cauchy functions using mechanisms of different sensitivities. This meant that the whole CSF was obtained by pooling of responses from many mechanisms. In order to

perform hyperacuity tasks the pooling was considered to occur over a quite short range. This had the effect of degrading information on absolute location while allowing fine relative localisation judgments to be made.

c). A contrast response function (which relates d' , the signal detection parameter, to the stimulus strength) was included. This predicted the response of the proposed mechanism at suprathreshold contrast levels.

d). Finally, account was taken of eye movements which degrade absolute, but not relative, location information.

They found good agreement between predicted and actual results and showed that such performance could be explained using cells no more sensitive than the simple cells found by Hubel and Weisel (1968). The model essentially combines features of both channel and "local-sign" theories. The "viewprints" provided by the output of a range of filter sizes allow both an implicit representation of the stimulus and an explicit location of individual features of the stimulus. This means that the model can operate either using the filter outputs directly for small separations, or by using the positional information and then performing a relative localisation (Morgan, 1991). Which method is adopted will depend on the relative sensitivity of the two systems. This point will be considered further in chapters 8 and 9.

3.3.4: Wilson (1986)

The most complete model, and the one subject to the most rigorous comparison with experimental data, is that proposed by Wilson and his co-workers (Wilson and Bergen, 1979; Wilson and Gelb, 1984; Wilson and Regan, 1984). It is summarised in Wilson (1986) which explains both the details and some of the tests to which it has been subjected.

The model proposes that there are six channels each tuned to a particular spatial frequency with specific orientation and frequency bandwidths. These are summarised in *Table 3.01*. Note that each receptive field has an excitatory center with two inhibitory flanks, the height of the central excitatory area being 3.2 times its width. In *Table 3.01* the width shown is that of the excitatory center (*Figure 3.09*).

Table 3.01:

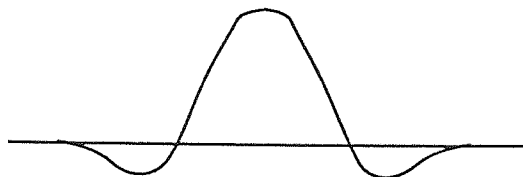
Peak spatial frequency	Peak sensitivity	Receptive field		Orientation bandwidth
cycles/degree		height	width	degrees
		minutes of arc		
0.8	30.0	75.0	23.4	30.0
1.7	70.0	35.3	11.0	30.0
2.8	140.0	21.4	6.7	20.0
4.0	170.0	15.0	4.7	20.0
8.0	76.7	7.5	2.3	15.0
16.0	18.4	3.8	1.2	15.0

The model differs from that proposed by Carlson and Klopfenstein (1985) in that it operates in two dimensions and therefore provides a general model covering a range of hyperacuity configurations.

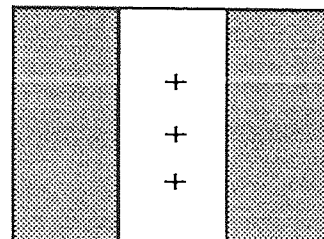
Figure 3.10 outlines a the response of different filters to a small vernier offset. Note that the small offset results in a larger differential response in the narrowly tuned high spatial frequency filter compared to that with a broad bandwidth low spatial frequency tuning. It should be apparent that the differential response has to have sufficient magnitude to allow it to be detected against the background noise within the channel and their larger differential response will make this easier to achieve with the high frequency channels. It is also apparent that the largest differential response occurs not at the point of peak sensitivity but towards the edge of the excitatory center where the sensitivity is changing most rapidly. It should be noted, however, from *Table 3.01* that the most sensitive cells are not those with the highest spatial frequency tuning. Peak sensitivities occur for cells tuned to a spatial frequency around 4 cycles per degree which compensates, to some extent, for their lower differential response. This reinforces the importance of inputs from all the filters not just the most precisely tuned or most sensitive in order to reliably detect small offsets. For vernier tasks, using two dots, the separation of the stimulus features is also important. With small vertical separations the two dots will lie well within the smallest filter and will not provide a strong stimulus to the orientationally tuned filters. When the two dots lie near

the upper and lower edge of the smallest filter (that is with a separation in the region of 4 minutes of arc) they provide a much stronger stimulus for orientationally tuned filters (Figure 3.11).

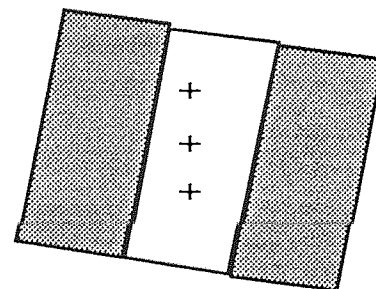
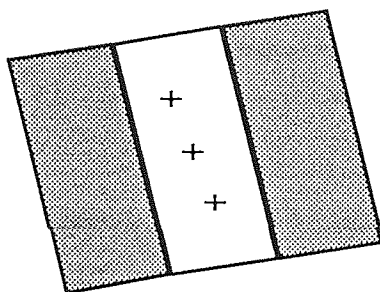
a)



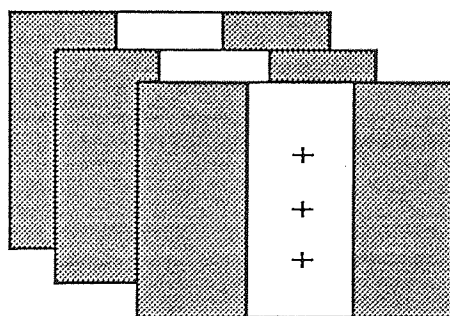
b)



c)



Orientated units



Displaced units

Figure 3.09: (a) The profile for an on-center receptive field which has a central excitatory peak with two inhibitory flanks (from Enroth-Cugell and Robson, 1966). (b) a schematic diagram of the same receptive field. (c) the layout of the fields with orientated and displaced filters (from Wilson, 1986). Within a group of filters it is proposed that all possible orientations are covered together with the six spatial frequencies listed in Table 3.01. In addition, the stimulus will be centered on some fields but displaced on others. The responses from all the fields are pooled in order to obtain thresholds to hyperacuity precision.

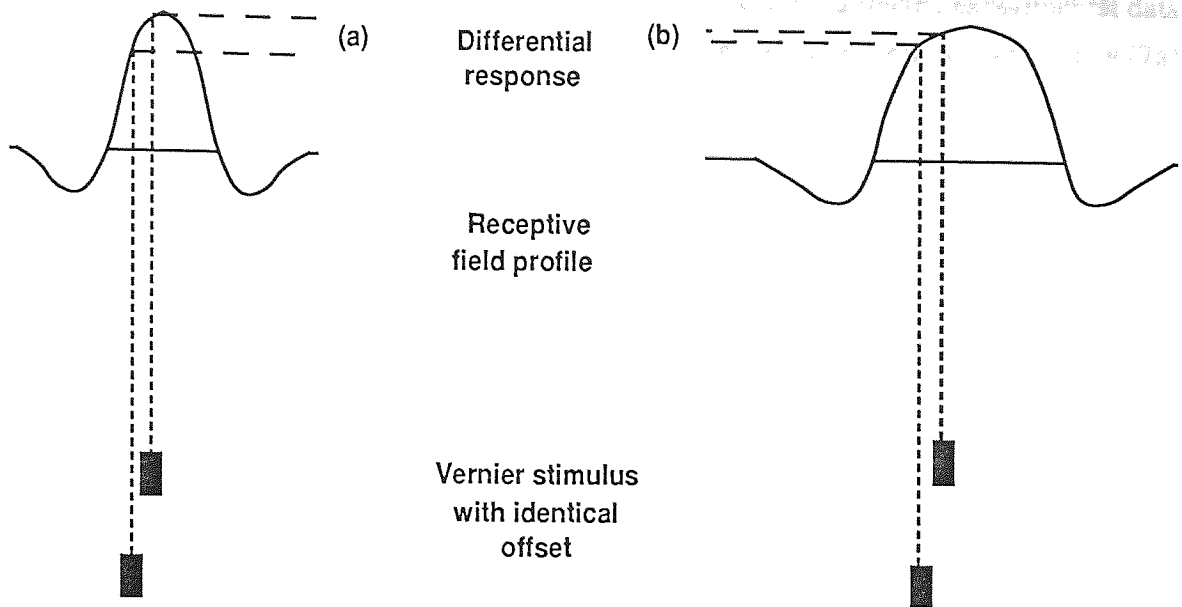


Figure 3.10: The receptive field profile for a high spatial frequency (a) and a lower spatial frequency (b) filter. Note that the differential response to the same offset, at the same relative location within the field, is greater for the high spatial frequency filter compared with the lower frequency.

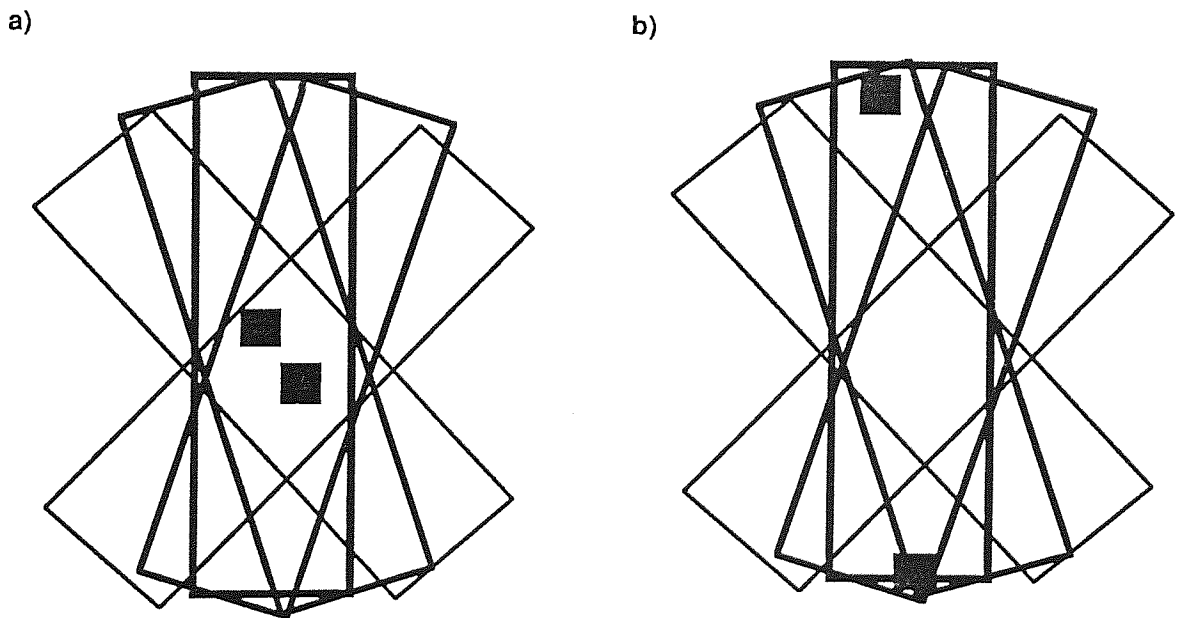


Figure 3.11: The two dots at a small separation (a) all lie within the excitatory center of the field regardless of the orientation of the field. The differential output of the fields will, therefore, vary over a relatively small range. In (b) the two dots are widely separated so that they lie almost at the extremes of the receptive field. In this case the dots will fall within the inhibitory flank of fields at certain orientations and cause a very much larger variation in the outputs.

The model has been used to compute thresholds for many hyperacuity tasks under a variety of conditions. These have then been compared to many sets of published experimental data under the same conditions. The results from Westheimer and McKee's (1977a) experiments on vernier acuity, both as a function of line length and separation, and also their chevron acuity data were compared against the model. There was a broad agreement although the levelling off predicted by the model occurred for line lengths over 8 minutes of arc rather than the 4 minutes of arc found by experiment. For chevron acuity the expected thresholds were generally too large, although the model correctly predicts the increase in threshold with increasing angle. The separation results, however, were a particularly good fit to the experimental data and can be easily explained using the model. For close separations all six filters are available to allow a judgment to be made. However, for very short lines and very close separations even the smallest filter will not be optimally stimulated (*Figure 3.11*). In these cases thresholds will be relatively poor but would be predicted to improve with increasing line length or separation. Around 4 minutes of arc separation the thresholds would be expected to reach a minimum as at this point the smallest filter is optimally stimulated. With further increases in separation the smallest filter, which gives the most accurate response, ceases to contribute towards threshold as none of the stimulus falls within its receptive field. Thresholds would therefore be expected to worsen as less accurate filters have to be used and this would continue as more filters fall out of use (*Figure 3.12*).

The model was also tested against periodic vernier acuity, the ability to differentiate between a straight line and a sinusoidally modulated one. The results of Tyler (1973) showed a very good fit with both the shape of the function and the minimum threshold value at 3 cycles per degree being correctly predicted.

Vernier acuity using cosine gratings was also used as a comparison. This time the data of Morgan (1984) and Bradley and Freeman (1985) was used. Once again good correlation was found, although for Bradley and Freeman's data the result was qualitative rather than quantitative. For the data from Bradley and Freeman the model also correctly predicted the effect of altering contrast on vernier acuity. In chapter 8 the results of the experiments investigating vernier acuity as a function of spatial frequency and grating separation also closely match the Wilson model.

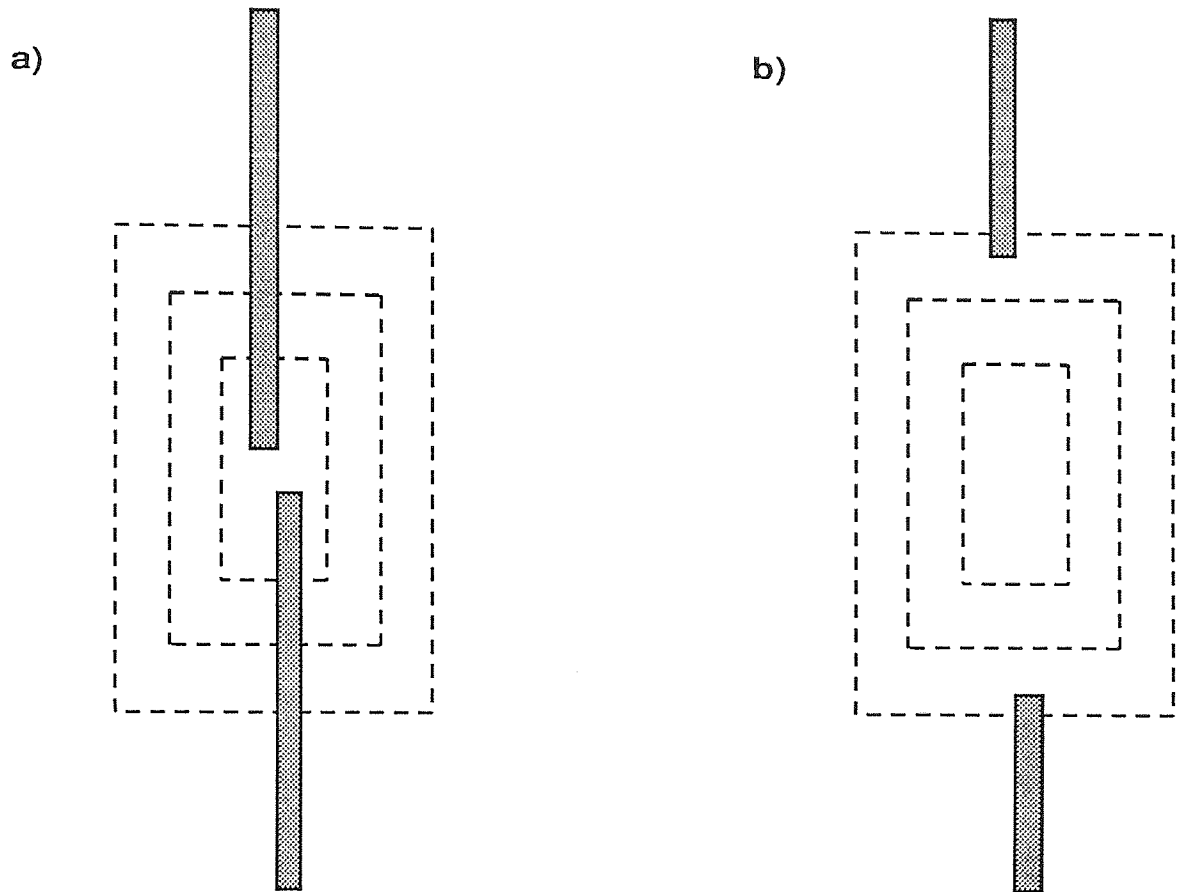


Figure 3.12: The left hand diagram (a) shows the filters used in determining the offset of abutting vernier line stimuli, the right hand diagram (b) the effect of separating the two lines. The smallest, most finely tuned filter can be used for abutting lines which results in the lowest threshold values (around 6 seconds of arc). As the lines are separated the smallest filter no longer encompasses both parts of the stimulus and cannot, therefore, contribute towards an estimate of the offset. The larger, less finely tuned filters are less sensitive to displacements of the stimulus and give correspondingly higher thresholds. It should be clear that the model is limited to stimuli which fall wholly within at least the largest filter (≈ 75 minutes of arc), thus placing an upper ceiling on the separation within which the filter models would be expected to determine thresholds

The model was also compared with two other sets of experimental data. The first was that of Klein and Levi (1985) using bisection acuity. Here there seems to be a good correlation, with the model correctly predicting the notch in the data at about 2 minutes of arc separation and the very low threshold value of around 1 second of arc (*Figure 2.10*). However, other notches predicted by the model are not seen in the data. These notches are a direct result of the use of six discrete filters and occur as the separation exceeds the size of a filter. Stimulus detection then falls within the next largest filter which means that thresholds initially worsen and then improve steadily as the stimulus becomes more optimal for the larger filter. Two points have to be made with regard to this data; first the low thresholds, at around 1 minute of arc separation, are probably due to luminance clues and should be considered as detection thresholds rather than localisation thresholds. Second, the choice of only six filters is subject to some disagreement. In the monkey, DeValois *et al.* (1982) showed a continuum of spatial frequency and orientation tuning, albeit in the overall range between approximately 0.5 cycles per degree and 16 cycles per degree. If this continuum is applied to the model, instead of discrete filters, then the absence of notches in the actual data can be explained. Wilson concedes that such a continuum could be applied to the model but argues that the six filters used by the model are sufficient. Therefore, extra filters will merely supply redundant information.

A continuum would also provide a better fit to the data of Levi, Klein and Aitsebaomo (1985) who confirmed previous work by Westheimer and Hauske (1975) on the effect of flanking lines on vernier thresholds (see chapter 2). They found a two to threefold increase in thresholds when the flanking lines fell about 3 minutes of arc from the main stimulus. The position of this peak is correctly predicted although the worsening in thresholds is slightly less than that found. The choice of discrete filters again introduces notches into the model result which do not appear in the experimental data.

On the other hand, Hirsch and Hylton (1982), in an experiment comparing spatial frequency discrimination as a function of spatial frequency, found steps in their data which could be explained on the basis of discrete filter sizes. Furthermore, Watt and Morgan (1983b) found a similar stepped pattern in their spatial interval detection task.

Finally, it has to be said that the model correctly predicts the results of an impressive array of experimental data albeit with some reservations.

3.3.5: Morgan and Regan (1987)

A modification of the basic Wilson model was put forward by Morgan and Regan (1987). Their model used receptive fields which were spatially separate on the retina but linked by coincidence detectors at higher cortical levels. These respond much more vigorously if both fields are optimally stimulated than if both receive non-optimal stimulation or there is unequal stimulation. In the example given in *Figure 3.13a*, for two straight vertical lines with no horizontal offset, the coincidence detector receiving input from the fields BB' will respond much more than those receiving input from AA' and CC'. In *Figure 3.13b* a vernier offset has been introduced with the upper line moved to the left. In such a situation the coincidence detector receiving input from the fields BB' will respond with slightly less vigour as the two lines no longer provide optimal stimulation of the two fields. The coincidence detector linked to fields AA', which would be silent in the example given in *Figure 3.13a*, will now respond albeit rather weakly. The coincidence detector linked to the fields CC' will remain silent as no part of the stimulus elements fall within these fields. The opponent element of the system then detects that the field pairs AA' and CC' have a differential response relative to each other and will as a result signal that the two lines must be offset relative to each other.

Evidence for this model comes from work done by Morgan *et al.* (1990) who used interfering features placed between two vernier stimuli. They found that the spurious features had no effect on threshold unless they were placed close to one or other of the main vernier stimulus components and would, therefore, fall within the receptive fields detecting the stimulus feature. While these results can be explained using the coincidence detector model they are harder to explain using the Wilson model since any feature located between the main stimulus features would be expected to disrupt the signal. On the other hand, the coincidence detectors would require an impressive organisational structure in the cortex as each detector would have to know its position with regard to all the others to a high degree of accuracy.

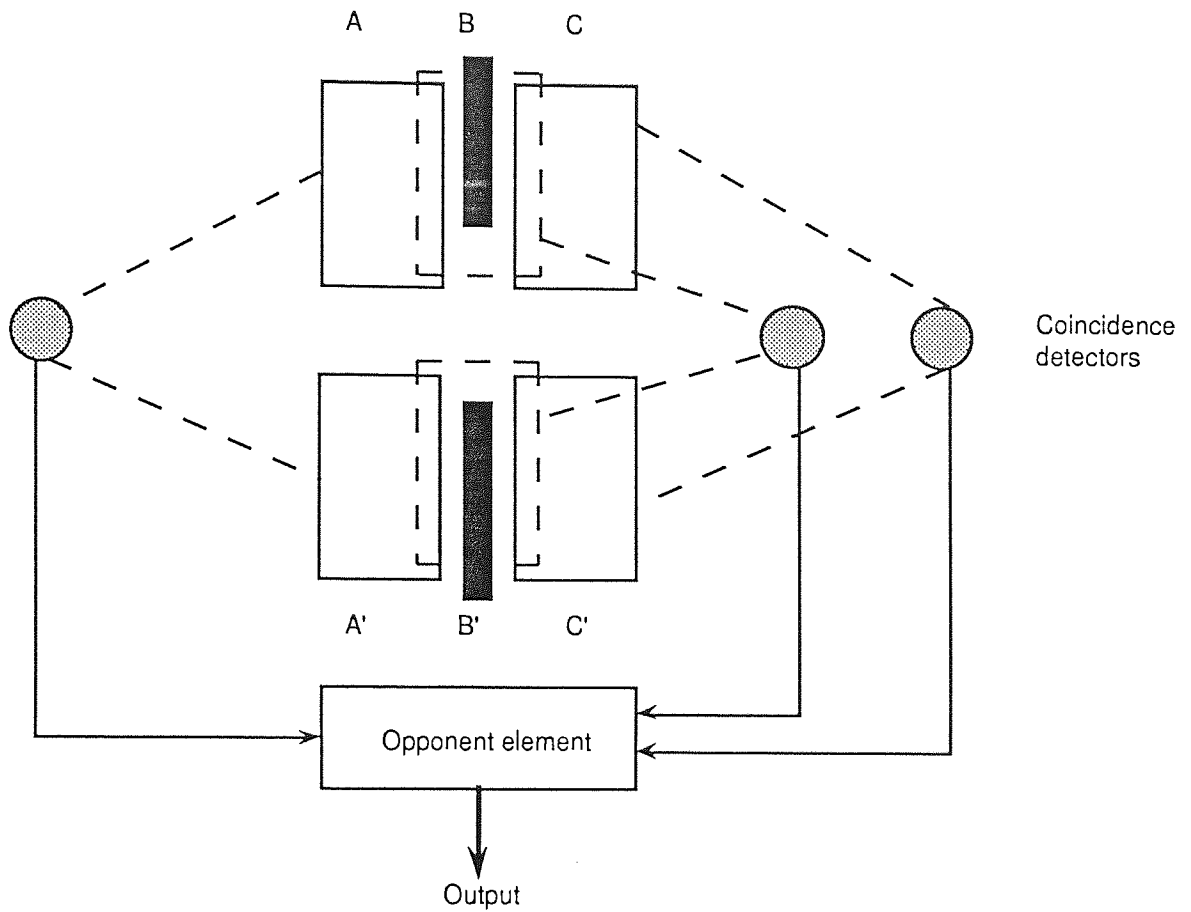


Figure 3.13a : The coincidence detector model of Morgan and Regan (1987). The three receptive field pairs A-A', B-B' and C-C' are linked by coincidence detectors such that equal stimulation of both fields is needed to give an optimum output. In this example the coincidence detector linked to fields B-B' responds maximally while the other two, linked to fields A-A' and C-C', are silent.

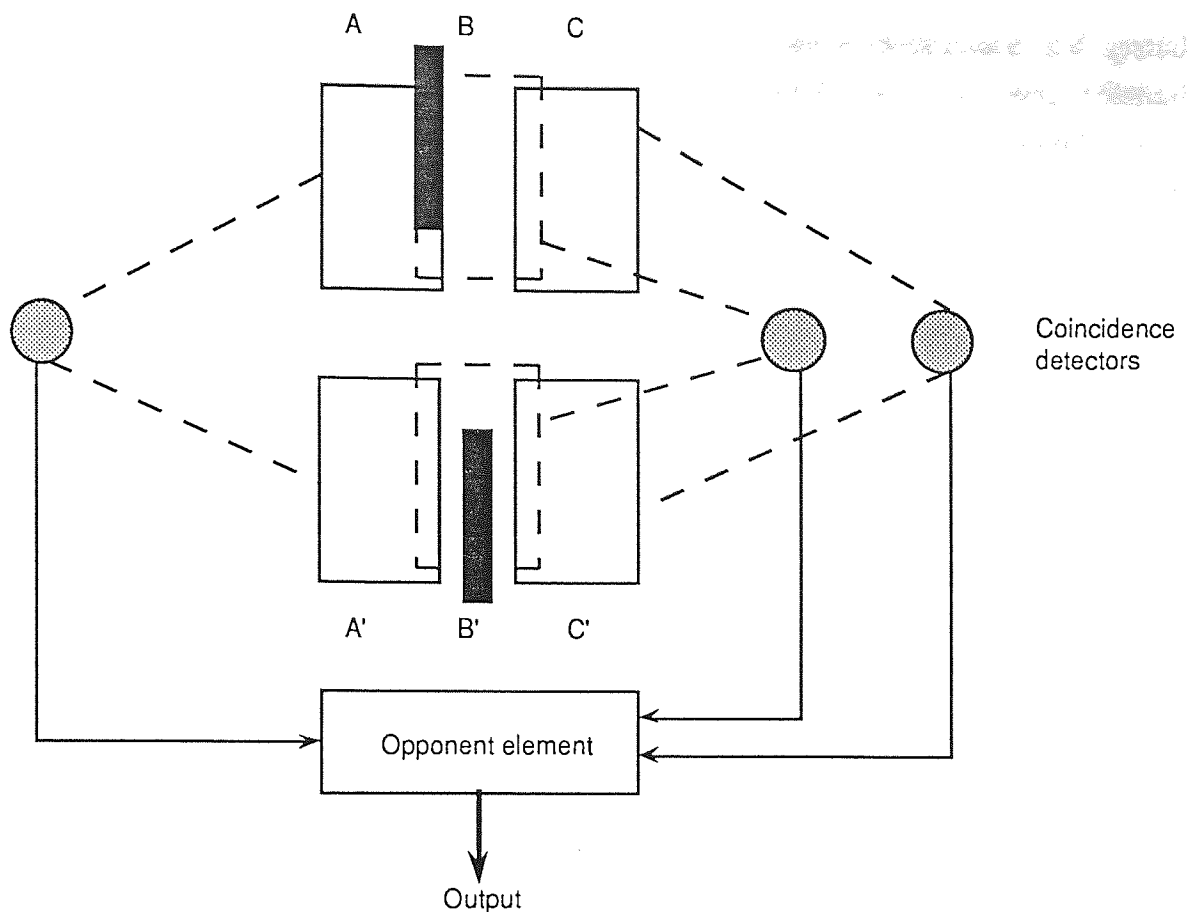


Figure 3.13b: The same model but this time with the two bars offset relative to each other. On this occasion the coincidence detector linked to field pair B-B' responds less strongly than before as the stimulus elements no longer provide optimal stimulation. The coincidence detector linked to the fields A-A' now respond weakly while the coincidence detector linked to fields C-C' remains silent. This change in the relative outputs of the three coincidence detectors is processed by the opponent element to signal that a horizontal offset is present.

3.3.6: Paradiso (1988)

The model put forward by Paradiso (1988) is based on the neural structure of the mammalian visual cortex, in particular the visual orientation hypercolumns (Hubel and Wiesel, 1974). It has long been known that many cortical neurons are orientation selective (Hubel and Wiesel, 1962). Their distribution was found to be highly organised with columns of cells arranged perpendicular to the surface of the visual cortex each of which covered about 1 mm^2 of the surface. Within each column, cells were found which were tuned to all possible orientations. As was mentioned earlier, DeValois *et al.* (1982) supported this and further developed the idea of a "Cortical Integration Area" - a set of three

columns within which were represented orientation, ocular dominance and spatial frequency. Paradiso (1988) attempted to model an orientation hypercolumn using statistical estimation theory and to compare his result with actual anatomical data. As with Geisler's (1984) ideal observer, similarity between the two would be an indication that the model might reflect the actual mechanism involved. Several properties of cortical neurons were considered including orientation selectivity, response amplitude, internal and external noise and the number of cells. The results showed that even a quite small number of cells, approximately 2000, is sufficient to discriminate orientation differences comparable to the performance of human observers. The advantage of this form of cortical organisation is that all the cells within the hypercolumn can be used to good effect, even unresponsive cells providing some information. It is this pooling of responses which is the central feature of many of the channel models; the individual cells can be quite coarse in their responses but as a group are able to signal changes in the stimulus to a high degree of accuracy.

3.3.7: Channel models, the final answer?

One of the critics of the channel models as proposed by Wilson (1986), at least as the sole determinant of threshold performance, is Burbeck (1987, also Burbeck and Yap, 1990a, 1990b). She argues that large scale localisation cannot possibly be performed by single filters on the basis that there are none large enough. Her experiments suggest that location of widely separated features, which she argues also applies to more short range separations, is carried out by individual filters, as per the Wilson model. The difference occurs in that these filters merely attribute location to the particular feature. Relative localisation, over whatever range, is carried out by secondary processing using the output from these small filters. In this respect it bears some resemblance to the Morgan and Regan (1987) model. However, Paradiso *et al.* (1989) disputed whether hyperacuity was determined by the comparison of responses from cells in the striate cortex; they concluded that some token was assigned at the early detector level (retinal ganglion cells) and passed to higher neural centers where comparisons would be made. The nature of this token was not considered but could clearly be some form of local-sign.

There is also some dispute as to whether or not location is made explicit in the channel models. It is possible that an explicit representation of the visual image may be produced in the visual cortex using the closely packed cells in striate cortex area IVc (Crick, Marr and Poggio, 1980; Barlow, 1981). They show the correct inter-cell separation required (about 5

to 6 seconds of arc) and are not in themselves inconsistent with this model. Wilson (1986) argues against this and cites the results of Klein and Levi (1985) as evidence for threshold values as low as 0.8 seconds of arc. Cells packed together such that inter-cell separations are less than 1 second of arc have not been found and such a threshold could not, therefore, be explicitly represented in the cortex. However, these thresholds are probably not representative of hyperacuity judgments and need not be contradictory. On the other hand, one strong argument against this explicit representation is the finding by Parker and Hawken (1985) that there are very few cells in cortical area IVc which are sufficiently sensitive to produce thresholds in the hyperacuity range. While the idea of explicit representation cannot be ruled out it is not an absolute necessity in the performance of tasks to hyperacuity levels of precision. Hyperacuities, as defined in chapter 1, are based on relative locations of stimulus features and as such do not require the absolute locations to be known. In defence of the channel models it has to be said that they are all limited to spatially localised stimuli. Once separation exceeds the largest filter size the models fail to predict experimental data. In these circumstances the tasks are almost certainly performed by another mechanism linking spatially separate areas as suggested by Morgan and Regan (1987) and Burbeck and Yap (1990b).

There is merit in the conclusion reached by Morgan *et al.* (1990) that a combination of local-sign and channel models could well explain the situation. They propose that the local-sign assigns position and size to the relevant features and thus allows the intelligent choice of a suitable filter to perform the task required to be made. Evidence for the two models will be considered in chapter 8, dealing with spatial frequency and separation for a vernier stimulus, and in chapter 9 which more closely investigates the "centroid" as a possible local-sign.

3.4: Can single cell responses determine hyperacuity?

It was mentioned in chapter 1 and is an underlying tenet of all the models discussed here that in order to achieve hyperacuity levels of performance some form of neural interpolation or pooling is required. There is, however, some evidence that individual cells may be able to reliably signal changes in stimulus parameters with sufficient fineness to meet the observed human performance levels in certain hyperacuity tasks.

Scobey and Horowitz (1972) showed that cat ganglion cells would respond to the

displacement of a spot of light even when the displacement was much smaller than the receptive field diameter. This was particularly apparent for peripheral movement where displacements of as little as 2 minutes of arc were detected by ganglion cells whose receptive fields were over 3.5 degrees across.

The responses of cortical neurons in the cat to stimuli of differing orientations and spatial frequency was investigated by Bradley *et al.* (1985). They found examples of cells which could reliably signal differences in orientation of 1.84 degrees and differences in spatial frequency of 5%.

Parker and Hawken (1985) recorded the ability of individual cortical cells in the vervet monkey (*C. Aethiops*) to perform a grating resolution task and of cells in the macaque (*M. Fascicularis*) to detect differences in both spatial frequency and phase. They found that individual cells could reliably signal the presence of a 55 cycle per degree grating, discriminate between spatial frequencies differing by as little as 3.7% and localise objects to within 11 seconds of arc.

A comparison of results obtained from human psychophysical experiments (orientation discrimination and spatial frequency discrimination) with the results of direct measurements of single cells within the visual cortex of cats was carried out by Skottun, Bradley, Sclar, Ohzawa and Freeman (1987). These were measured over a range of contrast values between 1 and 80%. Individual cells were found which could signal orientation changes of under 5 degrees and discriminate between spatial frequencies differing by less than 10%. Contrast had little effect on performance except close to contrast threshold (between 2 and 5%). The human observers produced threshold values for orientation discrimination around 0.5 to 1 degree and for spatial frequency discrimination around 5%; again, these were essentially independent of contrast above the 5% level.

Swindale and Cynader (1989) measured activity in area 17 of the cat's visual cortex. They used a bar stimulus with a vernier offset and recorded cell response to bars of different lengths and velocities. They suggested that their results indicated that vernier acuity could be mediated by responses from single orientationally tuned cells.

In all the cases listed here the point has to be made that while the individual neurons may be able to reliably signal the changes in orientation and spatial frequency considerable care is

needed before translating this into actual occurrence. The cells under consideration are those which give the "best" response and as such do not reflect the general response characteristics of individual cells. The animals in the studies were all deeply anaesthetised which has the effect of considerably reducing the resting level of the cells. In addition, cat / monkey neurophysiology results and human psychophysical results may not be directly comparable owing to species differences. Finally, it is most unlikely that a single cell can differentiate between the causes of a response. Cells respond to many stimulus parameters (contrast, spatial frequency, orientation, color, luminance etc...) and it may not be possible to isolate the parameter under consideration from all the other features leading to a response. It would still be necessary, therefore, to compare several neurons in order to isolate the required response even though the individual neuron may have the ability to discriminate differences to the required precision.

3.5: Parallel pathways and their relationship to hyperacuity

Even though single cells may be able to signal parameter changes to the necessary accuracy to allow hyperacuity performance levels it is more likely that some cortical processing is needed to extract the signal from the larger mass of interfering noise. This clearly necessitates the transfer of information through the visual system. Present thinking considers that there are two, essentially parallel, pathways by which information is transferred from the retina to the cortex and beyond. The idea of parallel visual pathways took form following the discovery of X and Y cells in the retinae of cats (Enroth-Cugell and Robson, 1966). They showed a differential response from the two cell types, X cells giving a sustained response to a stimulus, Y cells giving a short transient response. This was reinforced when the dichotomy was also shown at the LGN (Cleland, Dubin and Levick, 1971; Derrington and Fuchs, 1979) and the visual cortex (Ikeda and Wright, 1974, 1975).

In primates a similar neurological dichotomy has now been further developed into the Parvocellular pathway, which detects form and pattern and is also color sensitive (Zeki, 1978, Livingstone and Hubel, 1987), and the Magnocellular pathway which detects motion together with luminance and contrast variation (Zeki, 1974; 1978; Kaplan and Shapley, 1982). The two pathways are subserved by two classes of retinal ganglion cells, the *P(alpha)* for the magnocellular and the *P(beta)* for the parvocellular (Leventhal, Rodieck and Dreher, 1981). They continue through the LGN where the pathways go to the two

magnocellular and four parvocellular layers from which they get their names. Finally they project to different regions of the primary visual cortex (Hubel and Wiesel, 1972; Zeki, 1969) (*Figure 3.14*).

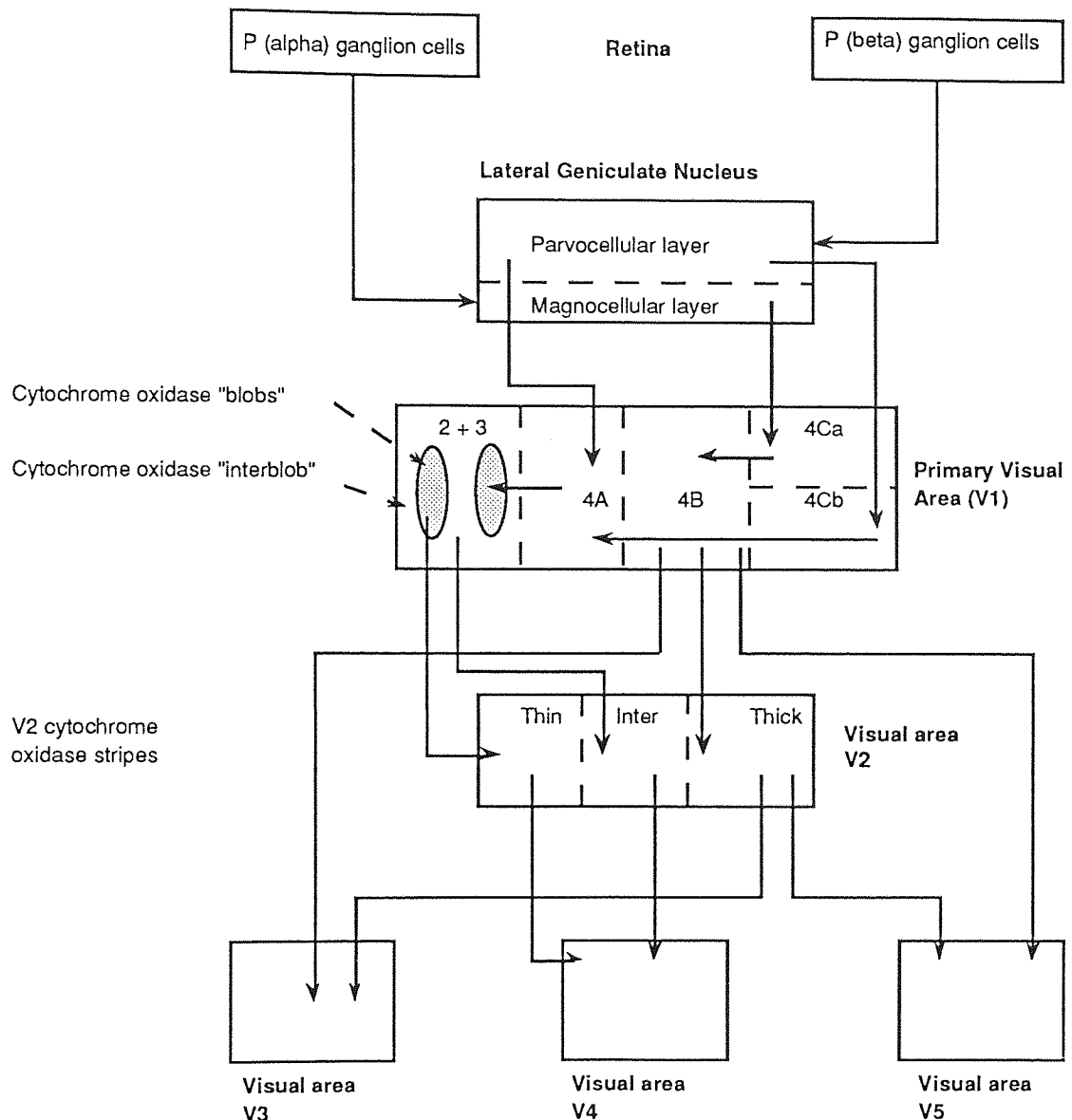


Figure 3.14: A simplified diagram of the known connections of the Magnocellular and Parvocellular pathways. Cortical area V1 is shown divided into layers 2, 3 and 4. Layers 2 and 3 are characterised by the cytochrome oxidase blobs, which stain darkly, and the interblobs, more lightly stained. Cortical area V2 also stains with cytochrome oxidase into thin and thick stripes separated by lightly stained interstripes. The Magnocellular pathway appears primarily concerned with orientation selectivity and direction selectivity. The Parvocellular pathway, which can be subdivided into the blob and interblob streams, has strong wavelength selectivity (via the blob stream) and also appears to deal with form (via the interblob stream) (Lehmkuhle, Kratz and Sherman, 1982). DeYoe and Van Essen (1988) and Zeki and Shipp (1988) both review the two pathways and the evidence for their underlying functional significance. The diagram is a simplified version of that given in figure 1 of the Zeki and Shipp review. These and other features of the two pathways are discussed in the text.

There are several major differences between the two pathways which are relevant to the information requirements of hyperacuity performance.

a). **Conduction velocity:** the difference in axonal diameter and myelination of the fibers in the pathways mean that the magnocellular pathway has a faster conduction velocity than the parvocellular (Marrocco, 1976; Kaplan and Shapley, 1982). In addition the magnocellular cells have a shorter latency than the parvocellular (Marrocco, 1976). The result is that information via the magnocellular pathway arrives at the cortex before that via the parvocellular.

b). **Contrast sensitivity:** The magnocellular pathway is most sensitive at low spatial frequencies and medium temporal frequencies. Conversely, the parvocellular pathway gives a maximal response for high spatial and low temporal frequency stimuli. Magnocellular cells have been shown to have much greater contrast sensitivity than parvocellular, at least for low and medium spatial frequencies. They respond to contrast levels below 1% but their responses tend to saturate at levels around 15 to 20% (further increases in contrast producing no increase in response). Parvocellular cells have very low response rates for contrast levels below about 10% and show little evidence of saturation with increasing contrast level (Kaplan and Shapley, 1982; Derrington and Lennie, 1984; Merigan and Eskin, 1986; Sclar, Maunsell and Lennie, 1990). Tootell, Silverman and Hamilton (1988), using 2-deoxyglucose uptake measurements in monkeys, found that high spatial frequency stimuli caused most uptake in the parvocellular areas of the cortex while the converse was true for low spatial frequency targets. One result of this difference is that high contrast, high spatial frequency stimuli should be preferentially processed via the parvocellular pathway. Studies using low contrast and low spatial frequency targets should, on the other hand, preferentially stimulate the magnocellular pathway. Contrast sensitivity may, however, be largely mediated via the parvocellular pathway. Merigan and Eskin (1986) found, after selective degeneration of the parvocellular pathway, that in monkeys (*M. Nemestrina*) the contrast sensitivity declined substantially. This would appear to indicate that the high level of contrast sensitivity usually attained could be explained by use of summation between individually insensitive parvocellular neurones.

c). **Other parameters:** The two pathways have also been found to respond differently to other parameters. The receptive fields of parvocellular ganglion cells are smaller than those

of magnocellular cells at corresponding retinal eccentricities. In the peripheral retina, however, both types have larger receptive fields compared with the fovea (Leventhal *et al.* 1981). The parvocellular pathway has high spectral sensitivity while the magnocellular does not respond at all to color (Derrington, Krauskopf and Lennie, 1984; DeYoe and Van Essen, 1988). Finally, the magnocellular pathway has been strongly linked with the detection of movement due to its strong projection to area MT in the cortex (Zeki, 1974). Work on monkeys has shown that selective degeneration of area MT causes defects in the ability to detect and compensate for moving stimuli (Newsome, Wurtz and Dursteler Mikami, 1985). This has been reinforced by the finding that patients with lesions in area MT show transient defects in movement perception (Andersen, 1989).

The different response characteristics of the two pathways have led to the suggestion that both contribute toward the visual image, the faster magnocellular pathway giving a coarse global picture which has local detail added by the slower parvocellular pathway (Breitmeyer and Ganz, 1976; Wong and Weisstein, 1983; Bassi and Lehmkuhle, 1990). Watt (1987) has made a similar suggestion, that low frequency filters are used initially to obtain information on the geometry of the stimulus with the high frequency filters coming into play later to convey more detailed information on to higher neural areas for further processing.

The classical stimulus used in hyperacuity tasks is usually highly localised in space and contains broad spatial frequency information. Such a stimulus would be expected to stimulate both pathways. A reduction in threshold values after removal of the high spatial frequency content of the stimulus, for example by blurring, would be indicative of a shift to mediation primarily by the magnocellular pathway. Certain hyperacuties, however, show resistance to blur which suggests that hyperacuity levels of performance may not be specific to one or other pathway. Indeed it is quite likely that each pathway has a range over which it is the chief determinant of threshold but that there is also a large common range over which both pathways may contribute.

Chapter 4: Psychophysics

4.1: Introduction

The concepts upon which modern psychophysical methods are based were conceived by Fechner (1860). It was he who first brought together the idea of the sensory threshold and the use of experimental methods which could be used to determine what this threshold was. His work has been described as marking the beginning of the science of experimental psychology (Green and Swets, 1966).

4.2: The sensory threshold

In its original form the sensory threshold was thought to be the smallest signal to which an organism would respond. Lower signal strengths were believed to have no effect on the organism while larger strengths produced no increase in the response. In effect the organism reacted with an all or nothing response (*Figure 4.01a*). Experiments showed, however, that this was not the case. If responses to a particular signal are measured for differing signal strengths there is not a clear cut-off below which no response is elicited and above which all stimuli produce a full response. Rather, the level of response falls along a curve described by a sigmoidal function (*Figure 4.01b*). This is known as the psychometric function. The threshold value is usually taken to be the 50% point on the curve where the slope is steepest which yields the maximum information about the positioning of the curve (Pentland, 1980).

4.3: Classical psychophysical methods

4.3.1: The method of adjustment

The method of adjustment involves the observer altering the value of a continuously variable stimulus until it is just visible or just noted as different from a standard stimulus. This adjustment can be either from below threshold, measuring the point at which it is just seen, or from above threshold measuring the point at which it just disappears. It is usual to take several measurements and calculate a mean value and standard deviation. If both ascending and descending measurements are taken the effects of observer response delay and anticipation can be reduced at the cost of a larger standard deviation. The method is subject to

criterion differences between observers which can strongly influence the result but it does have the considerable advantage of being quick to use. The various problems of criterion dependent methods will be considered later.

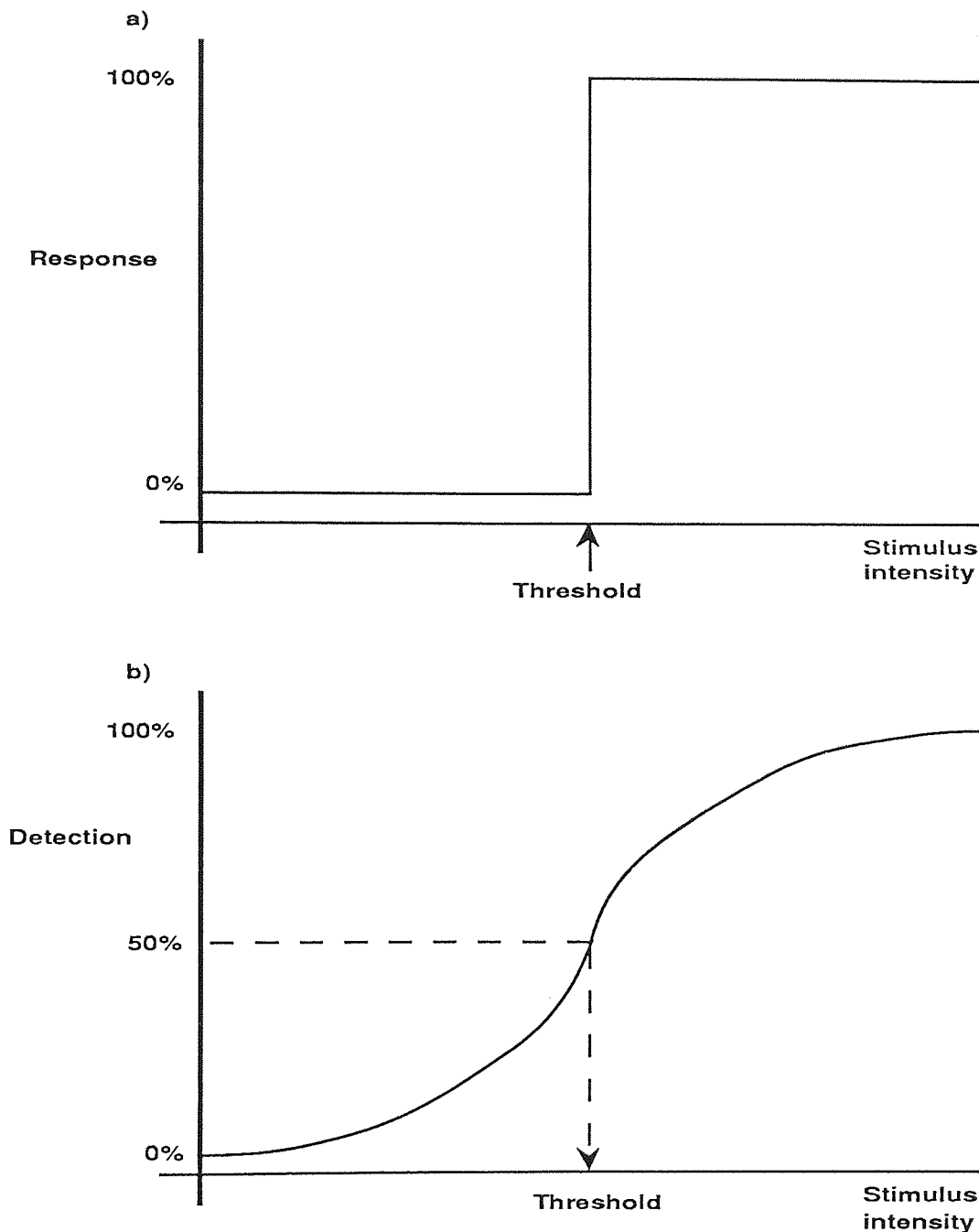


Figure 4.01: The response of an organism to a stimulus. Figure 4.01a shows a typical all-or-nothing response which commonly occurs in electronics, for example, and was at one time also thought to occur in physiology. Figure 4.01b shows the typical psychometric function of a human observer. The detection threshold for a stimulus is usually taken to be the 50% response point in such experiments.

4.3.2: The method of limits

The method of limits involves presenting stimuli at discrete values to either side of threshold such that the observer will respond "yes" to those stimuli seen, or noted as different from the standard, and "no" to those not seen. Again, the values are often presented either increasing from below threshold or descending from above threshold. A problem with the method is that if the sequence is known the observer will be able to predict whether the next presentation is to be greater or smaller than the last. This observer anticipation can have a strong influence on the threshold value obtained. The use of a technique, where ascending and descending presentations are randomly interleaved, can avoid this problem.

4.3.3: The method of constant stimuli

This method is an attempt to plot discrete data points on the psychometric function and then interpolate the curve of the function between them. Usually an equal number of presentations at a certain number of stimulus values are given to the observer and the percentage correct at each point plotted against the stimulus value. These points are then fitted with an interpolated curve from which the value of the threshold can be estimated. The 50% correct response value can then be read off the curve. The major disadvantage of the method of constant stimuli is that if the whole psychometric function is estimated the number of trials required is very large if a reasonably accurate curve is to be plotted. In addition, a large number of the points are going to lie well away from the 50% level leading to a very inefficient use of the observer's time and effort. Clearly, a more efficient method would be to plot only that part of the psychometric function lying around the estimated threshold value. If this version is employed it is obviously necessary to first obtain an estimate of threshold prior to performing the experiment.

4.3.4: Criterion dependency

One of the chief problems associated with psychophysical methods is criterion dependency - that is, the result is dependent to a greater or lesser extent on the observer's psychological attitude which in turn is usually unpredictable and not easily measured. These psychological factors include the observers keenness to do well, their knowledge of the experiment and its aims, the state of alertness and adaptation to the experimental environment and the

instructions given and their interpretation by the observer. As an example, a very keen observer who wishes to do well will give a positive response when he or she is not really sure whether or not they can actually see the stimulus. On the other hand, a cautious observer will not give a positive response until he or she is absolutely sure that the stimulus is visible. *Figure 4.02* graphically illustrates the difference that this criterion dependency may make to threshold values obtained even when the true thresholds of both observers are identical.

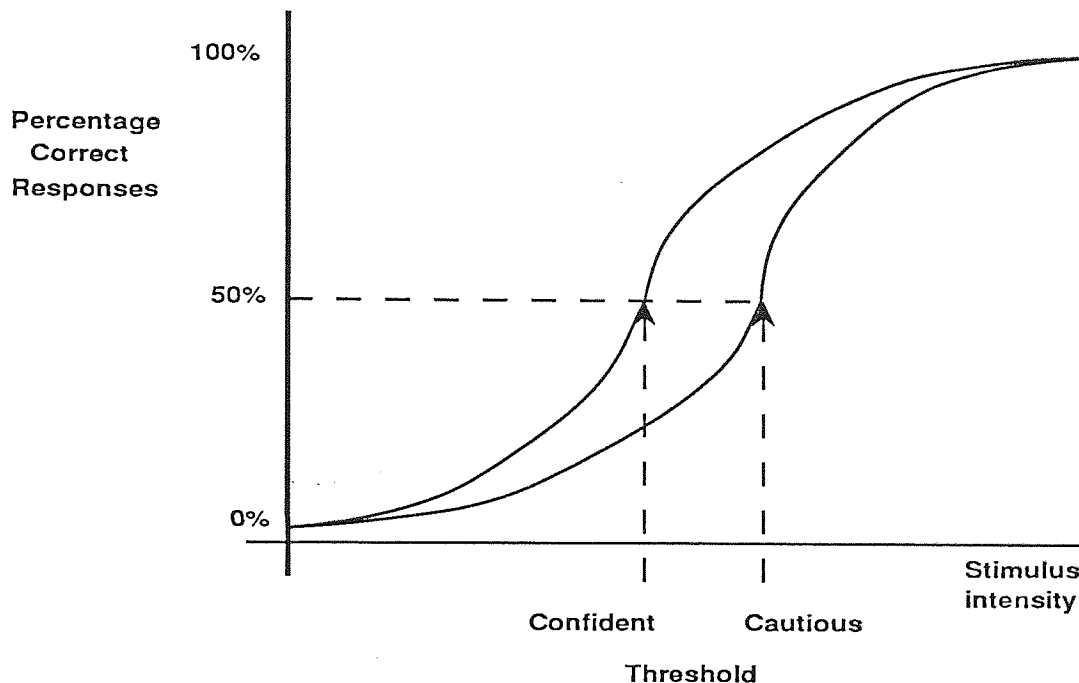


Figure 4.02: The effect on estimated threshold of variation in response criterion between observers. The confident observer appears to have a lower threshold value than the cautious even when both have identical true thresholds. The confident observer's function may be better visualised as not falling to 0%, but instead giving positive responses when the stimulus intensity is zero.

4.4: Forced choice measurements

The technique employed throughout this thesis, in an attempt to overcome criterion dependency, is to force the observer to make a decision, either up/down, left/right etc., which is independent of their actual threshold. In effect, when the stimulus value lies below the observer's threshold they will have to use what information is available to guess. As an example, in the classic vernier task the upper line may be offset to the right or left of the lower. When using a forced choice procedure the observer must respond "left" or "right". In

particular, they are not allowed to respond "don't know" or "straight above" etc.. Clearly, this limit to the possible responses alters the range of values over which the psychometric function is allowed to run. If pure guesswork were invoked then the number of correct responses would be 50% in a two alternative forced choice procedure. The psychometric function would therefore have ordinal values from 50 to 100% and the value which represents threshold is then often taken to be around the 75% correct point (*Figure 4.03*).

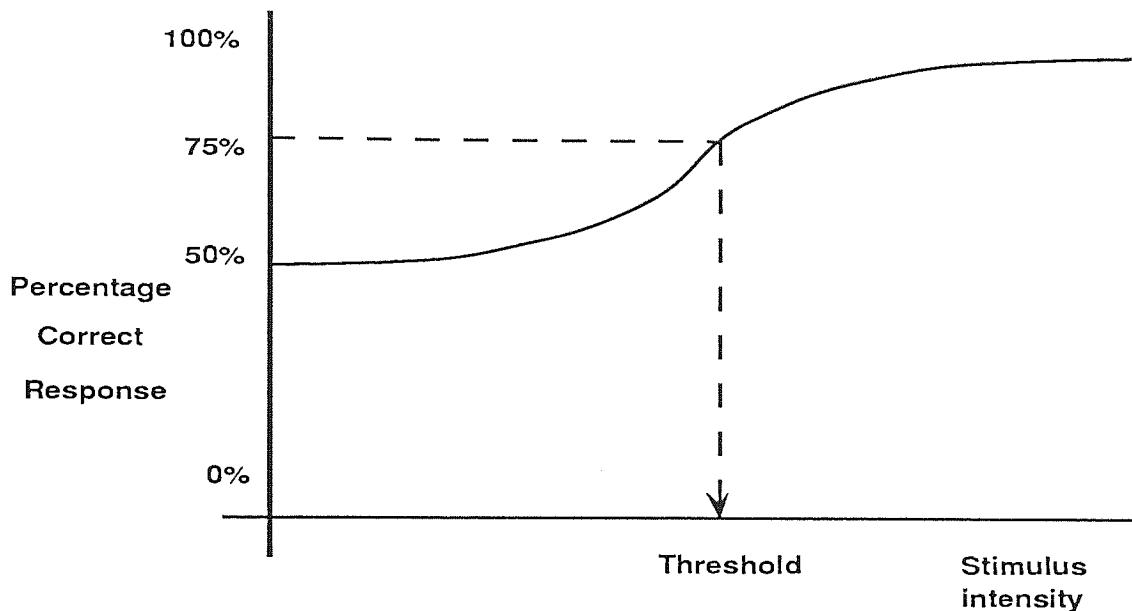


Figure 4.03: The psychometric function obtained using a two alternate forced choice technique. In this case the observer can obtain a 50% correct response simply by guessing so this is taken as the lowest ordinate value. Threshold is commonly taken to be around the 75% correct response level.

4.5: The staircase routine

Dixon and Mood (1948) suggested an up and down, or staircase, method for estimating the 50% point on the psychometric function. Essentially, the magnitude of the stimulus was altered in discrete steps, either up or down, depending on the observer's responses. *Figure 4.04* shows an example, the crosses representing incorrect responses following which the magnitude of the stimulus is increased. The open squares represent correct responses following which the magnitude of the stimulus is reduced. Threshold is determined in two stages. First the magnitude of the stimulus at the points of reversal (where the observer gives a correct response following one or more incorrect responses or vice-versa) is noted. An estimate of the final threshold can then be obtained by simply adding all these values together

and taking a mean. However, it is more usual to pair the reversals, one correct and one incorrect. The average value of this pair is then taken as an estimate of the threshold value. Logically, the threshold should lie between a correct and incorrect response. Clearly one reversal pair is only going to give a very approximate value, a problem which is overcome by taking several reversal pairs. The mean of all the individual threshold estimates thus obtained is then taken to be the final threshold.

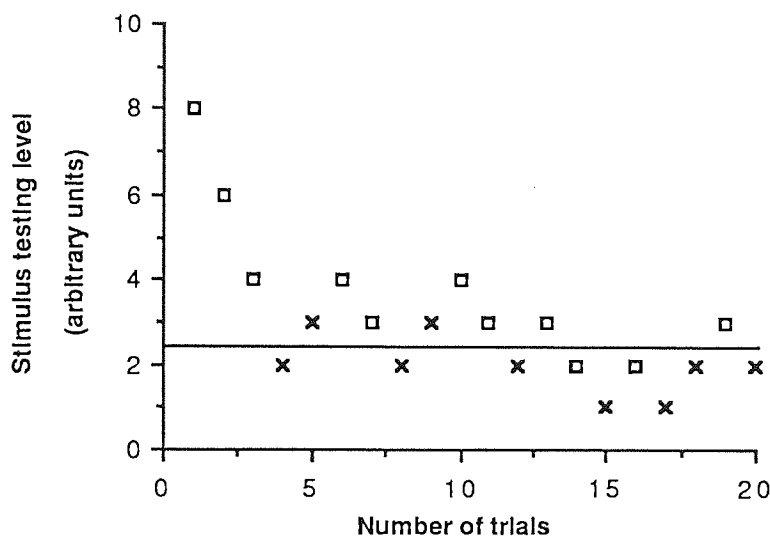


Figure 4.04: Example of a staircase routine. The open squares indicate a correct response the crosses incorrect responses. The horizontal line shows the estimate of threshold obtained. Note that throughout this chapter the stimulus intensity is in arbitrary units. As an example, in a vernier task the upper target may be left or right of the lower. In this thesis it was usual to consider values to the left negative and those to the right positive.

There are several factors which have to be considered if the staircase is to give a result which is not unduly biased by the choice of parameters. Cornsweet (1962) considers the following four:

- 1. Where to start:** It is usual to start close to threshold, usually above threshold in order to give some initial encouragement to the observer. The value of threshold has then either to be estimated from preliminary measurements or has already to be approximately known.
- 2. The step size:** The step size is the change in stimulus values when the method requires a move from one testing level to another. Its value is of critical importance; too large a step

size merely results in alternate correct / incorrect responses (*Figure 4.05*) with the threshold value lying somewhere in between but with a value whose magnitude can only be coarsely guessed at. Too small a step size can be equally troublesome, it usually results in long sequences of correct or incorrect responses between reversals with a consequent loss of efficiency as many trials will be needed to obtain a sufficient number of reversals.

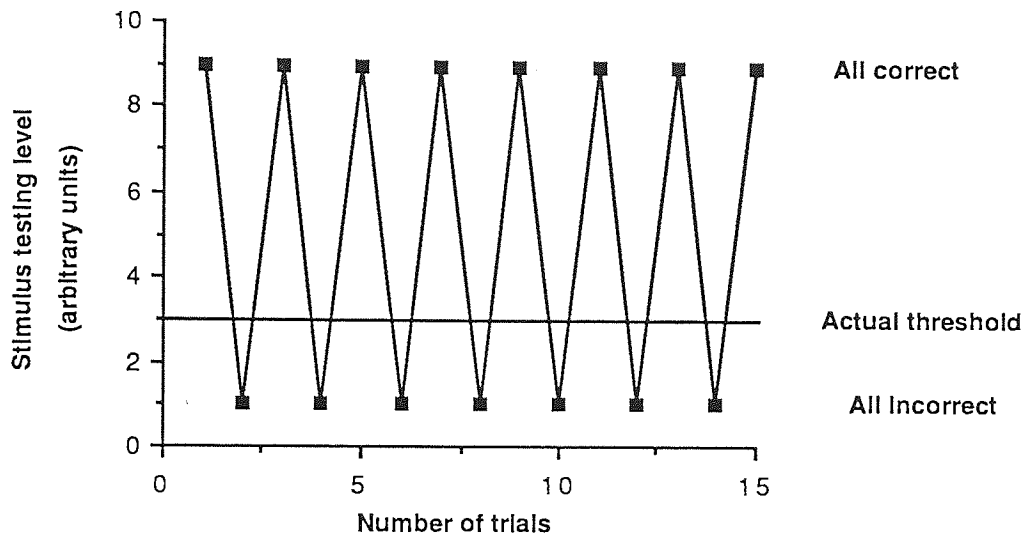


Figure 4.05: Too large a step size results in a succession of alternating correct / incorrect responses. The threshold value clearly lies somewhere in between but its magnitude can only be guessed at.

3. Modification of the step size: If, as is usual, the initial starting point is chosen not from a predetermined estimate of the threshold value but at a magnitude which is known to be some way above or below threshold then it is useful to have a larger step size in order to more rapidly approach threshold in these early stages. Once the presentations are occurring at magnitudes close to threshold then the step size needs to be reduced in order to gain a more accurate estimate of the final threshold value.

4. The end point: As has been intimated above this is usually taken to occur after a number of reversals although it is possible, as an alternative, to end after a fixed number of trials. Ideally the number of reversals should be sufficient to allow their averaged values to be asymptotic, or nearly so. However, one has to weigh this ideal against the number of trials required to obtain it (Pentland, 1980). There is also the problem that the early reversals are biased to some extent by the choice of starting point and it is useful to attempt to eliminate

this by ignoring the first few reversals.

In addition to the four points mentioned above, the use of the staircase with a simple yes / no type of response is open to distortion by certain psychological factors. The most obvious is that given a single staircase the final threshold value can be manipulated by the observer given a knowledge of the way the staircase is going. Indeed, any reasonably observant individual would have little difficulty in predicting the value of the next stimulus presentation after only a few trials. This clearly reduces the value of the final threshold estimate and would hold equally, although with slightly more difficulty, for a forced choice technique. To overcome this problem, Cornsweet (1962) suggested that two staircases be interleaved, one starting above and the other below threshold. This would make the prediction of the next presentation considerably more difficult. For the stimulus configurations used in this thesis, vernier acuity for example, one staircase starts with the offset of the upper target to the left the other to the right. *Figure 4.06* shows how the two staircases then converge towards the final threshold estimate.

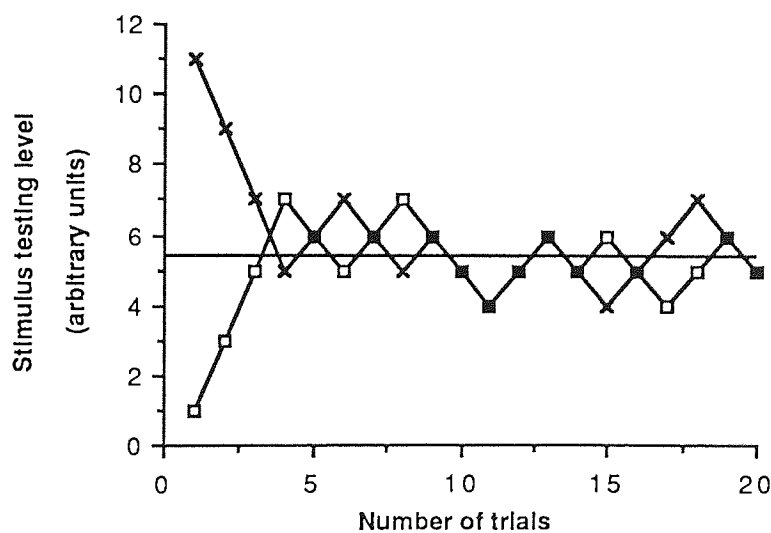


Figure 4.06: An example of two interleaved staircases one starting above threshold and the other below. In practice both staircases rarely produce exactly the same estimate of threshold, and the final threshold is taken to be an average of the two estimates.

4.6: The Up and Down Transformed Rule (UDTR)

As described above, the threshold estimate for a yes/no procedure is made at the 50% point on the psychometric function. For a forced choice technique this is an inappropriate measure since a 50% correct response can be obtained by simple guesswork. Estimation of threshold therefore requires the use of a different point on the psychometric function. Wetherill and Levitt (1965) showed that a simple transformation of the up and down rule would allow suitable points to be estimated. They proposed that instead of a single correct answer causing the testing value to be decreased, two or more consecutive correct responses should be required. Other combinations (one correct response followed by one incorrect or any single incorrect response) are treated as incorrect and cause an increase in the testing value. *Table 4.01* shows how various points on the psychometric function can be obtained by using different response sequences.

Table 4.01

Consecutive correct responses (decrease test value)	Consecutive incorrect responses (Increase test value)	Estimated point on psychometric function
1	1	50.0
2	1	70.7
3	1	79.4
4	1	84.1
5	1	87.0
1	2	29.3
1	3	20.6

From the table it can be seen that the 71% point can be estimated by requiring two consecutive correct responses before ordering a decrease in the testing value. The chance of obtaining such a sequence at the 50% level is $\sqrt{0.5} = 0.707$ or approximately 71% and it is to this point on the psychometric function that the sequence will converge. The advantages claimed for this method are...

a. It is simple to use and allows the experimenter to quickly determine the reliability of the observer's responses.

b. Thresholds can be determined quickly and efficiently and by use of two interleaved staircases using a two alternative forced choice paradigm many of the criterion dependent features can be eliminated.

There are, as always, some disadvantages; the first is that the responses may not be independent. If a sequence occurs, say several left presentations, the observer will begin to expect a rightward presentation and may give incorrect responses in anticipation of this. Similarly, the observer may note some sequential presentation and respond accordingly, although as has been noted the use of interleaved staircases make this unlikely. The point also has to be made that the greater the number of consecutive correct or incorrect responses used the larger the number of trials required. Wetherill and Levitt estimate that the 71% point requires around 3 - 4 trials per reversal whilst the 87% point requires 9 - 10 trials per reversal.

4.7: The Parameter Estimation by Sequential Testing method (PEST)

The Parameter Estimation by Sequential Testing or PEST technique was developed by Taylor and Creelman (1967) to allow determination of independent variables in psychophysical tests. As with the up and down transformed rule the magnitude of the stimulus is varied according to the responses given by the observer. For PEST there are three important decisions to be made during the test.

1. When to change the testing level: Starting at a particular testing level the number of correct responses (R_C) and the total number of trials (Tr) are counted. The value of R_C has to fall within bounds determined by the number of trials, if the value of R_C is higher than a certain percentage of the trials then the decision is made to reduce the testing level and vice-versa. At threshold, one would expect the number of correct responses to be given by...

$$R_C = P_t \times Tr$$

P_t is adjusted according to the point on the psychometric function which is being estimated, thus if the 75% point is being sought then at threshold three in every four responses should be correct and P_t would have the value 0.75. Clearly, away from threshold the value of P_t

varies and the testing level then needs to be adjusted to take account of this. The bounding values (N_b) which determine whether the testing value is too large or too small are given by...

$$N_b = R_c \pm W \text{ (where } W \text{ is a constant called the deviation limit of the sequential test)}$$

In effect if $R_c > N_{b(\text{upper})}$ then the testing level is reduced while if $R_c < N_{b(\text{lower})}$ the testing level is increased. W determines the speed and accuracy of the test. If W is small then the test rapidly converges towards the threshold value but gives a final result which is relatively inaccurate. If W is large then many more trials are needed but the final result is much more precise.

2. The step size: The direction of the change in testing level in PEST is determined as described above, the size of that change is determined by the responses to previous testing levels. The first step size is usually large and the test starts at a value above threshold to encourage the observer with a few easy trials. Taylor and Creelman (1967) suggested the following rules to determine the subsequent step sizes.

- a). At each reversal, halve the step size. Clearly, if two trials have given opposite results then the threshold value is most likely to lie in between - a trial half way between is a sensible option.
- b). The second step in the same direction should be the same as the first. When testing close to threshold the observer is more likely to give an incorrect response (*i.e.* a positive response when actually below threshold or vice - versa) and it is useful to check the validity of the response with a large step size.
- c). The fourth and subsequent steps in the same direction should be double the first subject to some upper limit in the value of the step size. If several moves in the same direction have not produced a reversal then the current test level is clearly some way from threshold and a rapid shift in testing level is called for. Observers, however, respond badly to large differences in the magnitude of sequentially presented stimuli and there should be some upper limit on step size to avoid this.

d). The third successive step in the same direction is double the value of the second if the step size leading to the most recent reversal was not the result of a doubling of values or vice-versa. This avoids multiple testing at the same level and simulation showed that the efficiency of the test was about 20% better using this rule.

3. The end point: PEST stops when the rules call for a step size smaller than some predetermined minimum value. The choice of step size clearly has an effect on the accuracy of the final threshold estimate as was shown in *Figure 4.05*. In the PEST routine it is usual to make the final step size small to counteract this. The actual threshold is the testing value asked for by the last step.

4.7.1: PEST modification

Findlay (1978) suggested some modifications to the PEST technique which allow it to operate either more speedily or with greater accuracy. He proposed two alterations to make use of information which was otherwise discarded.

The first modification involved the alteration of the step size, in the original PEST proposal this was independent of the number of trials (N_T) at the previous testing level. Thus if the 50% point (for a simple yes/no procedure) on the psychometric function were being estimated and $W = 1$ then the original PEST would not differentiate between, for example, a four correct responses out of five sequence and a nine correct responses out of fifteen sequence. However the first is in all likelihood further from threshold than the second. Findlay proposed that if the number of trials at a particular level exceeds a preset level then the stimulus level is reduced to give more rapid convergence towards threshold.

The second modification involved the value of W (the deviation limit of the sequential test). The proposal was for this to vary through the test in order to allow a more rapid convergence toward threshold in the early stages (W small) but when close to threshold use a larger value of W in order to increase the accuracy of the final threshold estimate. This modification is achieved by making W a function of the number of reversals.

Throughout this thesis it has been necessary to compromise on the use of the technique as outlined above. In particular, the rules used to determine the step size suggested by Taylor

and Creelman were not used apart from (a). In addition, we only used the second modification suggested by Findlay. While this compromise means that more trials may be needed in order to obtain a threshold estimate it was felt that this did not affect the accuracy of the final result to a significant extent. However, in order to simplify the computer software it was felt that this somewhat easier technique was justified.

4.8: Bias

It is usual to assume that threshold has a certain value combined with a standard deviation which represents the degree of uncertainty of the value. In some of the experiments carried out in this thesis there is a further complication, observer bias, which has to be addressed. For example, in the vernier task the observer does not always align the two features one above the other when there is no physical offset between them. It is more common for him to state that the two features are aligned when there is in fact a slight physical offset, the value of this offset being a measure of observer bias. It is a common procedure when estimating thresholds to define the value relative to a zero offset. If, therefore, the observer bias moves the subjective zero away from this objective zero the final estimate is going to contain a constant error (Andrews, 1967). Using the staircase routine it is possible to allocate a value to observer bias and thus eliminate this constant error from the estimation of threshold. Again, using the example of vernier acuity, two interleaved staircases are used one starting with the upper block to the left the other to the right. These measure the 75% point on the psychometric function for both leftward and rightward responses. The two values can then be used to determine observer bias which can now be defined as the point of subjective alignment of the two features and can be expressed as the mean of the two final threshold values. Acuity, or the observers actual threshold, can then be defined as the mean of the absolute values of the thresholds obtained. In the following example let us assume that the final threshold values from the two staircases were +25 units and -15 units, where + values are taken to be right and - values left of the zero physical offset. The observer bias is $(+25 + (-15)) / 2 = +5$ units and the acuity is $(25 + 15) / 2 = 20$ units. If only one staircase were used clearly neither of the two threshold values obtained would be correct as they would include a contaminating factor from the observer bias.

4.9: Conclusion

Throughout this thesis the UDTR method or the PEST technique have been used in order to estimate threshold values. The actual parameters used; step size, reversals, initial offset etc. were varied depending on the purpose of the experiment and these figures will be given in the chapters referring to the individual experiments. In addition, where it was necessary to take steps to separate observer bias and acuity this will be noted.

Chapter 5: Equipment

5.1: Introduction

All the experiments described in this thesis were carried out using stimuli generated on a cathode ray tube (CRT) under the control of a microcomputer. Programming was carried out either by myself or my supervisor, Dr. D. Whitaker. This chapter outlines details of the equipment used and the environmental factors which influenced the conduct of the experiments.

5.2: The RM Nimbus AX

The majority of the experiments utilised the Research Machines Nimbus AX microcomputer coupled with an EIZO 8060H high definition color monitor. *Figure 5.01* shows a photograph of the equipment and experimental set up, while *Figure 5.02* is a schematic diagram of the same. The AX is an IBM clone with a built in Winchester hard disk giving 32 Mb of memory.

The monitor allowed control of screen luminance and contrast the values of which will be noted, where appropriate, in the chapters on the individual experiments. The horizontal pixel separation was 0.3 mm which, depending on the working distance used, allowed a range of minimum offset values to be obtained (*Table 5.01*). In the vertical direction the pixel separation measured 0.7 mm but thresholds were never obtained in this direction. The observer had to respond to the stimulus generated on the monitor either via the keyboard or the mouse. The data was stored during the experimental run and then analysed to give the results. Finally, it was possible to print out both the data and the results via an Epson RX80 printer. Usually, however, the results were presented on the monitor and a hard copy written down.

5.2.1: Stimulus generation

The actual stimuli are described in the chapters referring to particular experiments, including the range of stimulus parameters dealt with. The stimuli took the form of bars, dots or clusters of dots either with or without fixed references. A range of hyperacuity configurations

could be generated including vernier, bisection and oscillatory displacement. The last example was, however, limited to a square wave oscillating form because of the limitations of the software used. In addition, it was possible to produce moving targets of both continuous and stop-go-stop variety (see chapter 7). It should be noted that the continuous movement actually consists of a series of displacements in discrete, sub-threshold steps due to the pixel spacing of the CRT. Stimulus size, offset and presentation duration could be varied between stimulus presentations by use of suitable commands in the programs. All the stimuli were generated using programs written in RM Basic. The programs followed a standard pattern consisting of...

1. Inputting of details relating to the stimulus required (*e.g.* working distance, size, separation etc..)
2. Generation of the stimulus and its presentation on the monitor.
3. Reading the responses from the observer (*i.e.* correct / incorrect response and the offset in pixels) and then adjusting the stimulus parameters according to the psychophysical technique being employed.
4. Storing the details of the observer's responses.
5. Processing the data and then calculating the result. This is then presented on the monitor and may also be printed out.

The use of Basic has the advantage that it is relatively simple to use and can be considered adequate for the experiments performed here. It does, however, have the disadvantage of being rather slow in operation, especially in the production of complex stimuli.



Figure 5.01: A photograph of the equipment used in conjunction with the Nimbus AX microcomputer. The observer is seated next to the computer station using the headrest when appropriate. The microcomputer and monitor are together in the center of the picture. A simple vernier stimulus consisting of two vertical bars with a small horizontal offset is displayed on the monitor. The keyboard and mouse which are used by the observer to signal his or her response to the stimulus are seen on the left. To the right can be seen the Epson RX80 printer which could be used to obtain a hard copy of the data and results if required. It was usual, for all working distances over 2 meters, for the stimulus to be viewed via a mirror placed at half the working distance in front of the observer and the monitor (see *Figure 5.02*). For shorter working distances it was usual to view the monitor directly.

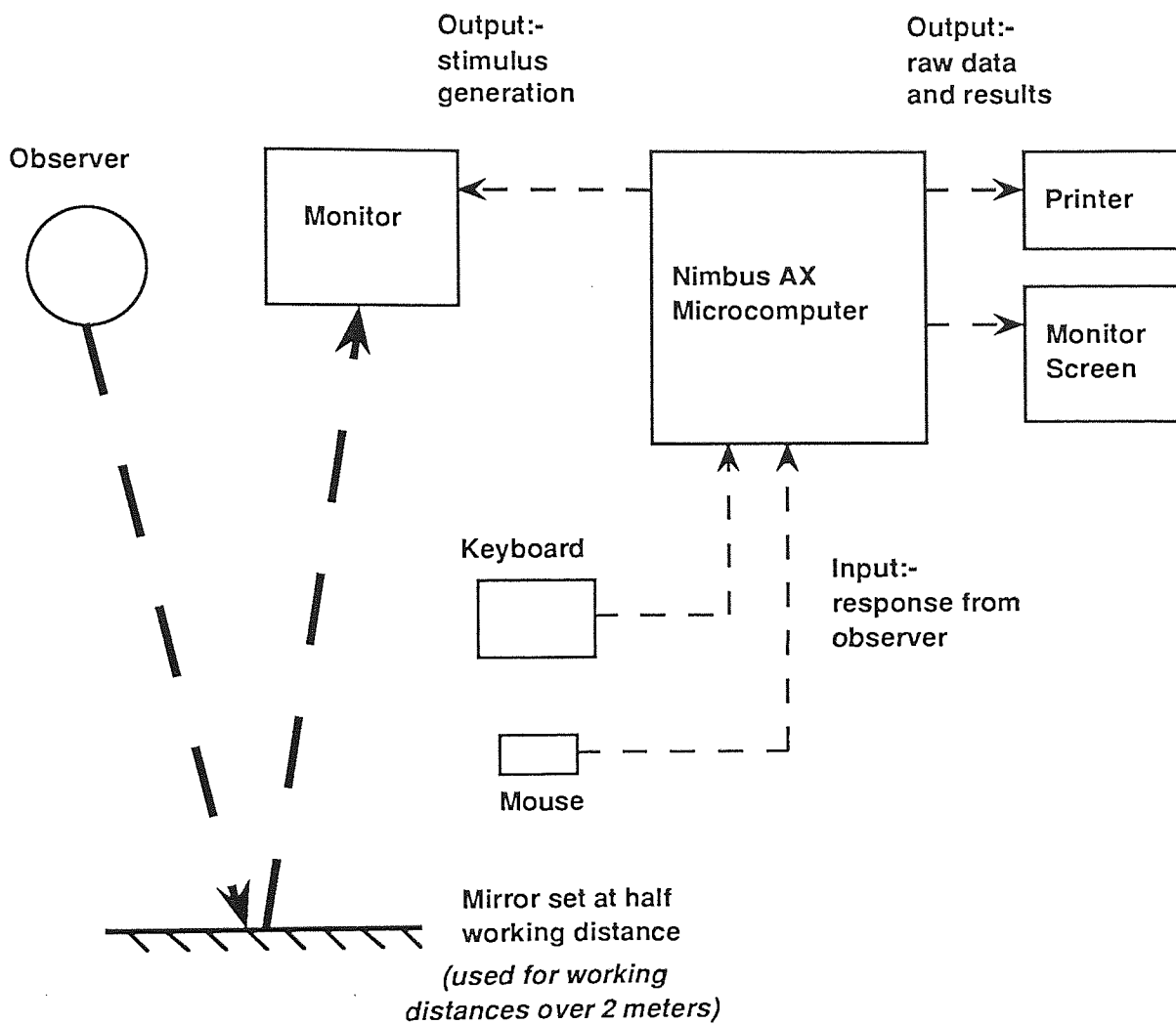


Figure 5.02: A schematic diagram of the experimental set up when using the Nimbus AX microcomputer. Details of the various items of equipment and the general experimental set up are mentioned in the text together with any restrictions on stimulus generation and presentation imposed by the equipment.

5.2.2: The experimental environment

The equipment was set up in a room fitted with total blackout curtains. This allowed a range of room illumination levels, ranging from complete darkness to bright photopic levels, to be obtained. The most commonly employed level of room lighting was in the mesopic range.

The working distances available, using a mirror, were up to a maximum of 10 meters wholly within the room, or 28 meters if an adjoining room was also used. The working distance was a critical value in certain of the experiments as it allowed the minimum threshold value obtainable by the limitations of the pixel size to be adjusted until they were well below the expected threshold. Clearly, running an experiment where the threshold value is close to, or less than, the minimum pixel size can lead to erroneous results.

For certain experiments an offset value of zero means that the targets are geometrically aligned, or, if an oscillating movement stimulus is being employed, are stationary. If this occurs during an experiment the value zero is counted as a reversal and the stimulus is presented with an offset of 1 pixel. If this second presentation leads to another reversal then the estimated threshold value is taken to be 0.5 pixels. *Table 5.01* lists the offset values, in seconds of arc, corresponding to this value together with the offset value for 1 pixel.

Table 5.01:

Working distance (meters)	Minimum threshold (seconds of arc)	
	0.5 pixel	1.0 pixel
10.0	3.1	6.2
8.0	3.9	7.7
2.5	12.4	24.8
1.5	20.7	41.3
1.0	31.0	61.9

From *Table 5.01* it can be seen that altering the viewing distance is a useful way of adjusting the minimum threshold. This was particularly important in certain experiments using

eccentric viewing where it was necessary to scale the stimulus to take account of the cortical magnification function. By altering the working distance it is possible to scale all stimulus features equally without reverting to complicated calculations in the software (see chapter 10).

The observers in most of the experiments were myself and Dr. Whitaker. Volunteers for what are generally long and somewhat tedious observation sessions are usually difficult to find. In order to iron out intra-observer variability, and hence improve the reliability of the results, it was usual to take four readings and then average them to obtain an estimate of threshold. However, in some of the experiments it was possible to use final year students as part of their dissertation. In addition, there were other experiments which required naive observers in order to eliminate practice effects (Westheimer and McKee, 1978), and one where a range of observer ages were needed. Using such naive observers it was usually only possible to perform one run for each stimulus configuration. This then introduces the problem of inter subject variation which can become a significant factor, especially if some clinical application is being sought. In these circumstances it is necessary to use a large number of observers in order to obtain a good estimate of the mean threshold value. The price of this is usually a large spread of individual results. If the spread of results from the normal group of observers overlaps, to a significant degree, the spread of results from the pathological group it can adversely affect the sensitivity of the test. Clearly, in such circumstances the accurate diagnosis of pathology is going to be compromised to a certain extent.

5.3: The VENUS stimulator

Two of the experiments, which required the use of sinusoidal gratings as stimuli, were carried out using the VENUS stimulator. *Figure 5.03* shows the equipment and experimental set up with *Figure 5.04* a schematic diagram. As with the Nimbus, the equipment consists of a microcomputer coupled to a high resolution color monitor on which stimulus parameters are input and data displayed. For the VENUS there is a second monitor which is used solely to present the stimulus after generation. The stimuli were produced using application software written in Microsoft C by Dr. Whitaker. This allowed the spatial and temporal output to predetermined areas of the stimulus monitor to be controlled independently. The actual stimulus details are given in chapter 8. The stimulus monitor had a mean luminance of 120 cd

m-2 when shrunk to the appropriate size for our experiments, and it had a refresh rate of 120Hz. Again the experiments were carried out under mesopic lighting conditions this time with a fixed working distance of 6 meters. The minimum possible offset available using the VENUS was a constant 1.4 degrees of phase angle. This allowed minimum threshold values of 0.875 seconds of arc for a 16 cycle per degree grating and 14 seconds of arc for a 1 cycle per degree grating.



Figure 5.03: A photograph of the equipment used in conjunction with the VENUS stimulator. The observer is seated alongside the right hand monitor on which the stimuli are presented and directly in front of the second monitor. The microcomputer and second monitor are together on the left of the picture and are used for programming and input of the stimulus parameters. The keyboard, with which the observer responds can be seen between the two monitors. When using the VENUS stimulator the observer always viewed the monitor via a mirror set at half the working distance.

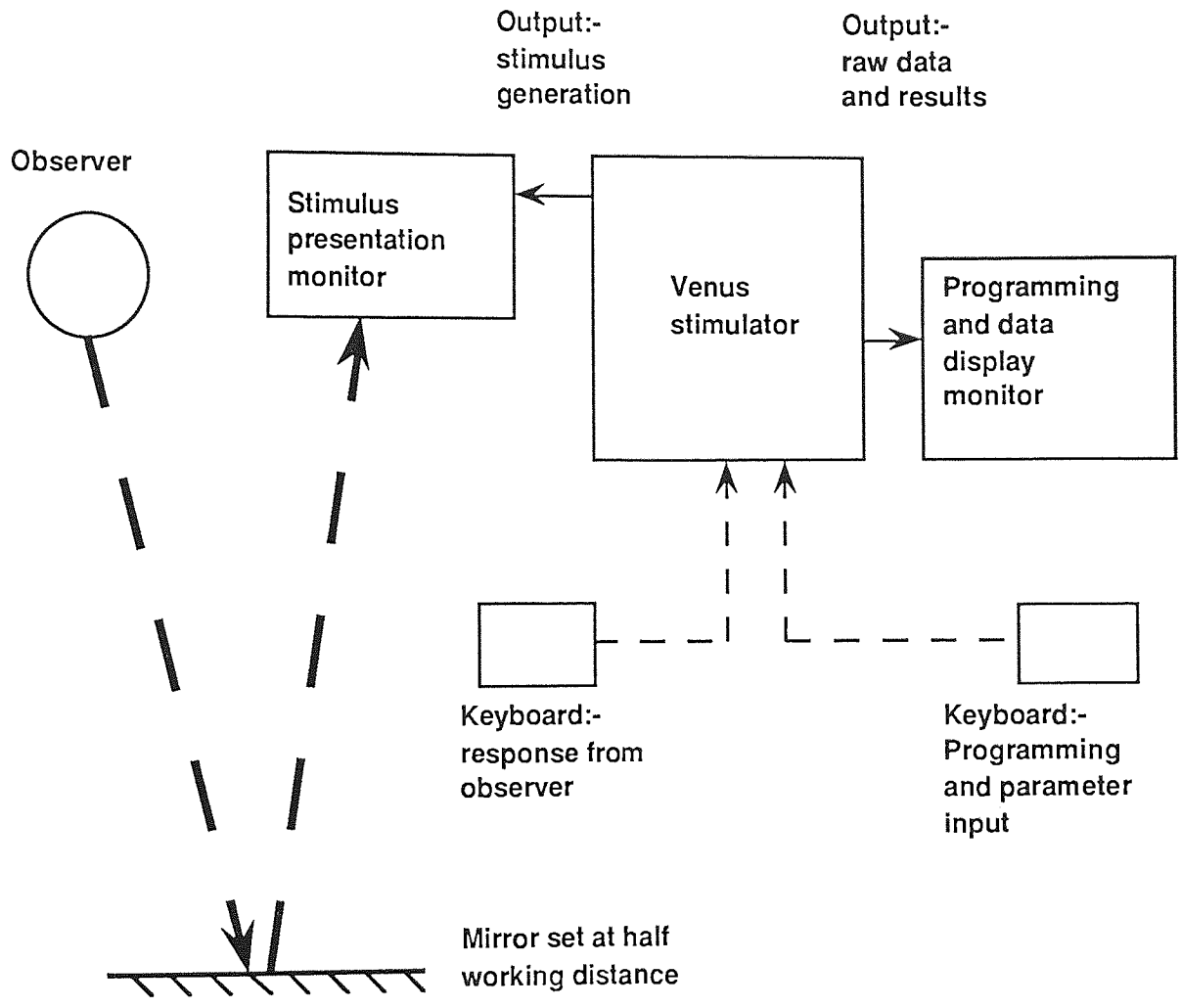


Figure 5.04: A schematic diagram of the experimental set up when using the VENUS stimulator. Details of the various pieces of equipment and their uses together with any restrictions on stimulus generation and presentation imposed by the equipment are mentioned in the text.

Chapter 6: Hyperacuity and contrast

6.1: Introduction

There has been considerable interest over recent years concerning the effect of stimulus contrast on hyperacuity performance. The findings of several studies seem to indicate that the contrast response of vernier acuity differs from that of other hyperacuties. This chapter deals with experiments carried out in an attempt to put forward some explanation for this apparent dichotomy.

6.1.1: Vernier acuity and contrast

Bradley and Skottun (1987) measured vernier acuity using a stimulus consisting of abutting, vertically orientated sinusoidal gratings. They obtained thresholds for a variety of spatial frequencies (between 0.25 and 10 cycles per degree) and contrasts (between 1 and 80%). Their findings are illustrated in *Figure 6.01* and show that vernier thresholds improve consistently with increasing contrast over the entire range of contrast levels studied.

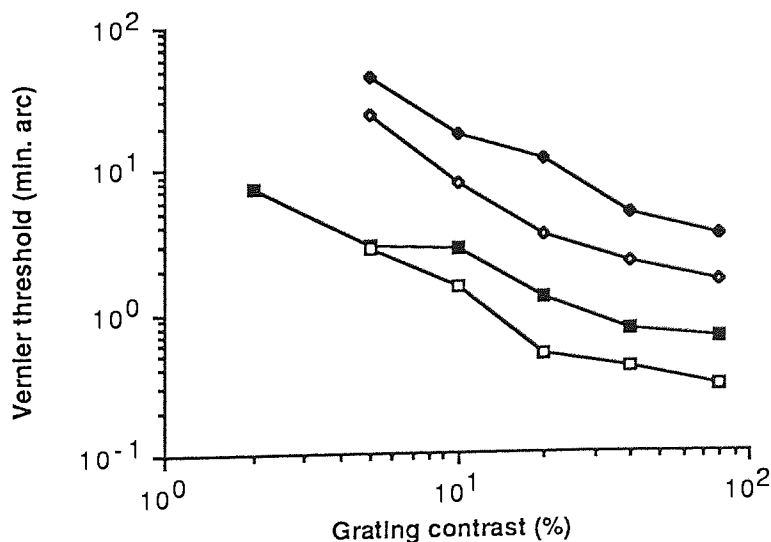


Figure 6.01: Vernier thresholds plotted against contrast level for different spatial frequencies. It is clear that thresholds improve, for all frequencies, with increasing contrast (from Bradley and Skottun, 1987). The improvement in threshold values with increasing spatial frequency is also apparent. Filled diamonds are results for a spatial frequency of 0.25 cycles per degree, open diamonds 0.75 cycles per degree, filled squares 2 cycles per degree and open squares 8 cycles per degree.

Krauskopf and Farell (1991) have confirmed these results using Gaussian modulated gratings, while previous reports by Foley-Fisher (1977), Wilson (1986) and Morgan and Regan (1987), all using line targets, and Watt and Morgan (1983b), using a Gaussian blurred edge, have each found a consistent improvement over the full range of contrast levels investigated. However, a recent paper by Wehrhahn and Westheimer (1990) has reported that vernier acuity levels off at a contrast level of around 20%. Increases in contrast level above this produce no further improvement in threshold. Their stimulus was unusual in that it consisted of a vertical division of a CRT with one side darker than the other. The divide contained a horizontal step offset equivalent to the horizontal offset of the two elements in more traditional vernier configurations. The observer had to decide whether the offset was to the left or the right. Weighed against this, another paper using separated blocks shows the same consistent improvement with increasing contrast as did all the other reports (Westheimer and Pettet, 1990). The evidence, therefore, seems to point toward vernier acuity improving consistently with increasing contrast over the whole range of contrasts investigated.

Watt and Morgan (1983b) suggest that vernier sensitivity improves in proportion to the square root of contrast, that is the exponent relating contrast to threshold is around -0.5. However, Bradley and Skottun (1987) reported a selection of results which showed wide variations in the exponent relating vernier acuity to contrast (*Table 6.01*). This variability is probably a result of the large range of stimulus configurations employed.

Table 6.01:

Investigators and year	Contrast range (%)	Exponent
Foley-Fisher (1977) §	≈ 10 to 100	0.15
Watt and Morgan (1983) §	10 to 80	0.50 to 0.60
Wilson (1986) §	25 to 100	0.67 to 0.94
Bradley and Skottun (1987) §	10 to 80	0.77 to 0.84
Morgan and Regan (1987) §	10 to 75	≈ 0.5
Krauskopf and Farell (1991)	multiples of detection threshold	0.40 to 0.63

§ indicates those results quoted by Bradley and Skottun (1987).

6.1.2: The effect of contrast on other hyperacuties

Other hyperacuties do not seem to respond in the same manner. Wright and Johnston (1985) used an oscillating sinusoidal grating and found that above about 10% contrast level there was no further improvement in displacement thresholds. Whitaker and Elliott (1989), using an oscillating bar of light, found that for low temporal frequency oscillations (2 Hz) there was no effect on thresholds between 6% and 96% contrast level. However, at higher temporal frequencies they found that changes in contrast had a marked effect on displacement thresholds. The clear conclusion is that displacement thresholds seem, under certain conditions, to exhibit a form of contrast saturation with increasing contrast producing no parallel increase in sensitivity (*Figure 6.02*). Indeed, Nakayama and Silverman (1985) using displacement of a sinusoidal grating found that saturation may occur at a contrast level as low as 2%.

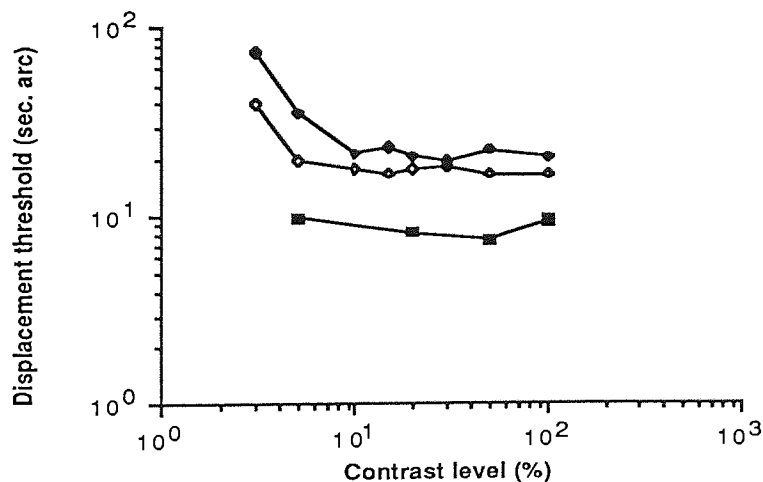


Figure 6.02: Displacement thresholds plotted against contrast level for subject AJ (filled diamonds) and subject MW (open diamonds) from Wright and Johnston (1985). The filled squares are the average results from the two observers used by Whitaker and Elliott (1989).

Morgan and Regan (1987) found similar saturation for a spatial interval detection task. They varied contrast between 10 and 75% and found essentially no change in threshold values. Skottun and co-workers (Skottun, Bradley and Freeman, 1986; Skottun *et al.* 1987) have found a similar independence to suprathreshold contrast for orientation and spatial frequency discrimination.

The obvious question is why vernier acuity seems to behave in one fashion and these other hyperacuities in another. It is possible that as contrast is progressively decreased the visual system, where possible, summates the signal from a greater extent of the stimulus. In such circumstances so long as the improvement in threshold gained from summation counteracts the effect of reducing contrast then saturation is found. In this experiment displacement thresholds for line targets have been measured as a function of line length and contrast and show that the effect of contrast on displacement thresholds is highly dependent on line length. The results have been confirmed using a bisection task with a broadly similar stimulus configuration.

6.2: Methods

6.2.1: Stimulus configuration

The experiments were performed in a darkened room with the stimulus presented on the face of a high resolution color monitor under the control of the RM Nimbus AX microcomputer. The stimulus, for the displacement and bisection tasks, consisted of three vertical lines, positioned side by side, each 4 minutes of arc wide. The length of the lines was varied between 4 and 64 minutes of arc. For the displacement experiment the lines were separated by 30 minutes of arc. It has been previously shown that displacement threshold are independent of separation over the range 5 to 80 minutes of arc (Whitaker and Elliott, 1989). Bisection thresholds, as was shown in chapter 2, are highly dependent on separation (Westheimer and McKee, 1979; Klein and Levi, 1985). In particular, too small a separation risks introducing a strong luminance clue which artificially lowers threshold values. The bisection task was, therefore, carried out at a separation of 8 minutes of arc which produces threshold values comparable to the displacement task but without introducing a luminance clue. The 100% contrast targets consisted of white lines on a black background while the lower contrast stimuli consisted of light grey lines on a dark grey background. For all experiments the mean screen luminance, defined as $(L_{\max} + L_{\min})/2$, was maintained at an arbitrary 18 cd m^{-2} for all contrast levels. The contrast was defined by the Michelson equation:

$$\text{Contrast} = (L_{\max} - L_{\min}) / (L_{\max} + L_{\min})$$

6.2.2: Observations

Observations were carried out by myself (DM) and my supervisor (DW), both of us being experienced in hyperacuity tasks. In the displacement threshold experiment one of the outer two lines was oscillating in a square wave form at 2 Hz, while the other two remained stationary to act as references. The task was to decide which of the outer two bars was moving. Having decided, the observer responded via the keyboard. Threshold was determined using a two alternate forced-choice staircase which estimated the 71% point on the psychometric function (Wetherill and Levitt, 1965). The staircase ran for 10 reversals, the last seven of which were averaged to produce the final threshold estimate. If the stimulus offset level fell to zero then a reversal was accepted at zero and the test was continued with an offset of 1 pixel.

For the bisection experiment the observer's task was to decide whether the center line was closer to the right or left hand outer bar. Again, the decision was conveyed to the computer via the keyboard. For this experiment thresholds were determined using the PEST technique described in chapter 4, with the 71% point on the psychometric function being estimated to allow comparison with the displacement results. As was pointed out in chapter 4, this method allows observer bias and threshold to be readily separated which is an important consideration in the bisection task.

6.3: Results

Figure 6.03 shows displacement thresholds as a function of line length for each of four contrast level. *Figure 6.04* shows the bisection thresholds, again as a function of line length, at the same contrast levels. For both tasks thresholds are independent of line length at high contrast levels. As the contrast level is reduced thresholds start to increase and, while for the longer line lengths this increase is quite small, it becomes very pronounced as line lengths are reduced.

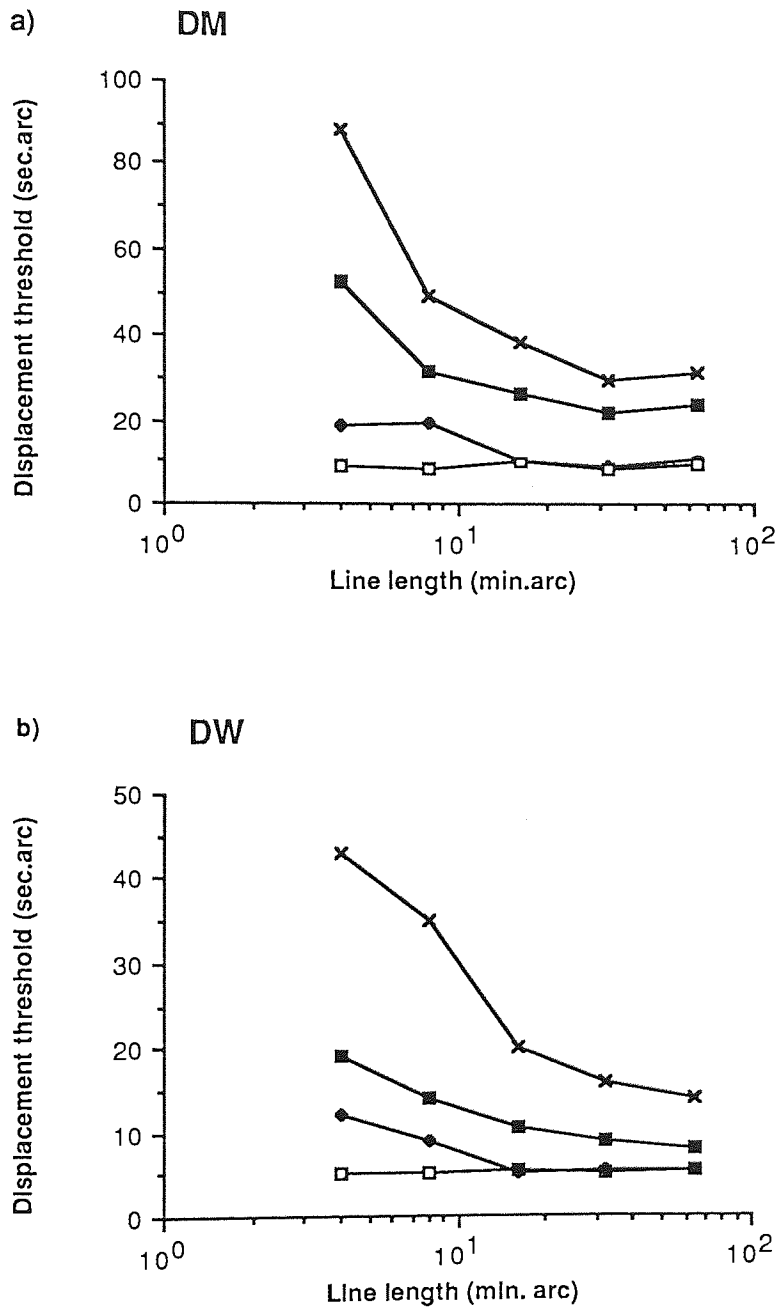


Figure 6.03: Displacement thresholds, for subject DM (a) and subject DW (b), plotted against line length. Four different contrast levels are shown; 100% (open squares); 20% (filled diamonds); 10% (filled squares) and 5% (crosses). For clarity, the standard error bars are not shown on the figure but were on average 20% of threshold for subject DM and 18% of threshold for subject DW. The results are discussed in the text.

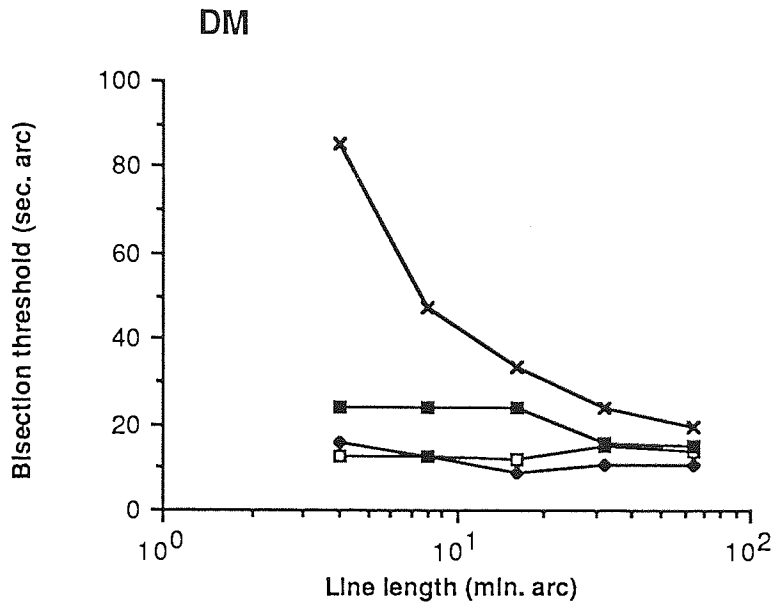


Figure 6.04: Bisection thresholds plotted against line length. Four different contrast levels are shown; 100% (open squares); 20% (filled diamonds); 10% (filled squares) and 5% (crosses). Again to improve clarity the standard errors are not shown but were on average 19% of threshold. The results are discussed in the text.

Table 6.02 shows the exponents relating threshold to line length at each contrast level. The data relating thresholds to line length was fitted with a logarithmic curve at each contrast level. The exponents of the curves vary from close to zero at high contrast levels to approximately -0.5 at the lowest contrast level. Sensitivity is, therefore, approximately proportional to the square root of line length at the 5% contrast level. It is also apparent that this applies to both the displacement and bisection tasks.

Table 6.02:

Displacement

Contrast	Exponent	
	DM	DW
100.0	+0.03	-0.03
20.0	-0.22	-0.30
10.0	-0.28	-0.34
5.0	-0.41	-0.47

Bisection

100.0	+0.04
20.0	-0.13
10.0	-0.19
5.0	-0.52

6.4: Discussion

Figure 6.05 shows the data for displacement detection replotted with contrast as the abscissa. Similarly, *Figure 6.06* shows the results for bisection acuity. It is clear that below 20% contrast the threshold values exhibit an approximately linear improvement with increasing contrast for all line lengths, although the sensitivity is greater for longer lines. The exponent value is around -0.75 which compares favorably with the exponent values quoted earlier (*Table 6.01*) for vernier acuity. Clearly, at these contrast levels vernier acuity, bisection acuity and displacement detection all show a similar contrast response.

Above 20% contrast, however, a difference becomes apparent. For bisection and displacement tasks longer line lengths exhibit contrast saturation. The shorter line lengths, in particular the 4 minute of arc line, do not, however, show saturation. In these cases thresholds continue to improve with increasing contrast.

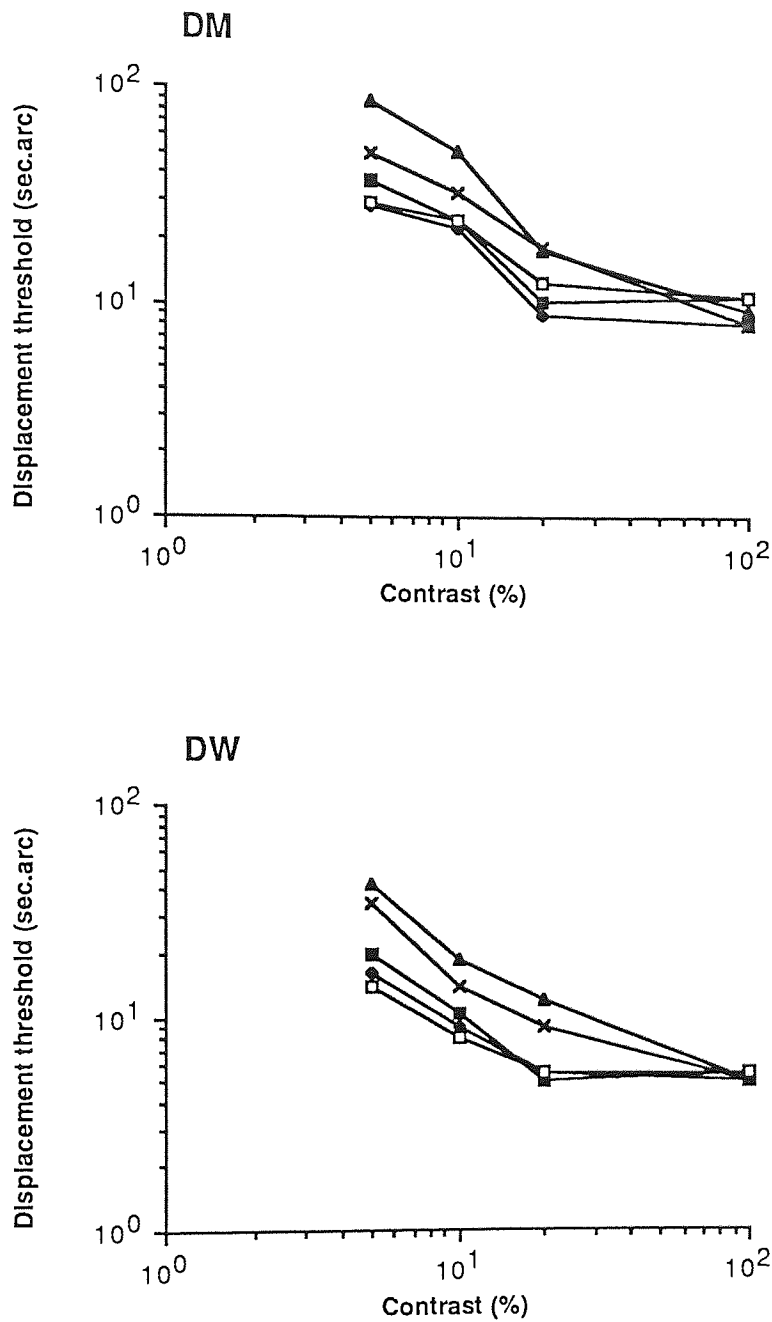


Figure 6.05: Displacement thresholds, for subject DM (upper) and DW (lower), plotted against contrast for different line lengths. The line lengths are 4 minutes of arc (filled triangles); 8 minutes of arc (crosses); 16 minutes of arc (filled squares); 32 minutes of arc (filled diamonds) and 64 minutes of arc (open squares). Note the saturation which occurs for longer line lengths. Standard errors are the same as for *Figure 6.03*, approximately 20% of threshold for subject DM and 18% of threshold for DW.

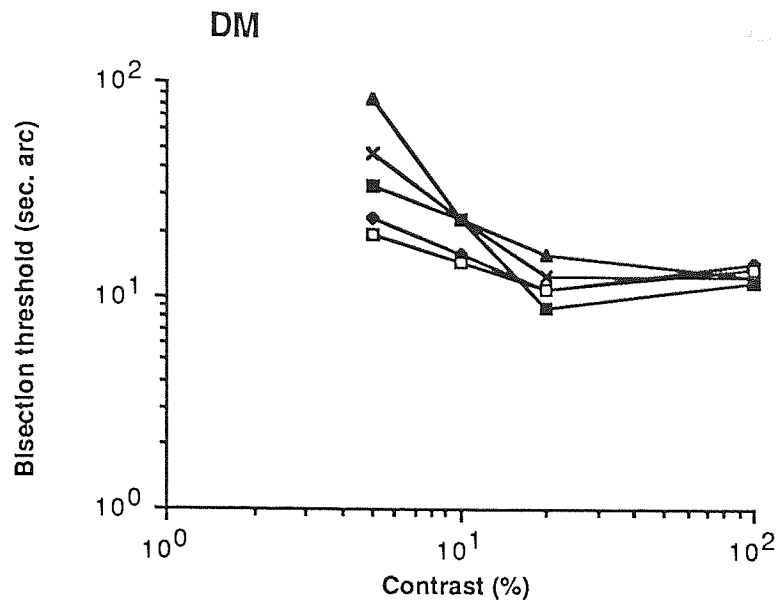


Figure 6.06: Bisection thresholds plotted against contrast for different line lengths. The line lengths are 4 minutes of arc (filled triangles); 8 minutes of arc (crosses); 16 minutes of arc (filled squares); 32 minutes of arc (filled diamonds) and 64 minutes of arc (open squares). Standard errors are the same as *Figure 6.04*, approximately 19% of threshold.

The consistent improvement in thresholds for displacement and bisection tasks with short lines and also for vernier acuity would point towards some mechanism whose operation is dependent on contrast. For longer lines, however, the displacement and bisection tasks would seem to possess some further mechanism which is not available for the other tasks. That mechanism, I would suggest, is that spatial summation, along the length of the stimulus, occurs as contrast level falls. This would allow a trade-off between reducing contrast level and increasing spatial summation. If one considers *Table 6.02* the increase in exponent with decreasing contrast would support this premise. For high contrasts it can be seen that thresholds are independent of line length, a situation which changes dramatically as contrast is reduced. This trade-off could explain the contrast saturation found for the longer, but not the short, lines in displacement and bisection tasks. Why, then, does this not have the same effect on vernier acuity?

The answer becomes apparent if one considers the configurations employed in performing the different tasks. For vernier acuity, as was shown in chapter 2, not all parts of the stimulus give information which allow the task to be performed optimally. It has been

demonstrated that as line length increases thresholds level out for line lengths over about 5 minutes of arc, no further improvement occurring above this level. Similarly, for two dot configurations, the lowest thresholds occur around a separation of 5 minutes of arc, becoming worse as separation varies from this value (Westheimer and McKee, 1977a). Clearly, therefore, the information from parts of the stimulus features away from this optimal location is far less important in allowing the task to be performed. The question regarding which part of the vernier stimulus is important in determining the offset will be considered further in chapter 8. It would seem that while summation can, and probably does take place, the extra information is not sufficient to compensate for the reducing contrast level. For the displacement and bisection tasks the stimulus features lie side by side and it is possible to perform the task equally well using any or all parts of the stimulus feature. In this case, where all parts of the stimulus are equally important in determining the threshold, it is clear that summation, when available, would allow the effect of contrast reduction to be overcome. It would require, however, that the length of the stimulus feature available allowed for sufficient summation to completely compensate for reducing contrast. For short line lengths it would appear that this process fails and, therefore, the displacement and bisection tasks give the same contrast response as the vernier task. Only for longer line lengths, over some 16 minutes of arc, does summation succeed in overcoming the effect of reducing contrast level. It has also to be pointed out that this applies only for contrast levels over about 20%. At lower contrast levels it would appear that summation cannot outweigh the deleterious effect of the lower contrast regardless of line length.

Contrast saturation has been investigated at various stages in the visual pathway of the macaque monkey (Sclar *et al.* 1990). They examined the response to stimuli of varying contrast at the LGN, visual area V1 and also area MT. As was explained in chapter 3, current thinking is that the visual signal is processed in parallel by two distinct pathways, the magnocellular and the parvocellular. The contrast response of the two pathways is markedly different. At the LGN magnocellular cells show greater sensitivity than parvocellular neurons, especially at low contrast levels below about 10%. In visual area V1, comparing simple and complex cells, a spread of responses which seems to combine both pathways was found. Finally area MT, the visual motion area, gave responses which were sensitive to very low contrast levels and showed saturation, in some cases, for contrasts of only 5%. This difference in contrast response of the two pathways has been well demonstrated by Kaplan and Shapley (1982) and Derrington and Lennie (1984).

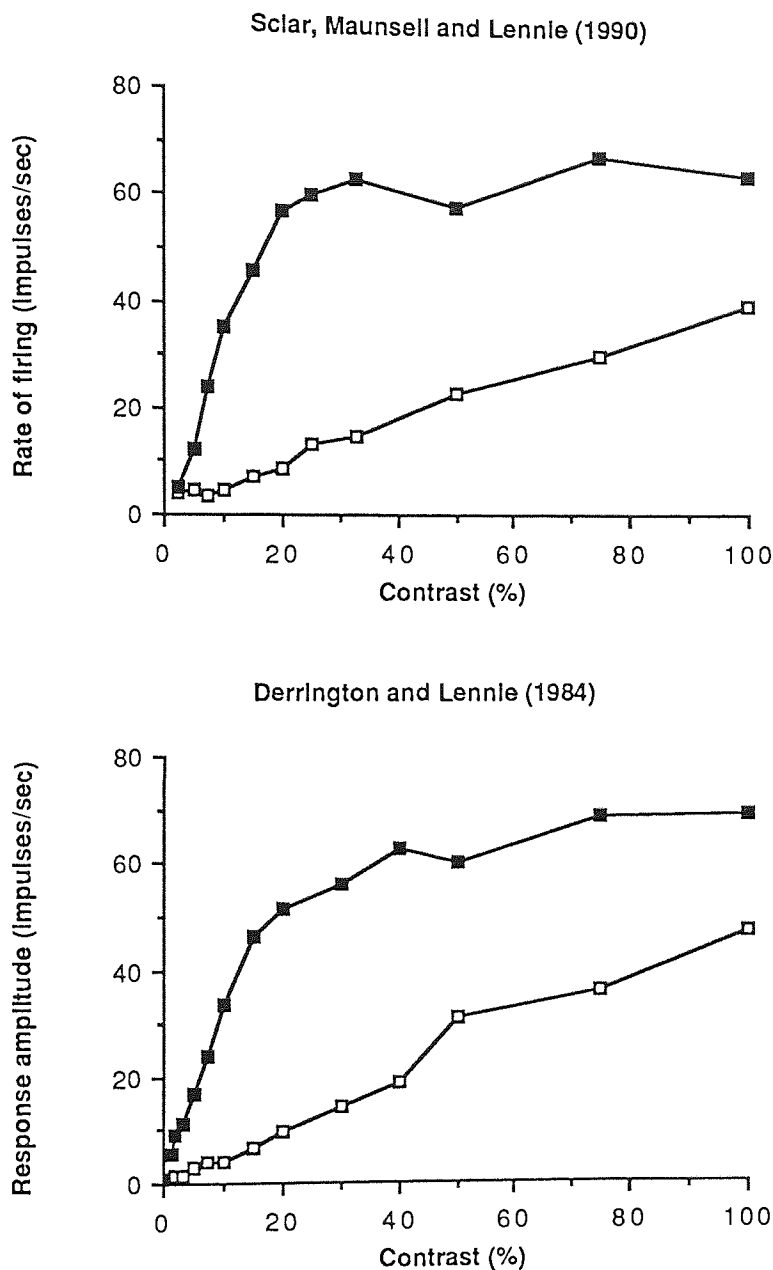


Figure 6.07: The contrast response of magnocellular (filled squares) and parvocellular (open squares) neurones at the Lateral Geniculate Nucleus (upper) and in the cortex (lower). Note that in both cases there is evidence of saturation in the magnocellular pathway but not the parvocellular.

Given the evidence for saturation at moderate contrast levels, demonstrated by certain displacement and bisection configurations, one could, perhaps, consider that the responses of magnocellular units are responsible for these thresholds. On the other hand, those thresholds

which fail to show such saturation would suggest, logically, a parvocellular input. There is, however, evidence that the parvocellular system, despite its poor response at low contrast levels, could mediate hyperacuity performance over the full contrast range. Sclar *et al.* (1990) point out that the contrast response of many cells in area MT, for example, is greater than that found in individual cells lower in the visual pathway. This points towards summation of input from individually less sensitive units combining to give a greater sensitivity to units higher in the visual pathway. It was also postulated by Derrington and Lennie (1984) that, while psychophysical contrast sensitivities could be explained by single magnocellular units they could also be obtained by summation among many parvocellular units each having a lower individual contrast sensitivity. In fact, they point out that as few as ten parvocellular units would be sufficient to match the peak contrast sensitivities found by psychophysical investigation. Further evidence for a parvocellular input comes from a report by Merigan and Eskin (1986). They found that selective degeneration of the parvocellular pathway reduced contrast sensitivity even at low and medium spatial frequencies. As was reported in chapter 3 it is the magnocellular pathway which is most sensitive to such frequencies. Sclar *et al.* (1990) go on to show that the saturation found in area MT could be explained on the basis of spatial summation. Sensitivity of MT cells was maximal for stimuli which filled the receptive field and, in such cases, saturation occurred at very low contrast levels. As the stimuli became smaller saturation occurred at progressively higher contrast levels. The sensitivity of the MT cells was shown to increase in proportion to the square root of stimulus area.

If one accepts that the mechanism which underlies hyperacuity averages the outputs of filters of many sizes and tuned to several orientations and spatial frequencies then an argument explaining the saturation found in these experiments can easily be constructed. The smallest line lengths will only completely fill the smaller filters thus causing their responses to saturate. However, the larger filters are not completely filled and as such their responses do not saturate. The overall response of the filters as a group, therefore, would be expected to show little evidence of contrast saturation. For the longer lines, on the other hand, progressively more filters will saturate as the stimulus fills their receptive fields. In such circumstances it is the contrast response of the filters which determines whether or not saturation occurs. Now the cells which display the best contrast sensitivity and also show saturation at around a 20% contrast level are magnocellular. While this might be used as an argument supporting a role for magnocellular cells in the experiments described here, it is not one which can be made with any certainty for the reasons described above.

This summation process offers several advantages to the visual system. First, it allows the output of the receptors to be averaged to overcome noise. Consider the retinal ganglion cells which have been shown to be capable of detecting small displacements within their receptive field (Scobey and Horowitz, 1972). This peak sensitivity has been found to occur toward the edge of the field where the sensitivity profile is changing most rapidly. However, as has been pointed out in chapter 3, this signal would be difficult to isolate from the competing signals caused by all the other factors eliciting a response from the cell, including changes in luminance, spatial frequency, orientation etc. In addition, cells all have a background discharge rate which has to be exceeded before a response can be elicited. It has been shown that noise grows as the square root of the number of active inputs (Barlow and Levick, 1969). The signal, on the other hand, grows in proportion to the number of active inputs. Therefore, the signal-to-noise ratio grows in proportion to the square root of stimulus area. If, in the situation described in the experiments here, spatial summation takes place over a large area relative to the size of the stimulus then all inputs will contribute noise but only a few signal. However, as the stimulus area grows the signal-to-noise ratio improves. This reasoning explains the optimal sensitivity to stimuli filling the receptive field found by Sclar *et al.* (1990). Summation, under the right conditions, therefore, would allow the signal to be extracted more easily from the background noise.

The second point to be considered is that the tuning functions of the cells to different stimulus features vary. By summing inputs from many cells with different tuning functions it is possible to more clearly extract the signal (see for example Paradiso, 1988).

Finally, it has been shown that there are individual cells sufficiently sensitive to reliably detect changes in orientation and spatial frequency to hyperacuity levels (Bradley *et al.* 1985). The majority of cells, however, are insufficiently sensitive and in order to produce thresholds in the hyperacuity range it would be necessary to average across many cells.

6.5: Conclusion

The conclusion to be drawn from this experiment is that displacement and bisection tasks produce a different contrast response to vernier acuity. However, the results suggest that the mechanism underlying the tasks is the same. On the other hand, the method by which the information is extracted from the stimulus does appear to differ. It is proposed that the stimulus configuration is the crucial feature underlying this difference. In particular, for

vernier acuity the optimal information used to determine the offset is provided by a limited spatial extent of the stimulus. Information from other parts of the stimulus is less useful. For the bisection and displacement tasks this is not so, information from all parts of the stimulus being equally useful in determining the offset.

Chapter 7: Displacement detection and reference features

7.1: Introduction

Movement of an object usually occurs in the presence of other stationary information within the visual field. Normally this is in the form of the background to the moving stimulus which forms a reference grid against which object movement can be discerned. Clearly, in this situation any object movement must involve a change in position relative to this reference grid, hence this type of movement is known as *relative* movement. It is most unusual to have movement of an object without any available reference point. An example would be the movement of an aeroplane against a clear blue sky. This type of movement is known as *absolute* movement. In this latter case it would seem necessary, in the absence of any other information, to assume that the movement is detected directly. In the former case, however, while there is a possibility that movement could be directly detected it is also possible that movement can be inferred from the change in position of the object relative to the references.

It has been suggested that the visual system has two mechanisms by which movement can be detected. Bonnet (1975, 1984) has proposed that the two mechanisms involve a movement analysing system (MAS) and a displacement analysing system (DAS).

7.1.1: The Movement analysing system (MAS)

Early models of movement detection were based upon the concept of directional selectivity, in which a unit only responds to movement in a specific direction (Reichardt, 1961). Directionally selective neurones have been found in the cortex of cats (Hubel and Wiesel, 1959) and also in the retinae of rabbits (Barlow and Hill, 1963). These units discharge strongly when stimulated by an object moving through the receptive field in the preferred direction. In the opposite direction there is either a weak discharge or none at all. Models for directionally selective units can be built quite conveniently using combinations of basic neural elements (Barlow and Levick, 1965; Marr and Ullman, 1981).

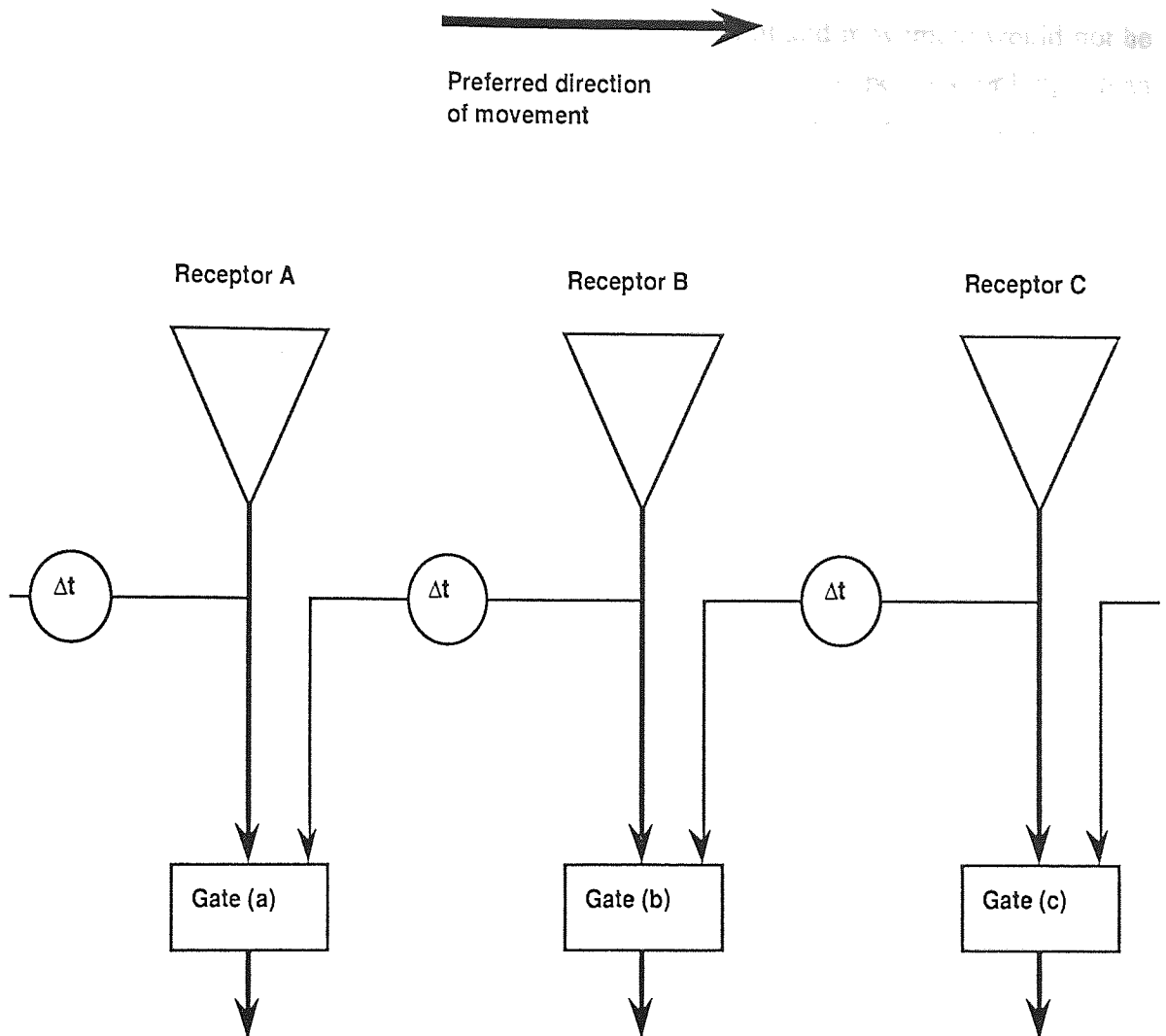


Figure 7.01: The model suggested by Barlow and Levick (1965). The preferred direction is from left to right, the operation of the model is explained in the text.

Barlow and Levick's model of a directionally selective sequence of units which could discriminate movement is shown in *Figure 7.01*. In the preferred direction the stimulation proceeds from receptor A to B then C. Receptor B, which is stimulated after receptor A, sends out an inhibitory signal to gate "a". This signal is subject to a time delay (Δt). The excitatory signal from receptor A thus arrives at gate "a" before the inhibitory signal from receptor B and allows the signal to be transmitted to higher centers. This is repeated in the direction of movement and activity spreads from left to right indicating movement. In the reverse direction, however, the inhibitory signal from receptor C to gate "b", again subject to a time delay (Δt), arrives at the gate simultaneously with the direct stimulation from receptor B. This time the two signals cancel and the gate effectively vetoes transmission of the

message. Thus in this direction the sequence fails to transmit and movement would not be indicated. The delay is not strictly necessary so long as the inhibition persists for longer than the excitation. Barlow and Levick also suggested an anatomical basis for their model using the known neural components of the retina.

Marr and Ullman (1981) also proposed a mechanism from which directionally selective units could be constructed. The model involves detecting zero-crossings in the convolved second derivative of the retinal light distribution (Marr and Hildreth, 1980). This detection is carried out by spatial (S) units which, following combination with temporal (T) units, respond to movement of the stimulus across the detecting units.

While these models provide a mechanism by which movement can be directly detected and are present in some form in the visual system they are not essential if one considers movement in terms of displacement of the stimulus relative to other features in the visual field.

7.1.2: The Displacement analysing system (DAS)

The DAS can be considered in the same light as the mechanisms proposed to explain the other hyperacuties, such as vernier acuity and bisection acuity (Westheimer, 1979, 1981). These reflect the highly specialised ability to localise objects relative to one another in the visual field. As originally proposed by Bonnet (1975), the DAS was assumed to operate at low velocities where the position of the stimulus over time could be remembered. That is, the initial position of the stimulus is encoded in some way and a subsequent position compared with this. It is clear that any difference between the two positions would mean that movement had occurred. This memory model was suggested by Kinchla and Allan (1969) and was supported by Henderson (1971) who found that the discrimination of movement was determined solely by its stationary components. It also finds support from Sperling's (1966) proposition that for high speed movement real and apparent motion are perceived similarly and that the motion phase is an ineffective stimulus. This would point toward the DAS operating independent of velocity rather than being restricted to low velocities only. It would seem likely that the DAS uses the same relative localisation mechanism as the other spatial hyperacuties with the addition of a temporal comparison.

An interesting investigation by Nakayama and Tyler (1981) sought to isolate the two

systems. They used two types of stimulus which would preferentially stimulate one or other of the two mechanisms. The first used random-dot patterns which give little position information and would, therefore, be a poor stimulus for the detection of relative displacement. The second type of stimulus consisted of lines which contain much more positional information and would, they concluded, be a poor stimulant for a motion detecting system. Their results confirmed that, using the random-dot pattern, the movement within the stimulus was detected by a velocity sensitive mechanism rather than a position sensitive mechanism. Using the line stimulus the opposite was found, that position information rather than movement *per se* was the factor mediating threshold determination. These results clearly point towards the presence of two distinct mechanisms underlying movement detection in the visual system.

7.1.3: The effect of references

There have been many reports which have shown that the presence of references allows displacement detection to be greatly enhanced (Aubert, 1886; Leibowitz, 1955; Kinchla, 1971; Legge and Campbell, 1981; Johnson and Scobey, 1982; Bonnet, 1984; Whitaker and MacVeigh, 1990). There is, however, some disagreement about the efficiency of references with respect to the duration of movement. Some authors claim that stationary references only improve thresholds for long durations of movement (Leibowitz, 1955; Bonnet, 1984). Others find that thresholds improve over the entire range of movement duration (Johnson and Scobey, 1982; Whitaker and MacVeigh, 1990). Leibowitz (1955) found that references only improved thresholds for long durations of movement (16 seconds). At the short exposure duration (250 msec) he found no consistent effect. Bonnet (1984), using a spot of light moving across a CRT, also found that the presence of references only had an effect for longer durations of movement. In this case the references had a significant effect for durations over 180 msec. These results are at odds with those of Johnson and Scobey (1982) who, using a moving line target, found that references reduced the displacement thresholds for all durations of movement studied (10 to 3000 msec) (*Figure 7.02*). It was found, however, that the effect was slightly more marked for the longer exposure durations.

Intuitively, reference proximity should also have a bearing on the ease with which displacements are detected. It seems logical to suggest that as the stationary reference is positioned further away from the stimulus, it must eventually cease to be an adequate stimulus in the judgment of relative position. This is, for example, the situation found in

many of the static hyperacutities where performance is highly dependent on feature separation (Westheimer and McKee, 1977a; Klein and Levi, 1985). For displacement detection, however, this would appear to depend on the type of movement employed. Legge and Campbell (1981) carried out an experiment using an instantaneous type of stop-go-stop displacement (see chapter 2), that is with no delay between the stimulus disappearing in one position and reappearing in another. They found that a stationary reference, in the form of an annulus, could be positioned between 3 minutes of arc and over 5 degrees from the moving stimulus without having much effect on displacement thresholds. Kinchla (1971) used a discrete type of movement in his experiment. This is similar to that employed by Legge and Campbell but has a time delay inserted between the disappearance of the stimulus and its reappearance in the new position. Again, the reference improved displacement thresholds but this time the effect depended strongly on the reference proximity. In fact when the reference was over about 3 degrees from the target it seemed to have no effect on thresholds. Palmer (1986), again using discrete movement, also found that reference proximity had a substantial effect on displacement thresholds. He studied the range of separations between 3 and 90 minutes of arc and found that thresholds increased steadily as separation grew (*Figure 7.03*).

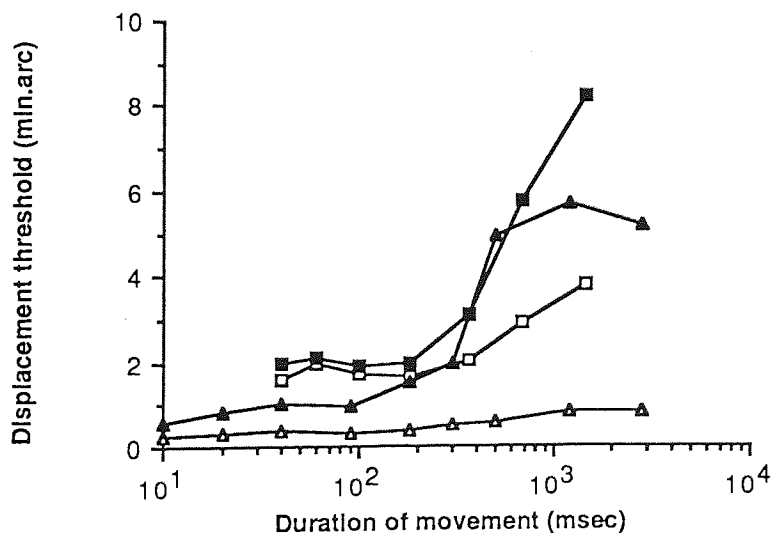


Figure 7.02: The effect of references on displacement thresholds for different durations of movement. The open squares are referenced motion and the filled squares unreferenced from Bonnet (1984). The open triangles are referenced and the filled triangles unreferenced for the observer (AM) from Johnson and Scobey (1982). The results are discussed in the text.

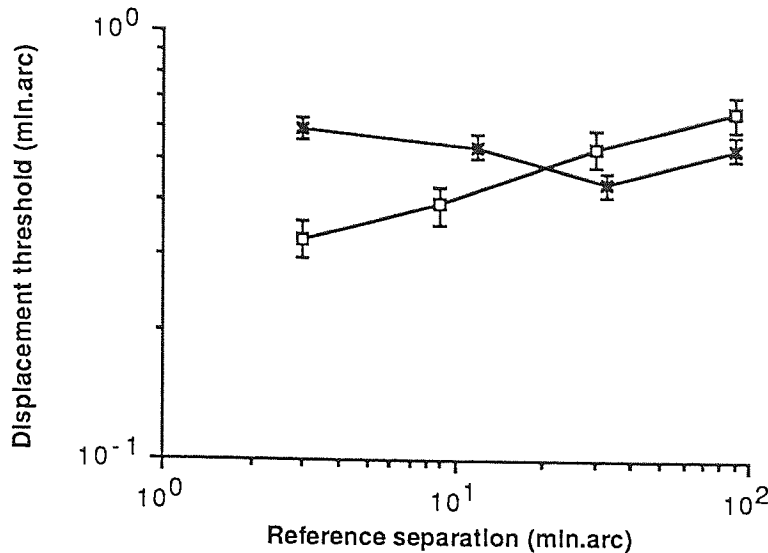


Figure 7.03: The effect of reference proximity on displacement thresholds. The crosses are the average of the two observers used by Legge and Campbell (1981) and show independence between thresholds and reference separation. The open squares are the average of the two observers used by Palmer (1986), this time it is clear that thresholds worsen as the reference separation increases.

The experiments performed here seek to answer two questions. First, over what range of temporal reference conditions are displacement thresholds improved by the presence of references? Second, what is the range of separations between the reference and stimulus over which the references aid detection of movement? An attempt will also be made to define those conditions in which movement is detected directly and those where movement is inferred by changes in the position of the stimulus relative to a reference.

7.2: Methods

The moving stimulus was presented on a high resolution color CRT under the control of the RM Nimbus AX microcomputer, details of which are contained in chapter 5. The stimulus always subtended 1 min. arc² at the eye of the observer who was positioned in a chin rest and viewed the screen from either 2 metres (experiments 1 and 2) or 6 metres (experiment 3). As was explained in chapter 5 the working distance has to be chosen with regard to the expected thresholds in order that the minimum offset produced on the CRT is well below threshold. The stationary reference, when present, consisted of a light annulus surrounding the moving stimulus. The radius of this ring determined reference separation and its width

subtended 1 minute of arc. The luminance of both moving stimulus and reference was 15 cd m^{-2} . The ring was presented on the monitor of the CRT whenever possible, but in certain conditions its diameter exceeded the dimensions of the screen. In these circumstances the reference was generated by a circular fluorescent tube masked down to the appropriate size and positioned in the same plane as the CRT screen. All experiments were conducted in total darkness so that no stationary reference points were available to the observer, apart from the circular reference when present.

As was explained in chapter 2 there are three forms of movement commonly employed in laboratory experiments. *Figure 7.04* illustrates their chief features. Discrete movement involves the stimulus appearing in one position for a certain time and then moving to another position. This movement can be either instantaneous, with no delay between disappearance in one position and reappearance in the next, or can have a temporal delay between the presentation of the stimulus in the two positions.

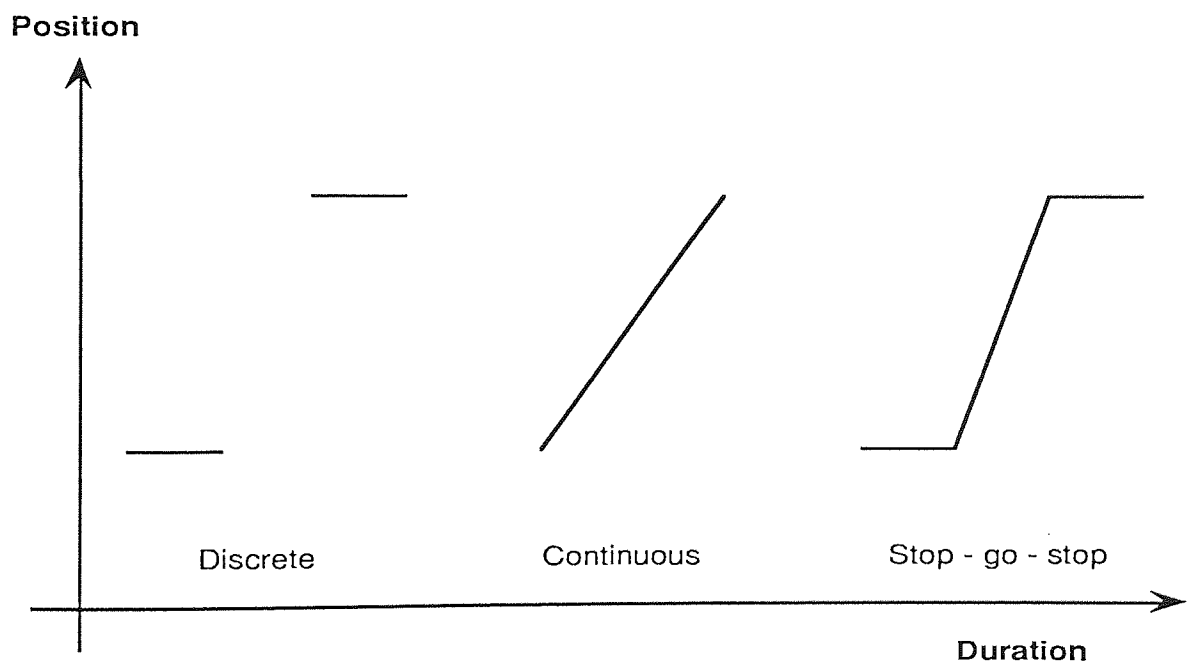


Figure 7.04: The three types of movement commonly employed in experimental situations. The duration of the stimulus exposure is shown on the x-axis. The y-axis shows the displacement of the stimulus. Thus for the discrete movement the stimulus appears for a certain period but does not move. It then disappears for another time period and then reappears at a different location where it remains for a third interval before finally disappearing. The features of the different movement types are fully explained in the text.

Continuous movement entails the stimulus appearing and immediately starting to move with a

constant velocity to a new position. Upon arrival at the new position it immediately disappears. In this situation there is no stationary position during presentation of the stimulus. Finally, in stop-go-stop movement, there is a combination of the other two with a stationary period preceding and following a period of continuous movement. In terms of the two systems discussed earlier it is clear that in order for the MAS to operate there has to be a continuous phase in the movement. The DAS on the other hand is better activated by stationary information, thus discrete movement would be the best stimulus. For stop-go-stop movement either system could conceivably be used to determine threshold.

For continuous movement the exposure duration was varied between 100 and 1000 msec. Values below 100 msec could not be replicated with sufficient accuracy owing to limitations in the computer hardware. In any case, an instantaneous continuous displacement would have no counterpart in nature. It would involve the stimulus appearing simultaneously at two different points instantaneously. This would then imply an infinitely large velocity in moving from one position to the next. Clearly such a configuration would be of no practical value. For stop-go-stop movement the moving phase lasted between 0 and 1000 msec. It was preceded, and followed, by stationary phases lasting 500 msec. The use of the 0 msec movement phase effectively replicates the instantaneous displacement stimulus used by Legge and Campbell (1981). The stimulus was made to randomly move either to the left or to the right as seen by the observer who responded via a mouse, pressing the right hand button if movement was to the right and vice-versa. From this response the computer determined the amplitude of displacement for the next presentation. Thresholds were measured using a staircase technique with presentations converging around threshold according to a transformed up-and-down rule (Wetherill and Levitt, 1965). In this way an estimate of the 71% point on the psychometric function was obtained. Initial starting point on the staircase was always clearly suprathreshold, and the step size was reduced during the run. The run terminated after ten reversals with thresholds estimated using the average of the last seven. The observers were myself (DM) and my supervisor (DW), both of whom were highly practised at these judgments. Both are moderately myopic and wore their full refractive correction during all experiments. Viewing was monocular with the dominant eye being used.

7.3: Experiment 1, the "no reference" condition

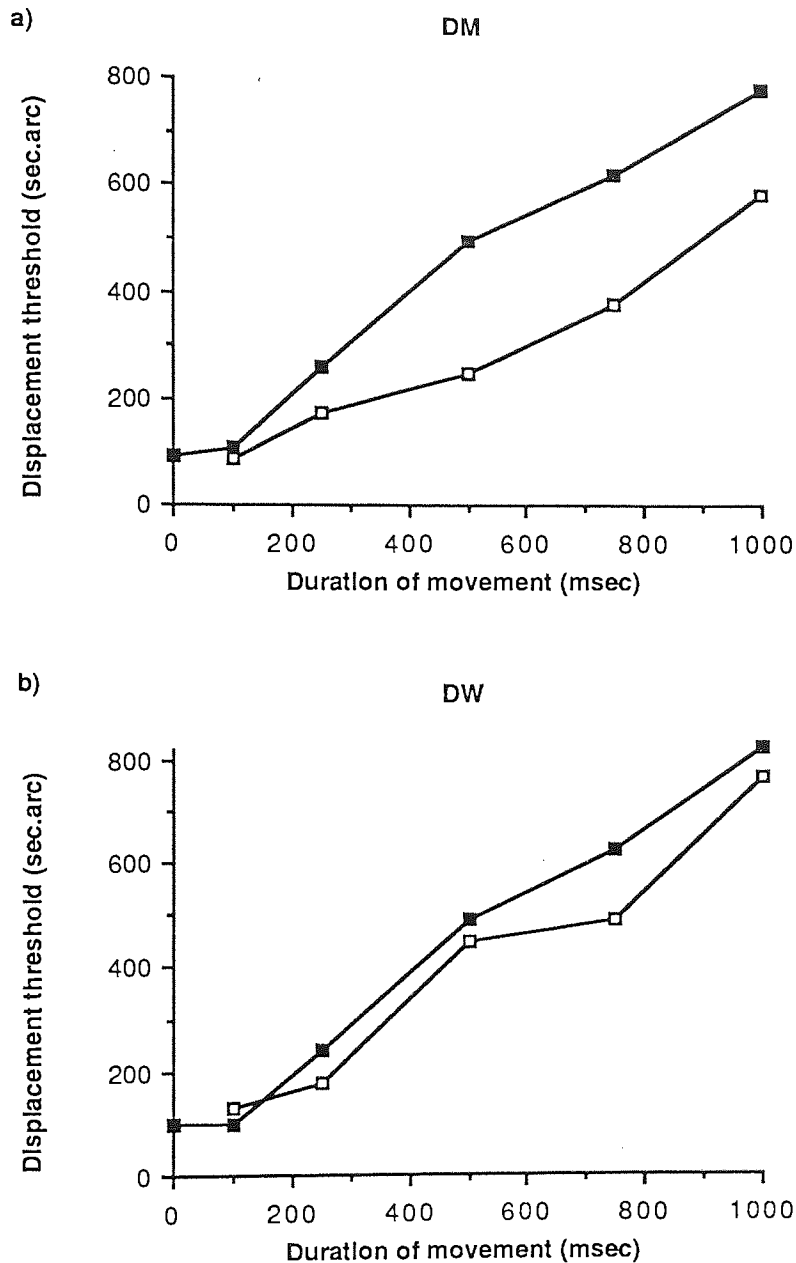


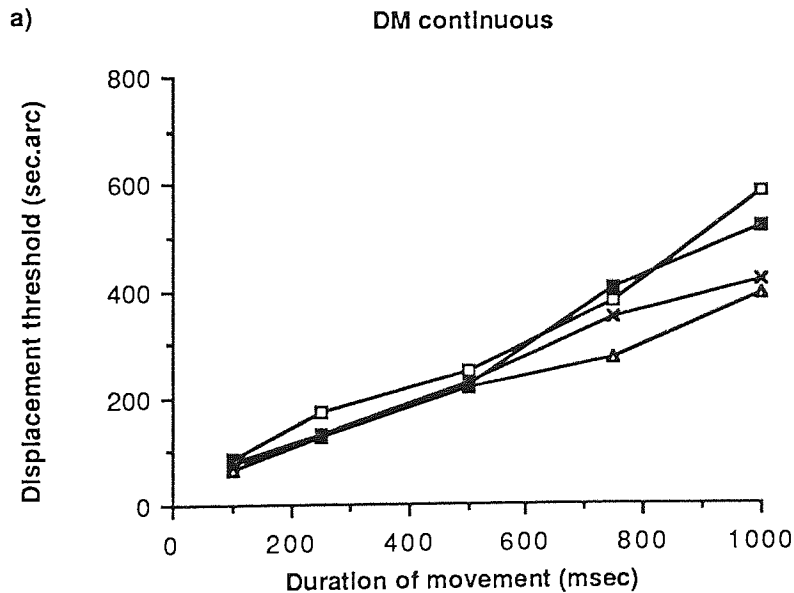
Figure 7.05: Displacement thresholds plotted against duration of movement for the two observers, DM (upper) and DW (lower). Solid squares represent stop-go-stop movement while open squares represent continuous movement. Each data point represents the average of four threshold measurements. The mean standard error, averaged across observers and types of movement, was 7% of threshold. Above 100 msec both graphs demonstrate that thresholds are proportional to duration, reflecting a constant velocity requirement to reach threshold. Below this value the stop-go-stop condition levels off thus departing from the constant velocity prediction.

The first experiment investigated displacement detection in the complete absence of references. *Figure 7.05* shows displacement thresholds plotted against duration of movement, for both observers, for continuous and stop-go-stop types of movement. Each data point represents the mean of four threshold estimates. For continuous movement it is clear that displacement thresholds increase approximately linearly as duration increases. Linear regression analysis of the data for DM reveals a slope of 9.3 min arc/sec ($r=0.99$). This result, therefore, indicates that if the stimulus velocity exceeds this value detection of movement will occur irrespective of its duration. The value for subject DW, under the same conditions, was 12.4 min arc/sec ($r=0.98$). This compares with results for continuous unreferenced movement obtained by Leibowitz (1955; ≈ 9 min arc/sec) and Bonnet (1984; 7.2 min arc/sec). The results for the stop-go-stop movement show a similar pattern for durations over 100 msec, with slopes of 14.1 min arc/sec for DM ($r=0.98$) and 14.3 min arc/sec for DW ($r=0.99$). However, below 100 msec this linearity fails and the threshold values depart from the constant velocity prediction. In fact below 100 msec there is an independence between displacement thresholds and exposure duration. Above 100 msec, therefore, stop-go-stop movement behaves in the same manner as continuous movement requiring a constant velocity to determine threshold. Below 100 msec, however, this relationship no longer holds true.

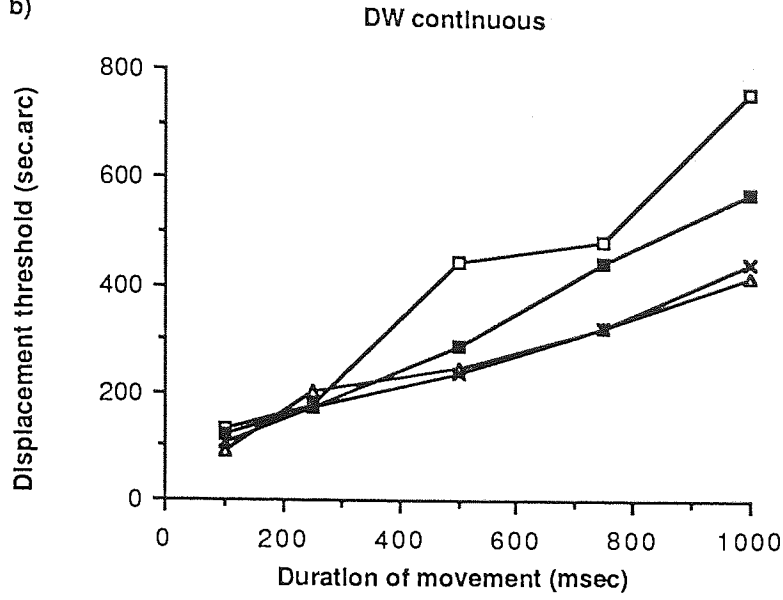
7.4: Experiment 2 - non simultaneous reference presentation

The second experiment demonstrates the effect of presenting a stationary reference immediately prior to the appearance of the moving stimulus. The references were displayed for a 500 msec period immediately before the stimulus appeared but were then extinguished. At no time, therefore, were the reference and stimulus visible together. The graphs again show displacement thresholds plotted against duration of movement, and, as in experiment 1, each data point represents the mean of four threshold estimates (*Figure 7.06*). The results for reference separations of 4, 40 and 400 minutes of arc are plotted on each graph together with the no reference condition from *Figure 7.05*. It should be noted that thresholds were also measured at separations of 12 and 120 minutes of arc. These followed the same pattern as the data presented here, but have been left out of the figure to improve clarity. For continuous movement presenting references in this manner improves thresholds slightly for long durations of movement. The effect is, however, only really apparent for the smaller reference separations. Stop-go-stop movement again shows a slight improvement in thresholds compared with the no reference condition. This time, however, the reference separation

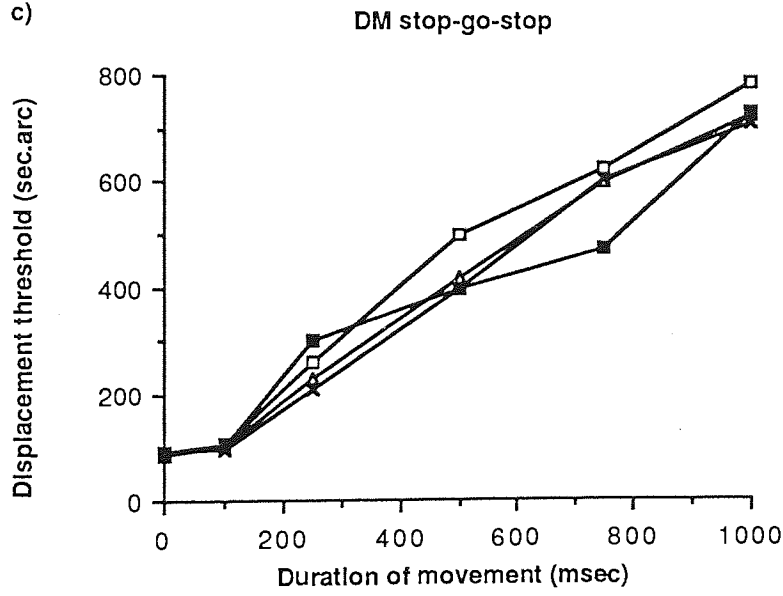
shows no consistent effect on thresholds. In the same manner as the unreferenced displacements, thresholds above 100 msec correspond well with a constant velocity prediction. Again this is not the case for the lowest duration where thresholds level off. In both the unreferenced experiment and this experiment, stop-go-stop thresholds for exposure durations over about 200 msec were found to be generally greater than continuous thresholds. This reflects reports from both observers that the stop-go-stop thresholds caused greater difficulty as movement was frequently seen in both directions during a single presentation. This is probably the result of the acceleration characteristics of the stimulus, with an apparent reverse movement occurring when the stimulus suddenly decelerates at its end point.



b)



c)



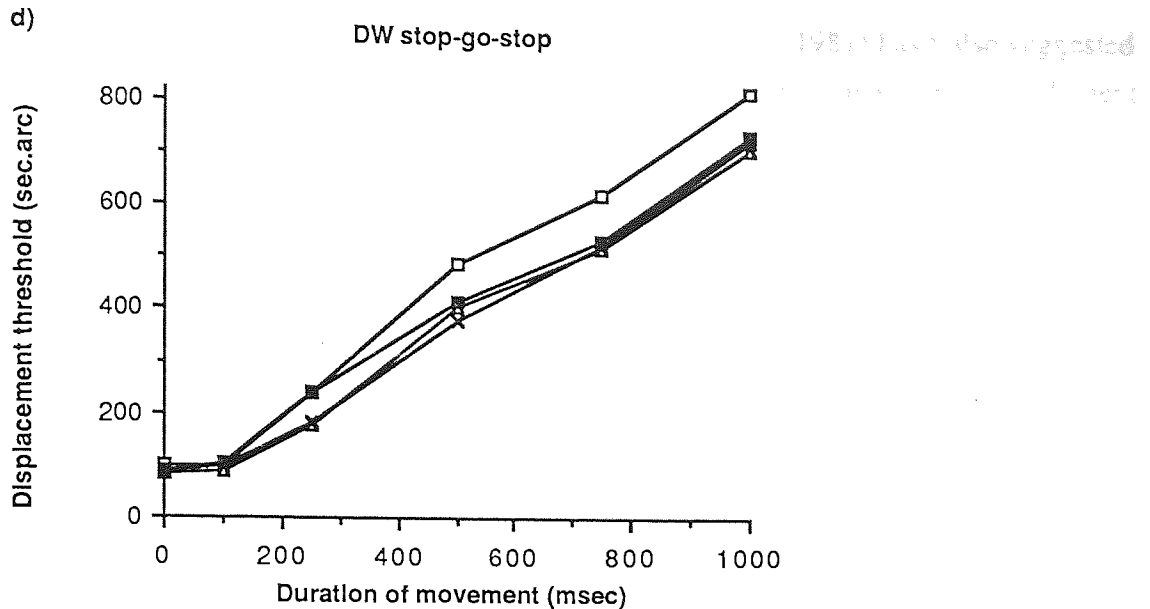


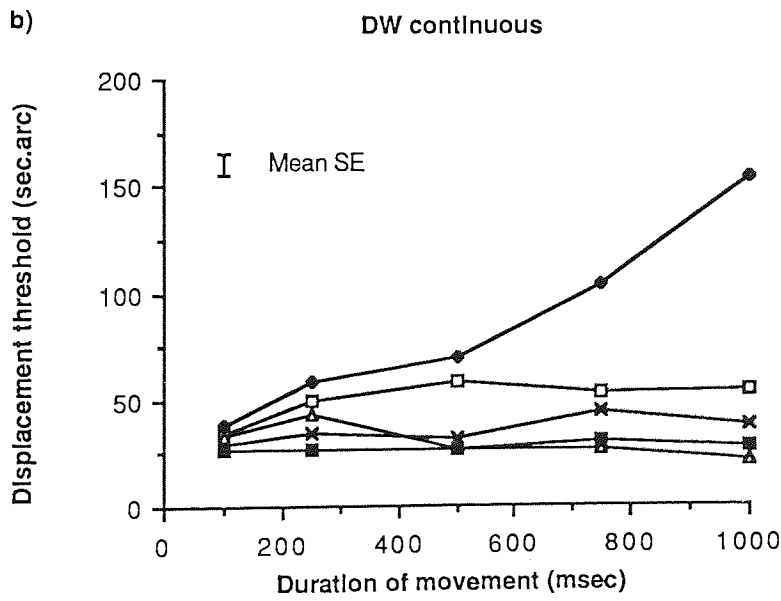
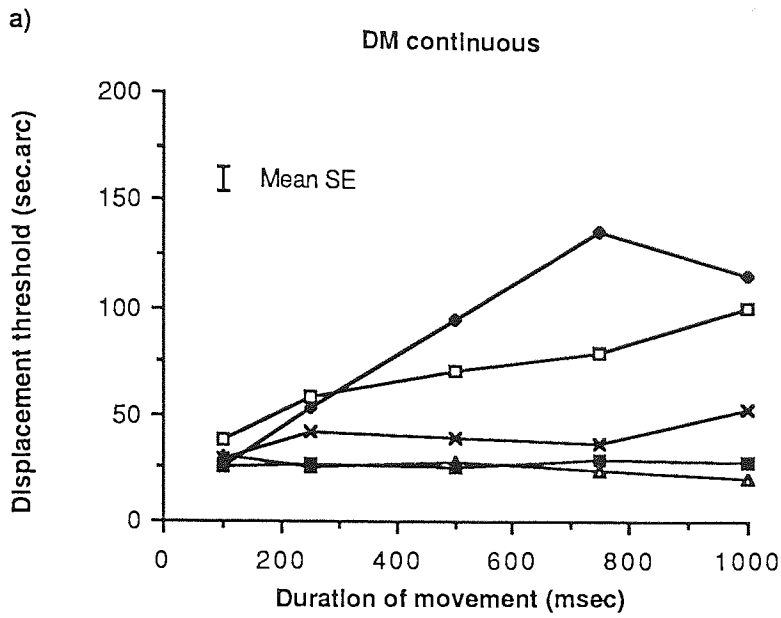
Figure 7.06: Displacement thresholds plotted against duration of movement for both observers. Two types of movement are involved, continuous (a/b) and stop-go-stop (c/d). Open triangles represent a reference separation of 4 minutes of arc; crosses 40 minutes of arc; filled squares 400 minutes of arc and open squares the no reference condition from *Figure 7.05*. The mean standard error, averaged across observers and types of movement, was approximately 8% of threshold. In this experiment the references were present for 500 msec prior to the movement phase of the stimulus but were then extinguished. Results were also obtained for reference separations of 12 and 120 minutes of arc but have been omitted for clarity.

7.5: Experiment 3 - continuous reference presentation

In this experiment the reference was displayed for 500 msec prior to the appearance of the moving stimulus, as in experiment 2. This time, however, it remained in place throughout the period of stimulus presentation. It quickly became apparent that, at least for stop-go-stop presentations, a bisection judgment of the final stimulus position relative to the reference provided a clue as to the direction of the movement. If, for example, the stimulus finished its movement phase nearer to the right side of the reference circle, it was an obvious deduction that it had moved rightward. For the smallest reference separation this decision could also be reached using a relative brightness clue as was discussed in chapter 2 (Klein and Levi, 1985). Clearly these clues had to be eliminated and in order to do this the starting position of the stimulus was randomly jittered to either side of the center of the circular reference with a standard deviation of 0.62 minutes of arc. A computer simulation was then run which revealed that thresholds, taking account of this random jitter, would be about four times greater than those observed if responses were made solely on the basis of final stimulus position. This clearly shows that the randomly varied starting position eliminates luminance

or bisection clues as mediators of the task. Legge and Campbell (1981) have also suggested that the mechanism underlying displacement detection does not rely on a bisection judgment for a reference separation greater than 20 minutes of arc.

Figure 7.07 shows displacement thresholds plotted against duration of movement for the five reference separations between 4 and 400 minutes of arc. Given the magnitude of the mean standard error shown in the figure, it is immediately apparent that both duration of movement and reference proximity are highly significant. In addition, there is clearly a significant interaction between these two variables. Thresholds for small durations show only a small dependence on reference separation. As duration of movement increases, however, there is a tendency for thresholds at the largest reference separations (120 and 400 minutes of arc) to be considerably greater than the smaller (4, 12 and 40 minutes of arc). It is also apparent that the presence of the reference greatly improves displacement thresholds at *all* durations of movement for both continuous and stop-go-stop presentations. This is reinforced by the fact that the y-axis extends only from 0 to 200 seconds of arc instead of 0 to 800 seconds as in *Figures 7.05* and *7.06*. It is, however, still true that thresholds are improved more markedly for the longer durations of movement. Indeed, when reference separations are small, under about 40 minutes of arc, displacement thresholds are essentially independent of the duration of the movement. The minimum velocity criterion for determination of displacement threshold no longer holds and, instead, a minimum displacement determines the detection of stimulus movement. Regardless of movement duration any displacement which exceeds this threshold will be detected. It should also be noted that the lowest minimum displacement thresholds obtained under these conditions approach an order of magnitude less than those obtained in the two earlier experiments. Indeed, under optimum conditions, these thresholds are as low as 10 seconds of arc which reinforces the view that the displacement threshold represents a hyperacuity. This time, now that references are constantly present, the stop-go-stop condition tends to give lower thresholds than the continuous mode, the reverse of what was found in the first two experiments.



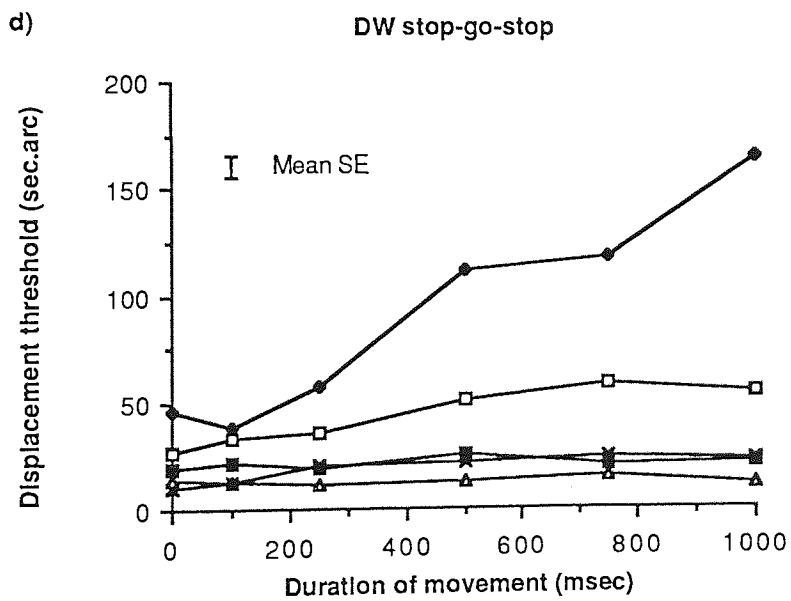
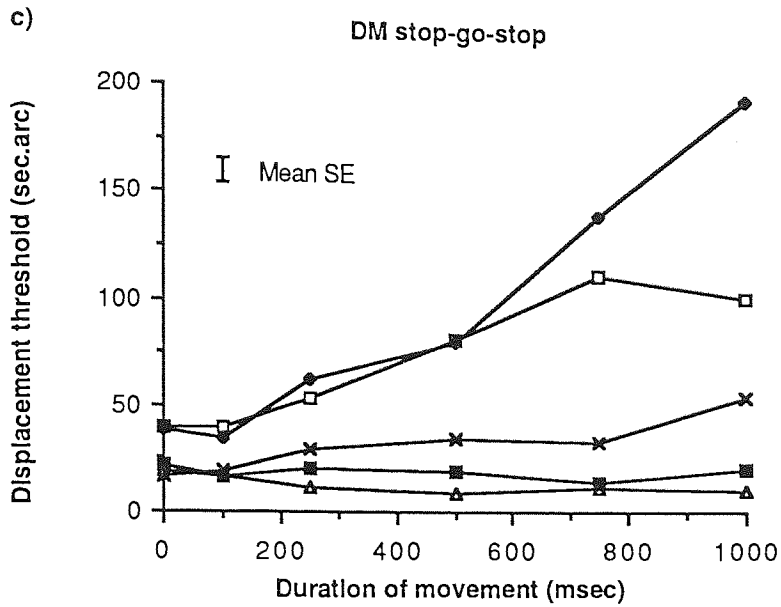


Figure 7.07: As for Figure 7.06 but this time with the references present throughout the presentation. (a/b) show the results for continuous movement, (c/d) for stop-go-stop. The reference separations are 4 minutes of arc (open triangles); 12 minutes of arc (filled squares); 40 minutes of arc (crosses); 120 minutes of arc (open squares) and 400 minutes of arc (filled diamonds). The mean standard error is shown for each graph.

7.6: Discussion

7.6.1: Movement detection in the presence of references

The results clearly show that the presence of nearby stationary references makes the detection of movement easier regardless of the duration or type of movement. This, therefore, agrees with the findings of Johnson and Scobey (1982), but not with Leibowitz (1955) and Bonnet (1984) both of whom suggested that references only had an effect at longer durations of movement. It is clear, however, that reference proximity is also an important factor. *Figure 7.07* demonstrates that, for references close to the moving stimulus, thresholds are essentially independent of movement duration. However, as the reference is moved away from the stimulus this independence no longer seems to hold. In similar fashion to the unreferenced condition, thresholds at longer durations of movement are higher, although the effect is much less marked. For small reference separations one would expect movement to become easily apparent because of the relative displacement of the stimulus and the reference. However, the larger the separation between reference and stimulus the less useful it should become in determining this relative displacement. The effect is, to some extent, clearly dependent on the duration of stimulus movement. Short exposure durations show little dependence on reference proximity, but at longer durations and larger separations the effect becomes quite marked. Thus, for long exposure durations or a long inter-stimulus interval for discrete movement, one would expect that the facilitatory effect of references would be pronounced only when they are close to the moving stimulus. This result therefore provides an explanation for the apparently inconsistent findings of Legge and Campbell (1981), who showed no effect of reference separation using an instantaneous type of displacement, and of Kinchla (1971) and Palmer (1986), who used a discrete type of movement with an inter-stimulus interval, and did find a separation effect. The obvious deduction to make from this is that the referenced results presented here provide evidence for a transition, with increasing reference separation and movement duration, from the DAS to the MAS in the determination of thresholds.

It has been stated several times already that the visual system is extremely sensitive to referenced displacement where two components have to be relatively localised. Thresholds well below the eye's resolution limit are frequently obtained. The results obtained here, at best around 10-15 seconds of arc, compare favorably with results found in such static hyperacuties as vernier and bisection acuity. These, of course, also require accurate relative

localisation of the stimulus components. There are two differences, however, between the static hyperacuties and displacement detection. The static hyperacuties, as was explained in chapter 2, are critically dependent on the spatial separation of the stimulus features (Westheimer and McKee, 1977a; Klein and Levi, 1985). This is thought to reflect the lower sensitivity of the larger receptive fields which have to be involved as the separation is increased (Wilson, 1986). Clearly, for short exposure durations, the present results demonstrate independence of displacement thresholds and reference separation. This has also been reported by Legge and Campbell (1981) and Whitaker and Elliott (1989). This may be due to the second difference between static hyperacuties and displacement detection. In the displacement task it is necessary to compare the stimulus over time. On the other hand, most of the static hyperacuties give all the information required to perform the task in one presentation. In the spatial domain it is assumed that interpolation amongst neural units allows the relative location of two objects to be determined even when they have noisy absolute locations. Indeed, a certain amount of noise in the form of blurring of the retinal image is a prerequisite for the attaining of hyperacuity levels of performance (see chapter 1). It has also been shown that some hyperacuties demonstrate a resistance to further optical blurring (Williams *et al.* 1984; Buckingham and Whitaker, 1986). For displacement detection one could conceive a similar situation in the temporal domain. This time the relative location of the stimulus features is compared over time and changes in this parameter used to infer movement. The results shown in *Figure 7.07* would seem to indicate that this is far more resistant to the effect of reference separation than the static hyperacuties. This would imply that despite the location of the stimulus relative to the reference becoming increasingly uncertain with growing separation the temporal comparison is relatively unaffected by the increasing noise in the system. However, the temporal comparison is markedly affected by any time delay interposed between the stimulus and reference. For displacement detection, therefore, it would appear that temporal separation of stimulus and reference is critical in order to allow hyperacuity levels of performance to be obtained.

7.6.2: Movement detection without references

It is readily apparent that in the absence of references displacement detection thresholds are entirely different from those obtained with references. *Figure 7.05* shows that both continuous and stop-go-stop movement, for durations of movement over 100 msec, require a certain minimum velocity to be detected. Under such conditions it is clear that a different system from the DAS suggested above must be operating, Bonnet's MAS being the obvious

candidate. For very short exposure durations this appears to break down and threshold values level off (Johnson and Scobey, 1980; Legge and Campbell, 1981; Post, Scobey and Johnson, 1984). Projecting the best fitting straight line through the data in *Figure 7.05* below 100 msec one would expect displacement thresholds to continue to reduce, eventually reaching close to zero when movement duration reached zero. As can be seen from the stop-go-stop results this is not the case with thresholds levelling off at around 100 seconds of arc. The original models of directional selectivity assume two spatially separate receptors, the response of one of these being subject to a short time delay (Reichardt, 1961; Barlow and Levick, 1965). *Figure 7.01* shows how a directionally selective unit may be constructed. More recently Van Santen and Sperling (1984) produced a modified version of the original Reichardt detector which eliminated the problems of aliasing found in the earlier model. All of these models impose a lower threshold of displacement approximately equal to the minimum receptor spacing. It will not respond reliably for stimulus displacements less than this spacing. On the other hand, Marr and Ullman (1981) and Watson and Ahumada (1985) have developed models which use a combination of spatial and temporal filters to encode information regarding image velocity and direction without the need for the stimulus to traverse two spatially separate receptors. These models should, therefore, be sensitive to extremely small displacements. However, these models cannot function properly for stimuli whose duration is shorter than the time constant of transient channels, this being dependent upon the state of adaptation. Adopting this model, therefore, imposes a lower threshold of exposure duration rather than displacement.

Previous investigations which have sought to study movement detection using instantaneous displacements must be treated guardedly. The fact that instantaneous displacements can be detected, even without references, begs the question as to which system is employed. The absence of a movement phase would appear to rule out the MAS in such circumstances. As an alternative certain researchers have suggested a "memory" model in which the new position of the stimulus is compared with its previous location (Boyce, 1965; Kinchla and Allan, 1969; Kinchla, 1971). The model could only be expected to operate over a relatively short time scale as eye movements would destroy the memory of previous location. Tulunay-Keesey and VerHoeve (1987), in an investigation into the role of eye movements in motion detection, found that stabilising the retinal image considerably improved sensitivity for long durations of movement but had no effect short durations. This clearly implies that for short exposure durations eye movements have no effect on motion detection. Instantaneous movement may, therefore, be detected using the retinal photoreceptor matrix as a grid. Elimination of eye movements would cause the movement across the retina to

stimulate different groups of photoreceptors. The fact that stimulation had moved from one group of photoreceptors to another would be an indication, in these admittedly artificial circumstances, that movement of the stimulus had occurred. For short periods it may therefore be possible that the sudden change in location of the retinal stimulation may act as a similar indicator of movement.

7.7: Conclusion

It is interesting that Westheimer and Hauske (1975) in their investigation into vernier acuity found that any temporal delay between the presentation of the two stimulus components markedly worsened thresholds. In addition, spatial interval detection in which the two stimuli are presented sequentially with a time delay, also worsen rapidly with increasing temporal delay (Westheimer, 1979). These results would suggest that in order to perform tasks with hyperacuity precision the information regarding the *spatial* localisation of the stimulus features has to be available simultaneously. In similar vein the results presented here suggest that in order for the displacement of an object to be detected with hyperacuity precision a spatial relative localisation is necessary. Thus, under these conditions, displacement can be thought of as a detection of changes in a succession of such relative localisations. Only when simultaneous presentation of targets and references is made can displacement detection be thought of as a hyperacuity.

In the absence of references, both in the spatial and temporal domain, the direct detection of the movement of the object would appear to mediate performance. There is one exception in that for stop-go-stop movement at very short durations (below 100 msec) some form of "memory" model may allow an explanation of the mechanism underlying detection. Previous investigations which have sought to study *movement* detection using instantaneous displacements should, therefore, be treated guardedly.

Chapter 8: Spatial frequency and vernier acuity

8.1: Introduction

Chapter 3 of this thesis outlined the concepts of the two models which have been developed to attempt an explanation for the phenomenon of hyperacuity. The local-sign models require the allocation of some tag to the stimulus features which enables their location to be defined. In order to carry out a relative localisation task, however, the positions of these tags then have to be compared, by means of some secondary processing, in order to enable the task to be performed with hyperacuity precision (Sullivan *et al.* 1972; Watt and Morgan, 1983; Morgan *et al.* 1990). The channel model does not require this explicit feature location to be known, instead computing an implicit representation of the stimulus using the outputs of filters tuned to different orientations, phase and spatial frequencies (Carlson and Klopfenstein, 1985; Klein and Levi, 1985; Wilson, 1986).

The extremely low threshold values characteristic of these hyperacuity tasks is, however, dependent on the exact stimulus configuration (Westheimer and McKee, 1977a). In the traditional vernier acuity task, for example, it is necessary for the lines to be at least 4 minutes of arc long (Westheimer and McKee, 1977a). Similarly, the two dot vernier acuity task requires that there is a gap between the dots of between 2 and 6 minutes of arc in order for optimum thresholds to be obtained (Sullivan *et al.* 1972; Westheimer and McKee, 1977a). Similar results have been obtained for spatial interval detection and in the judgment of orientation (Andrews *et al.* 1973; Westheimer, 1979). In addition, experiments using interfering targets in close proximity to the main stimulus features have shown that these strongly degrade vernier acuity if placed in a region centered around 3 minutes of arc from the stimulus (Westheimer and Hauske, 1975; Badcock and Westheimer, 1985). There are two clear implications from these results. The first is that the vernier task is carried out using information from a restricted area of the whole stimulus. The second that this zone extends beyond the stimulus to encompass an area of visual space approximately 6 minutes of arc in diameter.

Which of the two models can best explain this integration zone? Using the local-sign model it would seem, at first sight, unlikely that spurious features should have an adverse effect unless they are so close as to be optically inseparable from the main stimulus features. The presence of several local sign tags in close proximity could, however, make the secondary

localisation stage more imprecise. In the channel model the presence of interfering features can be explained simply because they would distort directly the output of the filters and thus introduce errors into the relative location of the stimulus features.

This would, on the grounds of parsimony if nothing else, support the channel model in preference to the local-sign models. There is a further area in which the two models would be expected to provide different results. It is this second area, the interaction between spatial frequency content and separation of the stimulus features, which the two experiments covered by this chapter seek to investigate.

A vernier acuity task was used in which the observer had to detect an offset between two sinusoidal contrast gratings. Traditional stimulus configurations, using dots and lines are usually high contrast, spatially localised and have a broad spatial frequency spectrum. The larger filters, which have lower spatial frequency tuning, have a broader orientation and spatial frequency bandwidth. This implies that such low frequency filters are less able to precisely locate the stimulus relative to higher spatial frequency tuned filters (see chapter 3). For the high spatial frequency filters small positional changes cause a relatively large change in the filter output. It is here that the difference between the two models should become apparent. The local-sign models would be intuitively expected to show a worsening in positional accuracy as the spatial frequency of the target is reduced. However, there is no reason to suppose that they would show a differential response to separation as a function of spatial frequency. The relative location of two local signs would be expected to become more uncertain with separation, but there is no reason why this should also depend on the precision with which the feature location is made. The channel models, on the other hand, automatically imply a relationship between separation and spatial frequency. As was mentioned in chapter 3, as the separation of the stimulus features increases, the high frequency filters are unable to provide the necessary information to enable relative location to be determined as they do not fully cover both parts of the stimulus. The result of this is that one would expect thresholds to worsen with increasing separation of the stimulus features, and this is what has been found. If, instead of using broad spectrum stimulus features, one uses gratings in which the spatial frequency content can be controlled, it would be expected that thresholds for high frequency gratings would worsen with increasing separation at a much faster rate than for low frequency gratings.

In addition, the vertical extent of filters tuned to low frequency stimuli would be expected to

be bigger than those for high frequency targets. Using thin strips of gratings, with various separations between them, optimum thresholds would be expected to be obtained from those strips separated sufficiently to give the best sensitivity at that particular spatial frequency. This is again based on the assumptions implicit in the channel models. For the same reason as given above, the local-sign model would not directly predict this result for gratings of different spatial frequencies.

8.2: Method

All the stimuli employed in this group of experiments consisted of vertically orientated sinusoidal gratings placed one above the other. The gratings were presented on a high resolution color CRT. Generation of the gratings was undertaken by the VENUS visual stimulator under application software control. In this way the spatio-temporal output to various pre-defined parts of the screen could be controlled independently. The screen refresh rate was 120 Hz.

For all experiments the stimulus consisted of two gratings which subtended 32 minutes of arc vertically and 1 degree horizontally (*Figure 8.01*). The mean luminance of the gratings was 120 cd/m^2 and contrast was maintained at 80% Michelson contrast. The upper grating was offset, either right or left, relative to the lower and the observer had to decide upon the direction of offset. Viewing distance was 6 meters under moderate room illumination. The minimum step size available was a constant 1.4 degrees of phase angle which allowed a minimum offset of 14 seconds of arc for a grating of 1 cycle per degree and 0.875 seconds of arc for a grating of 16 cycles per degree. These values are considerably smaller than the lowest vernier thresholds recorded during the experiments. With repetitive gratings the maximum offset is clearly 180 degrees of phase angle. At this angle the physical offset between the two gratings reaches a maximum value and then begins to reduce as the phase angle increases further.

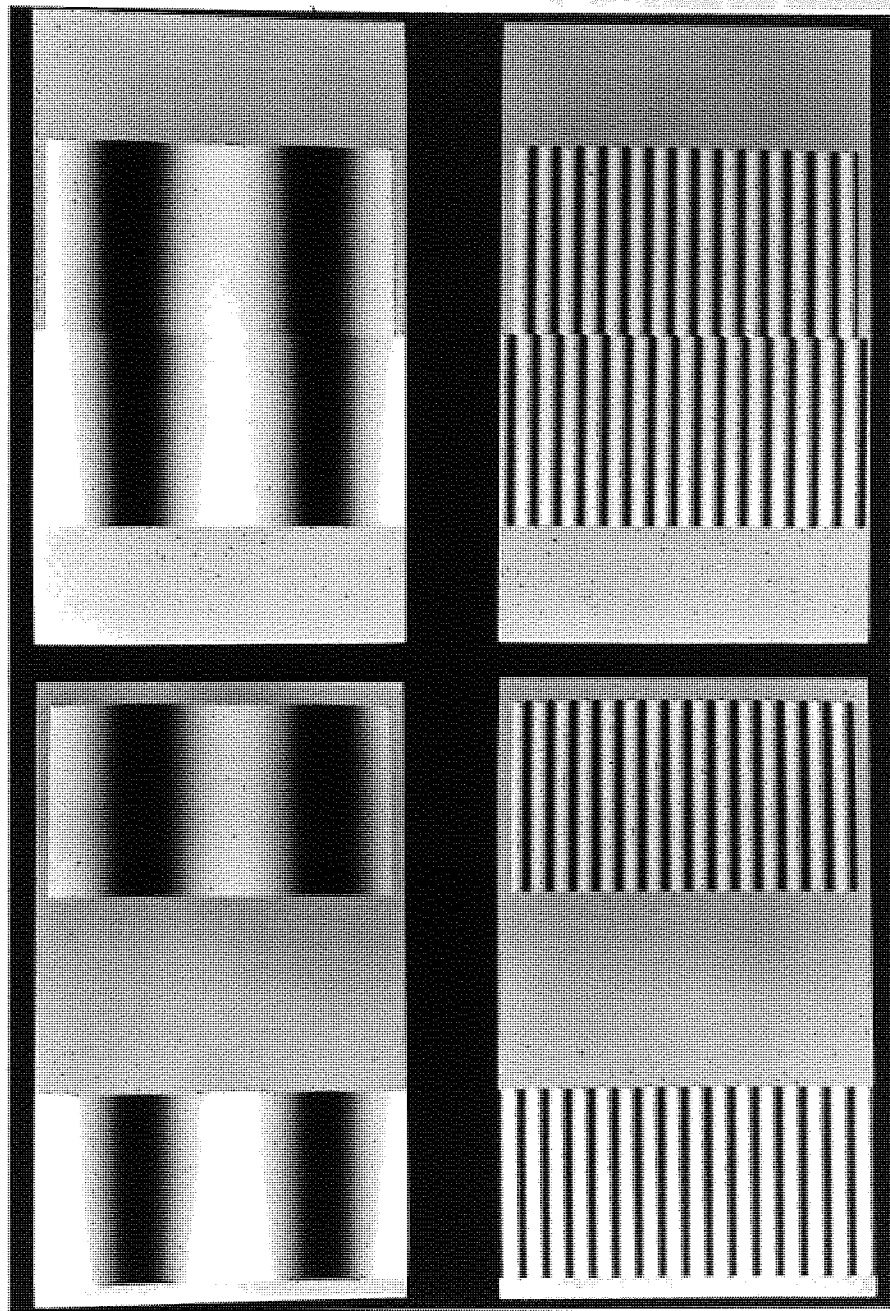


Figure 8.01: The stimuli used in experiment 1. The photographs give examples of the spatial frequency gratings employed. The upper left is a low (2 cycles per degree) frequency the upper right a high (16 cycles per degree) frequency. These represent the abutting stimuli, details of which are included in the text. The lower figures show the same gratings but with a 32 minute of arc separation between their inner edges.

The aim of the experiments was to determine vernier thresholds and with this in mind it was necessary to exclude the edge of the screen as a possible reference target. The horizontal position of the two gratings was therefore jittered at random between trials in the range 0 to 120 degrees of phase angle. In addition, the horizontal extent of the upper target was shortened to 55 minutes of arc in comparison to the 1 degree extent of the lower grating. This reduced the possibility of using luminance differences at the edge of the stimulus as a basis for deciding the direction of offset. Finally the observers, who both trained for a considerable period before data collection began, were instructed to concentrate on the center of the screen and attempt to ignore edge information as far as practicable. The observers, both moderately myopic, viewed the screen using their dominant eye and were fully corrected throughout the experiments. Each trial was presented until the observer responded via the keyboard. The initial offset was approximately 0.3 log units above threshold, calculated from the earlier practice runs. Subsequent presentations were determined by the computer using a modified PEST technique (see chapter 4). The 80% point on the psychometric function was estimated for two randomly interleaved staircases, one starting to the left, the other to the right. The mean value of these two estimates was taken to be the observer bias (position of subjective alignment). The threshold value was taken as half the distance between the two final estimates. This separation of sensitivity and bias is important in tasks such as vernier acuity as it cannot be assumed that the two values are independent of changes in the stimulus parameters. All results obtained are the mean of four individual estimates with all variable parameters, usually spatial frequency and separation, interleaved at random.

In experiment 1 the gratings were presented with a variable separation between them. The separations were 0, 4, 8, 16 and 32 minutes of arc. At each separation vernier thresholds were obtained for a selection of spatial frequencies. Threshold measurements for all separations were possible at 1, 2 and 4 cycles per degree. However, for 8 and 16 cycles per degree thresholds could only be obtained for the smaller separations since threshold values began to rapidly approach 180 degrees of phase angle as separation increased.

As was explained earlier the maximum offset possible corresponds to a 180 degree phase angle. A separate experiment, therefore, determined the spatial frequency, for each separation, at which the gratings could be identified as being in or out of phase. The PEST technique was employed in order to estimate the spatial frequency at which 80% correct phase identification could be determined, *i.e.* the cut-off frequency.

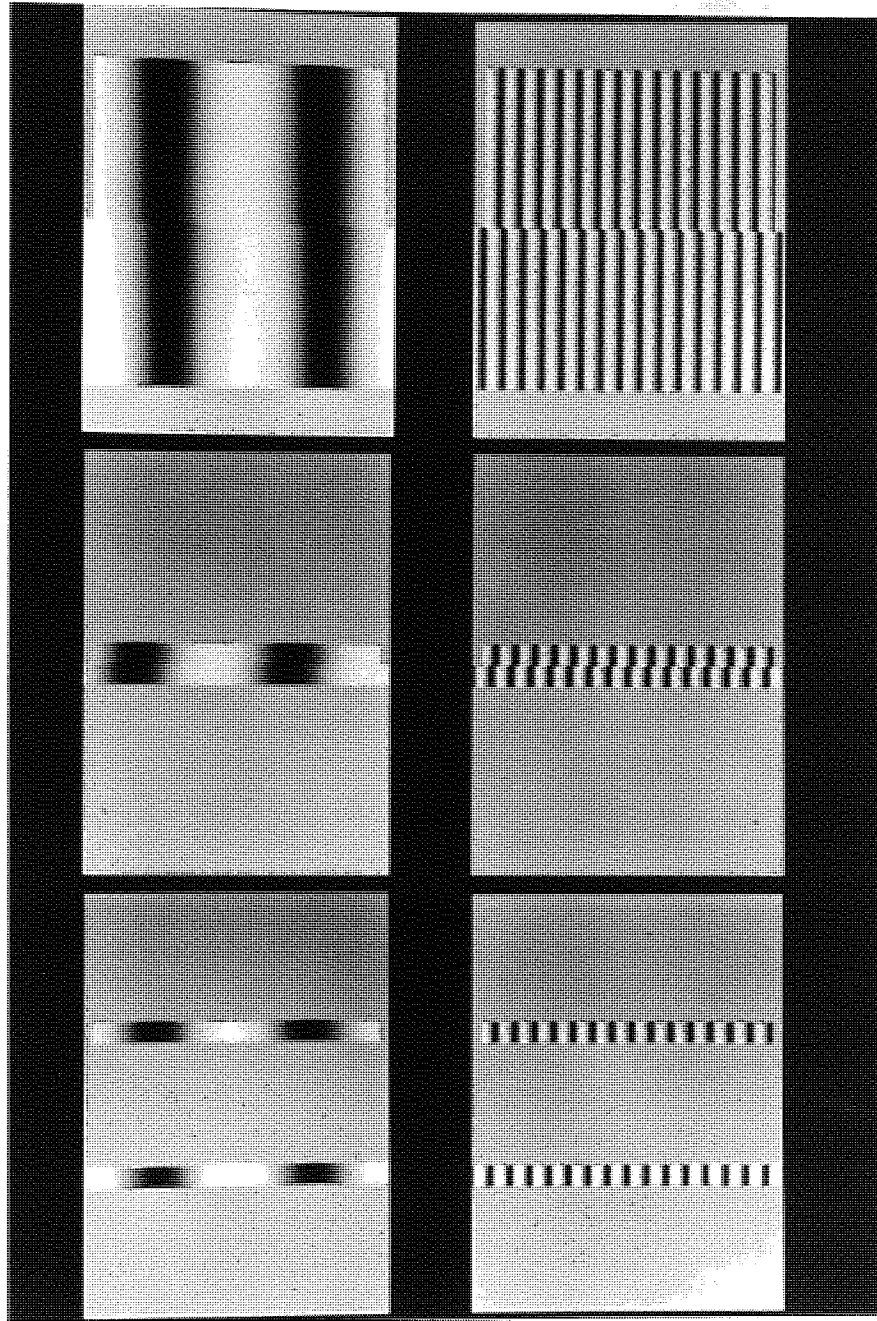


Figure 8.02: The gratings employed in experiment 2. The upper photographs show the full gratings with the low spatial frequency gratings on the left and the high spatial frequency gratings on the right. The center pair of photographs shows the abutting strips, each 4 minutes of arc wide. The lower photographs show strips from the centers of the full gratings their inner edges separated by 16 minutes of arc.

In order to decide which part of the stimulus gives information needed to carry out the vernier task, experiment 2 divided the gratings into horizontal strips, again with a variable separation between them. The strips were 4 minutes of arc high and represent different parts of the full grating (*Figure 8.02*). The inner edges of the strips were positioned between 0 and 16 minutes of arc from the center of the stimulus. Once again, the limiting spatial frequency for each separation was determined using a stimulus which estimated 80% correct phase identification.

8.3: Results

8.3.1: Experiment 1

Figure 8.03 shows the results of experiment 1 with vernier threshold plotted as a function of spatial frequency for different grating separations. For zero separation the optimum threshold is around 6 seconds of arc and occurs for spatial frequencies of 8 and 16 cycles per degree. Thresholds increase either side of this peak with the deterioration much more rapid for higher frequencies. In quantitative terms this experiment gives much lower threshold values than those obtained by Bradley and Skottun (1987). They do, however, correspond closely to the unpublished data of Morgan (1984) which is reported in Wilson (1986) and to the predicted values calculated using the spatial frequency model of Wilson (1986) (*Figure 8.04*).

The characteristic shape is also similar to that obtained by other workers. Bradley and Skottun (1987) proposed that this supported the existence of three regions determined by the differential response of vernier thresholds to spatial frequency and contrast.

1. At low spatial frequencies thresholds improve with increasing spatial frequency indicating that phase angle has a role to play in the determination of threshold.
2. The second region is a plateau where optimum thresholds are obtained over a range of spatial frequencies. This corresponds to an area where the improvement in vernier thresholds with increasing spatial frequency is countered by the reduction in contrast sensitivity.
3. As contrast threshold is approached there is a rapid deterioration in vernier thresholds.

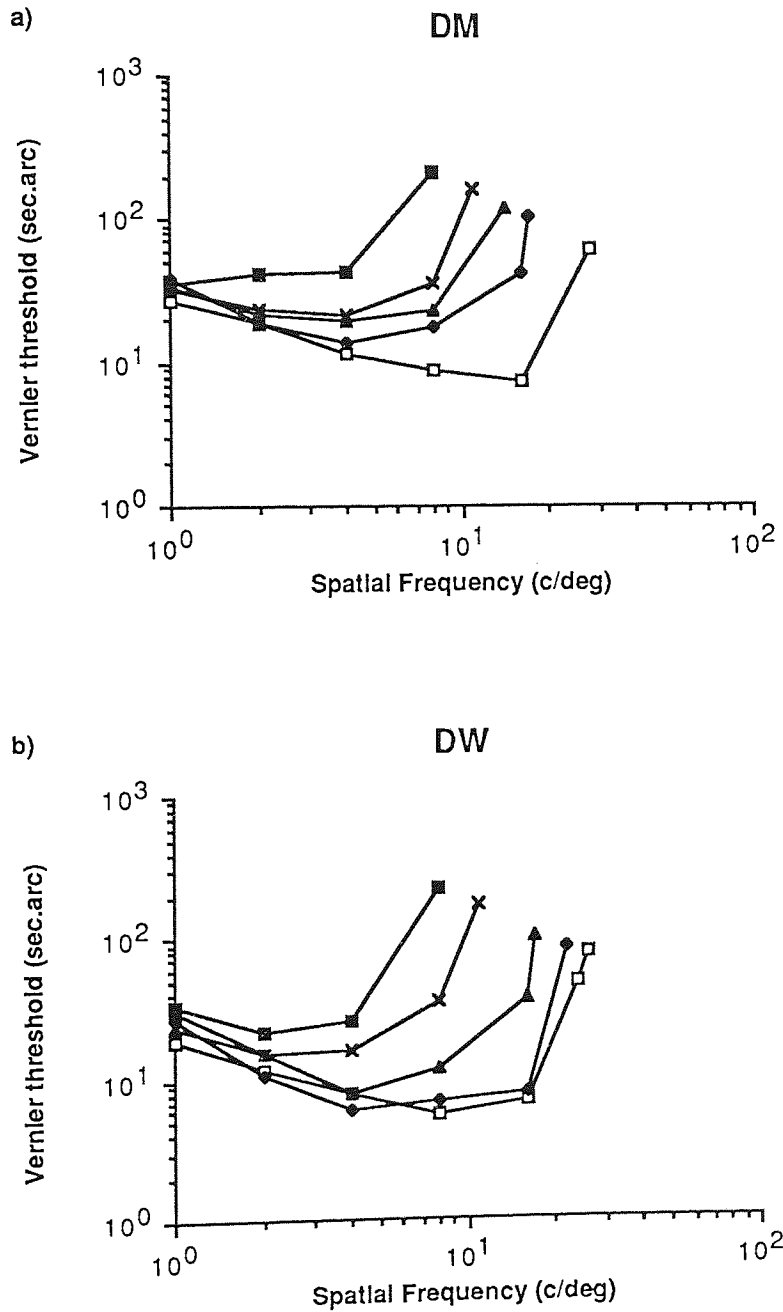


Figure 8.03: Vernier thresholds plotted against spatial frequency for gratings of different separations. The separations are zero minutes of arc (open squares), 4 minutes of arc (filled diamonds), 8 minutes of arc (filled triangles), 16 minutes of arc (crosses) and 32 minutes of arc (filled squares). Mean standard errors are not shown but were approximately 12% of threshold for subject DM and 14% of threshold for subject DW. The features of the curves are discussed in the text.

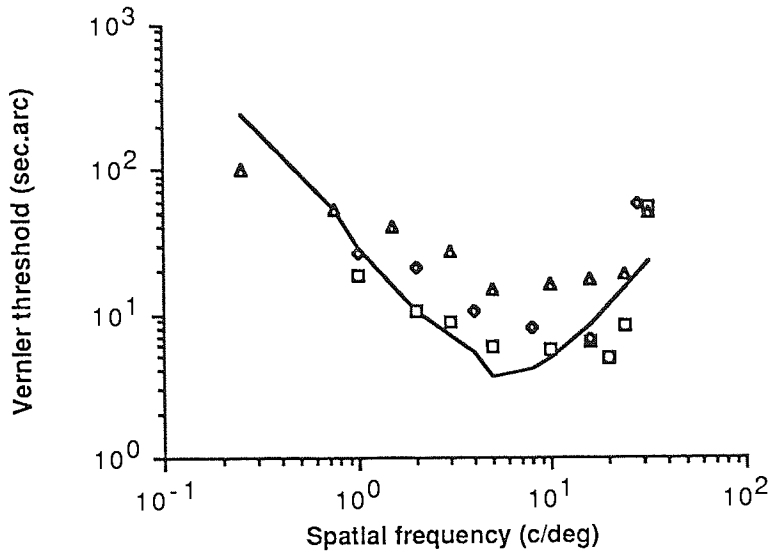


Figure 8.04: A comparison of results for vernier thresholds plotted as a function of spatial frequency. The open triangles are subject A.B. from Bradley and Skottun (1987); the open squares are subject R.J.W. from Morgan (1984) as reported in Wilson (1986); the open diamonds are the results for full gratings (experiment 1) of subject D.M. in the present study. The continuous line are the predicted values from the Wilson (1986) model.

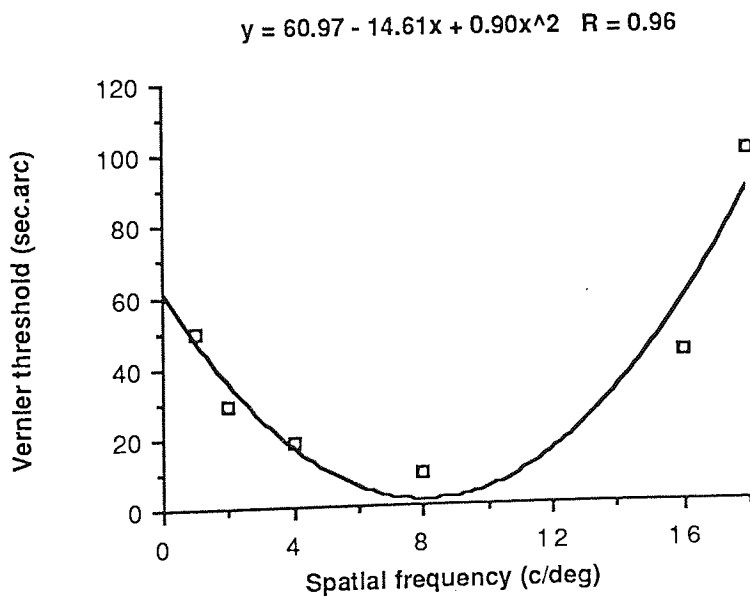


Figure 8.05: Vernier thresholds plotted as a function of spatial frequency for a separation of 4 minutes of arc. These results are from one of the four runs carried out by subject DM for the full gratings (experiment 1). It can be seen that a second order polynomial gives a good fit to the data. The optimum spatial frequency is clearly the point where the function has a minimum value (the optimum threshold) which occurs when the derivative of the curve has a zero value.

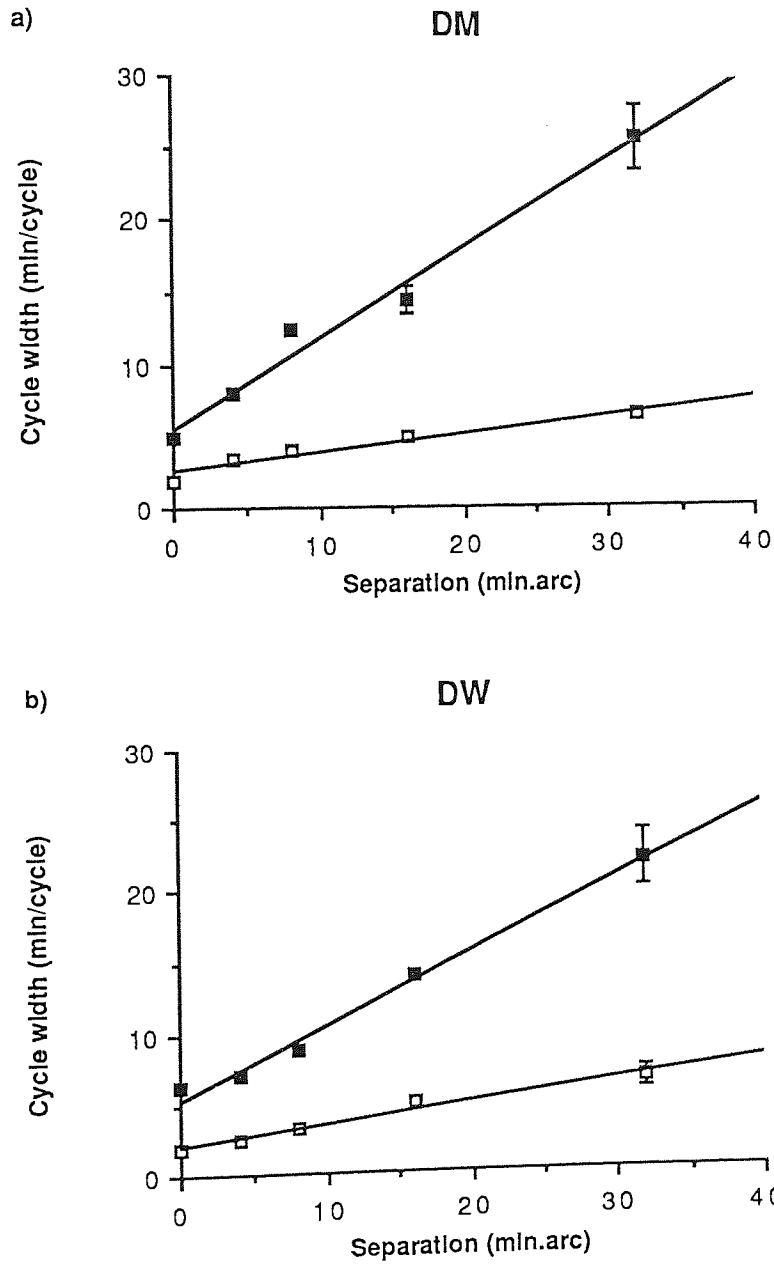


Figure 8.06: Cycle width plotted against separation for the optimum frequencies (open squares) and cut-off frequencies (filled squares). Standard error bars are as shown. If no error bars appear the standard error was too small to show at the scale of the graph, approximating to the size of the symbols.

It is observed there is a marked shift of the
 curve, indicating a change in vernier acuity
 with spatial frequency.

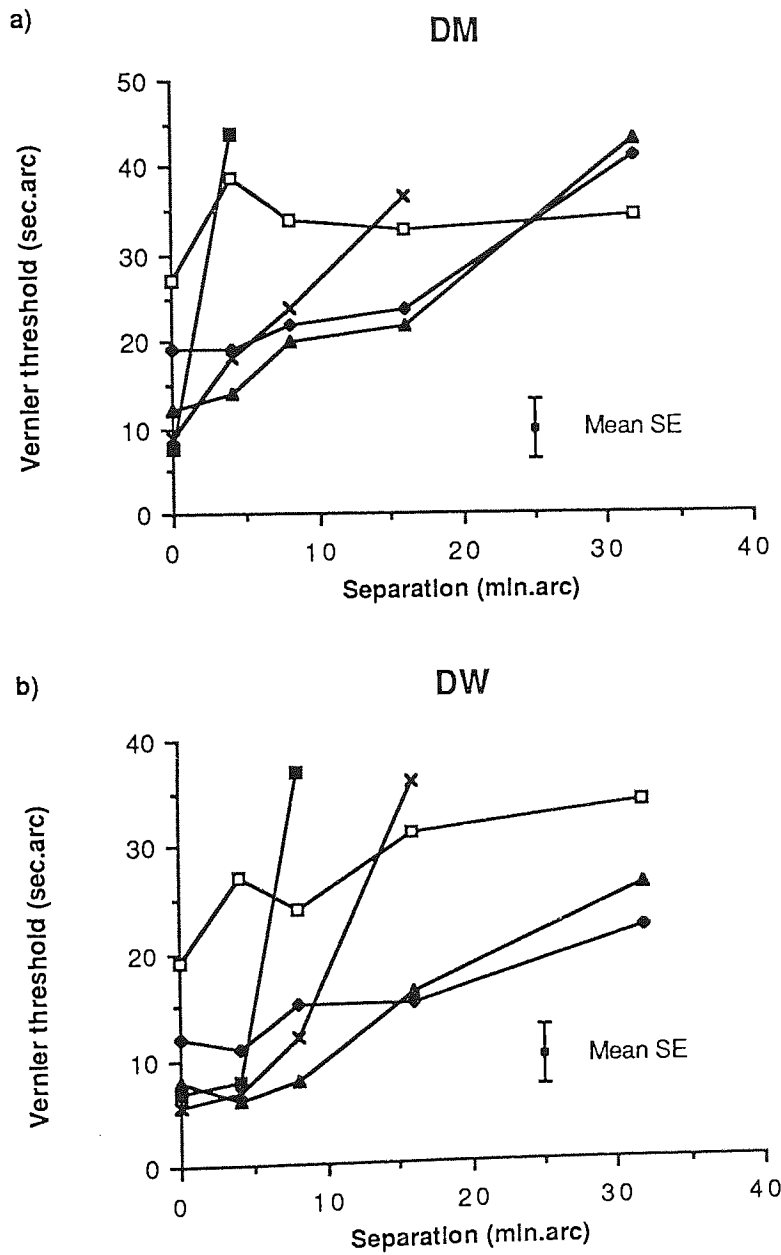


Figure 8.07: The data of *Figure 8.03* replotted with vernier thresholds against separation for different spatial frequencies. The spatial frequencies are 1 cycle per degree (open squares), 2 cycles per degree (filled diamonds), 4 cycles per degree (filled triangles), 8 cycles per degree (crosses) and 16 cycles per degree (filled squares). The mean standard errors are shown. The results are discussed in the text.

As the vertical separation between the gratings is increased there is a marked shift of the cut-off frequency (the frequency where the gratings can be correctly identified as being in or out of phase) toward lower spatial frequencies. In addition, the optimum threshold values are higher and occur at lower spatial frequencies. In order to quantify the spatial frequency at which this optimum threshold occurred, the data for each run at each separation were fitted, in turn, with a second order polynomial. This was carried out on the linear data and produced correlation coefficients between 0.9 and 1.0 (*Figure 8.05*).

Figure 8.06 shows the cut-off and optimum cycle widths (the inverse of spatial frequency) expressed in minutes of arc plotted against grating separation. The striking linearity of the two functions is apparent with all yielding correlations of at least 0.98.

Figure 8.07 shows the data of *Figure 8.03* replotted with separation rather than spatial frequency as the abscissa. It is clear that thresholds worsen with separation but this worsening is much more pronounced for higher spatial frequencies.

8.3.2: Experiment 2

Figure 8.08 shows vernier thresholds as a function of spatial frequency for different strip positions. The abutting strips produce thresholds in the order of 6 seconds of arc at spatial frequencies around 8 to 16 cycles per degree. The similarities between the two figures (*8.03 and 8.08*) are clear, reflecting the similarities between the stimuli. The cut-off frequency, the extreme right hand data point, falls as the strip is located further from the center of the stimulus. In addition, the same shape is found for both data sets. The effect of the strip position on threshold does become less marked as spatial frequency falls, the two becoming essentially independent for the lowest spatial frequency measured (1 cycle per degree).

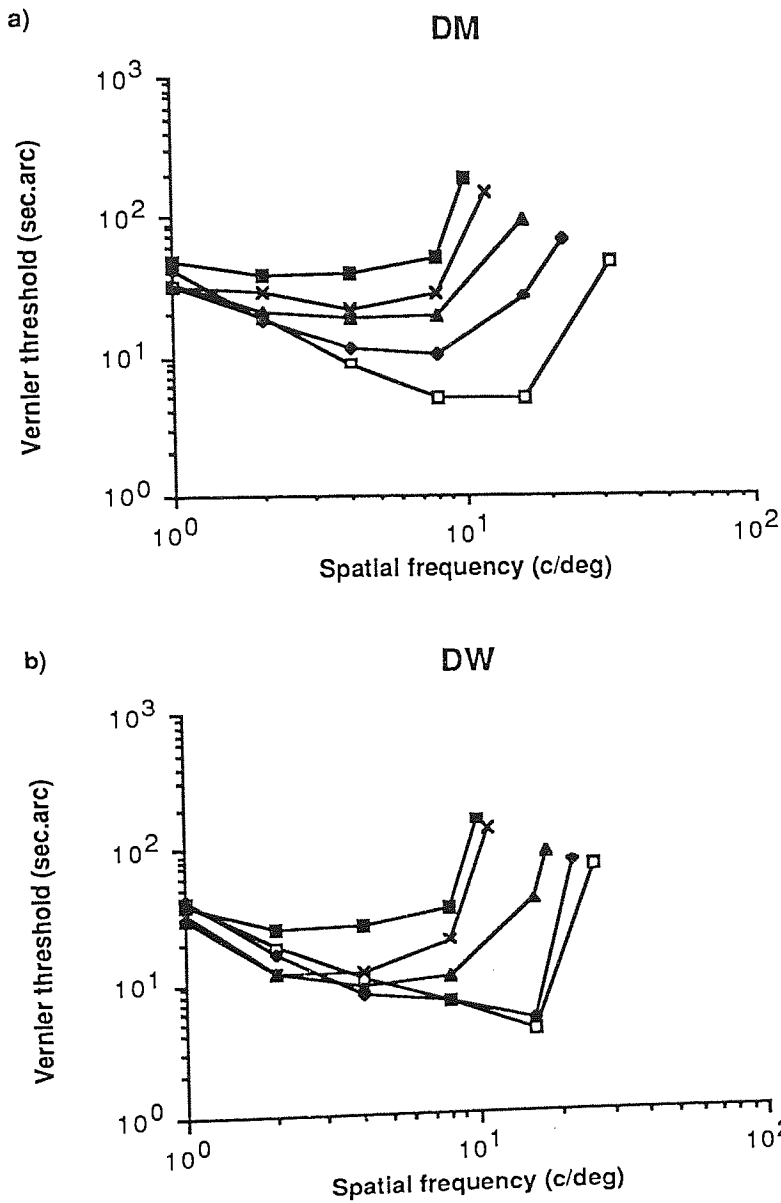


Figure 8.08: Vernier threshold plotted against spatial frequency for the grating strip stimuli at various separations, 0 minutes of arc (open squares), 4 minutes of arc (filled diamonds), 8 minutes of arc (filled triangles), 16 minutes of arc (crosses) and 32 minutes of arc (filled squares). Standard errors are not shown but were approximately 13% of threshold for subject DM and 14% of threshold for subject DW. The results are discussed in the text.

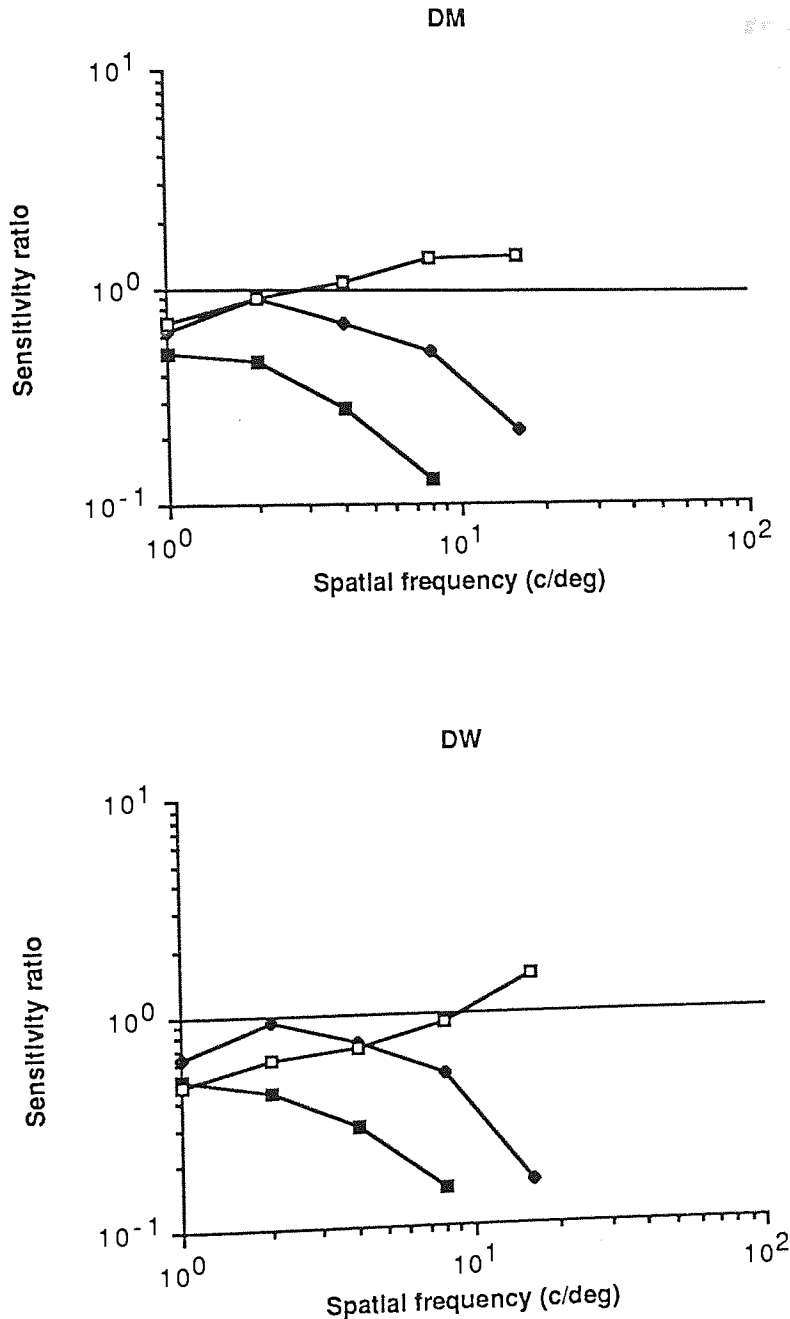


Figure 8.09: The sensitivity ratio (the ratio of the thresholds obtained with the full gratings to those obtained with the grating strips) plotted against spatial frequency for abutting stimuli (open squares), a medium separation (filled diamonds) and a wide separation (filled squares). The results are discussed in the text.

The thresholds for the strips are compared with thresholds obtained from the full gratings in Figure 8.09. The data are plotted as ratios of the threshold obtained with a full grating to that of the strips for three positions representing abutting, medium and large separations. The other separations have been omitted to improve the clarity of the figure but follow the same

pattern. The straight line represents unity, values below the line represent thresholds where the observer was less sensitive with strips than with the full gratings. Values above the line represent the opposite with the observer being more sensitive to strips than to full gratings. For the abutting stimulus thresholds are better with the strips than with the full gratings for high spatial frequencies. This is not true, however, at lower spatial frequencies. For the medium separation the thresholds approach unity for an intermediate spatial frequency (2 cycles per degree) and decline either side of this value. For the largest separation the thresholds with strips are always worse than with the full gratings, but reach their optimum value for the lowest spatial frequency measured (1 cycle per degree).

8.4: Discussion

The results obtained from the experiments reported here are clearly consistent with models based on the pooling of outputs among filters tuned to different spatial frequencies (Carlson and Klopfenstein, 1985; Klein and Levi, 1985; Wilson, 1986). *Figure 8.03* demonstrates that as separation increases vernier thresholds worsen. This is to be expected as a direct consequence of the need to use larger filters as separation increases in order for both parts of the stimulus to fall within a single filter. In addition, the very rapid rise in thresholds obtained at high spatial frequencies with increasing separation (*Figure 8.07*) is evidence that the highest tuned filters have a limited spatial extent which once exceeded results in such filters being unable to contribute usefully towards the determination of thresholds. The striking linearity of the functions in *Figure 8.06* reinforces this. The clear inference being that the horizontal and vertical extent of the receptive fields are proportional. This is implicit in the Wilson (1986) model and has also been demonstrated in neurophysiological studies (Dow, Snyder, Vautin and Bauer, 1981). They found that the ratio of field length to width ratio did not vary with eccentricity (over the range 0 to 120 minutes of arc) despite the fact that the more peripheral fields were larger.

It is the differential response amongst the filters which determines whether an offset is detected. Since a given spatial offset represents a much larger phase change in the small filters as compared with the large, it is the smaller filters which give the largest differential response to small offsets. The worsening of thresholds as separation increases is a direct consequence of this reduced response from the larger filters. *Figure 8.09* clearly shows the results of limiting the filters available. For the abutting stimuli thresholds are better with the strips than with the full grating at high spatial frequencies. This implies that in the full grating

the output from the larger filters has a detrimental effect on determination of thresholds. At lower spatial frequencies of course the smaller units have a reduced response and one would expect thresholds to be worse with abutting strips relative to the full gratings. As the strips and gratings are separated the smaller units cease to contribute towards threshold determination. In such cases the reduced output of the filters, caused by the stimulus failing to fill the full extent of the receptive field, would lead to thresholds being worse than with the full gratings with one exception. This was demonstrated in chapter 3 when a small vernier offset causes larger changes in orientationally tuned filters at the optimum feature separation which would occur, in this case, when the strips fall just inside the vertical extent of the filter. For the lowest spatial frequency investigated this situation never arises, the optimum separation would need to be approximately 60 minutes of arc, and therefore thresholds with the strips would not be expected to equal thresholds obtained with the full grating.

Using traditional stimuli, highly localised in space and with broad spatial frequency spectra, one could not predict this outcome. However, a study by Williams *et al.* (1984) investigated the effect of dioptric blur on vernier acuity. This has the effect of removing the high spatial frequency content of the stimulus *i.e.* low-pass filtering. They found that with increasing dioptric blur (equivalent to lowering the spatial frequency content) the separation at which optimum thresholds were obtained was increased. Given the argument mentioned above, that the optimum separation of the stimulus features becomes greater with reducing spatial frequency content, the relationship between dioptric blur and separation is not surprising.

While the evidence presented here tends to support the channel models a couple of notes of caution should be interjected. Firstly, there is a limit as to the extent of space over which the model will work. As the separation is increased it must eventually exceed the size of the largest filter and at this point the model must break down. Certain investigators have argued that the channel models cannot be correct precisely because of this. They point out that at large separations relative localisation is independent of the spatial frequency content of the stimuli (Burbeck, 1987; Toet and Koenderink, 1988). The threshold values obtained are, however, well outside the hyperacuity range and, it has to be said, extrapolation of the model to smaller scales would introduce unneeded complexity. The filter model requires only one processing stage, the pooling of the filter outputs. The alternative local-sign models require not only a positioning stage, which requires the pooling of two sets of filter outputs, but then a comparative stage in order to extract the offset. Three sets of processing are clearly less efficient than one and is unnecessary in order to determine the offset for targets at small

separations.

A second, more difficult, problem is the finding that supernumerary features placed between the two vernier elements has no effect on thresholds (Morgan and Ward, 1985; Burbeck and Yap, 1990; Morgan *et al.* 1990). These authors found that, provided the features were clearly resolved from the stimulus, they had no effect on performance. This is difficult to reconcile with a model in which both stimulus features are contained within the receptive field of a single filter since any filter containing both vernier elements must also contain the supernumerary feature. However, the feature separations used in these experiments were considerably greater than those employed in this set of experiments and, as stated earlier, produced threshold values outside the hyperacuity range.

Given that the channel models can only apply over a restricted range of separations it is not unreasonable for some other system to operate over large separations. As an example, the minimum spatial frequency tuning of foveal cells found by DeValois *et al.* (1982) was 0.5 cycles per degree. This would imply a maximum vertical field extent of around 120 minutes of arc. One possible alternative is the coincidence detector model of Morgan and Regan (1987) described in chapter 3. As with all human physiological systems one would not expect a sharp dividing line between the two systems and it is possible that the single filters operate in isolation over only a very restricted area while over part of their theoretical range the visual system will use whichever system gives the most reliable output. The presence of supernumerary features would clearly constrain the single filter model's operation and the intelligent selection of the alternative system could be used to overcome this (Morgan *et al.* 1990).

8.5: Conclusion

A number of conclusions can be drawn from these experiments. The first is that over the restricted range investigated the channel models can be used to explain how the vernier task is undertaken by the visual system. However, this would only be expected to be tenable up to the vertical extent of the largest filter and might, in all probability, fail well before this theoretical maximum is reached. The second conclusion to be drawn is that the critical separation, which is a feature of hyperacuity performance, should be considered as a consequence of the stimulus spatial frequency content rather than its spatial extent. For

example, if the stimulus contains high spatial frequency information, as do the dot and line configurations employed in the majority of hyperacuity studies, then the visual system will use two regions of the vernier stimulus separated by about 4 minutes of arc to achieve the characteristic hyperacuity thresholds. When high spatial frequency information is absent then more distant regions of the stimulus are employed with a consequent reduction in performance. The limitations imposed upon the choice of spatial frequency filters available to perform the task also explain the effect of separation on vernier acuity. For high spatial frequency targets the increasing separation quickly causes the stimulus elements to fall outside the range of the high spatial frequency filters resulting in a rapid decline in performance. However, for low spatial frequency stimuli the effect of separation is much less marked which is a direct result of the larger spatial extent of the low frequency filters employed. In short, the critical separation proposed in previous studies is perhaps best considered as a function of the spatial frequency content of the stimulus rather than a purely spatial feature. Clearly under such a proposition the critical separation ceases to be a fixed quantity but assumes a variable extent dependent on the underlying spatial frequencies present in the stimulus.

Chapter 9: Weighting functions for visual location**9.1: Introduction**

The previous chapter provided evidence that hyperacuity performance could be mediated by pooling the outputs of a group of filters tuned to different orientations and spatial frequencies. However, it was pointed out that the range of this model would be limited by the possible filters available. The lowest spatial frequency filters have a tuning peak at around 0.5 cycles per degree and would thus limit the separation over which relative localisation by this method could operate (DeValois *et al.* 1982). The obvious question, therefore, is what mechanism mediates relative localisation over greater spatial separations? Recently an idea has been put forward that relative localisation requires a two stage process in order to operate over a wide range of separations (Burbeck, 1987; Burbeck and Yap, 1990b). The model proposes that the stimulus features are located using the output of filters tuned to different spatial frequencies and these outputs are then compared by a separation or size discriminator. The exact nature of the secondary process is unclear at present but could be some form of coincidence detector (Morgan and Regan, 1987) or secondary spatial filter (Burbeck and Yap, 1990b).

This chapter addresses the primary representation of the stimulus features. There are two possible features of the stimulus which could be used in judging location. First, and most obvious, is the location of the edges of the stimulus. Logically the object can then be thought of as having a size measured by the distance between its two edges. For small objects, therefore, the mid-point between the two edges could be used to assign position. However, for large objects the position of the closest edge would be sufficient to allocate location. In this scenario the internal light distribution within the object is not used in positional judgments. However, it has already been mentioned, in chapter 3, that Watt and Morgan (1983a) have shown that the edge, defined as the point where the retinal light distribution of the object exceeded threshold, could not be the feature allocating location. Their conclusion was that edges in the primary retinal image were represented by zero-crossings in the convolution of the retinal light distribution with the second derivative of a Gaussian, as suggested by Marr and Hildreth (1980). Another of the possibilities which they considered was the mean of the retinal light distribution. This can be considered analogous to the center of gravity of a solid object and has been dubbed the "centroid" (Westheimer and McKee, 1977b; Whitaker and Walker, 1988).

Westheimer and McKee (1977b) used targets which were formed of strips combined to give wide bands of light (between 2 and 2.7 minutes of arc wide by 6.4 minutes of arc high). The strips were so close together as to be unresolvable. This meant that the internal light distribution of the band could be adjusted by altering the luminance of individual strips without altering the physical extent of the band. In their experiment the two bands had no physical offset. Within the two bands, however, one of the strips was brighter than the others and it was possible to simulate a vernier offset by shifting the brighter strip in the upper band relative to that in the lower. A subjective vernier offset was created even though there was no physical offset of the stimulus boundaries. The results also showed that vernier thresholds were essentially the same for this task as those obtained when the top and bottom bands were physically offset. Clearly, this indicates that the internal light distribution can influence the subjective position of an object.

Whitaker and Walker (1988) used a different target configuration consisting of clusters of random dots. Again the internal light distribution could be altered without affecting the physical extent of the cluster. This time vernier thresholds were obtained for pairs of clusters which had an extra dot placed within the cluster to move the centroid, a second pair which had an extra dot placed outside the dot which altered the apparent edge and finally a control pair with no distorting features. Their results clearly demonstrated that the additional dots changed the apparent position of the clusters and that, apart from very low dot densities, the change was consistent with that predicted by a change in centroid. It should be noted that both the distorted stimuli used by Whitaker and Walker had a shift in centroid position. The extra dot placed just outside the cluster edge was not resolvable from the rest of the cluster dots and as such would be expected to contribute to the overall light distribution. Its greater position from the centroid of the cluster means that it would be expected to have a greater effect, if centroid were the factor assigning location to the cluster, than the extra dot placed just inside the edge of the cluster. In fact the apparent change in position was always larger when the extra dot was placed outside the cluster boundary which can be taken as further evidence for the use of centroid in allocation of position.

Using a similar vernier task consisting of two random dot clusters Ward *et al.* (1985) also investigated the feature which might allocate position. They proposed that it could be one of three, the centroid (defined as the mean location of the dots along the x-axis), the overall slope of the whole vernier stimulus (as proposed by Andrews, 1967) and the relative positions of the extreme edge dot in the two clusters. Their results showed firstly that vernier thresholds improved dramatically as the dot density increased and secondly that either

centroid or edge proposals could determine location.

There is evidence, therefore, that the centroid of the internal light distribution is a strong contender as the tag used to allocate position to the cluster. If centroid is analogous to the center of gravity of a solid object then the influence of each dot within a dot cluster would be directly proportional to the distance of the dot from the geometric center of the cluster. Therefore, the effect of adding an extra dot would follow a linear function with increasing distance from the geometric center of the cluster. The following experiments employ stimuli which are designed to investigate the applicability of the use of the centroid in determining object location.

9.2: Method

All the stimuli consisted of a pair of pseudo-random dot clusters positioned one above the other. These were presented on a high resolution CRT under the control of the Nimbus AX microcomputer. The dots were 0.3 mm in diameter and were bright on a dark background. The viewing distance was 8 meters and the observers, two myopes wearing their full spectacle correction, used their dominant eye in all the experiments. The observations were carried out in complete darkness to remove all possible references. Presentation time was 500 msec following which the observer had to decide whether the upper cluster was to the right or left of the lower. Following the receipt of a response via the keyboard the computer then altered the offset depending on that response. A leftward response resulted in the next presentation being more to the right and vice-versa. Two interleaved staircases were used, one starting from the left the other from the right. In both cases the initial presentations were clearly suprathreshold. Each staircase ceased after 10 reversals with the final 8 being used in determination of threshold and bias values. For each staircase bias was taken to be the mean of the reversals while acuity was taken to be the standard deviation of the responses about this mean value. The two results thus obtained were then averaged to give a final estimate of vernier bias and acuity. In this experiment the physical offset associated with subjective alignment is the important value and hence we are more concerned with variations in vernier bias.

The control stimulus, on which all the others were based, consisted of clusters of 16 dots (*Figure 9.01a*). These were contained within an imaginary square measuring 400 seconds of arc on each side. The separation of the two clusters, measured between the closest edges, was a constant 400 seconds of arc. Within the squares the location of dots was not entirely

random, hence the term pseudo-random dot clusters. There were two major constraints on dot location:

a): A dot was always placed at the extreme left and right hand sides of the imaginary square which served to delineate the horizontal extent of the cluster. The vertical co-ordinates of these dots was entirely random.

b): All other dots were placed at random both along the horizontal and vertical directions except that for each dot placed to the left of the geometric center another dot was placed an equal horizontal distance to the right. The vertical co-ordinates of all the dots was entirely random. Clearly, this procedure results in all the dots balancing out so that the centroid always lies at the geometric center of the cluster.

For the various experiments modifications were performed to this basic cluster in order to vary the position of the centroid and the apparent edge as necessary.

9.3: Experiment 1

9.3.1: Stimulus configurations

In experiment 1 the prediction that the dots within the cluster are given equal weighting was tested. If the dots have an equal weighting then it should be possible to balance a dot positioned to one side of the geometric center with two dots placed half the distance to the other side. Three cluster configurations were used to test this. The first was the basic cluster used as a control. The second had an extra dot placed 16 seconds of arc within the apparent edge of the cluster with no counterbalancing dot to the other side (*Figure 9.01b*). These dots were placed so that they would tend to pull the centroid of the upper and lower dots in opposite directions and hence double the effect of each individually. The vernier bias would be expected to change by an amount equal to the relative change in centroid produced by the extra dot. The exact value can be calculated from the method of moments. Consider a cluster of D_n dots contained within an imaginary square of size S . If an extra dot is placed a distance d inside the edge of the cluster the centroid will move a distance c .

It follows that

$$(S/2 - d - c) = c \times D_n$$

therefore

$$c = (S/2 - d) / (D_n + 1)$$

This change occurs in both clusters, but in opposite directions, giving a relative change of

$$(S - 2d) / (D_n + 1)$$

This value represents the expected vernier bias if centroid were used in the determination of alignment (Whitaker and Walker, 1988; *Figure 4*).

The third stimulus configuration was arranged to maintain the centroid of the cluster at the geometric center but to alter the apparent edge of the cluster. An extra dot was placed 16 seconds of arc outside the cluster and this time balanced by two dots positioned, to exactly balance the extra dot, on the opposite side of the geometric center (*Figure 9.01c*). This time there were only 14 random dots within the cluster in order to keep the total number of dots within the clusters the same as in stimulus two.

Thresholds for each of the cluster configurations were measured as a function of cluster size. These were 100, 250, 400, 550 and 750 seconds of arc along each side. Depending on whether edge or centroid were used to allocate position, one would expect different results to be obtained from the three configurations. If centroid alignment were used then one would expect the second stimulus to show a linear increase in vernier bias with increasing cluster size. The rate of increase is given by the equation

$$d/dS ((S - 2d) / (D_n + 1)) = 1/(D_n + 1)$$

Edge position does not alter in this configuration so if this feature were employed in determining location then bias would not differ from the control stimulus. On the other hand the third stimulus would give vernier bias results identical with the control if centroid were used in determining position because the position of the centroid has not been altered. This time, however, if edge were used bias should be a constant 16 seconds of arc higher than the control stimulus.

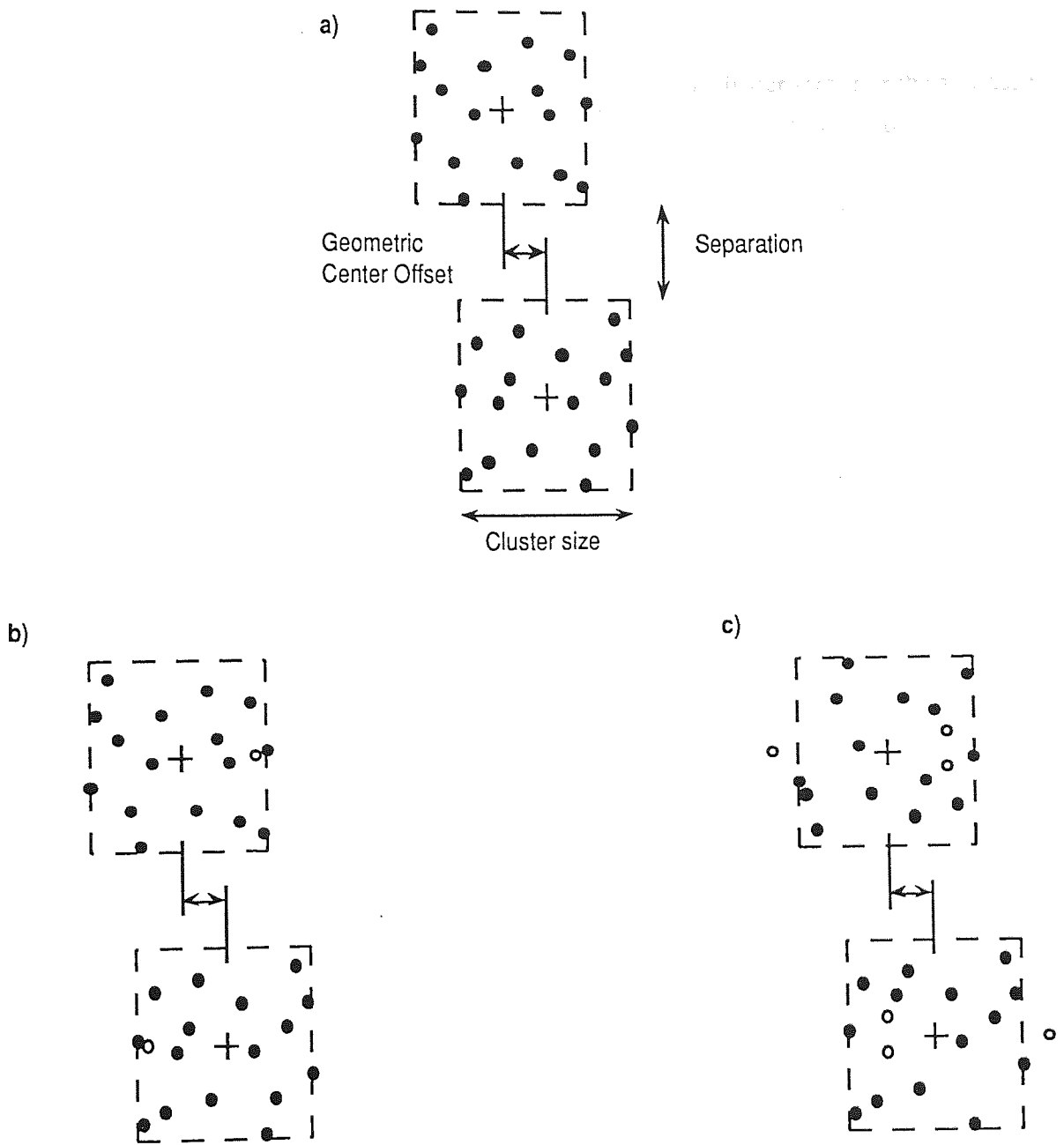


Figure 9.01: The stimulus configurations employed in this series of experiments, the restrictions on dot production and location are discussed in the text. (a) represents the basic 16 dot stimulus. The terms geometric center and geometric center offset are defined as is the cluster size and separation. The positioning of the dots was such as to locate the centroid at the geometric center. The dotted squares represent the limits beyond which dots were not placed (except as in (c) below) and thus demarcates the physical extent of the cluster. (b) shows the cluster with the distorted centroid. The extra dot (open circle) has the effect of moving the centroid away from the geometric center. (c) is the distorted edge cluster. For this stimulus configuration three extra dots were employed with the single dot placed outside the cluster balanced by a pair of dots within the cluster such that the centroid remains at the geometric center. In order to retain the same overall number of dots as in (b) there are only 14 random dots in this configuration.

9.3.2: Results

Figure 9.02a shows how vernier bias changes with increasing cluster size. For the standard stimulus there is little change in bias with increasing cluster size, with the value hovering close to zero. This means that the observers subjective position of alignment was very close to the true physical position of alignment. For the second stimulus, however, vernier bias increases steadily as the cluster gets larger. The straight line indicates a slope of $1/(D_n + 1)$ and represents the expected rate of increase in bias with increasing cluster size if centroid were the determinant of location. What is surprising is that the third stimulus also shows a steady increase in bias with increasing cluster size. In this third stimulus the centroid has been maintained at the geometric center by the additional balancing dots and one would expect, therefore, the result to mirror that from the control stimulus. Clearly, this is not happening and one has to conclude that the visual system is ignoring the presence of the balancing dots. This poses an interesting question: why does the visual system apparently ignore the two dots used in the third stimulus to balance the extra dot positioned outside the apparent cluster edge? Clearly, all the dots within the cluster cannot have an equal weighting.

Vernier acuity (shown in *Figure 9.02b*) shows a similar response to increasing cluster size for all three stimulus configurations. As cluster size increases there is an increase in threshold which varies from around 10 seconds of arc for the smallest cluster size to approximately 35 seconds of arc for the largest cluster size. This is consistent with the subjective appearance of the clusters as their sizes vary. The small clusters appeared as bright dots but as cluster size increases this appearance changes, the clusters becoming diffuse low contrast blobs. The well documented reduction in vernier acuity with reducing contrast (Bradley and Skottun, 1987; Morgan and Regan, 1987) and also with increasing spread (Toet, Van Eekhout, Simons and Koenderink, 1987) provide a ready explanation for this result.

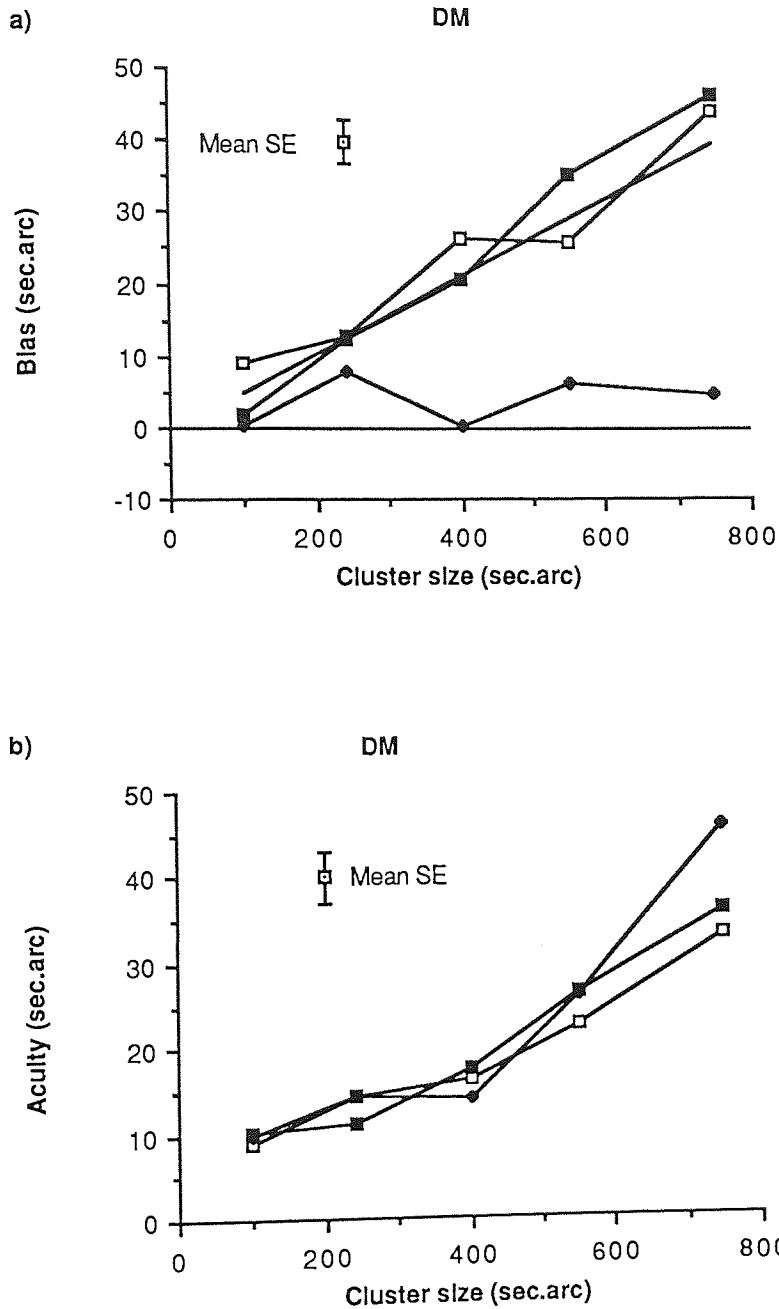


Figure 9.02: Vernier bias (a) and acuity (b) plotted against cluster size for the stimulus configurations described in *Figure 9.01*. The results for the control stimulus are shown by the filled diamonds, the distorted centroid stimulus by filled squares and the distorted edge stimulus by filled squares. Two other observers, one experienced, the other naive, also carried out this part of the experiment with results very similar to those shown. It should also be noted that the results are similar to those obtained by Whitaker and Walker (1988). In (a) the straight line indicates the result if centroid were used in determining offset. If, on the other hand, edge were the determining feature then a horizontal straight line with a bias value of 17 second of arc would be expected.

9.4: Experiment 2

9.4.1: Stimulus configuration

The results of experiment 1 seemed to imply that all the dots within the cluster were not given an equal weighting by the visual system. To investigate how this weighting changed with the position of the dot relative to the center of the cluster the following stimulus configuration was employed. The cluster consisted of 16 dots arranged as per the distorted centroid stimulus (*Figure 9.01b*). On this occasion, however, the extra dot was not placed at just one location. Instead it was placed at various points between 0 and 500 seconds of arc from the geometric center of the cluster. Measurements of vernier bias and acuity were made for each location both for this distorted centroid stimulus and the control stimulus. The two stimulus configurations were interleaved and estimates of vernier bias and acuity obtained as described in the methods. For this experiment we are interested primarily in the difference between the control stimulus and the distorted centroid stimulus which reflects the action of the extra dot. The net bias value, which appears in most of the figures throughout the rest of this chapter, is the difference between the actual bias obtained from the distorted centroid stimulus and that obtained from the control stimulus. As in the earlier experiment (1) the extra dot was placed such that it moved the centroid of the two clusters in opposite directions. The assumption is that changes in net bias as the dot moves further from the geometric center of the cluster gives an indication of the weighting attached to the dot at any position.

9.4.2: Results

Figure 9.03 shows the results for this experiment for a cluster size of 400 seconds of arc square, a separation between the clusters of 400 seconds of arc and a dot number of 16. The X-axis represents the offset from the geometric center of the cluster of the extra dot. In this case the edge of the cluster lies at 200 seconds of arc. The plot shows that for dots placed within the cluster (up to 150 seconds of arc offset) the effect on bias is quite small (less than 5 seconds of arc). As the dot approaches the edge and then is placed outside the cluster the effect on bias increases dramatically to peak at a value of around 55 seconds of arc at an offset of 300 - 400 seconds of arc. This corresponds to a dot position 100 - 200 seconds of arc beyond the edge the cluster. Further increases in offset produce an equally dramatic fall in bias values back towards zero. One should not be too surprised at this as the dot must eventually be perceived as separate from the cluster and is then ignored in performing the vernier task. The two lines drawn on the graph show the expected change in bias if edge or

centroid were to mediate performance. The actual plot clearly follows neither prediction exactly but falls somewhere in between.

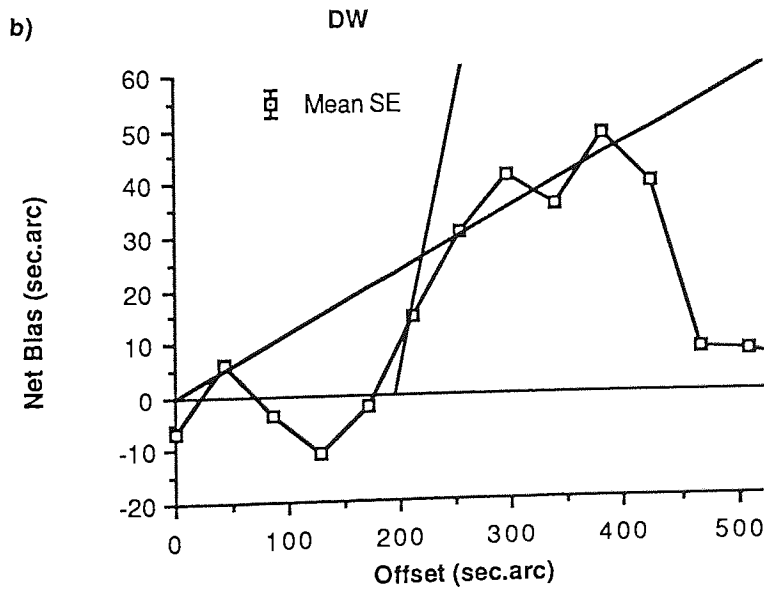
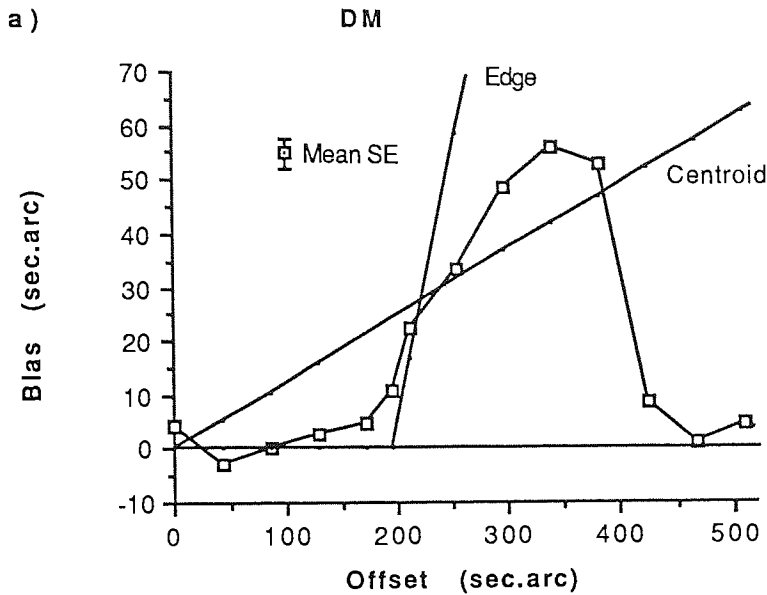


Figure 9.03: Net bias (bias obtained with distorted stimulus less bias from control stimulus) as a function of the offset of the centroid distorting extra dot. The two straight lines show the expected bias value if edge or centroid were used in determining offset. Note that neither correctly predict the observed results over the full range. The return to almost zero net bias with offset values over 450 seconds of arc occur when the extra dot becomes clearly separate from the clusters and is hence ignored in offset determination.

Near the edge of the cluster, however, the value falls close to that predicted by centroid and would, therefore, supply an explanation for the findings of experiment 1 and also those of Whitaker and Walker (1988). Had other offset positions been used the results would differ considerably from the predictions of the centroid model.

9.5: Experiment 3

9.5.1: Stimulus configuration

The next question to consider is whether the shape of the weighting function reflects some feature of the individual analysis of each cluster or whether it reflects the output of mechanisms which span the entire stimulus? In other words, does it represent the abstraction of a local-sign from the cluster or does it illustrate some feature of the filter outputs which create an implicit representation of the whole stimulus. One way of isolating these two possibilities is to alter the separation between the clusters. If the weighting function reflects the action of the orientationally tuned spatial filters used in carrying out the vernier task then these functions would be expected to vary with increasing separation as larger, more coarsely tuned filters are employed (Wilson, 1986). If the function reflects the individual analysis of the cluster then separation should have no effect on the shape of the weighting function so long as the cluster size is held constant. This experiment, therefore, uses the same cluster configuration as experiment 2 but alters the separation between the closest edges of the clusters. The standard cluster was used in all cases but with separation between the clusters tested at three values 0, 400 and 800 seconds of arc.

9.5.2: Results

The results (*Figure 9.04a*) show that the shape of the functions, and the position of the peak, do not vary with separation. There is, however, a trend toward a slightly higher peak bias value with increasing separation. This immediately suggests that the weighting functions do in fact reflect the individual analysis of the clusters. If the functions reflected the output of filters covering the whole stimulus one would expect changes in peak position, and possibly peak bias value, in line with the larger filters required at the greater separations. The values for vernier acuity (*Figure 9.04b*) show the expected increase in threshold with increasing separation. These values would, however, suggest that acuity is independent of the position of the extra dot as there is no systematic variation with increasing offset. This variation in acuity with separation could be explained on the basis of larger filters being required at larger

separations as proposed in the previous chapter. Equally, however, it can be explained by the assumption that the secondary processing of local-sign information becomes degraded with increasing separation. Given that the bias results (*Figure 9.04a*) do not indicate the use of different sized filters one has to conclude that some local-sign mechanism is being employed in this task.

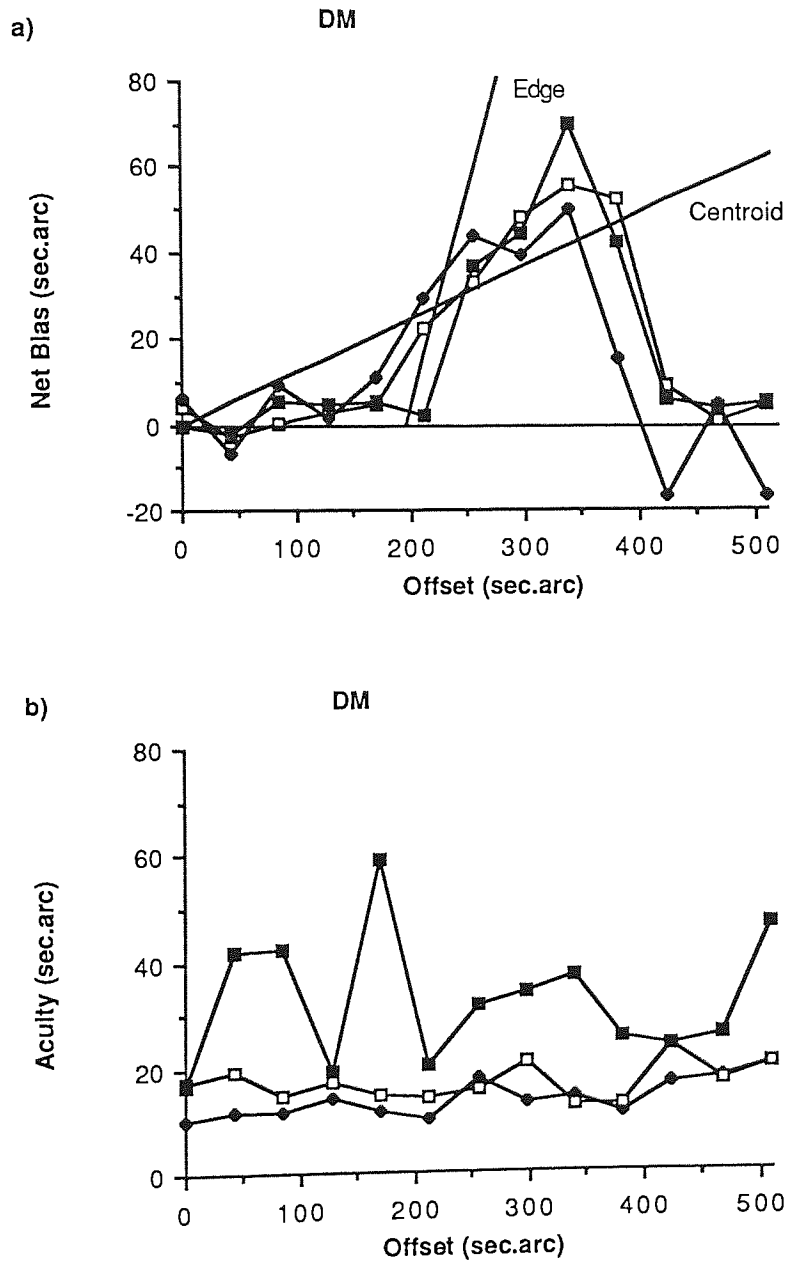


Figure 9.04: The effect of separation on net bias (a) and acuity (b). The separations are 200 seconds of arc (filled diamonds), 400 seconds of arc (open squares) and 800 seconds of arc (filled squares). For net bias there is little difference between the results except that the peak value may increase with increasing separation. For acuity there is the expected systematic increase with increasing separation. Results for the second observer (DW) are similar to those presented.

9.6: Experiment 4

9.6.1: Stimulus configuration

The next consideration is what specific cluster feature underlies the shape of the weighting function? Given that separation has no effect there remain two variables, cluster size and dot number. To examine these two factors each was varied independently. Firstly, the size of the cluster was altered while the dot number was kept constant. Cluster sizes of 200, 400 and 750 seconds of arc square were used. In all cases there were 16 dots per cluster together with the extra dot placed at discrete positions from the geometric center outward as in experiment 2. The second possibility was checked by maintaining the cluster size at 400 second of arc square but altering the number of dots contained within the cluster. In this case there were 8, 16 or 32 dots with again one extra dot placed as above to determine the weighting function. In all cases considered here the vertical separation between the nearest edges of the clusters was maintained at 400 seconds of arc.

9.6.2: Results

Figure 9.05 shows the result for the cluster 200 seconds of arc square. Two points stand out: the peak magnitude of the net bias is much lower (around 20 seconds of arc) than for the standard cluster and the weighting function now more closely follows the prediction for centroid than before. With the larger cluster size (750 seconds of arc) the opposite is true. This time the peak magnitude of the net bias is much higher (about 70 - 90 seconds of arc) and the weighting function closely follows that predicted by the use of edge in determining offset (*Figure 9.06*).

The results obtained by altering the number of dots within the square also differ from the standard result. *Figure 9.07* shows the results for a standard cluster with 32 dots. This time the peak value is again lower (around 22 seconds of arc) but the weighting function, certainly for subject DM, does not clearly follow either the edge or centroid prediction. On the other hand *Figure 9.09* shows the results with only 8 dots per standard cluster and again a striking change is apparent. This time the peak value is much larger than the standard cluster (around 100 seconds of arc). Again it seems unclear whether the weighting function follows the prediction of edge or centroid although for subject DM edge seems to be the more likely.

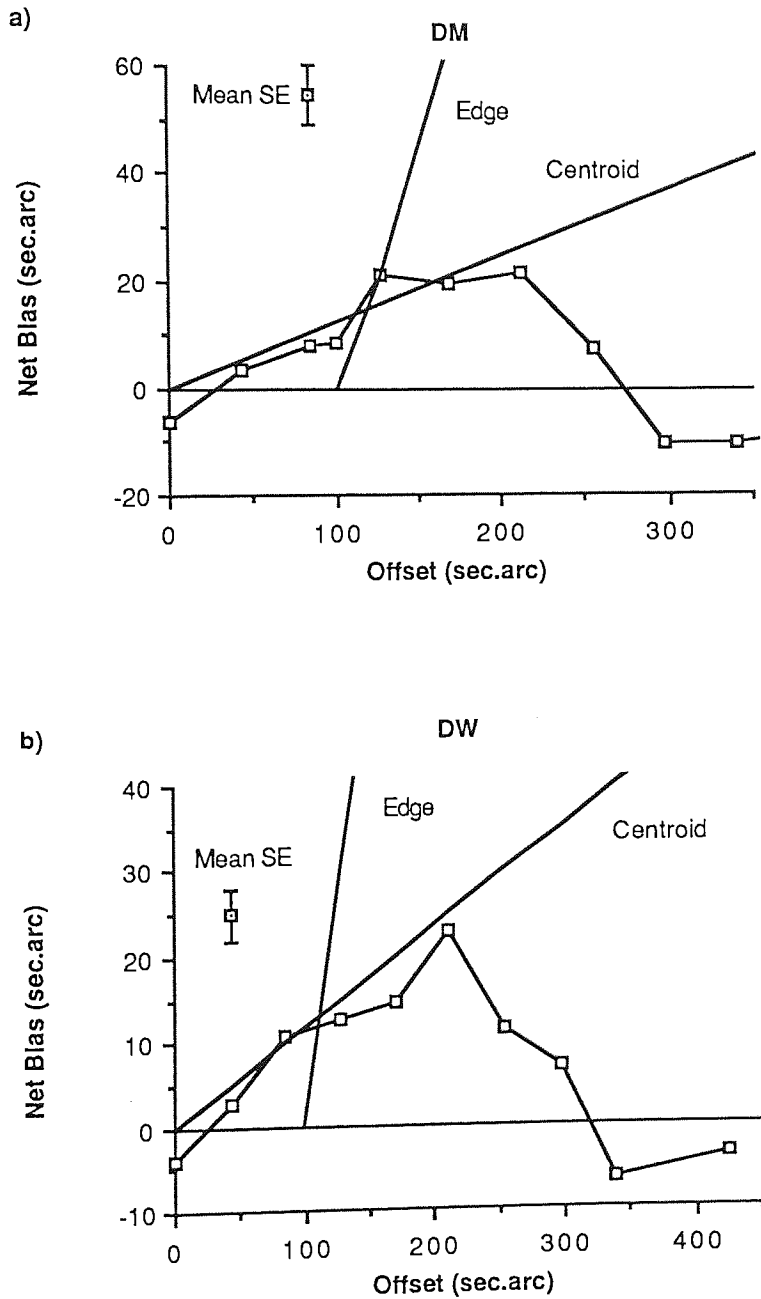


Figure 9.05: The effect on net bias of reducing the size of the cluster from 400 to 200 seconds of arc. Note that the peak value of the net bias is substantially reduced and its position moved closer to the cluster geometric center (the zero offset position). The weighting function follows the centroid prediction quite well until it falls back to zero when offset exceeds around 200 seconds of arc.

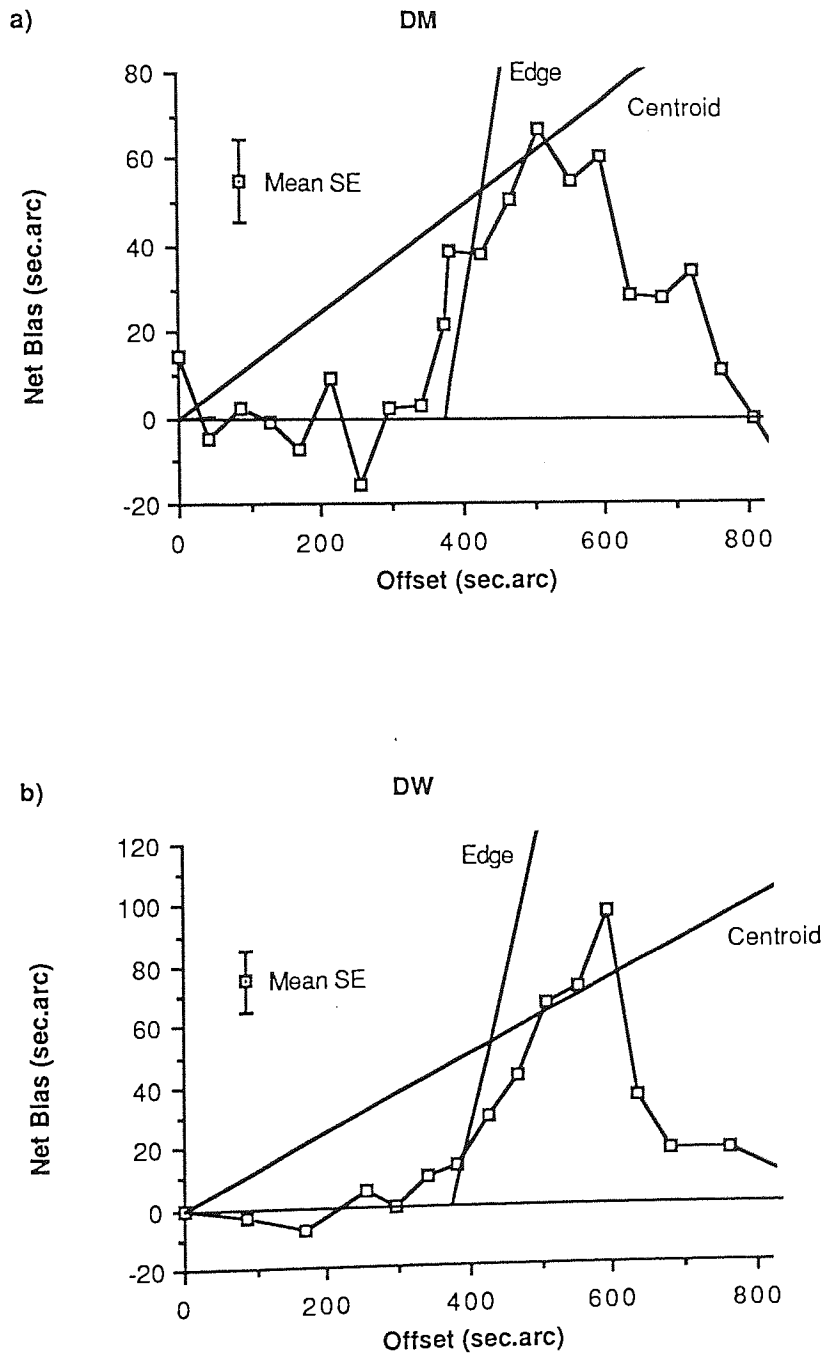


Figure 9.06: The effect on net bias of increasing the cluster size to 750 seconds of arc. Note that the weighting function more closely follows that predicted by edge.

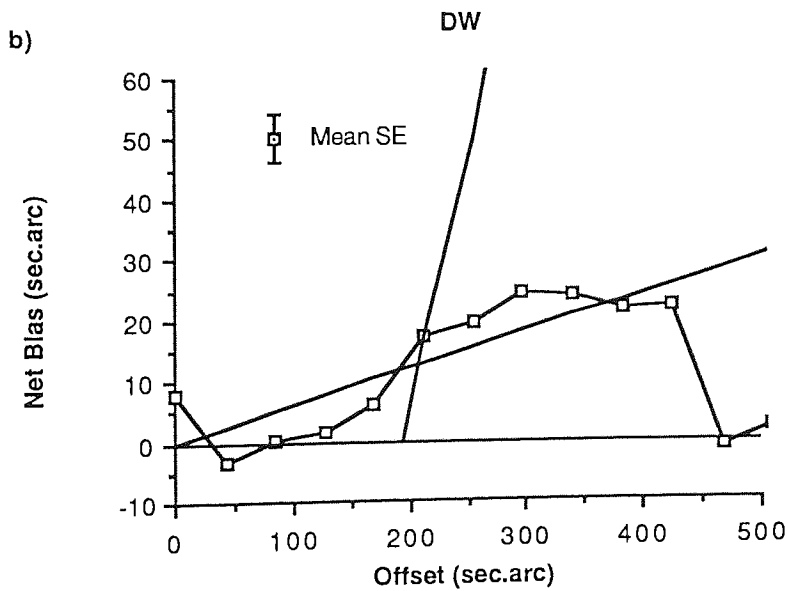
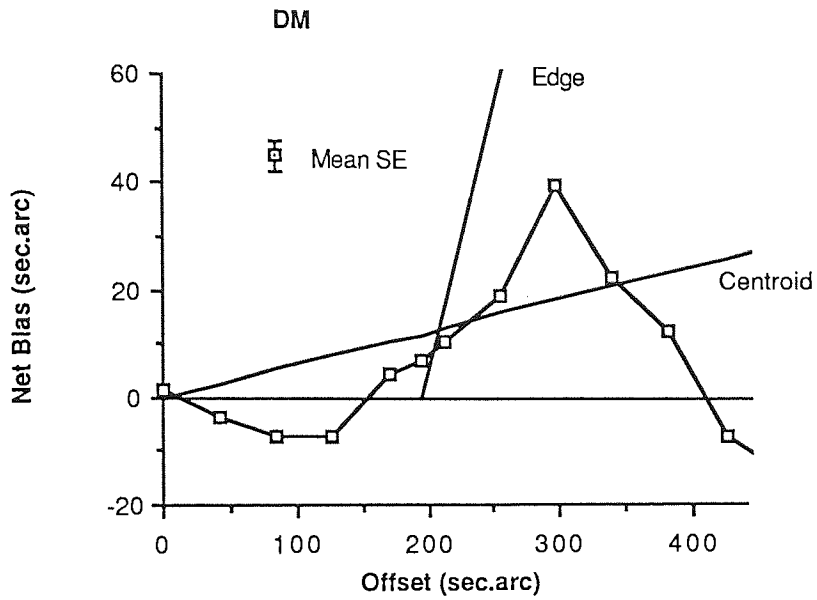


Figure 9.07: The effect on net bias of increasing the dot number to 32 while retaining the 400 second of arc cluster size. This time the weighting function closely follows that predicted by centroid especially for observer DW.

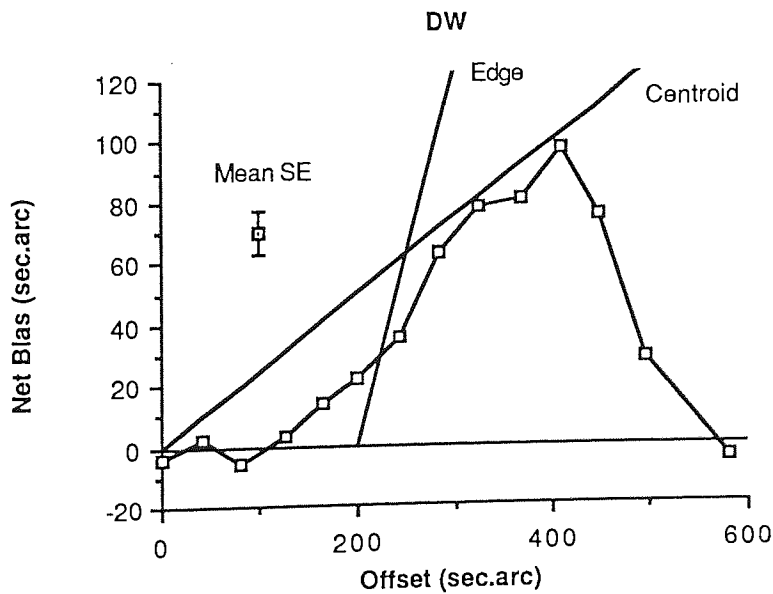
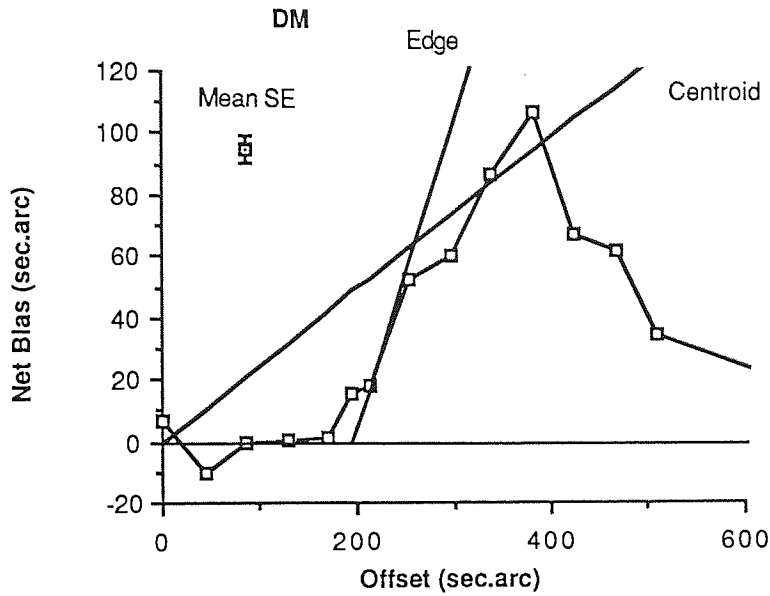


Figure 9.08: The effect on net bias of using only 8 dots within the standard 400 second of arc cluster. This time, certainly within the bounds of the cluster, the results more closely follow that predicted by the edge. Once the extra dot lies outside the cluster there appears to be a switch to use of centroid.

The results clearly show that the weighting function's peak amplitude varies with changes in cluster size and dot number. What common factor might be involved? In both cases the density of the dots within the cluster alters. The highest dot density occurs in the configuration shown in *Figure 9.05*. The weighting function closely follows the centroid prediction in this case. The lowest dot density occurs for the configuration shown in *Figure 9.06* where the weighting function closely follows that predicted by edge. The other configurations represent intermediate dot densities. The results, it has to be said, are not clear cut in all cases but the trend is there. This point is shown by *Figure 9.09* which shows peak amplitude plotted against dot density for both observers.

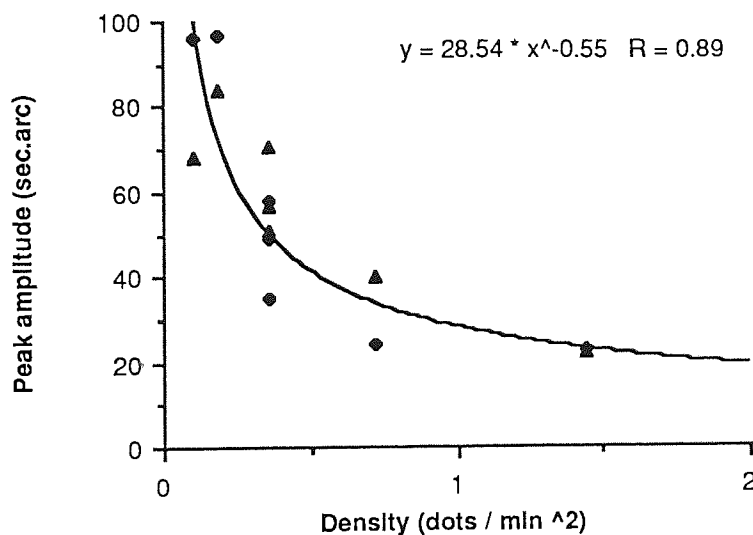


Figure 9.09: The peak amplitude of the weighting function plotted as a function of dot density. The filled diamonds are the results from observer DM, the filled triangles from observer DW. Note that the best fitting logarithmic curve has an exponent close to -0.5 indicating that the peak amplitude is inversely proportional to the dot density.

The data are best fitted by a logarithmic curve which has an exponent of around -0.5. This implies that peak amplitude is inversely proportional to the square root of dot density. In addition, it means that amplitude is inversely proportional to the density measured along the X-axis which is consistent with the idea that interpolation along the orthoaxial direction is used to determine location in a vernier task (Watt and Andrews, 1982; Watt and Morgan, 1983a). Cluster size does appear, superficially, to have an effect on the position of the peak effect. However, if the size of the cluster is subtracted from the position of peak magnitude one finds that the peak effect occurs around 150 seconds of arc outside the cluster edge in all cases. This is consistent with the view that this represents the limit beyond which the extra

dot is seen as separate and hence ignored in determining vernier offset. The limit is, however, due to two factors which co-vary depending on the cluster size. For the small cluster the dot is faint relative to the cluster and requires sufficient separation for its point spread function to be distinguished clearly from the much larger retinal light distribution of the cluster. For the larger cluster the inter-dot separation is large and in order to be clearly seen as separate the extra dot has to exceed this value. From the results obtained here it would seem that these two values are quite similar.

9.7: Discussion

The results show that altering the light distribution within the stimulus can have the effect of changing the apparent location of the object. This is confirmation of the findings of Westheimer and McKee (1977b), Ward *et al.* (1985), Levi and Westheimer (1987) and Whitaker and Walker (1988) who altered the internal light distribution of their stimuli. It also confirms the findings of Westheimer and Hauske (1975), Watt, Morgan and Ward (1983) and Badcock and Westheimer (1985) who introduced interfering features close to their stimuli. These reports found that interfering features had a peak effect on vernier thresholds if placed around 2 to 3 minutes of arc from the main stimulus features. This value coincides quite well with the value obtained in this series of experiments (approximately 2.5 minutes of arc). The weighting function is not linear but increases slowly within the cluster boundary and then more rapidly to peak between 2 and 3 minutes beyond the stimulus edge. In the case of the dot clusters the relationship between the amplitude of the peak effect is inversely proportional to the square root of the dot density. *Figure 9.02b* shows the relationship between vernier acuity and dot density and it can be seen that vernier thresholds deteriorate as dot density falls. This may be related to changes in stimulus contrast as was discussed in chapter 6. Certainly the subjective impression is that the clusters appear as low contrast blobs at low dot densities and as small high contrast dots at high dot densities.

The results also show that the determination of vernier thresholds cannot be explained simply on the grounds of single orientationally tuned filters nor on local-sign models whereby some feature of the stimulus is extracted to assign location. Instead, a combination of the two must be accepted which utilises information from both. This is consistent with several recent models concerning relative localisation (Klein and Levi, 1985; Morgan and Regan, 1987; Burbeck and Yap, 1990b). In the previous chapter strong evidence for the use of single spatial frequency selective filters in determining vernier acuity was put forward subject to limitations on the separations of the stimulus features. In this chapter the evidence points

toward some feature of the individual clusters being extracted and then compared to determine vernier offset. A logical combination, given this apparently conflicting evidence, would be that position is assigned using some feature of the stimulus and the output of this stage is then processed by orientationally tuned filters covering both clusters to signal the relative offset.

On the other hand, the stimuli used in this experiment and those discussed in the previous chapter are quite different. The fact that the repetitive gratings seem to support the use of filters tuned to different orientations, spatial frequency and phase while this experiment provides evidence for the extraction of a local-sign may reflect differences in the stimuli. Indeed, as has been suggested previously, it is possible that the strategy employed in performing a particular hyperacuity task may be dependent on the exact stimulus configuration used. It may be, therefore, that the use of "channels" or "local-sign" is not fixed but varies according to the exact task requirements (Klein and Levi, 1985; Morgan *et al.* 1990; Morgan, 1991).

The original premise of this investigation was that the position of the clusters was assigned by their centroid. However, in its strictest sense this would imply a linear relationship which we have not found. As a general statement we have to conclude that centroid is not the feature used to allocate position to an object. The dot density, and hence stimulus contrast, seems to have a controlling influence over the character of the weighting function. Indeed it may be that with a sufficiently low dot density the process of interpolation among the dots fails and the dots are then processed individually (Watt and Morgan, 1985; Whitaker and Walker, 1988). This may be a possible explanation for the shift from centroid to edge in assigning location which has been found here as the dot density falls.

Chapter 10: Spatial scaling of vernier acuity of M at the fovea center

10.1: Introduction

In chapter 2 it was explained that vernier acuity belongs to the group of relative localisation tasks whose thresholds surpass those imposed by the optical and anatomical limitations of the eye. Recently there has been some controversy about the variation with eccentricity of the hyperacuties and whether they differ in this respect from other threshold measurements such as visual acuity and contrast sensitivity. This chapter will detail a methodology which has been used to place a figure to the variation with eccentricity of vernier acuity.

10.2: Cortical magnification

It is well known that the extent of the visual cortex devoted to the processing of foveal vision is greater than that for the periphery. The way in which the foveal representation is magnified at the cortex compared with the retina has been given the term "Cortical Magnification", usually denoted by the symbol M (Daniel and Whitteridge, 1961). It is defined as the linear extent of visual cortex (in millimeters) per degree of visual angle. The reciprocal ($1/M$) has been found to increase linearly with increasing distance from the fovea. At the same time, many visual tasks have also been shown to decline linearly with increasing eccentricity. Clearly, if the two rates of change were found to be equal it would imply that the performance of the task is limited by the amount of cortical processing devoted to it at any location. The difficulty in determining whether this is so is that the stimulus configuration can make a significant contribution to the performance of the task. In some cases, therefore, failure to control the variation of the stimulus parameters with eccentricity can result in the rate of decline in performance due to eccentricity being altered by the concurrent variation in performance due to changes in the stimulus parameters.

10.2.1: Direct estimates of M

There have been several attempts to measure M directly in primates. The investigations usually use spots of light as stimuli with direct measurements, via electrodes, of cortical response to the stimulus. From this it is possible to calculate the change in M with eccentricity and hence to place a value on the rate of decline of inverse magnification ($1/M$).

It is also possible to estimate the value of M_0 , the hypothetical value of M at the very center of vision.

Early research in this field was carried out by Talbot and Marshall (1941) who attempted to plot the central visual field of a monkey onto the cortical surface. They devised an index of cortical representation which was based on the incremental angle, measured from the fovea, which occurred per millimeter of cortex. In essence, as the target is moved from the fovea into the periphery the cortical location stimulated varies. Thus, each millimeter of cortex will correspond with a particular extent of the visual field. The incremental angle is the change in visual angle corresponding to increments of one millimeter on the cortex.

This work was extended by Daniel and Whitteridge (1961) who mapped the visual field representation into the calcarine fissures. It was found that the inverse magnification ($1/M$) varied in proportion to the fall in human visual acuity with eccentricity as reported by Weymouth (1958). From this they asserted that, at any eccentricity, resolution required two areas of cortical excitation separated by, what they termed, the acuity distance, which depended on $1/M$. This can be thought of in a similar vein to the resolution limit imposed by photoreceptor spacing outlined in chapter 1. The two stimulated cortical areas must have an area of lesser stimulation between them in order to be resolved. At the fovea, where the extent of cortex per degree of visual angle is large, the acuity distance represents a small retinal separation. Conversely, in the periphery the extent of cortex per degree of visual angle is much smaller and the acuity distance represents a much larger retinal separation. If the concept of cortical magnification is correct it clearly follows that in cortical terms this acuity distance should be constant. In fact, Daniel and Whitteridge estimated that the minimum cortical separation of two objects had to be $67 \mu\text{m}$ in order for them to be resolved.

Rolls and Cowey (1970) investigated the magnification factors in the rhesus and squirrel monkeys. They checked their results by estimating the total area of the visual cortex from the magnification factors they had obtained and then compared this with anatomical data on actual cortical area. They obtained a value of 2900 mm^2 by calculation which compares well with estimates of human cortical area. These included those of Filimonoff (1932) as revised by Sholl (1956) and Cunningham and Brodmann (as cited by Polyak, 1957) who found values ranging from 3000 to 3500 mm^2 . They used this close agreement as strong evidence of the validity of their results.

In studies on receptive fields Hubel and Wiesel (1974, 1977) found that in the cortex there were blocks (hypercolumns; see chapter 3) approximately 1 or 2 mm in extent which acted in isolation from the surrounding areas. Essentially, at any cortical location there were a selection of receptive fields which varied in size and position and outlined an area which they called the aggregate field. They concluded that cortical magnification is related to receptive field size in order to maintain uniformity within the cortex. The blocks are essentially constant in size so for foveal vision they will represent a much smaller area of the visual field than in the periphery.

Dow *et al.* (1981) measured receptive field size and magnification in the striate cortex of rhesus monkeys. They confirmed the findings of Hubel and Wiesel (1977) but disputed whether the receptive field size is proportional to $1/M$. It was also found that the receptive field overlap at the fovea is far greater than in the periphery. This suggests that a single point of light will stimulate far more cortical cells if presented foveally compared with peripherally.

A method of 2-deoxyglucose (2DG) labelling was employed by Tootell, Silverman, Switkes and De Valois (1982) who used it to map the foveal representation. In this experiment monkeys were injected with 2DG. They then fixated a target consisting of concentric rings and spokes for 30 minutes. During this period the 2DG was concentrated in the cortex at locations where peak activity was occurring. When the cortex was investigated the outline of the 2DG was clear and allowed the location of activity to be plotted. Their investigation found a value for $1/M$ of 13.0 degrees per millimeter at the fovea.

Van Essen, Newsome and Maunsell (1984) made recordings from six macaque (*M. Fascicularis*) monkeys in order to map the striate cortex. They discussed their value of M_0 (13.0 mm/deg) in relation to the others mentioned here (see *Table 10.01*). It was suggested that the earlier results may have suffered from inaccuracies in technique and mathematical interpretation. In their considered view the value of M_0 which they and Tootell *et al.* (1982) had obtained was a good estimate. They also pointed out that the cortical representation of the fovea was considerably greater than that suggested by ganglion cell density which indicated that the cortex emphasised the fovea to a much greater extent than the retina. This had been previously proposed by Malpeli and Baker (1975).

Table 10.01

Investigation and year	Foveal Cortical Magnification (M_o) in millimeters per degree	Type of monkey
Talbot and Marshall (1941)	6.0	Rhesus
Daniel and Whitteridge (1961)	6.4	various
Rolls and Cowey (1970)	4.5	Rhesus / Squirrel
Dow, Snyder, Vautin and Bauer (1981)	30.0	Rhesus
Tootell, Silverman, Switkes and De Valois (1982)	13.0	Cynomolgus
Van Essen, Newsome and Maunsell (1984)	13.0	Cynomolgus

Table 10.01 lists the values of M_o which have been reported by various investigations using monkeys. The range of values obtained is quite large which immediately makes the interpretation of such results fraught with uncertainty. The reasons for the large variations may be due to inter species variability, differences in experimental methods and the improvements in available technology over the 40 years which the experiments cover.

All of the values of M_o listed in *Table 10.01* have been obtained using monkeys. There is, however, one study in which a human volunteer was used. Brindley and Lewin (1968) inserted a bank of electrodes over the striate cortex and used the phosphenes generated by this electrical stimulation to plot the subjects visual field. This report has been the subject of much analysis which has been used in conjunction with work done on monkeys (see above) to try and obtain an estimate of the value of M_o in man.

Cowey and Rolls (1974) used the data of Brindley and Lewin and calculated values for M_o using the angular separation and mean eccentricity of pairs of the phosphenes. They obtained a value of 15.1 mm/deg for M_o . As with Rolls and Cowey (1970) they then used an estimated value of cortical area compared with anatomical results to confirm the validity of their findings. They also found that $1/M$ is directly proportional to the minimum angle of resolution in man.

10.2.2: Indirect estimates of M

It is usually impossible to perform direct analysis on humans to estimate the value of M and indirect estimates have, therefore, had to be used. One obvious method is to measure the density of ganglion cells in the retina and use the result to infer a value for cortical magnification. The assumption which needs to be made is that cortical magnification will vary in proportion to ganglion cell density.

Drasdo (1977) investigated both ganglion cell receptive field density (D_r) and minimum angle of resolution data. Previous work on ganglion cell receptive field densities was corrected by the use of a specially designed schematic eye (Drasdo and Fowler, 1974). This reduced errors due to displacement of ganglion cells from their receptive fields and also due to shrinkage of the tissue used in the previous works. When compared with the minimum angle of resolution with eccentricity data of Weymouth (1958) a strong correlation was found. In addition, strong correlation was found with estimates of M obtained from the data of Brindley and Lewin (1968). The results showed that M^2 is proportional to D_r . He was able to suggest a value for human M_o of 11.5 millimeters per degree, somewhat lower than that proposed by Cowey and Rolls (15.1 mm/deg ; 1974).

Rovamo and Virsu (1979) compared the available data on the density of retinal ganglion cell receptive fields and previous estimates of M . They also found that M^2 was directly proportional to D_r in primates. They used this finding to calculate values for human M and expressed them in the form of four equations, one for each of the prime meridians. Using the values thus obtained they then scaled the retinal dimensions of test sinusoidal gratings in order to estimate the contrast sensitivity function at 25 locations across the retina. The results confirmed that by use of a suitable scaling factor it was possible to accurately predict visual acuity and resolution at any location. They also calculated a value for human M_o of 7.99 mm/deg which is lower than the two previous estimates mentioned above.

These values were obtained using the assumption that the magnification factor across the retina was equivalent to the magnification factor at the cortex. However, it has been shown that, certainly in monkeys, this may not be the case. The fovea has a much larger cortical representation than would be predicted by ganglion cell count alone (Van Essen *et al.* 1984). However, it is still unclear, and the subject of some debate, whether this is due to some

additional processing in the cortex or simply an underestimate of the true retinal ganglion cell density. This last point has been considered by Wässle, Grünert, Röhrenbeck and Boycott (1989, 1990) who proposed that the displacement of foveal ganglion cells and the presence of amacrine cells within the ganglion cell layer causes considerable errors in estimates of foveal ganglion cell density. In addition, they showed that the traditional belief of a one to one foveal cone to ganglion cell ratio was erroneous (for example Polyak, 1941). This had also been previously disputed by Schein (1988) who suggested a two ganglion cell per foveal cone ratio. Wässle *et al.* (1990) now suggest that this ratio is even higher (between 3.3 and 4 ganglion cells per foveal cone). This revision of the density and distribution of retinal ganglion cells alters the accepted retinal magnification factor substantially and allows of the possibility that retinal and cortical magnification factors may indeed be equivalent.

10.2.3: Psychophysical estimates

Psychophysical experiments cannot give an absolute value for the cortical magnification factor at any eccentricity as they need to assume a value for M_o . However, they can provide information as to how M varies with eccentricity. There have been several experiments which have shown that the decline in performance with increasing retinal eccentricity for several psychophysical tasks is approximately the same as the change in the original estimates of ganglion cell density. These include contrast sensitivity and visual acuity (Rovamo and Virsu, 1979; Virsu, Nasanen and Osmovita, 1987). The use of hyperacuity type stimuli has resulted in some dispute as to what scaling factor is appropriate and, indeed, whether there is a single scaling factor at all. In particular, Levi *et al.* (1985) investigated vernier acuity and found that performance fell much more rapidly than would be predicted by the estimates of human cortical magnification based on ganglion cell densities. They found that it scaled to the estimate of cortical magnification proposed by Dow *et al.* (1981). It was suggested that this indicated that vernier acuity was scaled according to true cortical magnification while contrast sensitivity and visual acuity reflected retinal processing. The more rapid deterioration, with eccentricity, of two dot vernier thresholds had previously been found by Westheimer (1982). On the other hand, he noted that the optimum separation for the two dots increased quite slowly with increasing eccentricity. This led him to suggest that hyperacuity tasks may not be scaled by a single factor over the whole of the visual field. In contrast to this, Beck and Halloran (1985), again using a two dot vernier task, found that over the limited range between 2 and 8 degrees thresholds appeared independent of eccentricity. Finally, further conflicting results were found by Virsu *et al.* (1987) who succeeded in scaling a two dot

vernier task according to the estimate of cortical magnification proposed by Rovamo and Virsu (1979) based on retinal ganglion cell density. This variability of results has led to the suggestion that several underlying mechanisms may contribute to the final threshold response and that these each scale in different ways with eccentricity (Yap, Levi and Klein, 1989; Hess and Watt, 1990).

10.2.4: Stimulus scaling

In order to obtain equivalent performance in a task foveally and in the periphery it is necessary to increase the parameters of the peripheral stimuli in line with cortical magnification. This magnification of the peripheral stimuli clearly requires the use of a suitable scaling factor. One of the problems with this type of psychophysical experiment is that improper scaling of the stimulus, or failure to scale some feature of the stimulus at all, may introduce distortions into the results. In particular, a prior choice of scaling factor may strongly influence the final result if this depends not only on eccentricity but also on stimulus dimensions. For example, if peripheral performance depends critically on the separation of the features, an underestimate of the scaling factor may result in peripheral targets being too close together and producing thresholds far worse than they should be. Clearly, any comparison with foveal data would be improper in such a circumstance.

There have been a couple of suggested procedures which might usefully be employed to counteract this problem (Watson, 1987; Johnston 1987).

Watson used a set of Gabor functions which were all magnified versions of each other. In his example the functions were placed on a progression in which each differed from those above and below by a factor of two. Each target, therefore, had a constant number of cycles and decreased in spatial frequency by a factor of two between each target. The procedure he adopted was to present each target foveally to obtain a contrast sensitivity function. The same set of targets is then presented at an eccentric point and another contrast sensitivity function obtained (*Figure 10.01a,b*).

Essentially the scaling factor to be employed is that which moves the second CSF so that it aligns with the first. To test the suggestion just such a target set were used, presented at 0 and 3 degrees, and a scaling factor obtained. It should be noted, however, that the lowest spatial frequency targets, after scaling, failed to match properly. This was put down to the

extended nature of such targets which results in not all parts of the stimulus lying at the same eccentricity. The results subsequently obtained from such extended stimuli cannot be considered a true measure of the *local* spatial scale.

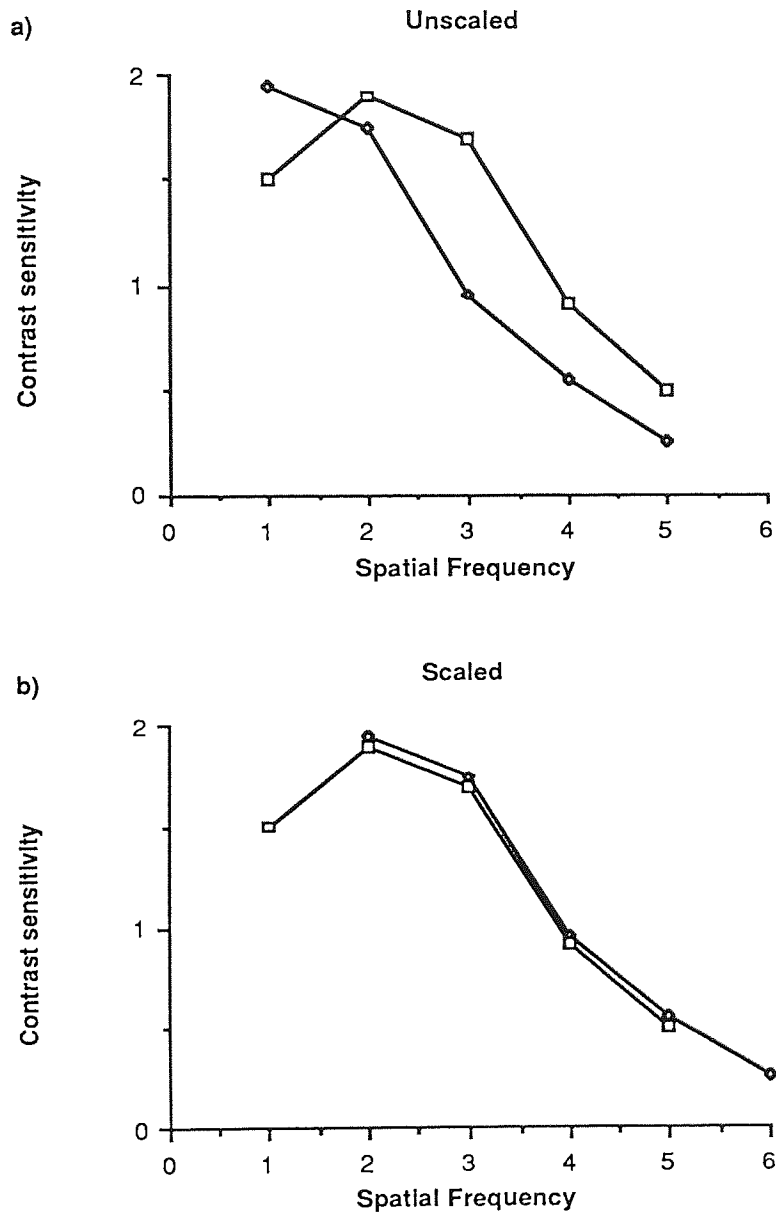


Figure 10.01: A schematic of the method proposed by Watson (1987) to estimate local spatial scale. (a) shows the results of presenting a selection of targets, each scaled versions of the others, foveally (open squares) and in the periphery (open diamonds). (b) shows the application of a scaling factor to the peripheral data which moves the curve to the right until it is superimposed on the foveal data. The scaling factor is the magnitude of the horizontal shift required.

Johnston (1987) proposed a similar method. In this case a selection of gratings were presented at various locations between 0 and 40 degrees eccentricity. The choice of an appropriate scaling factor then allowed all of the curves obtained to collapse to a single function. He also carried out an experimental study which covered a range of spatial frequencies presented between the fovea and 40 degrees eccentricity. The curves obtained were, by application of a suitable scaling factor at each eccentricity, again made essentially coincident.

In contrast sensitivity experiments the y-axis represents a measure of contrast modulation and is, therefore, independent of stimulus size. This is why in the experiments of Watson (1987) and Johnston (1987) spatial scaling of the results along only the x-axis was successful in making foveal and peripheral functions overlap. Most hyperacuity tasks are two dimensional where the threshold measure is itself magnification dependent. For instance, if a vernier stimulus is magnified by a factor of two not only does line length and width double, but so does the vernier offset. In such cases scaling factors need to be applied along both x and y-axes for foveal and peripheral functions to overlap.

This experiment set out to use the methodology described here to see if vernier acuity can in fact be scaled by a single factor and also to compare the results with the findings of previous workers.

10.3: Method

The stimuli were presented on a high resolution color monitor under the control of the Nimbus AX microcomputer as described in chapter 5. The stimuli consisted of white targets with a luminance of 34 cd/m^2 and consisted either of two lines of variable length or of two dots with a variable separation, presented against a dark background. The experiments were conducted in a darkened room to remove references, such as the edge of the screen, against which the vernier offset could be judged. The targets were presented for 250 msec following which the subject responded via the keyboard as to whether the upper line or dot was offset to the left or right of the lower. This, therefore, represents a two-alternate forced choice procedure as outlined in chapter 4. Onset and offset of the stimuli was instantaneous, due to software limitations, but the next stimulus presentation followed immediately after the subject responded which minimised problems due to accommodation and fixation fluctuations. The

PEST technique (see chapter 4) was employed to determine thresholds which were calculated from an estimate of the 75% point on the psychometric function for both left and right responses using a randomly interleaved procedure. Vernier bias was defined as the midpoint of the leftward and rightward estimate with half the distance between the two positions representing vernier threshold. As has been stressed the separation of bias and threshold is important in this type of experiment as bias cannot be assumed to vary in the same way as threshold. Four estimates of threshold (and bias) were obtained for each combination of line length/dot separation and eccentricity, the combinations being chosen at random. Each estimate required about 60 trials and to avoid fatigue the data was collected in several short 20 to 30 minute sessions. The subjects were highly experienced in both foveal and peripheral hyperacuity tasks. They wore their optimum spectacle corrections (both are moderately myopic) and viewed the stimuli monocularly with their dominant eye. It should be noted that the design of modern spectacle lenses produces negligible distortion at eccentricities up to 15 degrees. This factor can therefore be assumed to have no bearing on the results obtained.

Two groups of stimuli were employed, the first consisted of abutting lines of varying lengths and the other two dots with a variable vertical separation. As outlined above, a group of targets was presented foveally and at 5, 10 and 15 degrees in the nasal visual field (temporal retina). For the foveal targets the line lengths were 1, 2, 4, 8 and 16 minutes of arc while the width was a constant fraction ($1/9^{\text{th}}$) of the length. The two dot stimuli were presented foveally with separations of 1, 2, 4, 8 and 16 minutes of arc and consisted of dots whose height and width were equal to a constant fraction ($1/9^{\text{th}}$) of the separation. Therefore, for both sets of targets each stimulus presented was either a magnified or minified version of all the others.

In the periphery a fixation spot was used, and to avoid use of this as a reference the stimuli were jittered horizontally, relative to fixation, with a standard deviation equivalent to 0.5% of the eccentricity. Groups of successively larger stimuli, each magnified or minified versions of each other, were presented at each eccentricity. This was achieved by using different viewing distances. The foveal viewing distance was 10 meters reducing to 2.5 meters at 5 degrees, 1.5 meters at 10 degrees and 1 meter at 15 degrees eccentricity. The concept of local spatial scaling proposes that at any eccentricity a stimulus of a certain size should have a foveal equivalent which is simply a minified version of it. By altering the viewing distance it was possible to restrict the measurements to a range at each eccentricity which were likely to have an equivalent stimulus at the other eccentricities investigated. As an alternative it would

have been possible to simply extend the range of stimulus sizes covered. This would, however, have resulted in many observations being either impossible to perform, because of the small size of the stimulus, or wasteful because having no equivalent at other eccentricities they failed to supply any useful information. It has to be stressed that the targets are always magnified or minified versions of each other at each eccentricity and the change of viewing distance does not imply any initial assumption as to what that magnification factor may be. The choice of viewing distances was made following a series of pilot runs which were undertaken in the months before the final experiment was carried out. This also ruled out any possibility of practice effects being significant as the number of trials far exceeded that required to reach a performance plateau (Westheimer and McKee, 1978).

10.4: Results

10.4.1: Line stimuli

Figure 10.02 shows the vernier thresholds obtained from the abutting line stimuli as a function of the line length. The foveal data follows the well documented trend (see chapter 2) with thresholds improving as line length is increased to around 4 minutes of arc and then levelling off at a value of approximately 6 - 9 seconds of arc. As eccentricity is increased the thresholds increase in absolute terms for all line lengths but with the trend for lower sensitivity for the shorter lines remaining. The curves are clearly displaced relative to each other not only horizontally but also vertically. This reflects the fact that a vernier type task is two-dimensional, the offset being magnification dependent as well as the size of the stimulus. Contrast sensitivity, on the other hand, is one-dimensional since the y-axis represents contrast modulation which is independent of stimulus size. In the two experiments mentioned earlier (Watson, 1987; Johnston, 1987) the curves were displaced only along the x-axis for this very reason. It is possible, however, to modify the data presented here to make it comparable by expressing the vernier threshold not in absolute terms but relative to the size of the stimulus (*Figure 10.04*). This time the curves are simply displaced along the x-axis and if the concept of local spatial scale applies in this case the choice of a suitable scaling factor at each eccentricity should allow the peripheral curves to become coincident with the foveal curve.

In order to determine what the scaling factor might be it was necessary to find a factor which minimised the variance between the foveal data and the data at any eccentric point. As the

relationship (*Figure 10.04*) is not quite linear, when plotted on log-log co-ordinates, a second-order polynomial was employed, although this choice is not critical. The foveal data and the eccentric data, with an estimate of the scaling factor applied, were fitted with a second-order polynomial and the residual sum-of-squares deviation about this best fitting regression line calculated. This process was repeated until a minimum variance value was obtained. The value thus estimated was then taken to give an estimate of the actual scaling factor. The use of logarithmic data makes the intra-eccentricity variance constant which therefore minimises any contribution it might make to the final estimate of the scaling factor. In addition the use of logarithmic data gives equal weighting to foveal and eccentric deviations about the regression (Virsu *et al.* 1987).

It is possible to apply a similar process to the data shown in *Figure 10.02* but this time the scaling factor must be applied along both the x and y-axes. In fact, identical results were obtained from both methods but the use of the data from *Figure 10.04* is more like that proposed by Watson (1987).

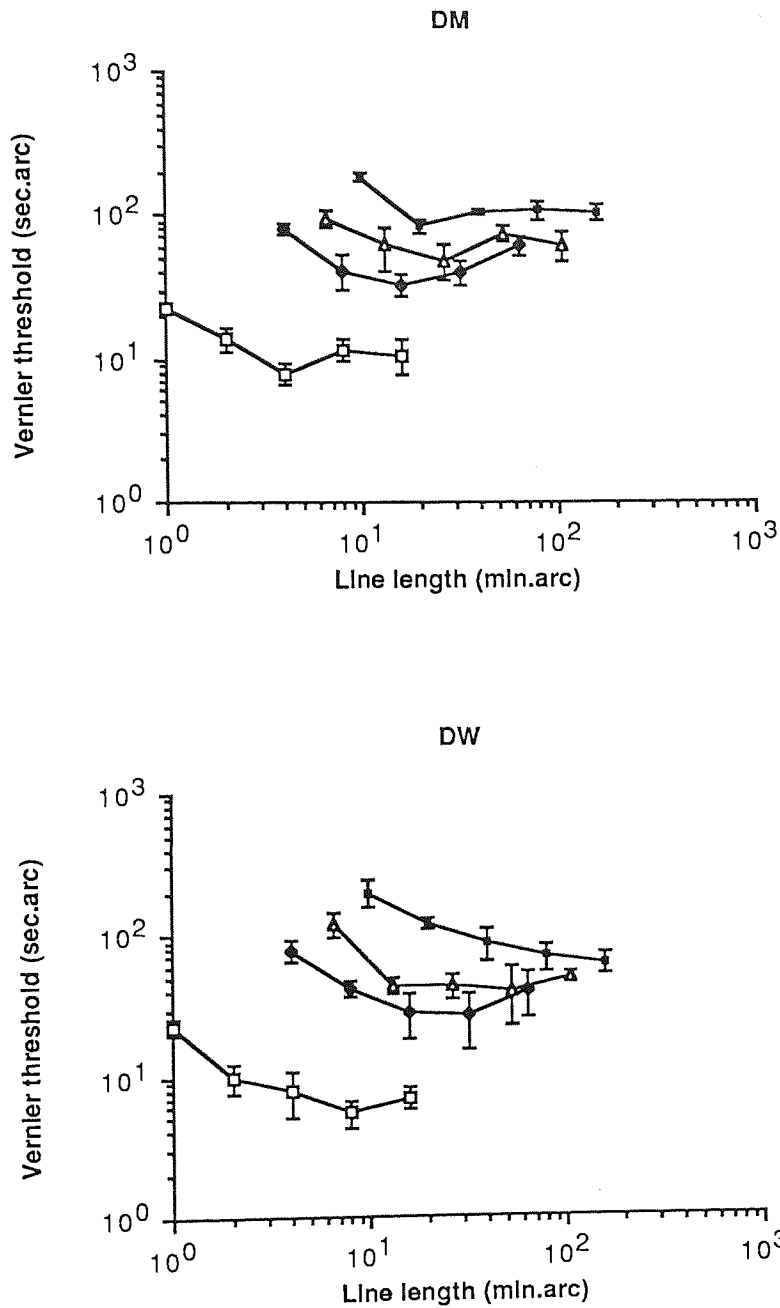


Figure 10.02: Vernier thresholds plotted as a function of line length for stimuli presented at different eccentricities. Foveal (open squares), 5 degrees (filled diamonds), 10 degrees (open triangles) and 15 degrees (filled squares). The results for both observer DM (upper) and DW (lower) are included and are discussed in the text.

The scaling factors were obtained for each eccentricity and are shown plotted against eccentricity in *Figure 10.05*. Because the scaling factors have been obtained relative to the foveal data the straight line is constrained to pass through the value of unity at zero eccentricity. The linearity of the result allows of the proposition that, over the range of eccentricities covered here, the scaling factor (F) can be related to eccentricity (E) by the equation....

$$F = S.E + 1$$

where S is the normalised gradient. The reciprocal of S represents the eccentricity at which F doubles, providing an indication of the rate of increase of F (Levi *et al.* 1985). This value (E_2) is given by the absolute value of the eccentricity where the scaling factor is zero, *i.e.* the projected x-intercept in *Figure 10.03*. The values for E_2 obtained in this experiment are 1.78 ± 0.13 for subject DM and 1.66 ± 0.14 for subject DW. *Figure 10.06* shows the result of scaling the curves from *Figure 10.04* according to the above equation. It is immediately apparent that there is minimal inter-eccentricity variance with no systematic variation between the data points at each eccentricity.

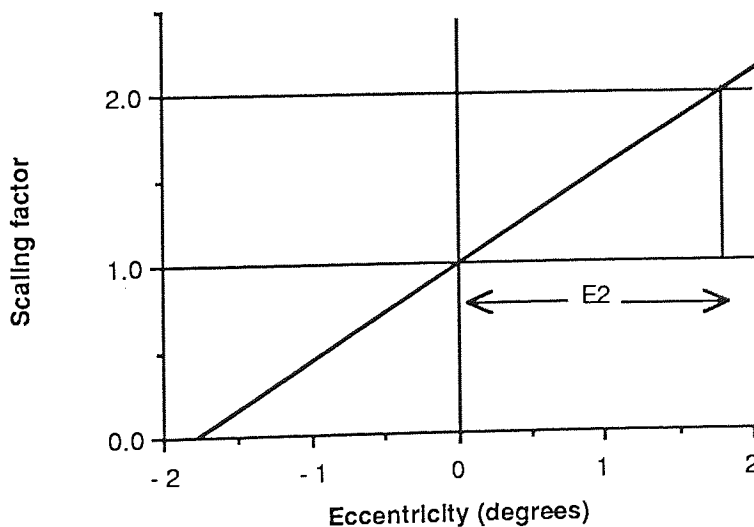


Figure 10.03: A plot of scaling factor against eccentricity. The normalised gradient (S) can be seen to intercept the x-axis at an eccentricity of approximately -1.75 degrees. E_2 , defined as the eccentricity where the scaling factor doubles clearly has the same value. The x-intercept therefore defines the value of E_2 .

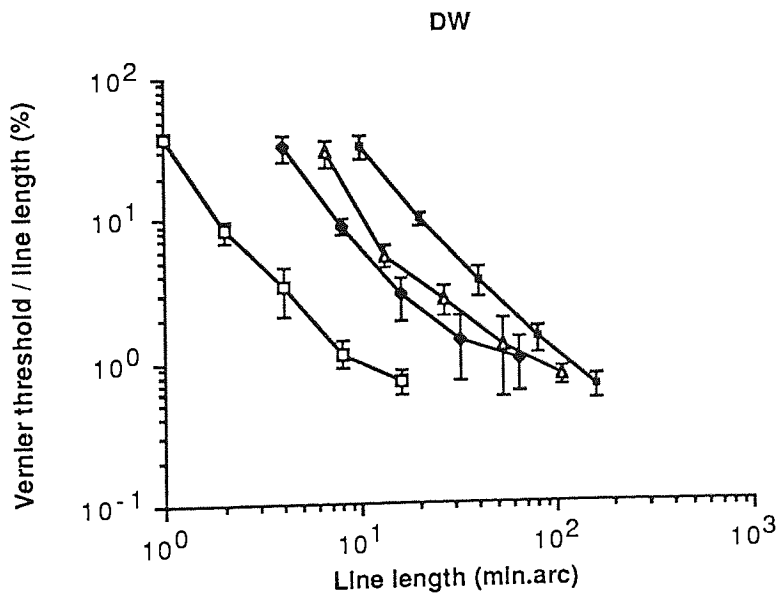
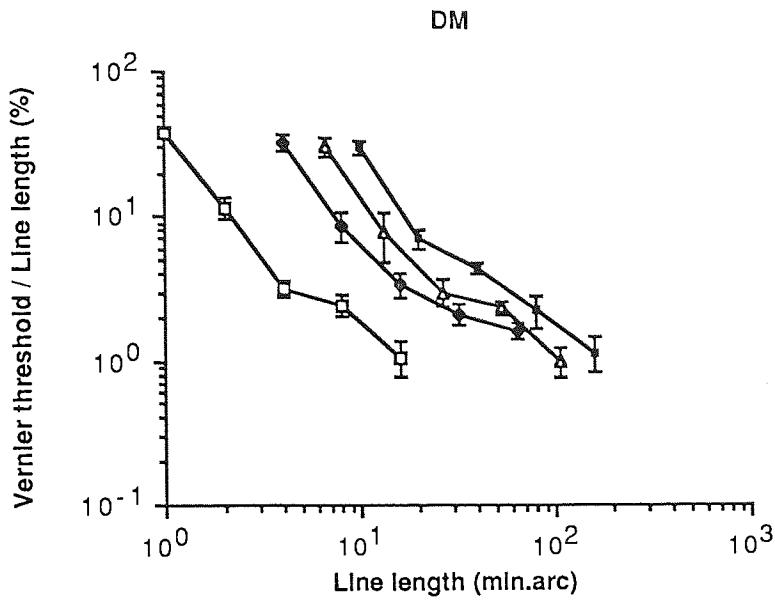


Figure 10.04: Vernier thresholds as a proportion of line length plotted against line length for the same eccentricities as Figure 10.02. This time the variance between the functions occurs only along the x-axis and choice of a suitable scaling factor should allow the curves to become coincident.

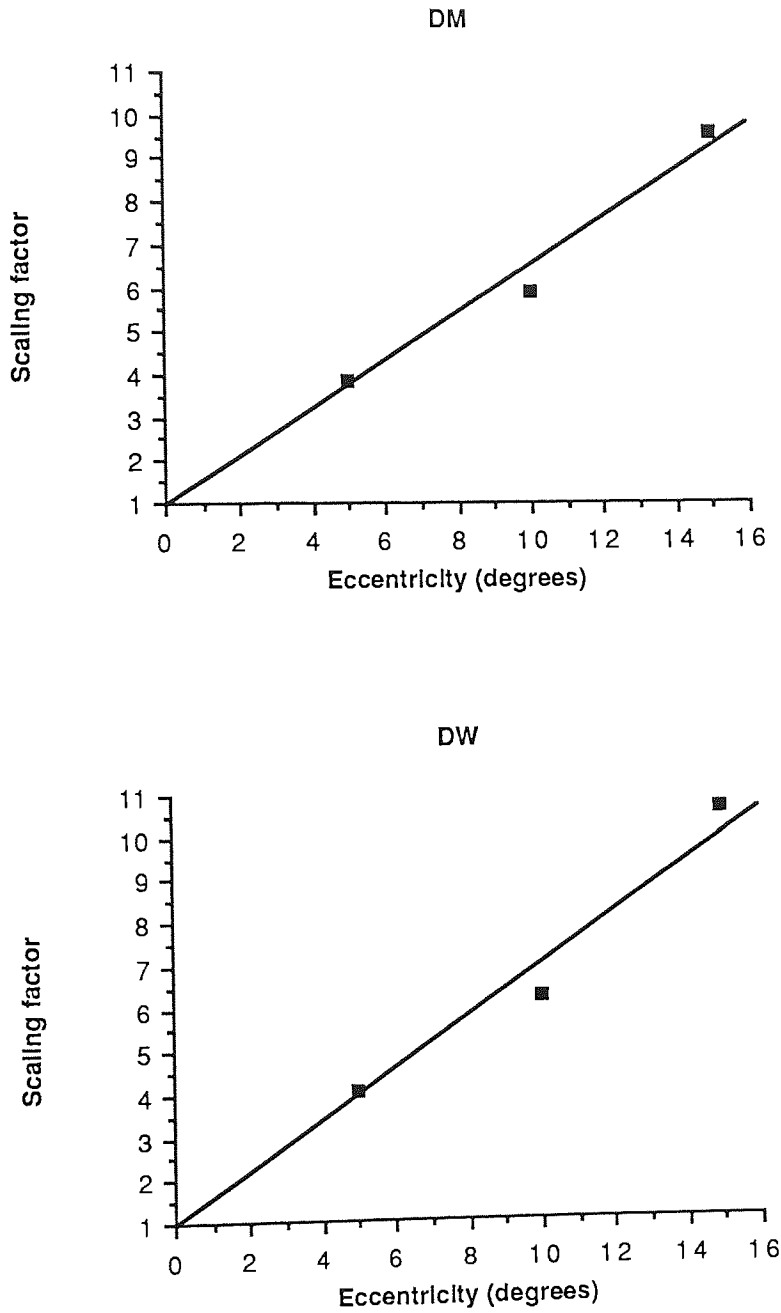


Figure 10.05: The scaling factor, found by the method discussed in the text, plotted against eccentricity. The linear fit is constrained to pass through 1 since the peripheral results are obtained relative to the foveal data.

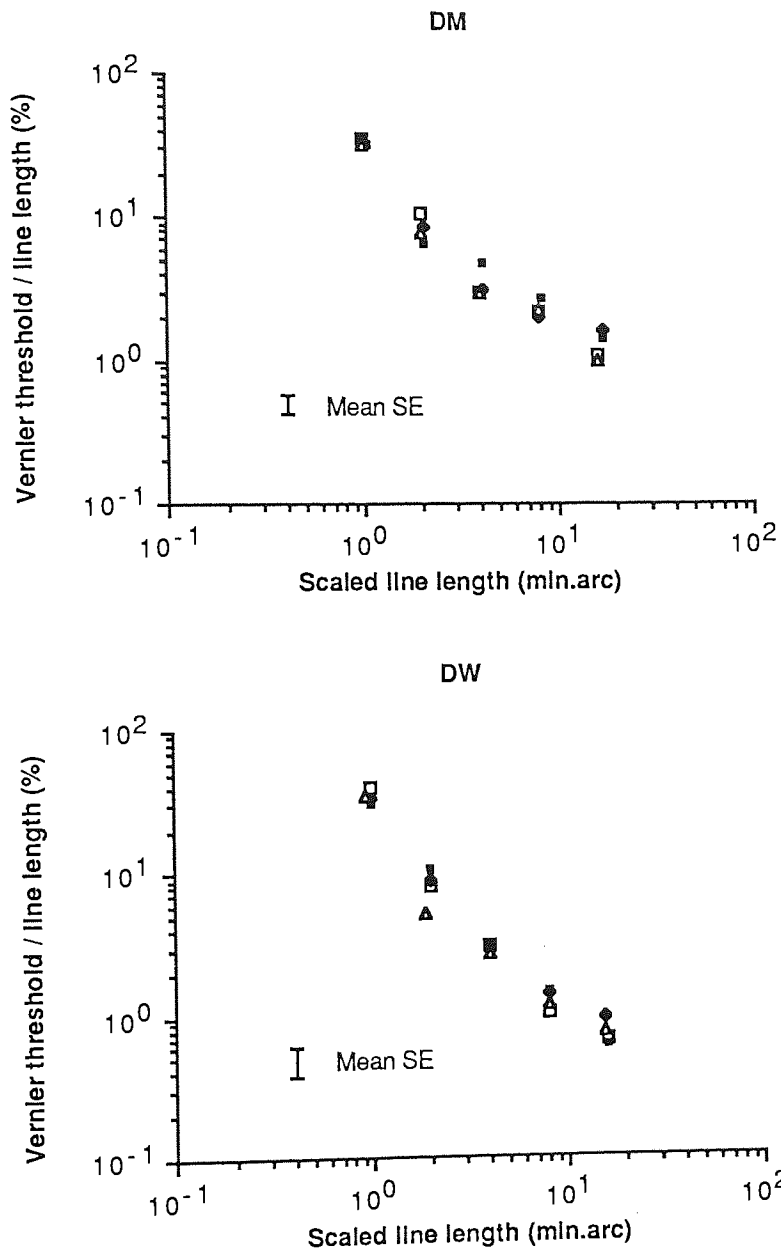


Figure 10.06: The data from Figure 10.04 after use of the scaling factor. Note how the curves become essentially coincident with no systematic variation apparent.

10.4.2: Dot stimuli

Figure 10.07 shows vernier thresholds plotted against separation for the two dot stimuli. Again the foveal data demonstrates the characteristic function obtained by previous experimenters (see chapter 2) with the minimum threshold value occurring at a separation of 4 minutes of arc. On this occasion, however, while the threshold values are in all cases higher with increasing eccentricity they differ in shape from the foveal function. It is clear that the foveal results have a characteristic U-shaped function while the peripheral results are much flatter and show a gentle rise in threshold values with increasing gap size. This difference in shape immediately suggests that scaling will not be as successful as it was with the line stimuli. The results support the finding of Westheimer (1982) that the optimum separation increases more slowly with increasing eccentricity than the vernier thresholds. This is apparent when one compares the optimum separation at the fovea (≈ 4 minutes of arc) with that at 15 degrees eccentricity (≈ 16 minutes of arc), a fourfold increase, and the optimum thresholds at the two points (≈ 6 seconds of arc at the fovea and ≈ 100 seconds of arc at 15 degrees), an eighteenfold increase. *Figure 10.08* shows the data with threshold expressed as a fraction of separation as was done for the two line data in *Figure 10.04*. Once again the foveal results show a different shape to the peripheral data with a steeper fall at small separations and a flattening off at larger separations.

Using the method outlined earlier scaling factors were obtained at each eccentricity and the data fitted by a linear regression (*Figure 10.09*). The values of E_2 thus obtained were 1.51 ± 0.18 for subject DM and 1.70 ± 0.08 for subject DW. *Figure 10.10* shows the data after application of the scaling factor and this time there is a systematic difference between the foveal and peripheral results. Essentially, thresholds are worse foveally for small separations but better at larger separations.

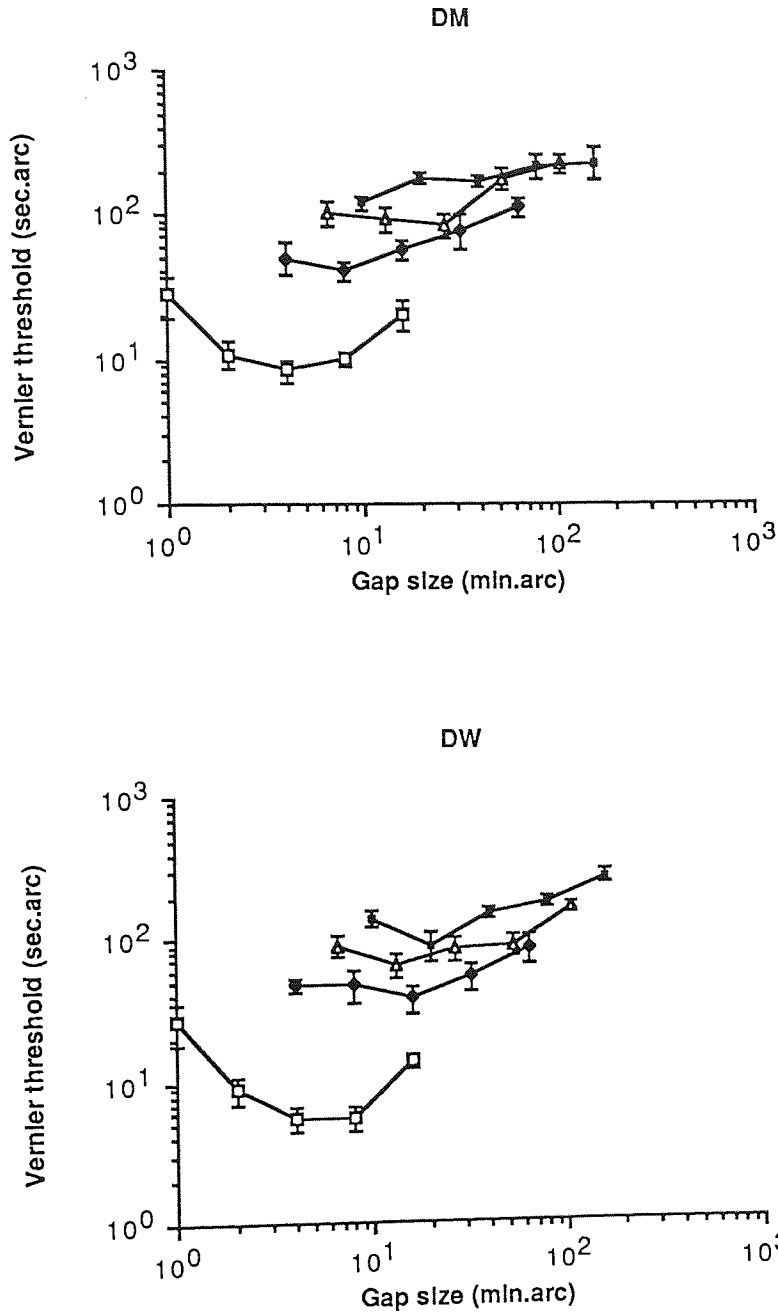


Figure 10.07: Vernier thresholds plotted as a function of gap size for stimuli presented at different eccentricities. The open squares represent foveal stimuli, the filled diamonds stimuli presented at 5 degrees eccentricity, the open triangles 10 degrees eccentricity and the filled squares 15 degrees eccentricity. Note the difference between the shape of the foveal function and the peripheral functions.

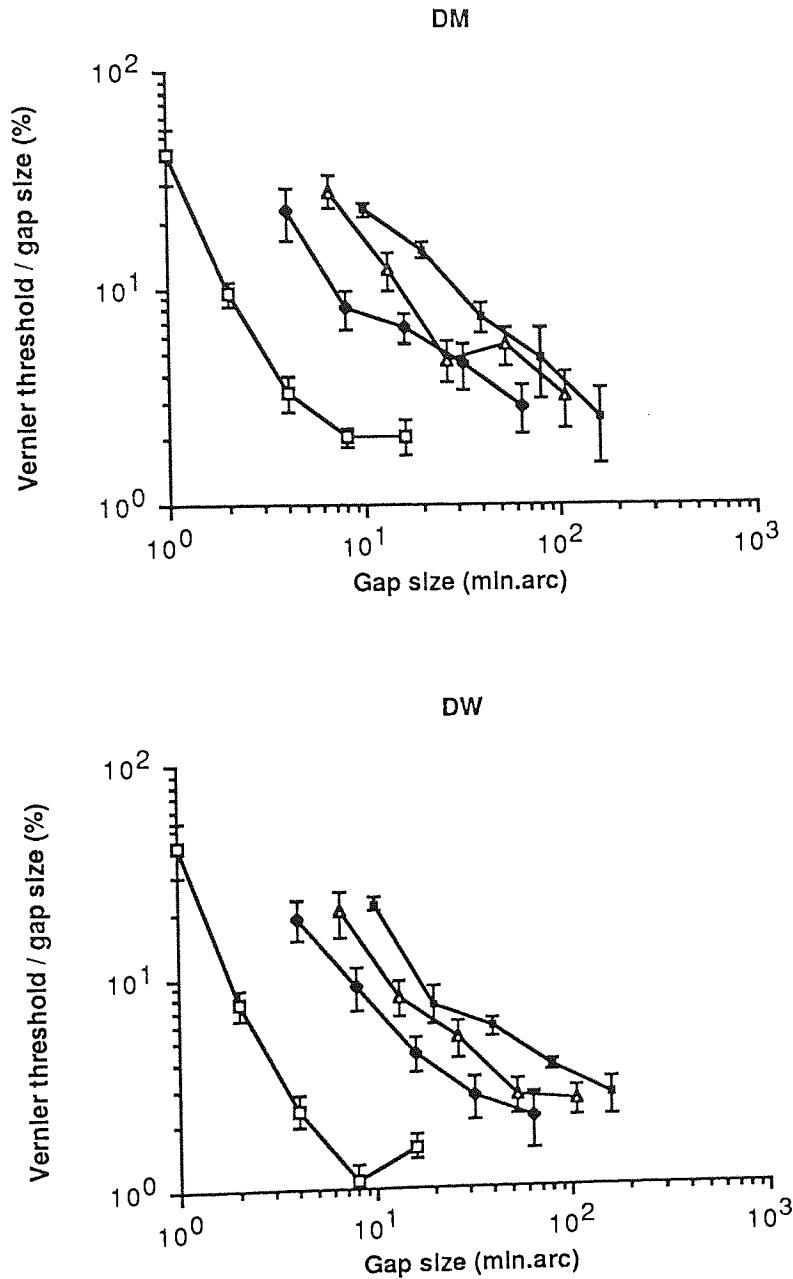


Figure 10.08: Vernier thresholds as a proportion of gap size plotted as a function of gap size for different eccentricities. The symbols represent the same eccentricities as Figure 10.07. Once again there is a difference between the foveal and peripheral results.

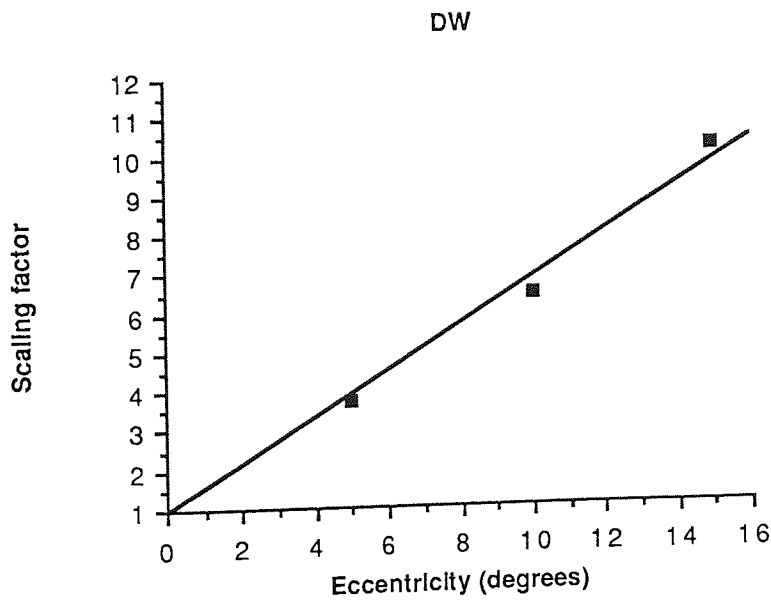
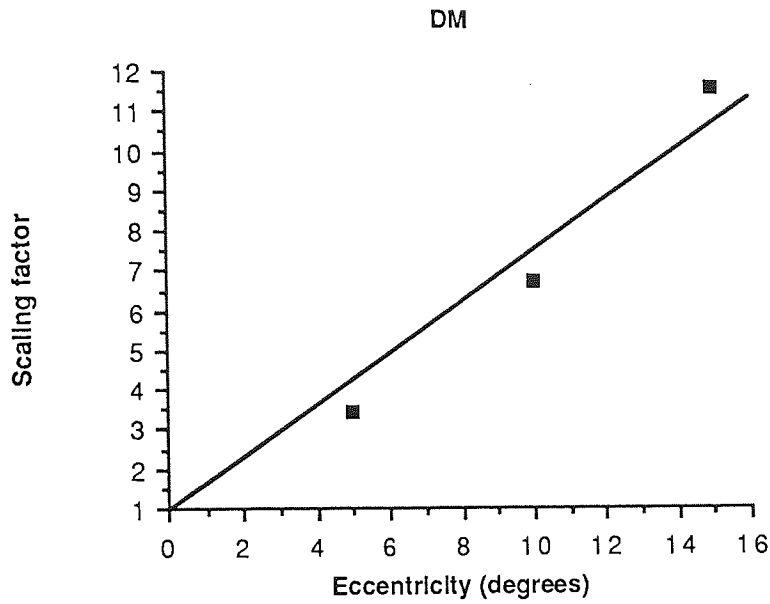


Figure 10.09: The scaling factors obtained for the two dot stimuli plotted as a function of eccentricity.

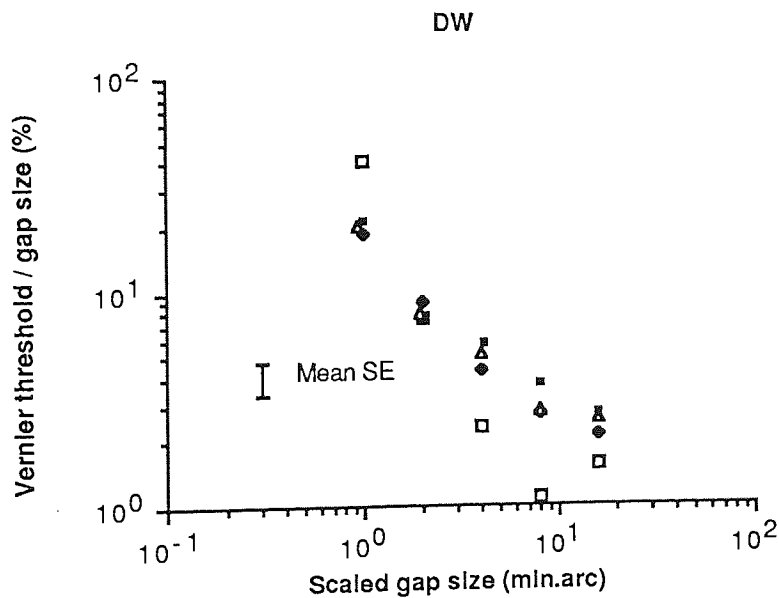
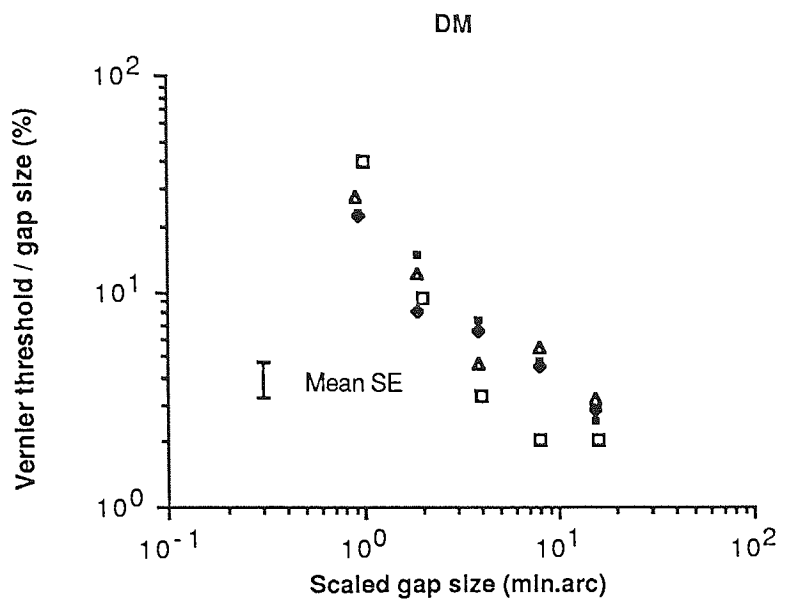


Figure 10.10: The data from Figure 10.08 after application of the scaling factors. This time while the peripheral data become essentially coincident there is a systematic variability for the foveal data. At small gap sizes foveal thresholds are relatively worse and at large gap sizes relatively better than peripheral thresholds.

10.4.3: Separation and eccentricity

Why is scaling more successful for line stimuli than separated dot stimuli? Suspicion falls, immediately, on optical factors which affect stimuli in close proximity to each other more than those further apart. For the two dot stimuli at small separations, and the line stimuli for short line lengths, the two images on the retina will overlap causing difficulty in detection of the vernier offset. In the periphery the gap sizes, and line lengths, are greater which will tend to reduce this effect, thus a shift from band-pass at the fovea to low-pass in the periphery would be expected. This is demonstrated by the more pronounced effect of artificial image degradation for two dot stimuli at small rather than large separations (Williams *et al.* 1984).

Apart from this factor there is also the problem that, for the two dot stimuli, increasing separation will alter the eccentricity of the two dots unless steps are taken to prevent this. The results outlined here may, therefore, reflect a combination of the effects of separation and eccentricity. This would be expected to affect the foveal data, where separation is large relative to eccentricity, more than the peripheral stimuli, where the separation is small relative to the eccentricity. A way of eliminating this problem is to place the stimuli on iso-eccentric arcs whereby the effect of separation on thresholds can be determined without being contaminated by the effects of eccentricity (Levi, Klein and Yap, 1988; Levi and Klein, 1990).

The two dot experiment was, therefore, repeated with the stimuli placed on iso-eccentric arcs. For the "foveal" data an arc of radius 16 minutes of arc was used which allows separations of up to 32 minutes of arc to be obtained. A 32 minute of arc separation would involve the two dots being placed above and below fixation. Lesser separations were obtained by moving the dots around the arc, in the nasal visual field, while maintaining fixation at the center. For the peripheral data the two dots were simply placed on iso-eccentric arcs of 5, 10 and 15 degrees radius.

Figure 10.12 shows the results obtained with this modification. This time the peripheral curves are similar to those found earlier (*Figure 10.07*). One should not be too surprised by this as the dot separation represents a small proportion of the eccentricity (at most around 6%). However, the 16 minutes of arc eccentricity curve obtained on this occasion differs markedly from the foveal curve found earlier (*Figure 10.07*). The shape of the new "foveal" curve now closely resembles the shape of the peripheral curves indicating that separation and

eccentricity both affect the foveal data. The steps taken here to dissociate these two variables are clearly important. When vernier thresholds are expressed as a percentage of the dot separation the curves again all show a similar shape (*Figure 10.13*). The same procedure as outlined earlier was then used to calculate scaling factors. *Figure 10.14* shows the increase in scaling factor with eccentricity. The linear fit has been constrained to pass through a value of unity at an eccentricity of 0.267 degrees. This is because the "foveal" data was actually obtained at this eccentricity. On this occasion the scaling factor (F) is related to the eccentricity (E) by the equation....

$$F = 1 + S.(E - 0.267)$$

where S is the gradient of the linear relationship shown in *Figure 10.14*.

This time, from *Figure 10.11* it is clear that

$$S = z / 0.267 = 1 - z / E_2$$

and therefore

$$S = 1 - 0.267S / E_2$$

thus E_2 and S are now related by the expression

$$E_2 = (1/S) - 0.267$$

Again values of E_2 , defined as the absolute value of the x-intercept of the straight line, were obtained. The values of E_2 are 1.88 +/- 0.22 for DM and 1.66 +/- 0.13 for DW. *Figure 10.15* shows the data following scaling and this time there is no appreciable evidence of any eccentricity dependent variance.

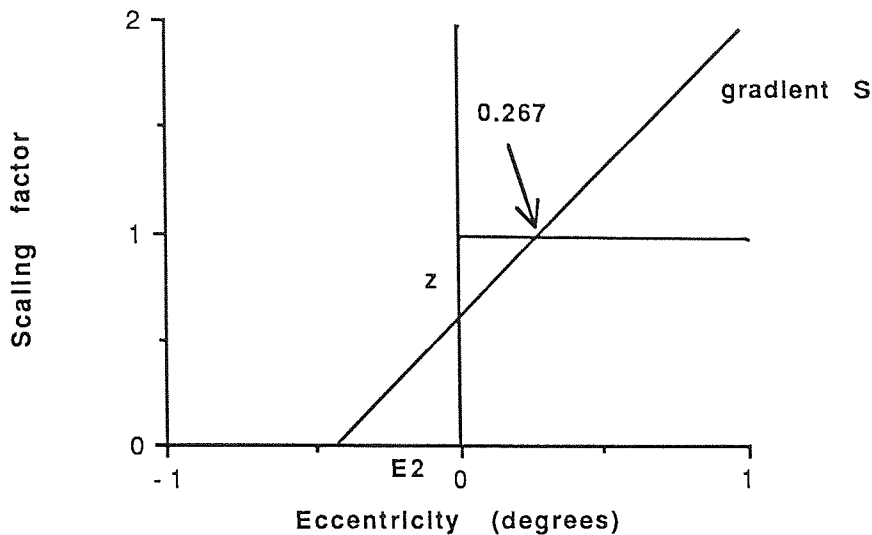


Figure 10.11: Scaling factor plotted against eccentricity for the data obtained using iso-eccentric arcs. See the text for details.

10.5: Discussion

10.5.1: A comparison of results

These results are in agreement with the principle of cortical magnification; the foveal results can be emulated in the periphery by scaling all features of the stimulus such that its cortical representation is equal in size both foveally and peripherally. A figure which provides a way of expressing this is E_2 , the eccentricity at which the stimulus size needs to be doubled in order to obtain equal detectability. It has to be pointed out that this only applies if the magnification increases linearly with eccentricity. The results obtained in the experiments reported here show that a single factor can be applied in both two line and two dot vernier tasks. The value of the scaling factor, averaged across both experiments and subjects, is 1.73 ± 0.10 degrees.

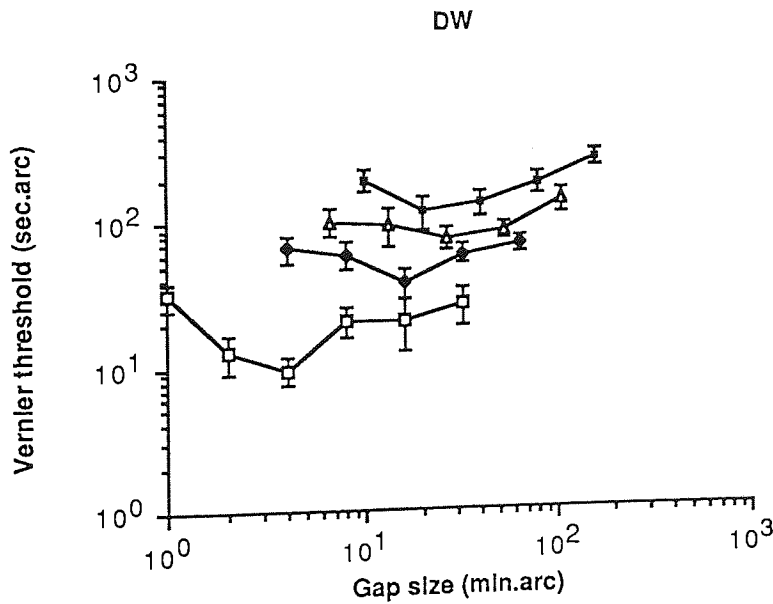
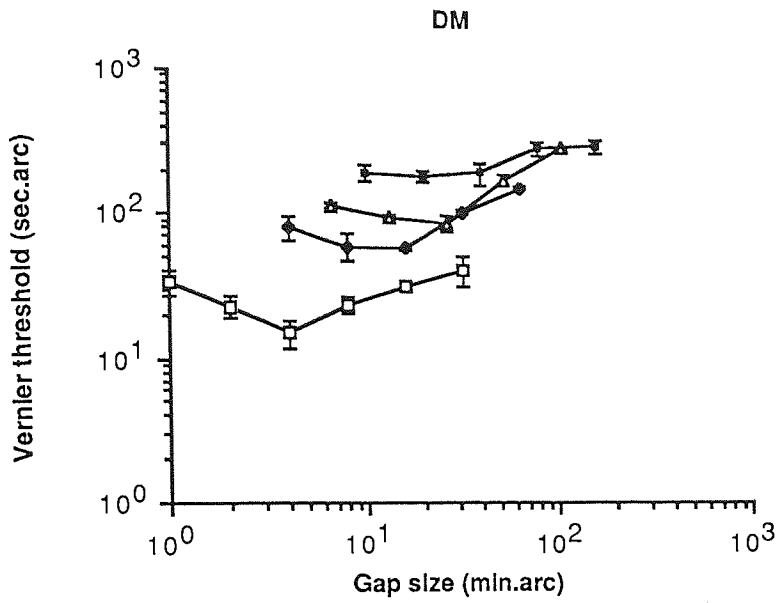


Figure 10.12: Vernier thresholds plotted as a function of gap size with the two dots placed on iso-eccentric arcs. This time the "foveal" function is very similar to the peripheral functions unlike the results shown in Figure 10.07. The symbols represent different eccentricities; open squares "foveal", filled diamonds 5 degrees, open triangles 10 degrees and filled squares 15 degrees.

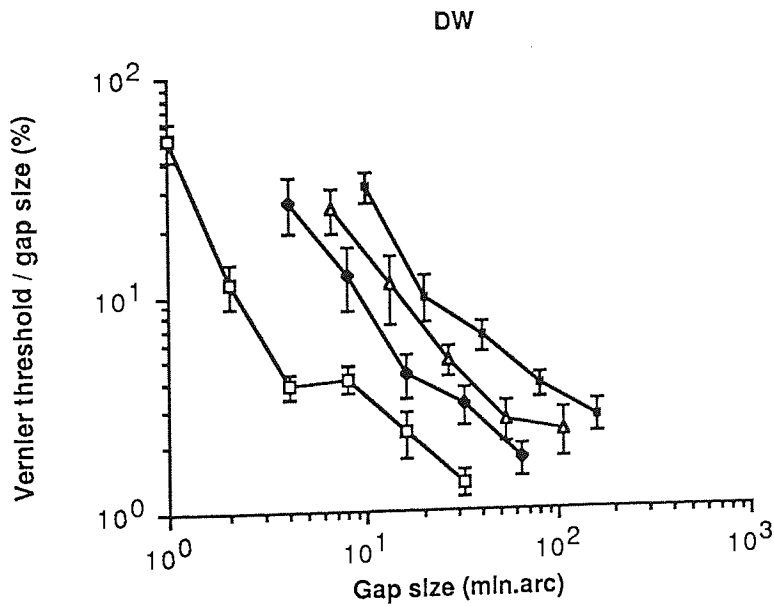
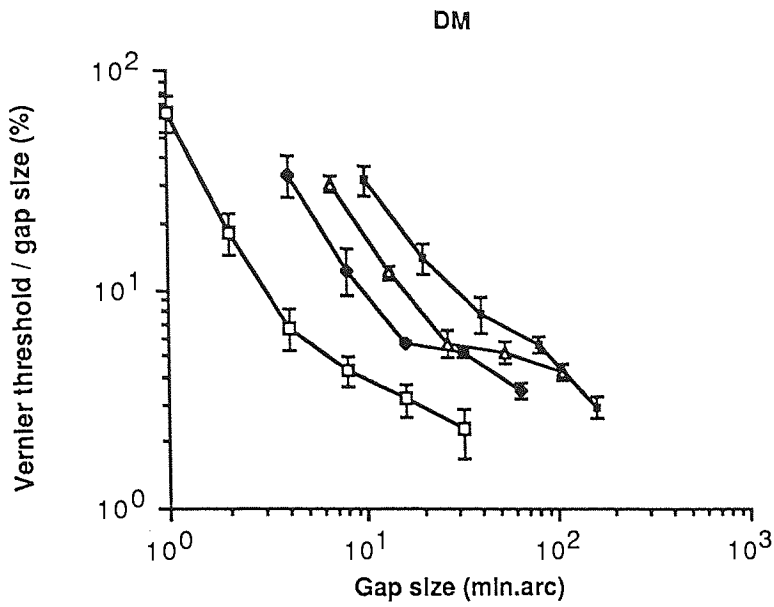


Figure 10.13: Vernier thresholds as a proportion of gap size plotted as a function of gap size. Again the placing of the two dots on iso-eccentric arcs results in the curves being similar in shape. The difference from the results shown in Figure 10.08 is quite marked.

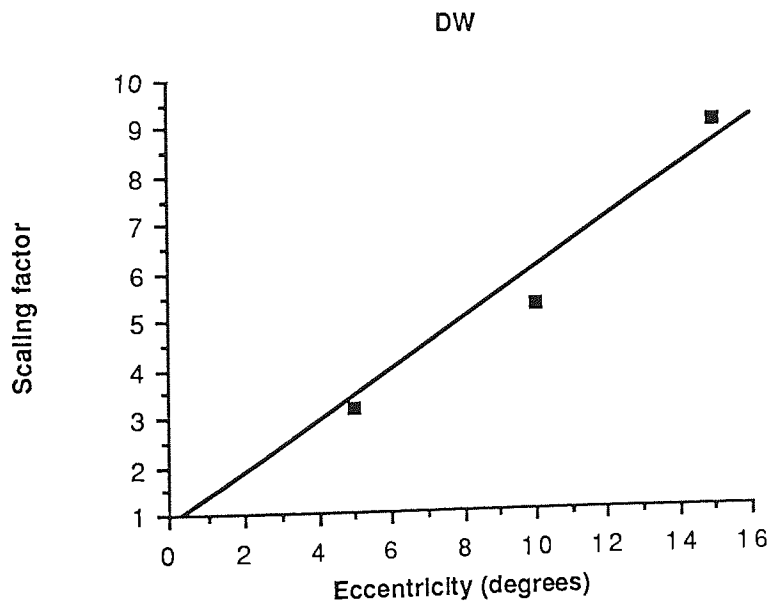
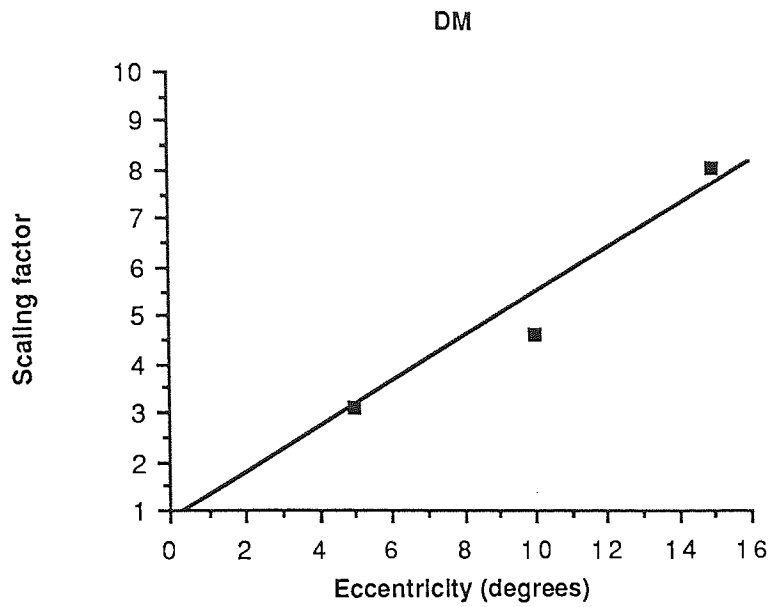


Figure 10.14: The scaling factors obtained for the two dot stimuli placed on iso-eccentric arcs plotted against eccentricity. The linear fit has been constrained to pass through a value of unity at an eccentricity of 0.267 degrees reflecting the fact that the "foveal" data was actually obtained at this eccentricity.

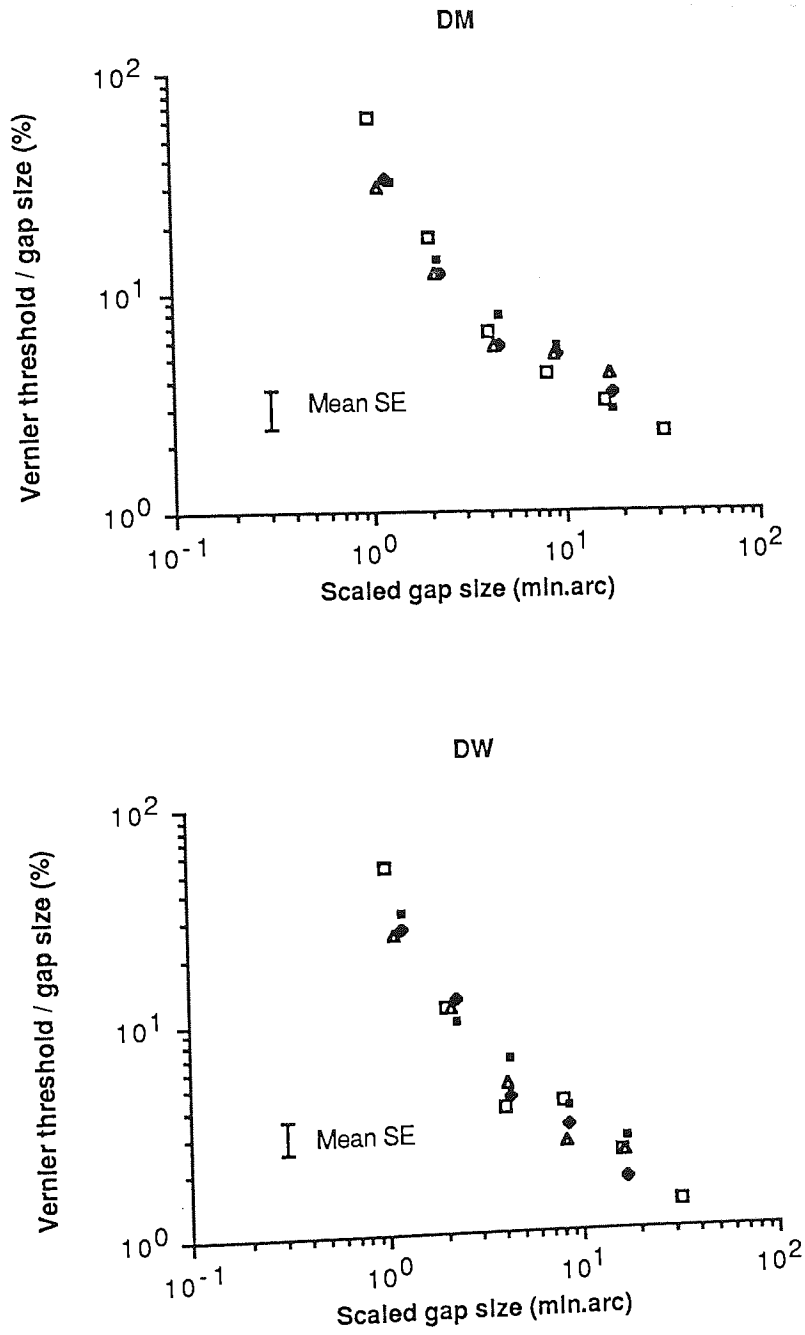


Figure 10.15: The data from Figure 10.13 after application of the scaling factors. This time there is no eccentricity dependent variability remaining.

It is important to stress the point that these results have been obtained using an assumption free spatial scaling technique. Many previous investigations have chosen to use a pre-determined scaling factor or have simply not scaled their stimuli at all. In this latter case the cortical size of the peripheral stimuli would have been considerably smaller relative to the foveal stimuli and the influence of peripheral undersampling may be reflected in the findings. The point also has to be made that all features of the stimulus need to be scaled. Beck and Halloran (1985), for example, chose to use a constant separation of 60 minutes of arc. For their lowest eccentricity this would have been a far from optimal separation. With increasing eccentricity, however, it would have become much closer to the optimum. Thus, the expected worsening of thresholds with increasing eccentricity would have been offset by the improvement as the separation became more optimal. This readily explains why they found no effect of eccentricity on vernier thresholds. Other studies using two dots (Westheimer, 1982; Virsu *et al.* 1987) failed to scale their stimuli with eccentricity and also allowed separation and eccentricity to co-vary. Their results, however, were completely different. Westheimer stated that two scaling factors, one each for separation and threshold, were needed. Virsu *et al.* on the other hand, found that two dot vernier acuity could be scaled to estimates of retinal ganglion cell density. The findings of the experiment reported here would seem to resolve this difference by ensuring careful scaling of the stimuli and that separation and eccentricity do not co-vary.

The two line results can be compared with those obtained by Levi *et al.* (1985). Their value of E_2 was between 0.6 and 0.8 degrees, well under half the value found here. Given that the foveal performance in both studies was comparable it implies that in this study peripheral performance was considerably better. The most significant difference between the studies is that Levi *et al.* assumed a scaling factor with which they altered the size of the peripheral stimuli. The value for E_2 used, 0.77, was based on the work of Dow *et al.* (1981) using monkeys. If it is assumed that the value of E_2 (1.73) found here is correct then clearly the stimuli used by Levi *et al.* were too large in the periphery. In these circumstances undersampling in the periphery can be discounted and there is no evidence that vernier acuity worsens with increasing line length (Sullivan *et al.* 1972; Westheimer and McKee, 1977a). It is possible, however, that the assumed value of E_2 may be the critical factor explaining the difference.

Levi *et al.* (1985) used their result to suggest that vernier acuity performance reflects cortical

rather than retinal magnification. However, modern estimates of ganglion cell receptive field density have shown that the foveal cone to ganglion cell ratio may be as high as four to one which greatly modifies the rate of decline in ganglion cell density with eccentricity. Drasdo (1991) has used the revised data to calculate an E_2 value for ganglion cell densities of 1.36. This value is somewhat less than the estimate of E_2 for vernier acuity found here. If it is assumed that the value of E_2 obtained here represents true cortical magnification then it is clearly not necessary to postulate an expansion of foveal projection at the cortex relative to the retina to explain the results.

However, the E_2 value found here should not be taken as implying that there is a single factor which covers all hyperacuity tasks. There are tasks in which performance declines much more rapidly than vernier acuity. Bisection acuity has been shown to fall into this category (Virsu *et al.* 1987; Klein and Levi, 1987; Yap, Levi and Klein, 1987) and even when a method of spatial scaling is employed there are tasks which fall off much faster than vernier acuity with eccentricity (Saarinen, Rovamo and Virsu, 1989). This latter study involved observers having to distinguish between patterns which were either identical or mirror symmetric and performance was found to decrease rapidly with increasing eccentricity. A suggestion which could explain these differences is the degree to which stimulus complexity determines the rate of increase in thresholds away from the fovea. The vernier task, for example, is relatively simple. Other hyperacuity configurations are more complex and would require greater neural processing to allow the task to be performed. On this basis the more complex the task the more likely that undersampling in the periphery will restrict the ability to successfully interpolate between receptors to allow completion of the task. The discrepancies in gradients found between different tasks may reflect the relative activity within separate channels each having their own magnification factor (Drasdo, 1989; 1991; Wilson, 1991).

10.5.2: A plea for standardised methodology

One of the chief problems associated with the determination of scaling factors for different visual tasks is the multiplicity of methods employed in different experiments. Clearly, in order to sensibly compare the scaling factors between different tasks it is necessary to find a method which can be standardised. It would seem that the methodology adopted here, which is free from prior assumptions, may have merit in this regard. It does, however, have some limitations. Chief among these is the fact that eccentricity is one of the variables under

consideration which must, of necessity, introduce difficulties with large, spatially extended stimuli. Indeed, Watson (1987) found that while spatial scaling was successful in matching small, high spatial frequency targets it was less so for large, low frequency targets. Clearly the larger stimulus will cover an area such that different parts will lie at different eccentricities. The use of small localised targets is, therefore, a prerequisite in such experiments. For hyperacuity type stimuli, which are commonly of this form, this should not pose a problem.

As was shown earlier, the introduction of variable separation between the stimulus components must also be strictly controlled if the effects of eccentricity are not to be confused with the effects of separation. The use of iso-eccentric arcs to separate the two effects is to be recommended in this regard.

Other external factors such as eye movements (Virsu *et al.* 1987; Drasdo, 1989) and optical image degradation (Charman, 1983) would be expected to degrade foveal vision more than peripheral vision thus having the effect of reducing the value of E_2 found. This is a variable which is difficult to quantify but clearly some regard to stimulus configuration is needed to reduce the impact of such features.

Finally, the range of eccentricities for which the spatial scaling holds would have to be stated. In fact the use of a linear regression on the data presented here has the effect of producing a slightly higher scaling factor because the 15 degree point always has a positive deviation from the linear regression (*Figures 10.05, 10.09 and 10.14*). It would appear, from this, that the value E_2 needs to have a range of eccentricities specified over which it was held to apply.

Notwithstanding this last point it would appear that, given sufficient regard to the constraints placed on the stimulus, it is possible to determine a scaling factor for vernier acuity over the range 0 to 15 degrees. The method employed may well be appropriate in attempts to scale other hyperacuity tasks in order to allow like-to-like comparisons to be made.

Chapter 11: Hyperacuity and age

11.1: Introduction

There is a vast library of evidence that visual function declines with increasing age. It has been claimed, however, that certain hyperacuties seem to contradict this general rule. This chapter will, therefore, consider the evidence for visual decline with age and investigate three hyperacuity configurations and their variation as a function of age. The configurations investigated are vernier acuity, bisection acuity and displacement detection.

11.1.1: Changes in visual acuity with age

Weale (1975) found that visual acuity in normal healthy adults fell from around 1.0 (the mean acuity expressed as a decimal) at age 20 years to approximately 0.75 at age 80 years. The decline is not regular but appears to accelerate after age 50 years. Other researchers have repeated these findings. Greene and Madden (1987) compared 24 young subjects (mean age 19.5 years) and 24 older subjects (mean age 68.4 years). They found a decline from around an acuity of 1.25 in the young group to around 1.0 in the older. Elliott *et al.* (1989) and Elliott and Whitaker (1991a) have also shown a similar decline. These two reports both show minimum angle of resolution as falling from around 40-42 seconds of arc (an acuity of ≈ 1.25) at age 20 years to around 55 seconds of arc at age 75 years (≈ 1.0). Visual acuity is, however, a measure of the ability to resolve small high contrast targets, usually in the form of letters. The range of stimuli presented to the eye covers a far larger spectrum in terms both of contrast and spatial frequency and, therefore, the contrast sensitivity function (CSF) represents a more complete measure of spatial vision.

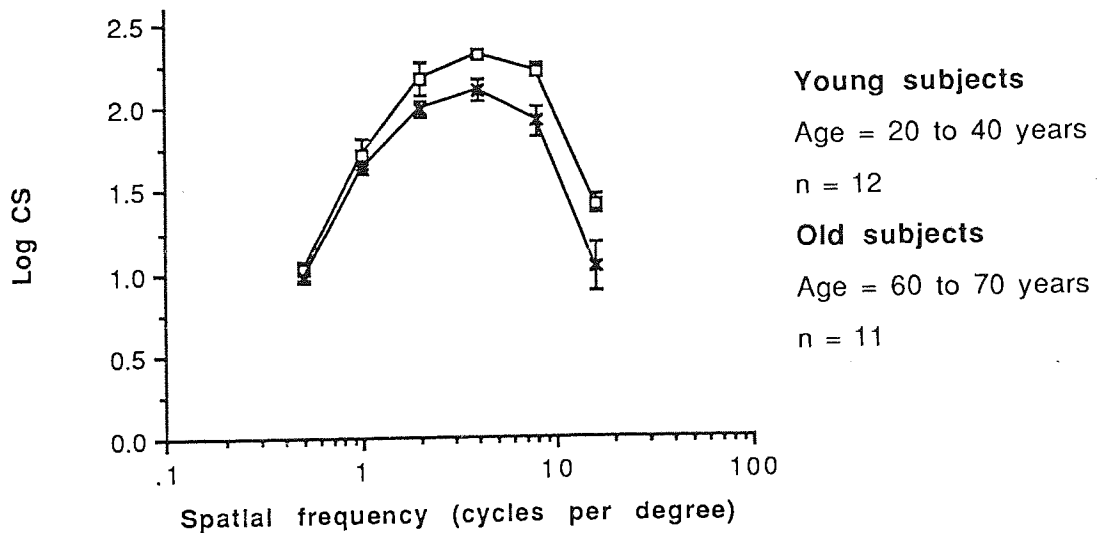
11.1.2: Changes in CSF with age

The effect of ageing on the CSF has been the subject of many investigations and some controversy as to the range of spatial frequencies over which a decline in sensitivity can be demonstrated. The vast majority of reports have shown a sensitivity loss at medium and high spatial frequencies only (Derefeldt, Lennerstrand and Lundh, 1979; Owsley, Sekuler and Siemsen, 1983; Kline, Schieber, Abusamra and Coyne, 1983; Elliott, 1987; Elliott, Whitaker and MacVeigh, 1990). There have, however, been some reports which show a loss at low spatial frequencies as well (Greene and Madden, 1987; Sloane, Owsley and Alvarez, 1988) and also one which showed a loss at low spatial frequencies only (Sekuler, Hutman and

Owsley, 1980). It is possible that criterion differences may explain the conflicting results. Higgins, Jaffe, Caruso and deMonastario (1988) found a loss at all spatial frequencies with age using a method of adjustment. When using a forced choice technique, however, they found a loss with age only for medium and high spatial frequencies. *Figures 11.01a to f* gives details of the results from a selection of the various reports.

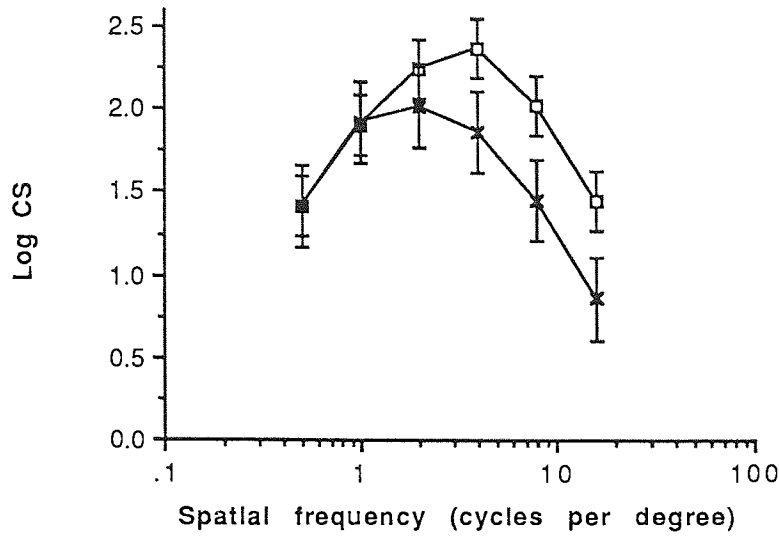
a)

Derefeldt, Lennerstrand and Lundh, 1979



b)

Owsley, Sekuler and Slemson, 1983



Young subjects

Age = 22 +/- 3 years

n = 12

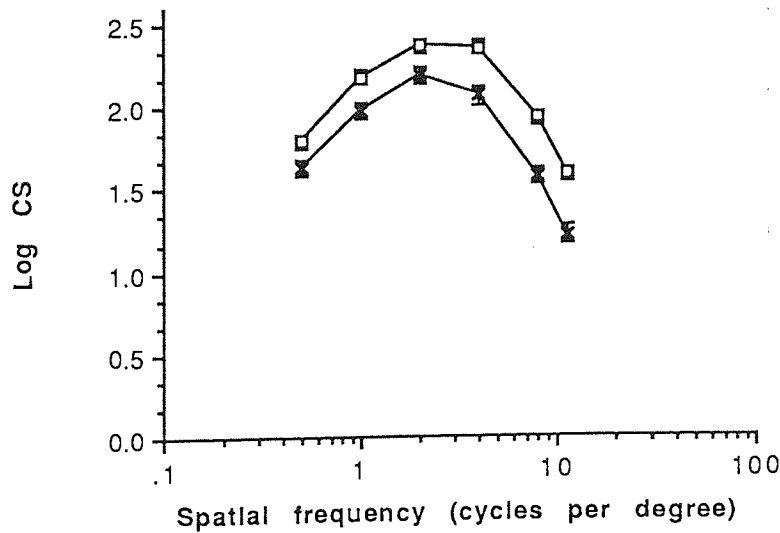
Old subjects

Age = 82 +/- 3 years

n = 14

c)

Sloane, Owsley and Alvarez, 1988



Young subjects

Age = 23 years

n = 12

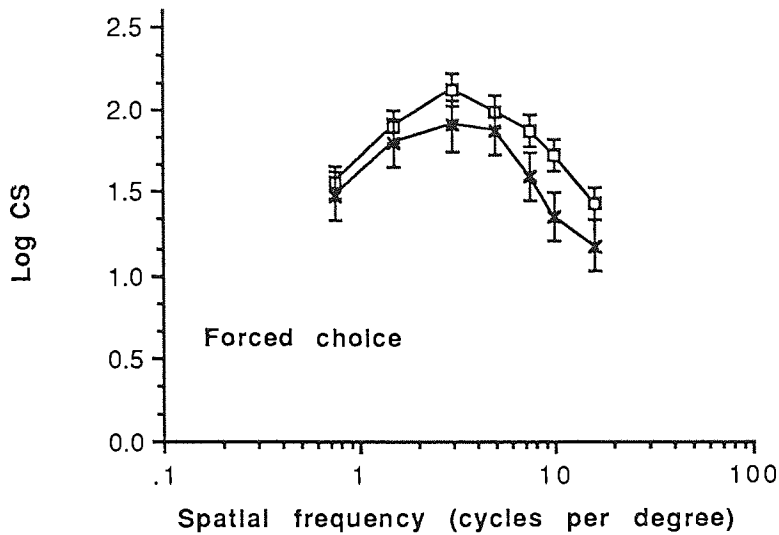
Old subjects

Age = 74 years

n = 11

d)

Higgins, Jaffe, Caruso and deMonasterlo, 1988



Young subjects

Age = 26.2 +/- 3.4 years

n = 10

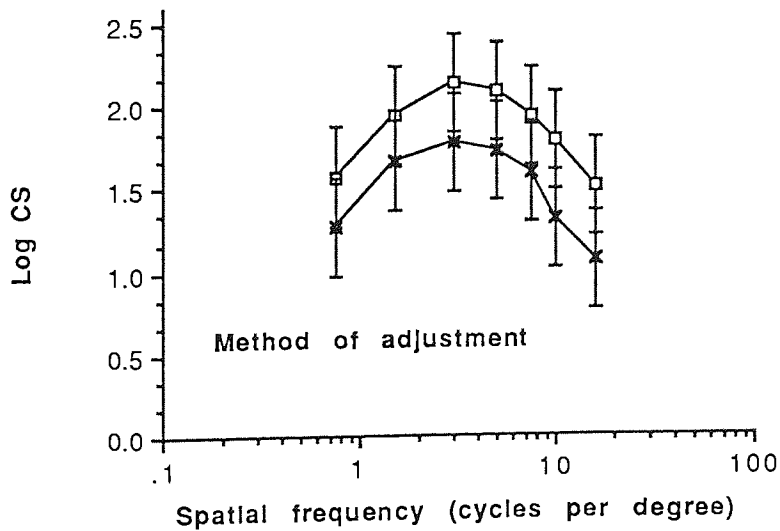
Old subjects

Age = 67.2 +/- 3.4 years

n = 10

e)

Higgins, Jaffe, Caruso and deMonasterlo, 1988



f)

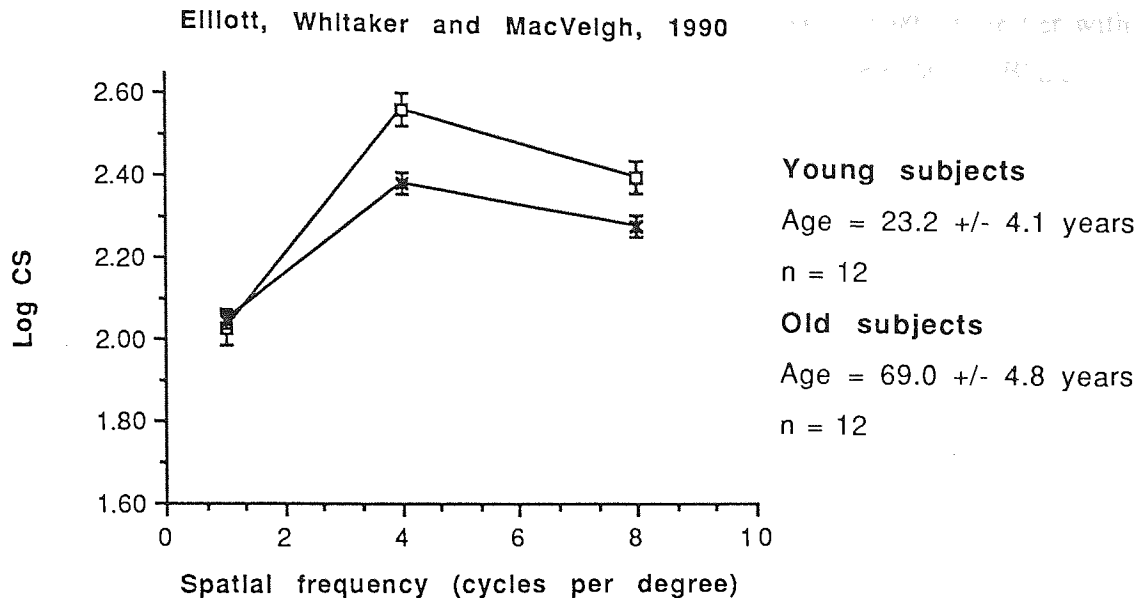


Figure 11.01: The effect of increasing age on contrast sensitivity found in a selection of studies (a to f). The results for the young subjects are shown as open squares, the older as crosses. It is apparent that there are significant differences between the findings of these studies.

11.1.3: Changes in other visual functions with age

Other measures of visual function also show a decline with increasing age. These include dark adaptation (McFarland, Domey, Warren and Ward, 1960), flicker sensitivity (Tyler, 1989) and photostress recovery time (Elliott and Whitaker, 1991b).

McFarland *et al.* (1960) tested dark adaptation in a group of subjects covering the age range 16 to 89 years. They found that luminance thresholds, following exposure to a bright white light source, rose uniformly with increasing age at all stages of dark adaptation.

Critical flicker fusion frequency in a group of observers between the ages of 5 and 75 years was investigated by Tyler (1989). He found an increase in sensitivity up to approximately 16 years of age then a gradual decline over the rest of the age range studied.

Elliott and Whitaker (1991b) measured the photostress recovery time in 61 subjects covering the age range 19 to 78 years. The subjects had their LogMAR acuity measured and were then exposed to a bright flash of light. Photostress recovery time measures how quickly the subjects acuity returns to its pre-exposure level. The results showed a decline in PSRT from

around 10 seconds at age 20 years to around 22 seconds at age 70 years indicating a decline in macular function with age. It has been proposed that this may be due to loss of retinal pigment epithelium cells and photoreceptors (Gartner and Henkind, 1980) together with degenerative changes in the macula evidenced by a rise in lipofuscin levels (Wing, Blanchard and Weiter, 1978).

11.1.4: Changes in hyperacuity with age

There have been relatively few investigations into the effect of age on hyperacuity. These few have, however, demonstrated a dichotomy between the age response of vernier acuity and displacement detection. Vernier acuity was investigated by Odom, Vasquez, Schwartz and Linberg (1989) who used a method of adjustment whereby the two component lines of the vernier stimulus had to be subjectively aligned. *Figure 11.02* shows their results which indicate that increasing age, far from causing a sensitivity decline in vernier acuity, would appear to have little effect or, indeed, may show a slight improvement!

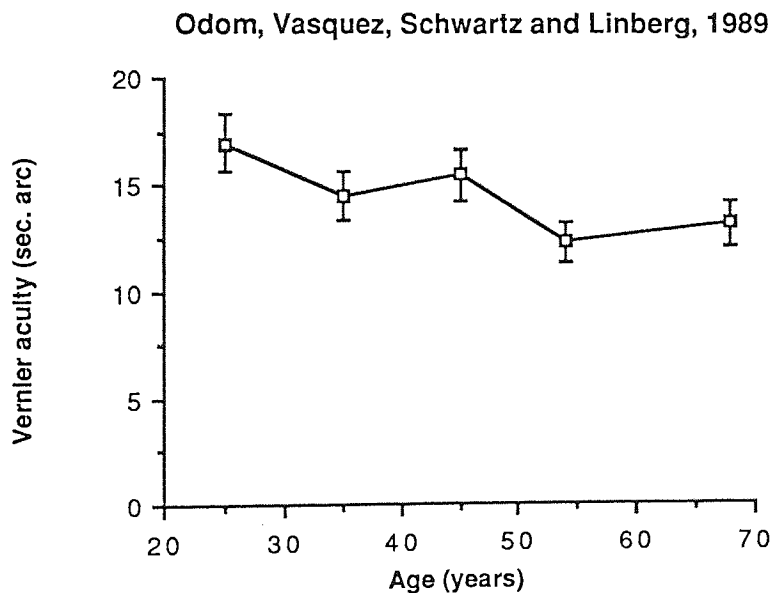


Figure 11.02: Vernier acuity plotted as a function of age. Note that threshold values vary little as a function of age.

Lakshminarayanan, Aziz and Enoch (1991) also investigated the effect of age and separation on vernier thresholds. Their results would also seem to indicate that thresholds are essentially independent of age. If one considers only the youngest and oldest age groups there is clearly little change in thresholds for any of the separations considered (*Figure 11.03*).

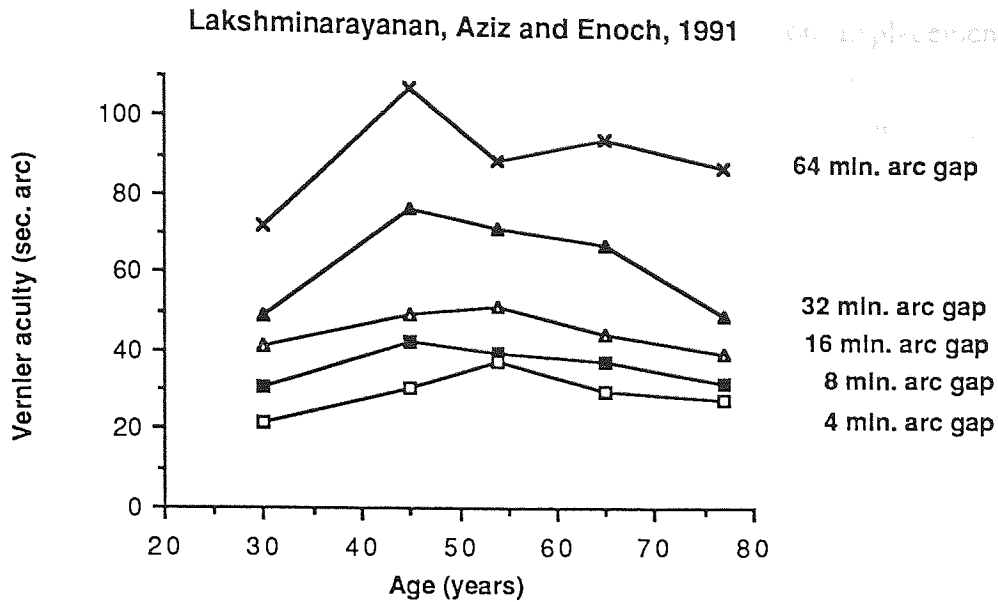


Figure 11.03: Vernier acuity plotted as a function of age. The stimulus consisted of two dots with a separation between them varying between 4 and 64 minutes of arc. The effect of increasing separation is to raise threshold values in line with the findings of Sullivan *et al.*, (1972) and Westheimer and McKee (1977a). However, it is clear that there is little effect on threshold values with increasing age for any separation value.

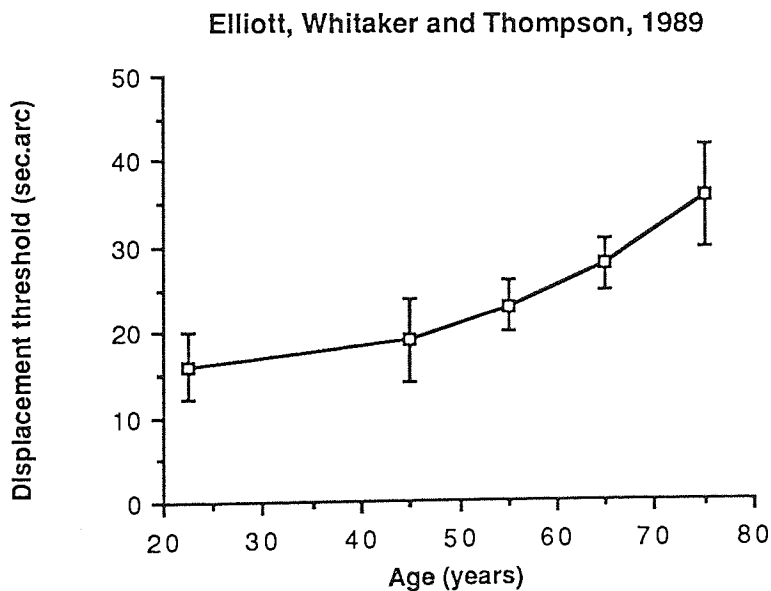


Figure 11.04: Displacement thresholds plotted as a function of age. Note the consistent increase in threshold values with increasing age.

On the other hand, displacement detection thresholds do seem to be affected by increasing age. Elliott *et al.* (1989) studied the effect of increasing age on displacement detection thresholds using an oscillating bar with a stationary reference bar on either side. The central bar oscillated with a simple harmonic motion at 2 Hz and thresholds were determined using the method of limits. Their results show a definite decline in displacement detection sensitivity with age (*Figure 11.04*). Why should there be this difference? One obvious possibility is that the mechanism underlying displacement detection is more seriously affected by age changes than that for vernier acuity.

11.1.5: Optical or neural factors in visual decline with ageing?

There are two factors which could underlie the altered performance of the elderly eye compared with the younger. These are changes to the eye's optics and changes to the neural processing and transmission system.

The optical factors include pupil miosis, increased light scatter and changes in the transmission characteristics of the ocular media, particularly the crystalline lens. It is well known that the pupil has a smaller diameter in the elderly. Loewenfeld (1979), in a study of over 1200 subjects, showed that dark-adapted pupil size was reduced from around 7 mm diameter at age 20 years to around 4.5 mm diameter at age 75 years. This pupillary miosis reduces retinal illumination which, in turn, can reduce visual performance. In compensation, however, it has been shown that a reduction in pupil size can improve performance by reducing ocular aberrations (Campbell and Green, 1965). The chief location for changes to the ocular media is the crystalline lens. In particular, the ageing lens suffers from alterations to its refractive index which results in increased light scatter and absorption and in consequence a reduced retinal contrast and illumination (Allen and Vos, 1967; Sigelman, Trokel and Spector, 1974). It has been estimated that due to these changes the 60 year old eye transmits only one third the light of the 20 year old eye (Weale, 1963). While these optical factors represent a logical explanation of reduced acuity in the older eye there are problems associated with their inability to fully explain the magnitude of the loss. Weale (1975) showed that optical factors (senile miosis, reduced transmission and light scattering within the eye) could not, of themselves, explain the observed drop in visual performance with age. Therefore, he put forward the alternative idea that loss of neural cells in the visual pathway and at the cortex could be the causative agent. Weale used data which showed that cell loss took place at a rate of about 2.5 per cent per decade. If one assumes that the visual information is transmitted via a series of relay stations then one can use this cell loss to

estimate the information loss throughout the visual system. The observed decline in visual acuity closely matched that predicted by this estimated cell loss while optical factors were unable to offer a complete explanation.

This controversy regarding neural loss against optical degradation has been investigated many times over the last few years. Several methods of separating optical and neural processes have been used. An obvious one is to evaluate visual function after cataract extraction (Owsley, Gardner, Sekuler and Lieberman, 1985; Jay, Mammo and Allan, 1987). This assumes that following cataract extraction there is no loss of retinal image quality due to reduced light transmission and increased scatter. Both of these investigations have shown a continuing decline in acuity measures after cataract extraction.

Using interference fringe methods, where the stimulus is projected directly onto the retina, it is possible to bypass the optics of the eye. Reports have shown that contrast sensitivity measured in this fashion continues to decline with increasing age (Morrison and McGrath, 1985; Elliott, 1987).

Finally, it is possible to mimic the optical changes in the older eye using young observers. Sloane *et al.* (1988) used artificial pupils and found that miosis did not reduce contrast sensitivity in young subjects. Sturr, Church and Taub (1988) adjusted stimulus luminance, to account for reduced transmission in the older eye. They found, at low spatial frequency (0.4 cycles per degree), no significant difference between young and old. However, initially they did find a difference at a higher spatial frequency (7.5 cycles per degree). This was eliminated by the simple expedient of correcting the older subjects refraction for the working distance employed (71 cms). The argument which they put forward suggesting that these findings point toward optical factors being significant in the decline of visual function with age is somewhat tenuous. Owing to the incorrect refraction the grating would, of necessity, be blurred which thus reduces the high spatial frequency content and provides a ready explanation for the poorer performance.

More recently Elliott *et al.* (1990) mimicked the effect of senile miosis and reduced retinal illumination and found that these had no effect on spatial or temporal contrast sensitivity. Elliott and Whitaker (1991a) added to this the effect of light scatter and found, again, that even a complete mimicking of the older eye's optics did not reduce the contrast sensitivity of the young observers to a significant extent. This inability, using a technique which simulates the optical quality of the older eye, to replicate the visual loss found in older eyes in young

subjects would strongly suggest that optical factors are not the underlying cause. In addition, those reports which bypass the optics of the eye but continue to show a decline in performance would seem to absolve the lens as the chief cause of visual loss. It has to be stressed, of course, that this applies to normal healthy eyes. In those situations where pathological changes to the media occur, for example in cataract, the extra loss in visual function is clearly due to optical changes.

As was commented on in chapter 2, hyperacuties have shown resistance to optical blur (Williams *et al.* 1984; Whitaker and Buckingham, 1987). Based on this it would appear reasonable to assume that the optical changes which occur with ageing would have relatively little effect on hyperacuity performance. The finding that displacement detection thresholds are affected by age, even though they are unaffected by optical blurring, can be taken as evidence that neural changes underlie this decline (Elliott *et al.* 1989). On the other hand, the slight decrease in sampling density occasioned by cell loss might not be expected to seriously impair hyperacuity thresholds. As was shown in chapter 1 hyperacuity performance is not limited by the sampling density of the visual system. The findings of Odom *et al.* (1989) and Lakshminarayanan *et al.* (1991) that vernier acuity is unaffected by ageing can be used as evidence supporting this premise.

While one or two of the studies reported here have given conflicting results the overwhelming evidence would appear to point toward neural changes as being responsible for reduced visual function in the elderly. The experiments reported here have extended the hyperacuties studied to include bisection acuity and will attempt to offer a possible explanation for the differential response of the hyperacuties with increasing age.

11.2: Method

The stimuli were presented on a high resolution CRT (0.3 mm pixel size) under the control of the Nimbus AX microcomputer. Three hyperacuity configurations were used; vernier acuity, bisection acuity and displacement detection. In all cases the stimuli were two or three bright bars on a dark background. The bars subtended 8 minutes of arc high by 1 minute of arc wide and had a brightness of 52 cd/m². For the vernier task there were two bars positioned one above the other with a gap between them of 4 minutes of arc. The observer had to decide whether the upper bar was to the left or right of the lower bar. For the bisection and displacement tasks there were three bars positioned side-by-side with a mean separation between them of 8 minutes of arc. In the bisection task the observer had to decide whether

the central bar lay closer to the left or right hand outer bar. For the displacement task one of the outer two bars was made to oscillate with a square wave form at a frequency of 2 Hz. The observer had to decide which of the outer two bars was moving. The viewing distance for all three tasks was 8 meters and the experiments were carried out under low room illumination using the observers dominant eye.

There were 60 observers whose ages ranged from 18 to 80 years, all were inexperienced in psychophysical tasks and were unaware of the purpose of the experiment. The observers were screened for media opacities and any ocular pathology and wore their spectacle refraction, when appropriate, in order to optimise their visual acuity. These were measured using a LogMAR chart at a luminance of 160 cd/m². Observers whose acuity was worse than +0.1 (Snellen $\frac{6}{7.5}$) were excluded from the experiment.

All three threshold estimates were made in a single sitting taking between 20 and 25 minutes. In order to exclude the effect of fatigue the three were measured in a random order. Initial presentations were suprathreshold which allowed the observer to become acquainted with the task. The thresholds were determined using a forced choice technique which demanded one of two answers from the observer (left or right in all cases). They were not allowed to give ambiguous responses. To reduce the effect of the slower response time in older subjects the stimuli were presented for an unlimited period which ended when the response was given. It is clearly important in studies such as this to eliminate criterion differences between the young and old observers. Higgins *et al.* (1988) in their comparison between the method of adjustment and forced choice concluded that the two methods were not equivalent in age related studies and that the method of adjustment was subject to the more conservative judgments of the older observers. As was suggested earlier, this may go some way to explaining the different results found in the studies on CSF and ageing mentioned in the introduction to this chapter.

The vernier and bisection thresholds were determined using two interleaved staircases converging from right and left. A right response from the observer led to the next presentation being more to the left and vice-versa. In all, 15 reversals were used with the first 3 being ignored in the final calculations. This allows bias (the mean of reversals) to be separated from acuity (the standard deviation of reversals around the mean) for each staircase. The estimates obtained from the two staircases were then averaged to give final threshold and bias figures. Bias can be expressed either as an absolute figure (independent of sign) or as an arithmetic figure, with bias to the right being arbitrarily defined as positive and

to the left negative.

Bias is not applicable to the displacement detection task. The same staircase method was used to measure displacement detection thresholds but with only a single staircase. The displacement offset was varied according to the subjects previous response. The offset was increased after an incorrect response and decreased after two consecutive correct responses. This allowed the 71% point on the psychometric function to be estimated. Again, 15 reversals were used with the first 3 being ignored in the final threshold determination.

11.3: Results

11.3.1: Acuity results

Figure 11.05 shows the changes in visual acuity with age amongst the observers used in the study. It follows previous reports in showing a reduction in acuity with age, regression analysis revealing that this reduction is highly significant ($r = 0.65$; $F_{1,59} = 42.7$, $p < 0.0001$). The three hyperacuity tasks produce different age responses. Displacement detection (*Figure 11.06*) shows a marked worsening of thresholds with age, thus confirming the finding of Elliott *et al.* (1989) ($r = 0.53$; $F_{1,59} = 23.6$, $p < 0.0001$). Bisection acuity (*Figure 11.07*) shows a significant but less pronounced deterioration with age ($r = 0.33$; $F_{1,59} = 7.2$, $p < 0.01$). Finally (*Figure 11.08*), vernier acuity reveals no significant variation with age ($r = 0.1$; $F_{1,59} = 0.57$, $p \gg 0.1$), which again confirms previous findings (Odom *et al.* 1989; Lakshminarayanan *et al.* 1991).

At any age, there is a large amount of variance in the data. This suggests that factors other than chronological age influence threshold. One of these may be the fact that visual performance is likely to be determined by biological rather than chronological age.



Figure 11.05: The effect of age on visual acuity for the subjects investigated. There is the expected decline in visual acuity with increasing age. The best fitting linear regression is given by the equation...

$$y = -0.12 + 0.0013x \quad (r = 0.65)$$

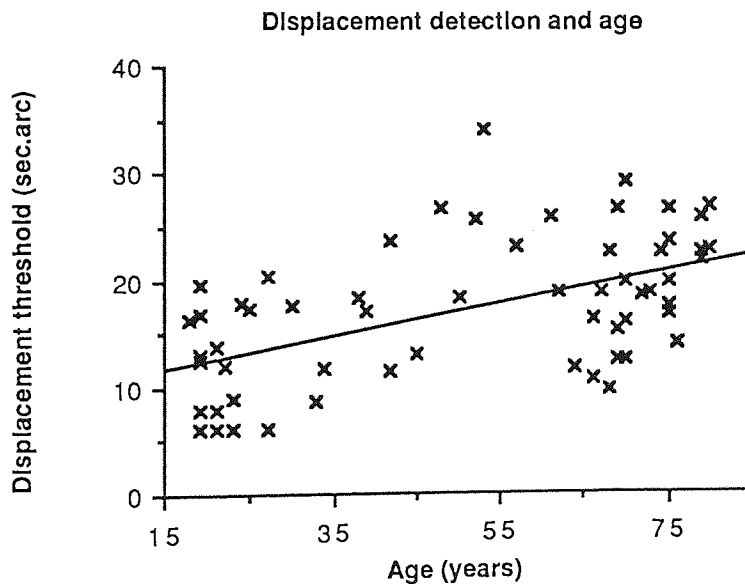


Figure 11.06: The effect of age on displacement detection thresholds. Again, there is a significant effect with thresholds worsening with increasing age. Thus confirming previous findings (Elliott *et al.* 1989). This time the equation of the best fitting linear regression is...

$$y = 9.28 + 0.156x \quad (r = 0.53)$$

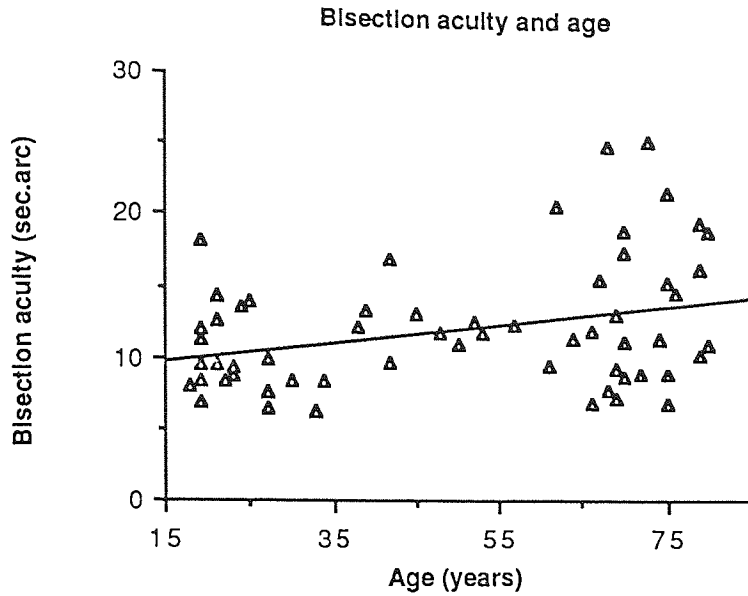


Figure 11.07: Bisection acuity measured as a function of age. There is an effect although less pronounced than that found for visual acuity and displacement detection. The best fitting linear regression has an equation of...

$$y = 8.84 + 0.066x \quad (r = 0.33)$$

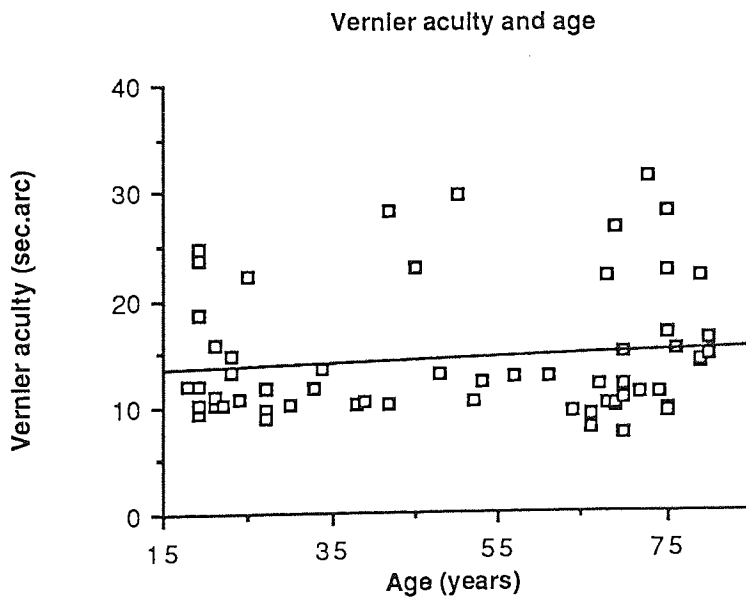


Figure 11.08: Vernier acuity as a function of age showing little change in thresholds with increasing age. Once again this confirms previous findings (Odom *et al.* 1989; Lakshminarayanan *et al.* 1991). The best fitting linear regression has an equation of...

$$y = 13.2 + 0.027x \quad (r = 0.1)$$

11.3.2: Bias results

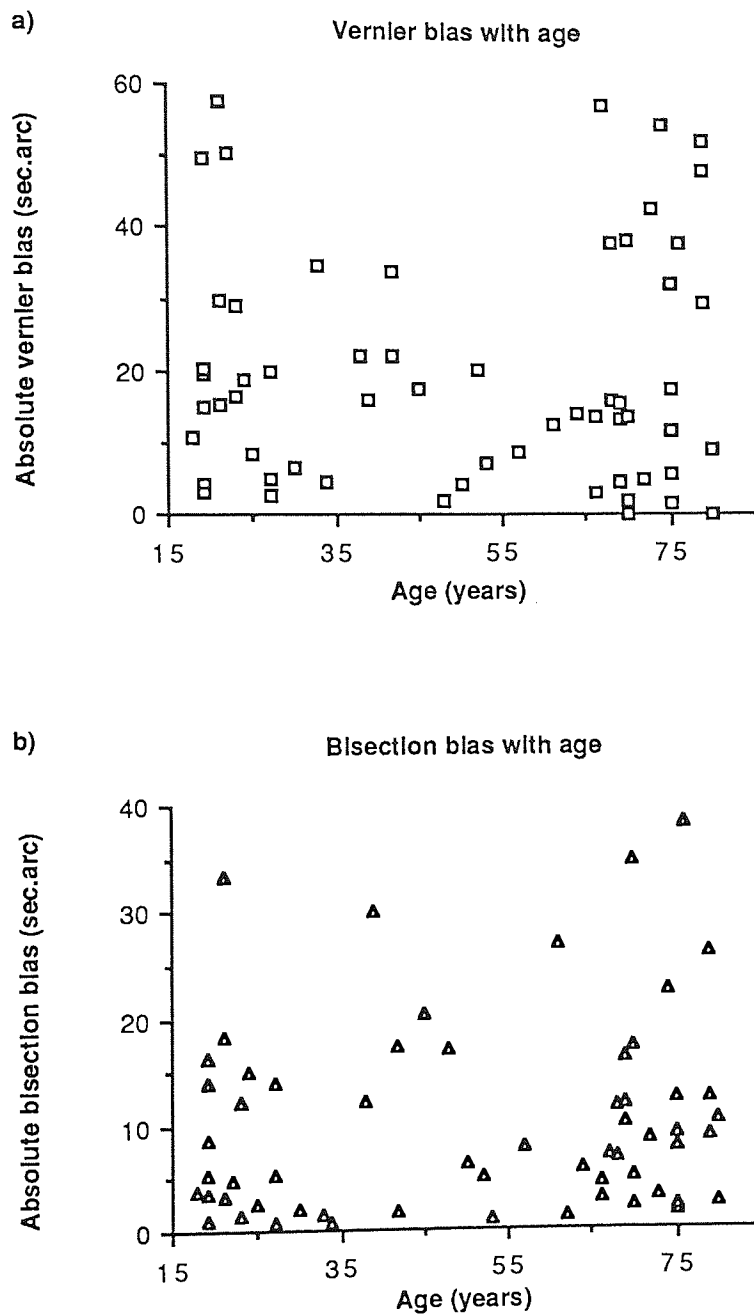


Figure 11.09: The effect of age on vernier bias (a) and bisection bias (b). Note that these are absolute values disregarding the sign. In both cases there is no significant variation with age and there is a large spread of values at all ages.

Odom *et al.* (1989), using a method of adjustment technique, reported that vernier bias increased with age. They found that bias values rose from around 3 seconds of arc at age 30 years to around 12 seconds of arc at age 40 years. It was suggested that this finding may be

linked with presbyopia or other changes in visual function which occur within this period. However, the results from this experiment show no systematic variation of either vernier or bisection bias with age (*Figure 11.10*). Indeed, both vernier and bisection bias vary over an enormous range in both young and old subjects. The mean arithmetic value for vernier bias was -3.5 ± 26.8 seconds of arc and for bisection bias -4.1 ± 13.3 seconds of arc. There was no significant change in this position of subjective alignment with age ($p > 0.1$). It seems in fact to have an extremely variable and seemingly unpredictable value. The most compelling argument to explain the difference between this report and that of Odom *et al.* (1989) would appear to be in the psychophysical techniques employed. This further reinforces the findings of Higgins *et al.* (1988) that method of adjustment and forced choice techniques do not produce equivalent results.

11.4: Discussion

The results presented here indicate that displacement detection deteriorates markedly with increasing age. Bisection acuity, to a lesser extent, also shows this age related decline in sensitivity. Vernier acuity, however, is seen to be unaffected by ageing. The decline demonstrated by both displacement detection and bisection acuity are clearly in line with the reduction in other measures of visual performance. This begs the question as to why this dichotomy, between vernier acuity and the other hyperacuities, should exist.

As was pointed out in chapters 3 and 8 there are two groups of models which attempt to explain the phenomenon of hyperacuity. The local-sign model proposes that some feature of the stimulus is extracted and used to assign a precise location to it. In order to perform this localisation the model requires that the retinal image is blurred. It would be reasonable, therefore, to suggest that further blurring, due to changes in the ocular media, would be unlikely to seriously affect the ability to carry out this localisation. This resistance to optical blurring has been demonstrated on several occasions (Williams *et al.* 1984; Whitaker and Elliott, 1989). Indeed, it has been shown that hyperacuity performance is still possible with quite severe cataracts when visual acuity is seriously degraded (Whitaker and Deady, 1989). It was also pointed out that hyperacuity performance approaches an order of magnitude finer than the sampling density of the retina (around 5 seconds of arc compared with 30 seconds of arc). It seems, therefore, that a further reduction in the sampling density, caused by cell loss within the visual pathway, may not cause a marked worsening of localisation ability. The local-sign model requires, however, that the relative locations of the stimulus features are then extracted by some comparative process. It would seem that the observed age response of the

hyperacuity configurations examined here would therefore have to occur at this secondary processing stage.

The alternative channel model does not require that the stimulus features are made explicit but that the responses from groups of spatial filters, with different spatial frequency, phase and orientation tuning, create an implicit representation of the whole stimulus. Therefore, by comparing the outputs of many cells, with overlapping receptive fields, the signal can be extracted from the background noise and an estimate of the relative location of the stimulus features obtained. Bisection acuity can be thought of as either a comparison of the two gaps separating the three stimulus bars or as a localisation of the center bar relative to the outer two. Regardless of which of these methods is employed a group of spatial frequency tuned filters centered on one of the gaps can extract information which indicates the spatial extent of the gap. This value can then be compared with the result of a similar estimate of the extent of the gap on the other side of the central bar. Clearly, for bisection acuity, this comparison will directly allow a decision as to which of the two gaps is larger or smaller, which then locates the central bar relative to the two outer bars. Displacement detection, however, requires that a temporal factor is taken into account. In the experimental set up used here one of the outer bars was oscillating at a 2 Hz frequency. The filters centered on the gap subject to the sudden change will obviously alter their output every time the outer bar moves. In order to carry out the task it is, therefore, necessary to be able to detect this *variation in output over time* and distinguish it from other possible causes of variability.

For vernier acuity such a comparison process is not required. The offset of one bar relative to the other can be signalled by the overall orientation of the stimulus. Thus in the channel model the offset can be determined by pooling amongst receptors selective for phase and orientation. The output of these receptors gives a direct indication of the direction of offset without the need for any comparison procedure.

The difference in the processing of vernier acuity and the other two hyperacuties considered here will apply regardless of which of the two models are assumed to be responsible. In the local-sign model the second comparative stage could be carried out by the same process which underlies the channel model. The obvious implication is that the mechanism responsible for vernier acuity is less affected by changes within the ageing visual system than other functions. If one accepts the majority view that such age changes are due to neural loss this should not be altogether surprising. The vernier task, as was stated above, is carried out by pooling amongst many receptors with their output giving a direct indication of the direction of offset. The loss

of some of these receptors would not be expected to seriously degrade the performance of the task. For bisection and displacement tasks the receptor outputs have to be compared in order to extract the necessary information. In the bisection task all the required information is present at any given time while for displacement a temporal comparison is needed in addition to the bisection judgment. We must assume that it is at this comparison stage that the age-related differences between vernier acuity on the one hand, and displacement detection and bisection acuity on the other, arises.

Chapter 12: Conclusion and further studies

12.1: Summary of experiment conclusions

What conclusions regarding visual hyperacuity can be drawn from the experiments described in this thesis? In order to answer this question it may be best to first give a brief resumé of the conclusions from each experiment.

12.1.1: Contrast

a). Displacement detection and bisection acuity thresholds were found to respond similarly to changes in contrast level. They both display evidence of contrast saturation for longer lines but not for short lines. In this respect they differ from vernier acuity which shows no evidence of saturation with increasing contrast.

b). It was concluded that spatial summation is taking place which, under certain conditions, counteracts the deleterious effect on thresholds of reducing contrast. For vernier acuity optimal information used to determine the offset comes from a limited spatial extent of the stimulus. On the other hand, displacement detection and bisection acuity can be performed equally well using any part of the stimulus. This difference is considered to facilitate the effect of summation for the latter two stimulus configurations.

c). Given the high contrast sensitivities of magnocellular cells and the fact that they exhibit contrast saturation at relatively low contrasts it is possible that the results could indicate preferential processing via the magnocellular pathway. However, there is also evidence that summation amongst relatively insensitive parvocellular units could produce the same effect. The experiment cannot differentiate between these two possibilities and the point was made that both pathways are probably used but that one or other will predominate depending on the exact stimulus parameters.

12.1.2: Displacement thresholds and references

a). The effect of references on a displacement detection task is to greatly enhance performance.

b). Both temporal and spatial reference separations were investigated and it was found that the effect of temporal separation is much more pronounced. This has also been found in purely spatial hyperacuity tasks. The clear conclusion to be drawn is that in order to obtain thresholds with hyperacuity precision simultaneous presentation of the stimulus features is required.

c). There was an obvious difference between the results obtained with a reference and those without. This pointed towards two mechanisms underlying displacement detection. With a reference the task requires relative localisation of the stimulus features, the same mechanism which underlies the spatial hyperacuties. If one accepts the channel model, for example, displacement detection in the presence of references would be signalled by changes, over time, in the output of the group of filters covering the area in which the stimulus is located.

d). In the absence of references a form of direct movement detection is chiefly employed. This does not produce threshold values within the hyperacuity range. The best unreferenced threshold values occur for an instantaneous stop-go-stop displacement. In this special case positional memory may be the mechanism which allows the task to be completed.

12.1.3: Spatial frequency and separation

a). These two factors co-vary in such a way as to suggest that vernier acuity, using sinusoidal gratings, is mediated by the differential response of filters tuned to differing spatial frequencies, phase and orientations.

b). In order to obtain the very low thresholds characteristic of hyperacuity tasks, the separation has to be limited to a maximum value of around 16 minutes of arc. This is sensible if one accepts that the filters need to cover both parts of the stimulus. However, it is proposed that this finding reflects, primarily, the restriction on the spatial frequency filters available to the visual system inherent in the choice of stimulus. For example, a low spatial frequency grating forces the visual system to rely on the outputs of low spatial frequency filters resulting in a marked worsening of threshold values. This proposition is entirely consistent with the operation of the channel models.

12.1.4: Weighting function

a). This experiment used random dot clusters and found that the weighting attached to different parts of the retinal light distribution when assigning location does not vary linearly with distance from the geometric center of the cluster. The weighting function did, however, demonstrate a relationship to dot density. For high dot densities there was a tendency for the weighting function to vary linearly while for low dot densities the weighting reflected the use of some edge feature of the cluster. This change was thought to reflect the variations in inter-dot separation and cluster contrast with changes in dot density.

12.1.5: Eccentricity

a). By prudent use of a technique which does not assume a prior value of the scaling factor it was possible to show that vernier acuity using two lines *and* two separated dots could be scaled by a single factor. This was opposed to certain views previously published but was felt to be sound given the steps taken to rigidly control the variables within the experiment.

b). The rate of decline of vernier acuity with eccentricity is much less steep than that found by some other investigations. Again, this may reflect the strict control on the experimental variables. In particular, steps were taken not to allow separation and eccentricity to co-vary.

12.1.6: Age

a). Three types of hyperacuity task (vernier acuity, bisection acuity and displacement detection) were investigated in a group of subjects between the ages of 18 and 80 years. Vernier acuity was shown not to vary significantly with age in contrast to the other two tasks which both showed a significant deterioration with increasing age.

b). The possible means by which vernier, bisection and displacement judgments are made were discussed. The differences in response with age were thought to arise at a secondary comparative stage, necessary when performing displacement and bisection tasks but not for the vernier task.

12.2: General conclusion

The results of this group of experiments can be used to make some tentative suggestions as to the underlying mechanism being employed to carry out the hyperacuity task. From chapter 8 there is evidence that single filters tuned to different orientations, phase and spatial frequency can best explain the findings. On the other hand, chapter 9 shows that some feature of the retinal light distribution is employed in assigning an explicit location to a random dot cluster, *i.e.* a local-sign. There are significant differences, however, between the two types of stimulus and it would not be unreasonable to conclude that both systems might be available to the visual system and that the exact stimulus configuration is the critical factor in deciding which is employed.

The use of single filters was shown to severely limit the spatial extent of the stimulus from which thresholds in the hyperacuity range can be obtained. The evidence, from chapter 8, appears to place this limit of feature separation at around 16 to 20 minutes of arc. Intuitively this leads towards the suspicion that a dual system must be employed in the performance of relative localisation tasks, as was suggested by Klein and Levi (1985) and Morgan *et al.* (1990). On the assumption that both systems operate simultaneously it is logical to predict that the most efficient should be preferentially employed. Thus for small separations single filters would usually be preferred. As separation increases the larger, low frequency filters which have to be used are significantly less efficient than the small, high frequency filters used at small separations. In such circumstances either system, or indeed both systems, may be utilised depending on the exact stimulus configuration. For very large separations, over about 60 to 75 minutes of arc, the lack of suitably large filters make the single filter system untenable necessitating the use of some form of local-sign system. The experiments described here may provide some support for this dual mechanism. Such dual mechanisms are also found elsewhere in the visual system. In chapter 7 it was shown that movement detection is thought to be mediated by two systems depending on the presence, or otherwise, of references. In addition, there are thought to be two, essentially independent, pathways by which information is transmitted between the retina and the cortex. These two pathways are discussed in chapter 6 with regard to their different contrast sensitivities. A further example of a dual mechanism in the visual system is the change from cone to rod response concurrent with a fall in luminance levels. It would be sensible to assume that all four dual mechanisms mentioned follow a similar path with regard to their spheres of operation. Thus, at the extremes one or other would predominate but there should be a gradual transition from one to

the other in moving from one end of the range to the other. Indeed, it may be that the need to operate over a vast range of stimulus parameters (size, contrast, luminance, velocity etc.) may make dual mechanisms a prerequisite for the efficient operation of the visual system.

12.3: Further studies

12.3.1: Use of strongly orientated interfering stimuli

In a recent paper, Morgan *et al.* (1990) suggest that their results question the ability of single filters to perform a vernier acuity task. They argue that instead an explicit representation of the target feature position would be needed. In their experiment vernier acuity was measured using two targets each 4.2 minutes of arc square. To this basic stimulus configuration various supernumerary features (squares of the same size, positioned as shown in *Figure 12.01*) were added.

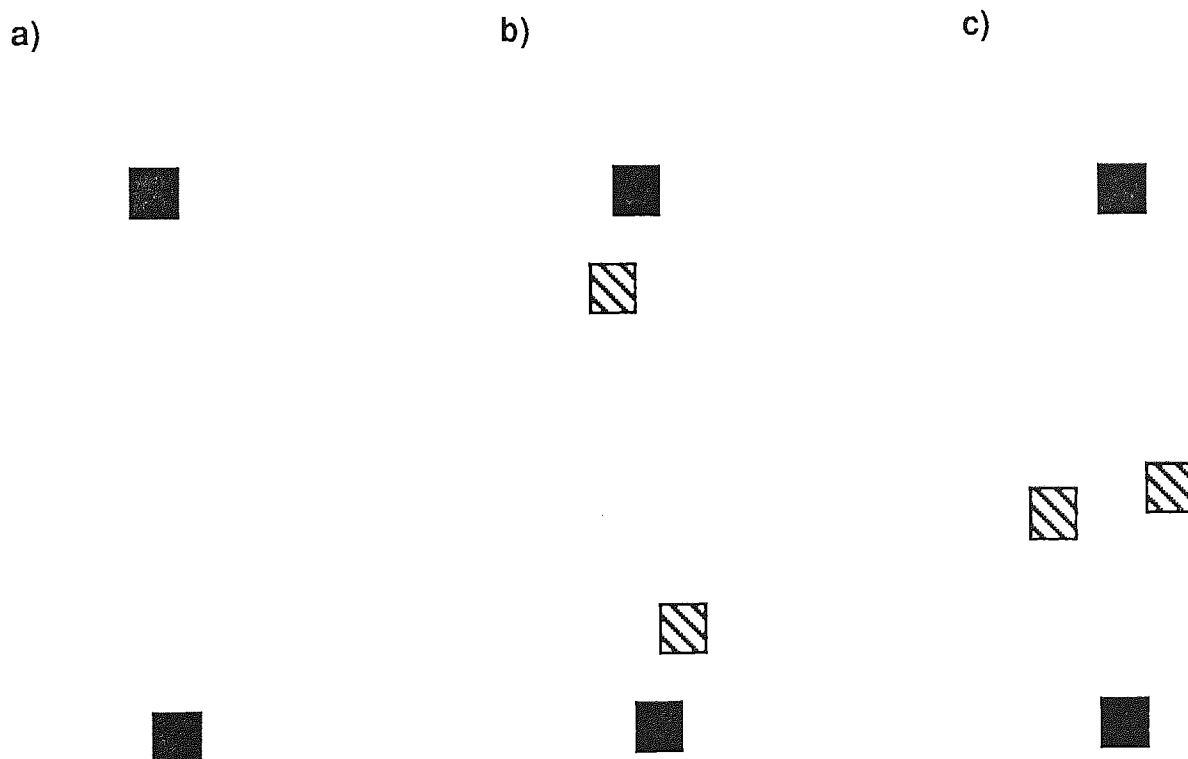


Figure 12.01: The stimuli used by Morgan *et al.* (1990). (a) is the control stimulus, a conventional two dot vernier task with the squares separated by 37.8 minutes of arc. (b) has two interfering squares (hatched lines) placed between the two main feature squares. The supernumerary squares are placed symmetrically with regard to the feature squares. The separation between the feature and supernumerary squares was either 4.4, 10.7 or 21.0 minutes of arc. The supernumerary squares were also jittered horizontally between 0 and 560 seconds of arc. (c) shows the experiment with supernumerary squares placed to either side of the imaginary line joining the feature squares. These squares were jittered by up to 140 seconds of arc, both horizontally and vertically, with the proviso that they did not cross the imaginary vertical line joining the feature squares.

The first experiment showed that the supernumerary squares had no effect on threshold values except when placed close to the feature squares. In the second experiment there was no effect on thresholds for either vertical or horizontal jitter of the supernumerary squares.

The argument against a single filter being able to perform the vernier task in these conditions is simple. In essence, the output of any filter which contains both target squares must also contain the supernumerary squares which will clearly have an effect on the output of the filter. Morgan *et al.* suggested that the results could only be explained by use of accurately located, orientationally tuned filters or by a form of coincidence detector (as suggested by Morgan and Regan, 1987; see chapter 3). Alternatively the local-sign model might be invoked whereby the target square positions are encoded with an explicit location and these are then compared to perform the vernier judgment. Their final suggestion was that a combination of local-sign and filter models might usefully be considered. In this the local-sign would allow the intelligent selection of filters which then enables the task to be performed regardless of the presence of disturbing features.

There is, however, one point which needs to be made regarding the experiment. The separation chosen (37.8 minutes of arc) would allow only the larger, less sensitive filters to operate. In such circumstances the local-sign model may well provide a more efficient method for completing the task than the single filter models. In addition, as was pointed out above, given a choice of either local-sign or channel model in the experimental set up used the visual system would clearly choose the local-sign model in order to overcome the presence of the disturbing features. At smaller separations the greater sensitivity of the channel models may make the forced selection of a local-sign model less easy.

A trial run using just such an experimental configuration has been performed. The stimulus features are two dots measuring one minute of arc across. The disturbing feature this time is a line 12 minutes of arc long positioned at various orientations between 40 degrees left of vertical and 40 degrees right of vertical. The dots were separated by 16 minutes of arc vertically while the end of the line was always at least 60 seconds of arc from the dots. Vernier thresholds were measured, using a PEST technique, for each orientation. The nine different orientations were randomly interleaved and all thresholds were obtained in a single sitting lasting about 25 minutes (*Figure 12.02*).

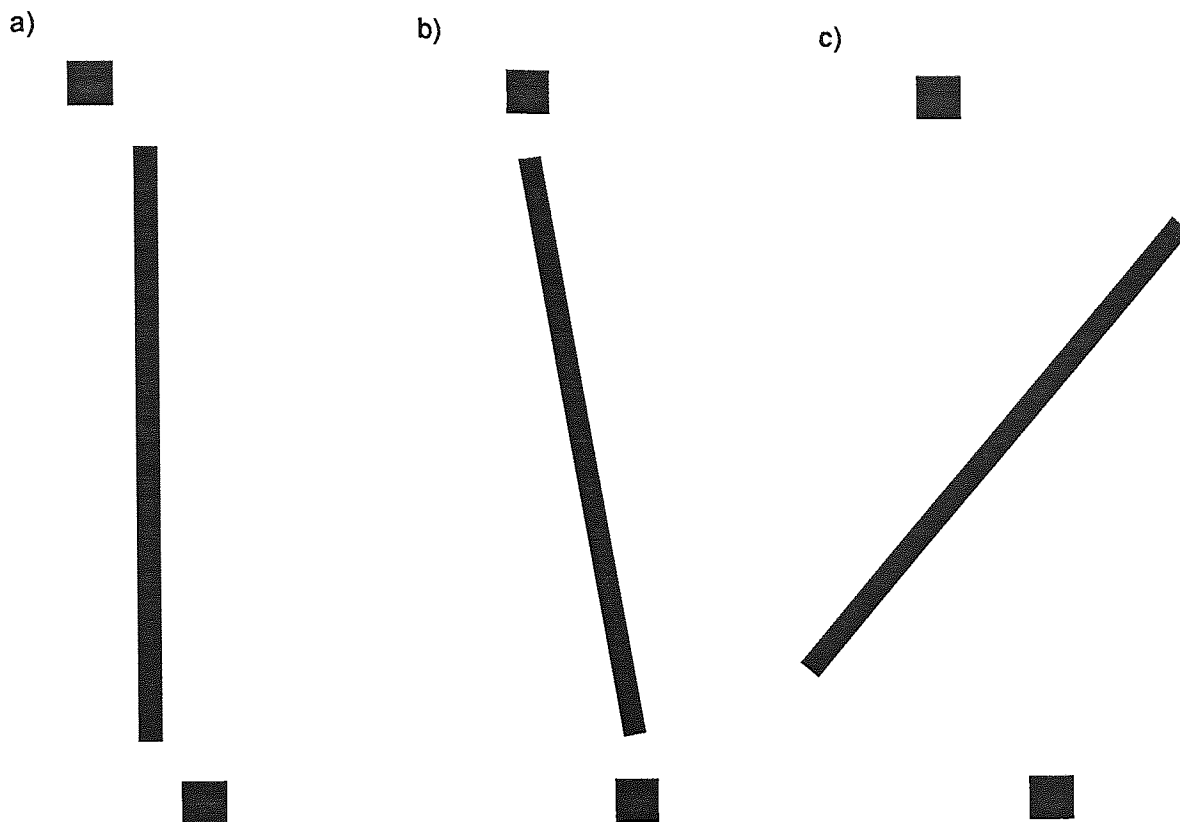


Figure 12.02: The configuration employed to investigate interference with orientationally tuned filters as described in the text. a) shows the disturbing line positioned vertically, b) with an orientation of 10 degrees to the left and c) an orientation of 40 degrees to the right.

The changes in bias (*Figure 12.03*) show that the orientated line appears to move the position of subjective alignment in the direction of the line orientation. Thus a 20 degree leftward tilt of the line causes a net bias of approximately 40 seconds of arc to the left. Note that there is a large variability of results, however, which means any conclusion must be viewed with caution. This variation can be explained on the basis of the orientationally tuned filters signalling a vernier offset. Clearly, the line is going to cause those filters tuned to its orientation to be stimulated. Given the close proximity of the line to the filters signalling the offset of the two dots averaging of all the filters responses would be expected to give results in line with those found here.

The changes in acuity are more problematic (*Figure 12.04*). A possible explanation is that the response from those filters signalling the offset of the two feature dots is distorted by the outputs from those filters signalling the orientation of the line. In effect, the increased noise caused by the presence of the line lowers the sensitivity of the filters signalling the offset.

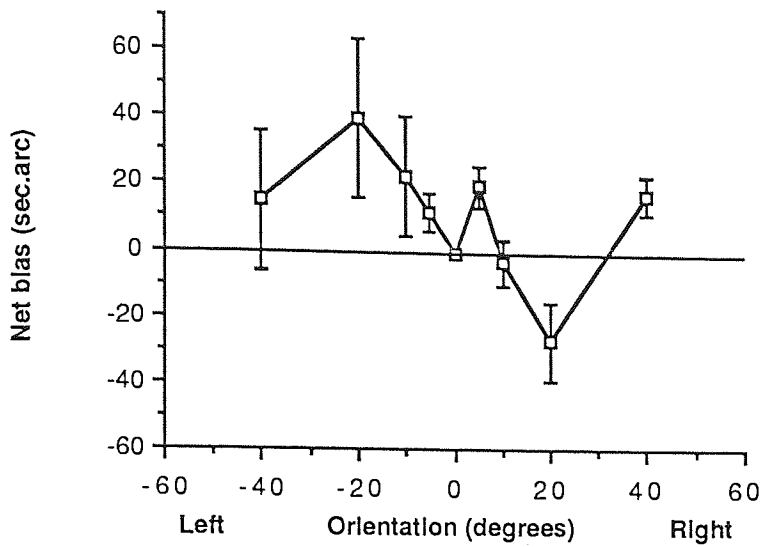


Figure 12.03: Net bias, bias value relative to that at zero orientation, plotted as a function of the orientation of the perturbing line, positive values indicate leftward bias and vice-versa. Despite the large variance there is a systematic trend for bias to be pulled in the direction of the orientated line the effect seems to peak at around 20 degrees.

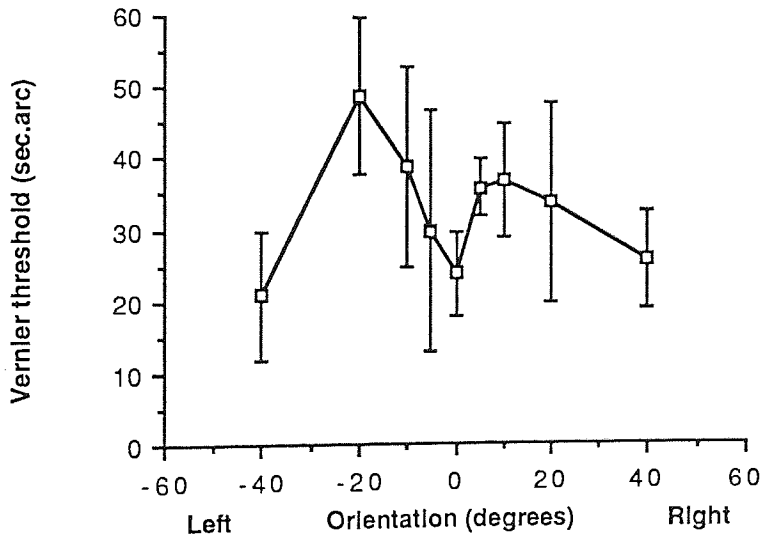


Figure 12.04: Vernier acuity plotted as a function of the orientation of the perturbing line. Note that acuity worsens as the orientation increases up to 20 degrees and then returns to a base level (comparable with that obtained with the zero orientation and also checked against results with no perturbing line in place).

Given these early results it would seem worthwhile to attempt to investigate a selection of stimulus parameters and experimental methods to see if a more repeatable set of results can be obtained. It would also be necessary to carry out the experiment on further subjects who would need to be naive as to the purpose of the experiment but experienced in hyperacuity tasks.

It is my contention that the outcome would be to add further evidence to the premise that, certainly over the small target separations where hyperacuity levels of performance are obtained, a channel model can be invoked as the underlying mechanism.

12.3.2: Spatial scaling as a clinical tool

There are several pathological conditions which in their early stages affect only part of the retina. Two common examples are Primary Open Angle Glaucoma (POAG) and Age-related Macula Degeneration (AMD). Early detection of such conditions greatly improves the efficacy of treatment in stabilising the situation and in many cases arresting further damage. Common techniques employed in screening for these conditions compare the results, obtained in a task such as light detection, contrast sensitivity etc., from a suspect patient to those from an averaged set of age matched normals.

POAG is a disease affecting the fibers of the optic nerve. It is a slow, insidious condition which can cause substantial damage without causing a detectable decline in function as measured using perimetry (Quigley, Addicks and Green, 1982). It has been suggested that use of a hyperacuity task which depends on processing by the retinal ganglion cells might be usefully employed as an early detector of damage (Fitzke, Poinoosawmy, Ernst and Hitchings, 1987). They carried out some preliminary work using an oscillatory displacement detection task. The results indicated that patients with ocular hypertension and POAG had higher thresholds than normal subjects. *Figure 12.05* shows the summary of their results. An important point to note is that there is a considerable overlap between the groups, in particular between the normals and ocular hypertensives. This immediately raises the problem of test selectivity, the ability to differentiate between normals and non-normals.

Use of the spatial scaling technique employed in chapter 10 may represent an alternative method whereby self matching within the same individual is employed. Early POAG affects sensitivity first at around 15 degrees from the fovea. In such circumstances performance at

15 degree eccentricity would be expected to be below normal in the affected eye. It would be logical, therefore, to assume that the fall off in performance with eccentricity for a psychophysical task would be faster than normal. By a similar argument, in AMD the macular area is affected causing a reduced foveal performance but a normal performance at 15 degrees. In such circumstances a slower fall in sensitivity with eccentricity would be expected.

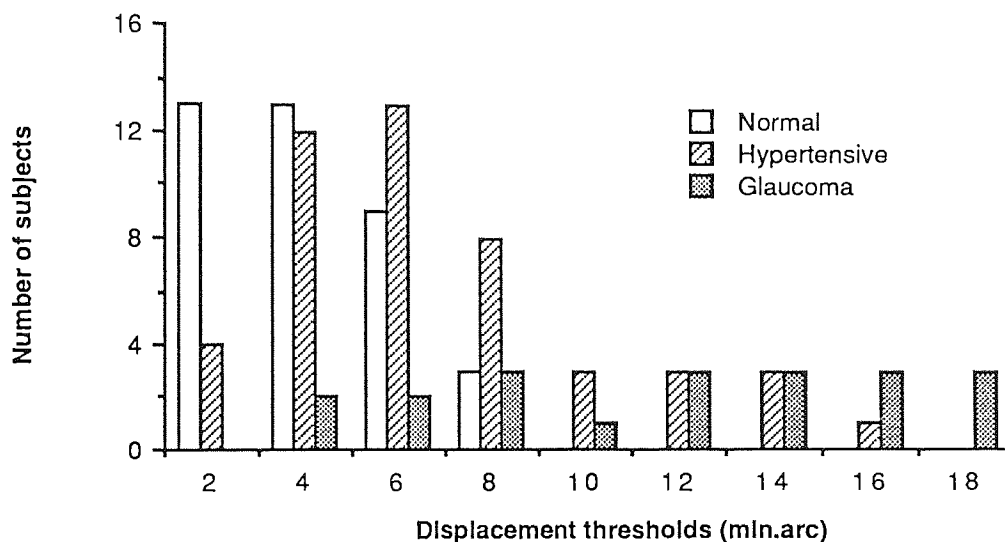


Figure 12.05: Displacement thresholds obtained by Fitzke *et al.* (1987) for three groups; normals, ocular hypertensives and diagnosed sufferers from POAG. The number of subjects falling into each category are shown and the overlap, especially between normals and ocular hypertensives is apparent. The mean displacement thresholds for the three groups were....

Normals	3.2 +/- 1.9
Ocular hypertensives	5.5 +/- 3.1
POAG	9.7 +/- 4.9

It is clear that the spread of results increases greatly for the POAG group compared with the normals and it is this spread which reduces the selectivity of the test.

With this in mind it may be worth investigating a selection of normal subjects, of various ages, to see if such a technique could be translated into a clinical method. The first difficulty would be the choice of a suitable hyperacuity paradigm. The clinical use of a two dot vernier task for estimation of retinal function behind media opacities has been suggested before (Enoch, Williams, Essock and Fendick, 1985). It suffers, however, from the relationship between separation, performance and blur. With increasing blur the separation has to be increased in order to enable the task to be carried out. But, as has been shown, performance declines with increasing separation (Westheimer and McKee, 1977a). However, for the early detection of POAG this may not be a critical factor. Many early sufferers fall in the 40

to 60 years age group where media opacities are much less common than in older age groups.

An alternative, which has also been put forward as a possible measure of retinal function behind media opacities, would be to use a displacement detection task (Whitaker and Deady, 1989). This has been shown to be more resistant to media changes (Whitaker and Buckingham, 1987) and has been shown not to be critically dependent on separation (Chapter 7).

In order to translate this suggestion into a clinical tool it will be necessary to investigate the variability of the gradients obtained in normal subjects. These subjects would have to cover a range of ages and would have to be free from ocular disorders. To reduce the time taken it may be necessary to measure only two points (for example, foveal and 15 degrees). It has been repeatedly shown that inter-observer variability is usually large which, in consequence, makes the interpretation of the results fraught with difficulty (see chapter 11, and *Figure 12.05*). This may, however, be less of a problem using the method proposed here. It may still be true that the absolute sensitivity at the points measured would vary greatly. However, because the gradient represents a ratio between two sensitivity values it is largely independent of the sensitivity values themselves. If this is so then the gradients should be broadly similar for a range of normal observers. Clearly, therefore, any abnormal gradient could be a strong indicator of an ocular defect and may well improve the specificity and sensitivity of the test.

Publications, Presentations and Posters

Publications.

Elliott, D. B., Whitaker, D. and MacVeigh, D. (1990) Neural contribution to spatiotemporal contrast sensitivity decline in healthy ageing eyes. *Vision Research* **30**, 541 - 547.

Whitaker, D. and MacVeigh, D. (1990) Displacement thresholds for various types of movement: effect of spatial and temporal reference separation. *Vision Research* **30**, 1499 - 1506.

MacVeigh, D., Whitaker, D. and Elliott, D. B. (1991) Spatial summation determines the contrast response of displacement threshold hyperacuity. *Ophthalmic and Physiological Optics* **11**, 76 - 80.

Whitaker, D. and MacVeigh, D. (1991) Interaction of spatial frequency and separation in vernier acuity. *Vision Research* **31**, 1205 - 1212.

Whitaker, D. and MacVeigh, D. (1991) Sequential mapping of weighting functions for visual location. *Spatial Vision*, (in press).

Whitaker, D., Elliott, D. B. and MacVeigh, D. (1991) Variations in hyperacuity performance with age. *Ophthalmic and Physiological Optics*, (in press).

Whitaker, D., Rovamo, J., MacVeigh, D. and Makela, P. (1991) Spatial scaling of vernier acuity tasks. *Vision Research*, (submitted).

Presentations.

Whitaker, D., Elliott, D. B. and MacVeigh, D. (1989) Spatiotemporal contrast sensitivity decline with age. *Association for Research in Vision and Ophthalmology Annual Meeting*, Sarasota, U.S.A. April 30 - May 5.

MacVeigh, D. (1990) Detecting the displacement of objects of varying size and contrast. *Society of Experimental Optometry*, Birmingham, U.K. July 24 - 25.

MacVeigh, D. and Whitaker, D. (1990) Do spatial frequency filters determine vernier acuity? *Applied Vision Association Postgraduate Open Contributions Meeting*, London, U.K. November 21.

Elliott, D. B., MacVeigh, D. and Whitaker, D. (1991) Variations in hyperacuity performance with age. *Non invasive Assessment of the Visual System*, Santa Fe, U.S.A. February 4 - 7.

Rovamo, J., Whitaker, D. and MacVeigh, D. (1991) Spatial scaling of vernier acuity tasks. *Association for Research in Vision and Ophthalmology Annual Meeting*, Sarasota, U.S.A. April 28 - May 3.

Abstracts.

Elliott, D. B., Whitaker, D. and **MacVeigh, D.** (1989) Spatiotemporal contrast sensitivity decline with age. *Investigative Ophthalmology and Visual Science (Suppl.)* **30**, 406.

MacVeigh, D. and Whitaker, D. (1990) Detecting the displacement of objects of varying size and contrast. *Ophthalmic and Physiological Optics* **10**, 410.

Rovamo, J., Whitaker, D. and **MacVeigh, D.** (1991) Spatial scaling of vernier acuity tasks. *Investigative Ophthalmology and Visual Science (Suppl.)* **32**, 1270.

Elliott, D. B., **MacVeigh, D.** and Whitaker, D. (1991) Variations in hyperacuity performance with age. *Non invasive Assessment of the Visual System, Technical Digest* **1**, 137 - 140.

List of references

- Allen, M. J. and Vos, J. J. (1967) Ocular scattered light and visual performance as a function of age. *American Journal of Optometry and Physiological Optics* **44**, 717 - 727.
- Andersen, R. A. (1989) Visual and eye movement functions of the posterior parietal cortex. *Annual Review of Neurosciences* **12**, 377 - 403.
- Andrews, D. P. (1967) Perception of contour orientation in the central fovea. Part 1: short lines. *Vision Research* **7**, 975 - 997.
- Andrews, D. P. and Miller, D. T. (1978) Acuity for spatial separation as a function of stimulus size. *Vision Research* **18**, 615 - 619.
- Andrews, D. P., Butcher, A. K. and Buckley, B. R. (1973) Acuities for spatial arrangement in line figures: Human and ideal observers compared. *Vision Research* **13**, 599 - 620.
- Aubert, B. (1886) Die Bewegungsempfindung. *Pflugers Archiv fur die gesamte Physiologie* **39**, 347 - 370.
- Badcock, D. R. and Westheimer, G. (1985) Spatial location and hyperacuity: The center/surround localization contribution function has two substrates. *Vision Research* **25**, 1259 - 1267.
- Barlow, H. B. (1979) Reconstructing the visual image in space and time. *Nature* **279**, 189 - 190.
- Barlow, H. B. (1981) Critical limiting factors in the design of the eye and the visual cortex. *Proceedings of the Royal Society of London, Series B* **212**, 1 - 34.
- Barlow, H. B. and Hill, R. M. (1963) Evidence for a physiological explanation for the waterfall phenomenon and figural after-effects. *Nature* **200**, 1345 - 1346.
- Barlow, H. B. and Levick, W. R. (1965) The mechanism of directionally selective units in rabbit's retina. *Journal of Physiology, London* **173**, 377 - 407.
- Barlow, H. B. and Levick, W. R. (1969) Three factors limiting the reliable detection of light by retinal ganglion cells of the cat. *Journal of Physiology, London* **200**, 1 - 24.
- Bassi, C. J. and Lehmkuhle, S. (1990) Clinical implications of parallel visual pathways. *Journal of the American Optometric Association* **61**, 98 - 109.
- Beck, J. and Halloran, T. (1985) Effects of spatial and retinal eccentricity in two dot vernier acuity. *Vision Research* **25**, 1105 - 1111.
- Bonnet, C. (1975) A tentative model for the detection of visual motion. *Psychologica* **18**, 35 - 50.
- Bonnet, C. (1977) Visual motion detection models: features and frequency filters. *Perception* **6**, 491 - 500.

- Bonnet, C. (1982) Thresholds of motion perception. In Wertheim, A.H., Wagenaar, W. A. and Leibowitz, H. W. (eds.) *Tutorials in Motion Perception*. Plenum, London.
- Bonnet, C. (1984) Two systems in the detection of visual motion. *Ophthalmic and Physiological Optics* **4**, 61 - 65.
- Boyce, P. R. (1965) The visual perception of movement in the absence of an external frame of reference. *Optica Acta* **12**, 47 - 54.
- Bracewell, (1978) *The Fourier transform and its applications* McGraw Hill, New York.
- Bradley, A. and Freeman, R. D. (1985) Is reduced vernier acuity in amblyopia due to position, contrast or fixation deficits? *Vision Research* **25**, 55 - 66.
- Bradley, A. and Skottun, B. C. (1987) Effects of contrast and spatial frequency on vernier acuity. *Vision Research* **27**, 1817 - 1824.
- Bradley, A., Skottun, B. C., Ohzawa, I., Sclar, G. and Freeman, R. D. (1985) Neurophysiological evaluation of the differential response model for orientation and spatial-frequency discrimination. *Journal of the Optical Society of America A* **2**, 1607 - 1610.
- Breitmeyer, B. G. and Ganz, L. (1976) Implications of sustained and transient channels for theories of pattern marking, saccadic suppression and information processing. *Psychological Review* **83**, 1 - 36.
- Brindley, G. S. and Lewin, W. S. (1968) The sensations produced by electrical stimulation of the cortex. *Journal of Physiology, London* **196**, 479 - 493.
- Buckingham, T. and Whitaker, D. (1986) Displacement threshold for continuous oscillatory movement: The effect of oscillation waveform and temporal frequency. *Ophthalmic and Physiological Optics* **6**, 275 - 278.
- Burbeck, C. A. (1987) Position and spatial frequency in large-scale localisation judgments. *Vision Research* **27**, 417 - 427.
- Burbeck, C. A. and Yap, Y. L. (1990a) Spatiotemporal limitations in bisection and separation discrimination. *Vision Research* **30**, 1573 - 1586.
- Burbeck, C. A. and Yap, Y. L. (1990b) Spatial filter selection in large-scale spatial-interval discrimination. *Vision Research* **30**, 263 - 272.
- Campbell, F. W. and Green, D. G. (1965) Optical and retinal factors affecting visual resolution. *Journal of Physiology, London* **181**, 576 - 593.
- Campbell, F. W. and Gubisch, R. W. (1966) Optical quality of the human eye. *Journal of Physiology, London* **186**, 558 - 578.
- Carlson, C. R. and Cohen, R. W. (1980) A simple psychophysical model for predicting the visibility of displayed information. *Proceedings of the Society of Information Display* **21**, 229 - 246.

- Carlson, C. R. and Klopfenstein, R. W. (1985) Spatial-frequency model for hyperacuity. *Journal of the Optical Society of America A* **2**, 1747 - 1751.
- Charman, W. N. (1983) The retinal image of the human eye. In *Progress in Retinal Research, Volume 2*. Osborne, N. and Chader, G. (eds.) Pergamon Press, Oxford.
- Cleland, B. G., Dubin, M. W. and Levick, W. R. (1971) Sustained and transient neurones in the cat's retina and lateral geniculate nucleus. *Journal of Physiology, London* **217**, 473 - 496.
- Cornsweet, T. N. (1962) The staircase method in psychophysics. *American Journal of Physiology* **75**, 485 - 491.
- Cowey, A. and Rolls, E. T. (1974) Human cortical magnification factor and its relation to visual acuity. *Experimental Brain Research* **21**, 447 - 454.
- Crick, F. H., Marr, D. and Poggio, T. (1980) An information processing approach to understanding visual cortex. In *The Cerebral Cortex*, Schmidt, F. O. and Worden, F. G. (eds.) MIT Press, Cambridge MA.
- Daniel, P. M. and Whitteridge, D. (1961) The representation of the visual field on the cerebral cortex in monkeys. *Journal of Physiology, London* **159**, 203 - 221.
- Derefeldt, G., Lennerstrand, G. and Lundh, B. (1979) Age variations in normal human contrast sensitivity. *Acta Ophthalmologica* **57**, 679 - 690.
- Derrington, A. M. and Fuchs, A. F. (1979) Spatial and temporal properties of X- and Y-cells in the cat lateral geniculate nucleus. *Journal of Physiology, London* **293**, 347 - 364.
- Derrington, A. M. and Lennie, P. (1984) Spatial and temporal contrast sensitivities of neurons in lateral geniculate nucleus of macaque. *Journal of Physiology, London* **357**, 219 - 240.
- Derrington, A. M., Krauskopf, J. and Lennie, P. (1984) Chromatic mechanisms in lateral geniculate nucleus of macaque. *Journal of Physiology, London* **357**, 241 - 265.
- DeValois, R. L., Albrecht, D. G. and Thorell, L. G. (1982) Spatial frequency selectivity of cells in the macaque visual cortex. *Vision Research* **22**, 545 - 559.
- DeYoe, E. A. and Van Essen, D. C. (1988) Concurrent processing streams in monkey visual cortex. *Trends in Neurosciences* **11**, 219 - 226.
- Dixon, W. J. and Mood, A. M. (1948) A method for obtaining and analyzing sensitivity data. *Journal of the American Statistical Association* **43**, 109 - 126.
- Drasdo, N. (1977) The neural representation of visual space. *Nature* **266**, 554 - 556.
- Drasdo, N. (1989) Receptive field densities of the ganglion cells of the human retina. *Vision Research*, **29**, 985 - 988.

- Drasdo, N. (1991) Neural substrates and threshold gradients in peripheral vision. In *Vision & Visual dysfunction, Volume 5*. Cronly-Dillon, J. R. (ed.) MacMillan, Basingstoke.
- Drasdo, N. and Fowler, C. W. (1974) Non-linear projection of the retinal image in a wide-angle schematic eye. *British Journal of Ophthalmology* **58**, 709 - 714.
- Dow, B. M., Snyder, A. Z., Vautin, R. G. and Bauer, R. (1981) Magnification factor and receptive field size in foveal striate cortex of the monkey. *Experimental Brain Research* **44**, 213 - 228.
- Elliott, D. B. (1987) Contrast sensitivity decline with ageing: a neural or optical phenomenon? *Ophthalmic and Physiological Optics* **7**, 415 - 419.
- Elliott, D. B. and Whitaker, D. (1991a) The effect of simulating optical changes associated with ocular ageing. *Investigative Ophthalmology and Visual Science (supp.)* **32**, 1275.
- Elliott, D. B. and Whitaker, D. (1991b) Changes in macular function throughout adulthood. *Documenta Ophthalmologica* **76**, 251 - 259.
- Elliott, D. B., Whitaker, D. and Thompson, P. (1989) Use of displacement threshold hyperacuity to isolate the neural component of senile vision loss. *Applied Optics* **28**, 1914 - 1918.
- Elliott, D. B., Whitaker, D. and MacVeigh, D. (1990) Neural contribution to spatiotemporal contrast sensitivity decline in healthy ageing eyes. *Vision Research* **30**, 541 - 547.
- Enoch, J. M., Williams, R. A., Essock, E. A. and Fendick, M. (1985) Hyperacuity: A promising means of evaluating vision through cataract. In *Progress in Retinal Research Volume 4*. Osborne, N. N. and Chader, G. J. (eds.) Pergamon Press, Oxford.
- Enroth-Cugell, C. and Robson, J. G. (1966) The contrast sensitivity of retinal ganglion cells of the cat. *Journal of Physiology, London* **187**, 517 - 552.
- Fahle, M. and Poggio, T. (1981) Visual hyperacuity: spatiotemporal interpolation in human vision. *Proceedings of the Royal Society of London, Series B* **213**, 451 - 477.
- Fechner, G. T. (1860, translated 1966) *Elements of psychophysics*. (Volume 1, translated by Adler, H. E.) Holt, Rinehart and Winston, New York.
- Fendick, M. and Westheimer, G. (1983) Effects of practice and the separation of test targets on foveal and peripheral stereoacuity. *Vision Research* **23**, 145 - 150.
- Filimonoff, I. N. (1932) Über die variabilität der Großhirnrindenstruktur. Regio occipitalis beim erwachsenen Menschen. *Journal Physiologische Neurologische, Leipzig* **44**, 1 - 96.
- Findlay, J. M. (1978) Estimates on probability functions: A more virulent PEST. *Perception and Psychophysics* **23**, 181 - 185.

- Fitzke, F.W., Poinosawmy, D., Ernst, W. and Hitchings, R. A. (1987). Peripheral displacement thresholds in normals, ocular hypertensives and glaucoma. *Seventh International Visual Field Symposium* Greve, E. L. and Heijl, A. (eds). Nijhoff, M. and Junk, W., Dordrecht.
- Foley-Fisher, J. A. (1977) Contrast, edge-gradient and target line width as factors in vernier acuity. *Optica Acta* **24**, 179 - 186.
- French, J. W. (1920) Height and width of vernier lines and separation. *Transactions of the Optical Society* **21**, 127 - 156.
- Funakawa, M. (1989) Relation of spatial and temporal frequencies to vernier acuity. *Spatial Vision* **4**, 267 - 274.
- Gartner, S. and Henkind, P. (1981) Ageing and degeneration of the human macula. 1. Outer nuclear layer and photoreceptors. *British Journal of Ophthalmology* **65**, 23 - 28.
- Geisler, W. S. (1984) Physical limits of acuity and hyperacuity. *Journal of the Optical Society of America A* **1**, 775 - 782.
- Green, D. M. and Swets, J. A. (1966) *Signal detection theory and psychophysics*. John Wiley and Sons, New York.
- Greene, H. A. and Madden, D. J. (1987) Adult age differences in visual acuity, stereopsis and contrast sensitivity. *American Journal of Optometry and Physiological Optics* **64**, 749 - 753.
- Hecht, S. and Mintz, E. V. (1939) The visibility of single lines at various illuminations and the retinal basis of visual resolution. *Journal of General Physiology* **22**, 593 - 612.
- Heeley, D. W. and Buchanan-Smith, H. M. (1990) Recognition of stimulus orientation. *Vision Research* **30**, 1429 - 1437.
- Henderson, D. C. (1971) The relationships among time, distance and intensity as determinants of motion discrimination. *Perception and Psychophysics* **10**, 313 - 320.
- Hering, E. (1899) Über die Grenzen der Sehschärfe. *Berichte über die mathematisch - physikalische Classe der Königl. Sächsischen Gesellschaft Wissenschaften, Leipzig Naturwiss Teil* pp. 16- 24.
- Hess, R. F. and Watt, R. J. (1990) Regional distribution of the mechanisms that underlie spatial localisation. *Vision Research* **30**, 1021 - 1031.
- Higgins, K. E., Jaffe, M. J., Caruso, R. C. and deMonastario, F. M. (1988) Spatial contrast sensitivity: Effects of age, test-retest and psychophysical method. *Journal of the Optical Society of America A* **5**, 2173 - 2180.
- Hirsch, J. and Curcio, C. A. (1989) The spatial resolution capacity of human foveal retina. *Vision Research* **29**, 1095 - 1101.

- Hirsch, J. and Hylton, R. (1982) Limits of spatial frequency discrimination as evidence of neural interpolation. *Journal of the Optical Society of America* **72**, 1367 - 1374.
- Hirsch, J. and Hylton, R. (1984) Quality of the primate photoreceptor lattice and limits of spatial vision. *Vision Research* **24**, 347 - 355.
- Hirsch, J. and Hylton, R. (1985) Spatial-frequency discrimination at low frequencies: evidence for position quantization by receptive fields. *Journal of the Optical Society of America A* **2**, 128 - 135.
- Howard, I. P. (1982) *Human visual orientation*. Wiley, Chichester.
- Hubel, D. H. and Wiesel, T. N. (1959) Receptive fields of single neurones in the cat's striate cortex. *Journal of Physiology, London* **148**, 574 - 591.
- Hubel, D. H. and Wiesel, T. N. (1962) Receptive fields, binocular interaction and functional architecture in the cat's visual cortex. *Journal of Physiology, London* **160**, 106 - 154.
- Hubel, D. H. and Wiesel, T. N. (1968) Receptive fields and functional architecture of monkey striate cortex. *Journal of Physiology, London* **195**, 215 - 243.
- Hubel, D. H. and Wiesel, T. N. (1972) Laminar and columnar distribution of geniculo-cortical fibers in macaque monkey. *Journal of Comparative Neurology* **146**, 421 - 450.
- Hubel, D. H. and Wiesel, T. N. (1974) Uniformity of monkey striate cortex: A parallel relationship between field size, scatter and magnification factor. *Journal of Comparative Neurology* **158**, 295 - 306.
- Hubel, D. H. and Wiesel, T. N. (1977) Functional architecture of macaque monkey visual cortex. *Proceedings of the Royal Society of London, Series B* **198**, 1 - 59
- Ikeda, H. and Wright, M. J. (1974) Evidence for 'sustained' and 'transient' neurones in the cat's visual cortex. *Vision Research* **14**, 133 - 136.
- Ikeda, H. and Wright, M. J. (1975) Spatial and temporal properties of 'sustained' and 'transient' neurones in area 17 of the cat's visual cortex. *Experimental Brain Research* **22**, 363 - 383.
- Jay, J. L., Mammo, R. B. and Allan, D. (1987) Effects of age on visual acuity after cataract extraction. *British Journal of Ophthalmology* **71**, 112 - 115.
- Johnson, C. A. and Scobey, R. P. (1980) Foveal and peripheral displacement thresholds as a function of stimulus luminance, line length and duration of movement. *Vision Research* **20**, 709 - 715.
- Johnson, C. A. and Scobey, R. P. (1982) The effects of reference lines on displacement thresholds at various durations of movement. *Vision Research* **22**, 819 - 821.
- Johnston, A. (1987) Spatial scaling of central and peripheral contrast-sensitivity functions. *Journal of the Optical Society of America A* **4**, 1583 - 1593.

- Kaplan, E. and Shapley, R. M. (1982) X and Y cells in the lateral geniculate nucleus of macaque monkeys. *Journal of Physiology, London* **330**, 125 - 143.
- Kinchla, R. A. (1971) Visual movement perception: a comparison of absolute and relative movement discrimination. *Perception and Psychophysics* **9**, 165 - 171.
- Kinchla, R. A. and Allen, L. G. (1969) A theory of visual movement perception. *Psychological Review* **76**, 537 - 558.
- Klein, S. A. and Levi, D. M. (1985) Hyperacuity thresholds of 1.0 second: theoretical predictions and empirical validation. *Journal of the Optical Society of America A* **2**, 1170 - 1190.
- Klein, S. A. and Levi, D. M. (1987) Position sense in the peripheral retina. *Journal of the Optical Society of America A* **4**, 1543 - 1553.
- Kline, D. W., Schieber, F., Abusamra, L. C. and Coyne, A. C. (1983) Age, the eye and the visual channels: Contrast sensitivity and response speed. *Journal of Gerontology* **38**, 211 - 216.
- Krauskopf, J. and Farell, B. (1991) Vernier acuity: Effects of chromatic content, blur and contrast. *Vision Research* **31**, 735 - 749.
- Lakshminarayanan, V., Aziz, S. and Enoch, J. M. (1991) Aging and the hyperacuity gap function. *Noninvasive assessment of the visual system, technical digest*. pp. 133 - 135.
- Legge, G. E. and Campbell, F. W. (1981) Displacement detection in human vision. *Vision Research* **21**, 205 - 213.
- Le Grand, Y. (1972) Spectral luminosity. In *Handbook of Sensory Physiology, Vol VII 14*. Fuortes, M. G. F. (ed.) Springer, Berlin.
- Lehmkuhle, S. W., Kratz, K. E. and Sherman, S. M. (1982) Spatial and temporal sensitivity of normal and amblyopic cats. *Journal of Neurophysiology* **48**, 372 - 387.
- Leibowitz, H. W. (1955) The effect of reference lines on the discrimination of movement. *Journal of the Optical Society of America* **45**, 829 - 830.
- Leventhal, A. G., Rodieck, R. W. and Dreher, B. (1981) Retinal ganglion cell classes in the Old World monkey: Morphology and central projections. *Science* **213**, 1139 - 1142.
- Levi, D. M. and Klein, S. A. (1990) The role of separation and eccentricity in encoding position. *Vision Research* **30**, 557 - 585.
- Levi, D. M. and Westheimer, G. (1987) Spatial interval discrimination in the human fovea: what delimits the interval? *Journal of the Optical Society of America A* **4**, 1304 - 1313.
- Levi, D. M., Klein, S. A. and Aitsebaomo, A. P. (1985) Vernier acuity, crowding and cortical magnification. *Vision Research* **25**, 963 - 985.

- Levi, D. M., Klein, S. A. and Yap, Y. L. (1988) "Weber's Law" for position: Unconfounding the role of separation and eccentricity. *Vision Research* **28**, 597 - 603.
- Livingstone, M. S. and Hubel, D. H. (1987) Psychophysical evidence for separate channels for the perception of form, color, movement and depth. *Journal of Neuroscience* **7**, 3416 - 3468.
- Loewenfeld, I. E. (1979) Pupillary changes related to age. In *Topics in neuro-ophthalmology* Thompson H. S. (Ed.), pp. 124 - 150. Williams and Wilkins, Baltimore.
- Ludvigh, E. (1953) Direction sense of the eye. *American Journal of Ophthalmology* **36**, 139 - 143.
- Malpeli, J. G. and Baker, F. H. (1975) The representation of the visual field in the lateral geniculate nucleus of *Macaca mulatta*. *Journal of Comparative Neurology* **161**, 569 - 594.
- Marocco, R. T. (1976) Sustained and transient cells in monkey lateral geniculate nucleus. Conduction velocities and response properties. *Journal of Neurophysiology* **39**, 340 - 353.
- Marr, D. and Hildreth, E. (1980) Theory of edge detection. *Proceedings of the Royal Society of London, Series B* **207**, 187 - 217.
- Marr, D. and Ullman, S. (1981) Directional selectivity and its use in early visual processing. *Proceedings of the Royal Society of London, Series B* **211**, 151 - 180.
- McFarland, R. A., Domey, R. G., Warren, A. B. and Ward, D. C. (1960) Alterations in dark adaptation as a function of age: I. A statistical analysis. *Journal of Gerontology* **15**, 149 - 154.
- McKee, S. P. and Westheimer, G. (1978) Improvement in vernier acuity with practice. *Perception and Psychophysics* **24**, 258 - 262.
- Merigan, W. H. and Eskin, T. A. (1986) Spatio-temporal vision of macaques with severe loss of P retinal ganglion cells. *Vision Research* **26**, 1751 - 1761.
- Miller, W. H. (1979) Interocular filters. In *Handbook of Sensory Physiology, Volume VII/6a*. Autrum, H., Jung, R., Loewenstein, W. R., Tueber, H. L. and Mackay, D. M. (eds.) Springer, Berlin.
- Morgan, M. J. (1984) Lecture at the Center for Visual Studies symposium. University of Rochester.
- Morgan, M. J. (1991) Hyperacuity. In *Vision & Visual dysfunction Volume 4* Cronly-Dillon, J. R. (ed.) MacMillan, Basingstoke.
- Morgan, M. J. and Regan, D. (1987) Opponent model for line interval discrimination: Interval and vernier performance compared. *Vision Research* **27**, 107 - 118.
- Morgan, M. J. and Ward, R. M. (1985) Spatial and spatial-frequency primitives in spatial-interval discrimination. *Journal of the Optical Society of America A* **2**, 1205 - 1210.

- Morgan, M. J., Ward, R. M. and Hole, G. J. (1990) Evidence for positional coding in hyperacuity. *Journal of the Optical Society of America A* **7**, 297 - 304.
- Morrison, S. D. and McGrath, C. (1985) Assessment of the optical contributions to the age-related deterioration in vision. *Quarterly Journal of Experimental Physiology* **70**, 249 - 269.
- Nakayama, K. and Silverman, G. H. (1985) Detection and discrimination of sinusoidal grating displacements. *Journal of the Optical Society of America A* **2**, 267 - 274.
- Nakayama, K. and Tyler, C. W. (1981) Psychophysical isolation of movement sensitivity by removal of familiar position cues. *Vision Research* **21**, 1663 - 1668.
- Newsome, W. T., Wurtz, R. H. and Dursteler Mikami, A. (1985) Deficits in visual motion processing following ibotenic acid lesions of the middle temporal visual area of the macaque monkey. *Journal of Neuroscience* **5**, 825 - 840.
- Odom, J. V., Vasquez, R. J., Schwartz, T. L. and Linberg, J. V. (1989) Adult vernier thresholds do not increase with age: Vernier bias does. *Investigative Ophthalmology and Vision Science* **30**, 1004 - 1008.
- Østerberg, G. (1935) Topography of the layer of rods and cones in the human retina. *Acta Ophthalmologica (Suppl.)* **65**, 1 - 102.
- Owsley, C., Sekuler, R. and Siemsen, D. (1983) Contrast sensitivity throughout adulthood. *Vision Research* **23**, 689 - 699.
- Owsley, C., Gardner, T., Sekuler, R. and Lieberman, H. (1985) Role of the crystalline lens in the spatial vision loss of the elderly. *Investigative Ophthalmology and Vision Science* **26**, 1165 - 1170.
- Palmer, J. (1986) Mechanisms of displacement detection with a visual reference. *Vision Research* **26**, 1939 - 1947.
- Paradiso, M. A. (1988) A theory for the use of visual orientation information which exploits the columnar structure of the cortex. *Biological Cybernetics* **58**, 35 - 49.
- Paradiso, M. A., Carney, T. and Freeman, R. D. (1989) Cortical processing of hyperacuity tasks. *Vision Research* **29**, 247 - 254.
- Parker, A. J. and Hawken, M. J. (1985) Capabilities of monkey cortical cells in spatial-resolution tasks. *Journal of the Optical Society of America A* **2**, 1101 - 1114.
- Pentland, A. (1980) Maximum likelihood estimation: the best PEST. *Perception and Psychophysics* **28**, 377 - 379.
- Polyak, S. L. (1941) *The retina*. University of Chicago Press, Chicago.
- Polyak, S. L. (1957) *The vertebrate visual system*. University of Chicago Press, Chicago.

- Post, R. B., Scobey, R. P. and Johnson, C. A. (1984) Effects of retinal eccentricity on displacement thresholds for unidirectional and oscillatory stimuli. *Vision Research* **24**, 835 - 839.
- Quigley, H. A., Addicks, E. M. and Green, R. (1982) Optic nerve damage in human glaucoma III. Quantitative correlation of nerve fiber loss and visual field defect in glaucoma, ischemic neuropathy, papilledema and toxic neuropathy. *Archives of Ophthalmology* **100**, 135 - 146.
- Rayleigh, Lord (1903) On the theory of optical images with special reference to the microscope. *Journal of the Royal Microscopical Society* p. 474.
- Reichardt, W. (1961) Autocorrelation, a principle for the evaluation of sensory information by the central nervous system. In *Sensory communication*, Rosenblith, W. A. (ed.), Wiley, New York.
- Rolls, E. T. and Cowey, A. (1970) Topography of the retina and striate cortex and its relationship to visual acuity in rhesus monkeys and squirrel monkeys. *Experimental Brain Research* **10**, 298 - 310.
- Rovamo, J. and Virsu, V. (1979) An estimation and application of the human cortical magnification factor. *Experimental Brain Research* **37**, 495 - 510.
- Saarinen, J., Rovamo, J. and Virsu, V. (1989) Analysis of spatial structure in eccentric vision. *Investigative Ophthalmology and Vision Science* **30**, 293 - 296.
- Sclar, G., Maunsell, J. H. R. and Lennie, P. (1990) Coding of image contrast in central visual pathways. *Vision Research* **30**, 1 - 10.
- Scobey, R. P. and Horowitz, J. M. (1972) The detection of small image displacements by cat retinal ganglion cells. *Vision Research* **12**, 2133 - 2143.
- Schein, S. J. (1988) Anatomy of macaque fovea and spatial densities of neurons in foveal representation. *Journal of Comparative Neurology* **269**, 479 - 505.
- Sekuler, R., Hutman, L. P. and Owsley, C. (1980) Human ageing and spatial vision. *Science* **209**, 1255 - 1256.
- Sholl, D. A. (1956) *The organization of the cerebral cortex*. Methuen, London.
- Sigelman, J., Trokel, S. L. and Spector, A. (1974) Quantitative biomicroscopy of lens light backscatter. *Archives of Ophthalmology* **92**, 437 - 442.
- Skottun, B. C., Bradley, A. and Freeman, R. D. (1986) Orientation discrimination in amblyopia. *Investigative Ophthalmology and Vision Science* **27**, 532 - 537.
- Skottun, B. C., Bradley, A., Sclar, G., Ohzawa, I. and Freeman, R. D. (1987) The effects of contrast on visual orientation and spatial frequency discrimination: A comparison of single cells and behaviour. *Journal of Neurophysiology* **57**, 773 - 786.

- Sloane, M. E., Owsley, C. and Alvarez, S. L. (1988) Ageing, senile miosis and spatial contrast sensitivity at low luminance. *Vision Research* **28**, 1235 - 1246.
- Snyder, A. W. (1982) Hyperacuity and interpolation by the visual pathways. *Vision Research* **22**, 1219 - 1220.
- Snyder, A. W. and Miller, W. H. (1977) Photoreceptor diameter and spacing for highest resolving power. *Journal of the Optical Society of America* **67**, 696 - 698.
- Sperling, G. (1966) Comparisons of real and apparent motion. *Journal of the Optical Society of America* **56**, 1442.
- Stigmar, G. (1971) Blurred visual stimuli. *Acta Ophthalmologica* **49**, 364 - 379.
- Stratton, G. M. (1902) Visible motion and the space threshold. *Psychological Review* **9**, 433 - 447.
- Sturr, J. F., Church, K. L. and Taub, H. A. (1988) Temporal summation functions for detection of sine-wave gratings in young and older adults. *Vision Research* **28**, 1247 - 1253.
- Sullivan, G. D., Oatley, K. and Sutherland, N. S. (1972) Vernier acuity as affected by target length and separation. *Perception and Psychophysics* **12**, 438 - 444.
- Swindale, N. V. and Cynader, M. S. (1989) Vernier acuities of neurons in area 17 of cat visual cortex: Their relation to stimulus length and velocity, orientation selectivity and receptive field structure. *Visual Neuroscience* **2**, 165 - 176.
- Talbot, S. A. and Marshall, W. H. (1941) Physiological studies on neural mechanisms of visual localization and discrimination. *American Journal of Ophthalmology* **24**, 1255 - 1264.
- Taylor, M. M. and Creelman, C. D. (1967) PEST; Efficient estimates on probability functions. *Journal of the Acoustical Society of America* **41**, 782 - 787.
- Toet, A. and Koenderink, J. J. (1988) Differential spatial displacement discrimination thresholds for Gabor profiles. *Vision Research* **28**, 133 - 143.
- Toet, A., Van Eekhout, M. P., Simons, H. L. and Koenderink, J. J. (1987) Scale invariant features of differential spatial displacement discrimination. *Vision Research* **27**, 441 - 451.
- Tootell, R. B., Silverman, M. S., Switkes, E. and De Valois, R. L. (1982) Deoxyglucose analysis of retinotopic organization in primate striate cortex. *Science* **218**, 902 - 904.
- Tootell, R. B., Silverman, M. S. and Hamilton, S. L. (1988) Functional anatomy of macaque visual cortex IV. Spatial frequency. *Journal of Neuroscience* **8**, 1610 - 1624.
- Tulunay-Keesey, U. and Ver Hoeve, J. N. (1987) The role of eye movements in motion detection. *Vision Research* **27**, 747 - 754.

- Tyler, C. W. (1973) Periodic vernier acuity. *Journal of Physiology, London* **228**, 637 - 647.
- Tyler, C. W. (1989) Two processes control variations in flicker sensitivity over the life span. *Journal of the Optical Society of America A* **6**, 481 - 490.
- Tyler, C. W. and Torres, J. (1972) Frequency response characteristics for sinusoidal movement in the fovea and periphery. *Perception and Psychophysics* **12**, 232 - 236.
- Van Essen, D. C., Newsome, W. T. and Maunsell, J. H. R. (1984) The visual field representation in striate cortex of the macaque monkey: Asymmetries, anisotropies and individual variability. *Vision Research* **24**, 429 - 448.
- Virsu, V., Nasanen, R. and Osmovita, K. (1987) Cortical magnification and peripheral vision. *Journal of the Optical Society of America A* **4**, 1568 - 1578.
- Volkman, A. W. (1863) Physiologische Untersuchungen *Gebiete der Optik*, Breitkopf and Hartel, Leipzig.
- Ward, R. M., Casco, C. and Watt, R. J. (1985) The location of noisy visual stimuli. *Canadian Journal of Psychology* **39**, 387 - 399.
- Wässle, H., Grünert, U., Röhrenbeck, J. and Boycott, B. B. (1989) Cortical magnification factor and the ganglion cell density of the primate retina. *Nature* **341**, 643 - 646.
- Wässle, H., Grünert, U., Röhrenbeck, J. and Boycott, B. B. (1990) Retinal ganglion cell density and cortical magnification factor in the primate. *Vision Research* **30**, 1897 - 1911.
- Watson, A. B. (1987) Estimation of local spatial scale. *Journal of the Optical Society of America A* **4**, 1579 - 1582.
- Watt, R. J. (1987) Scanning from coarse to fine spatial scales in the human visual system after the onset of a stimulus. *Journal of the Optical Society of America A* **4**, 2006 - 2021.
- Watt, R. J. and Andrews, D. P. (1982) Contour curvature analysis: hyperacuties in the discrimination of detailed shape. *Vision Research* **22**, 449 - 460.
- Watt, R. J. and Morgan, M. J. (1983a) Mechanisms responsible for the assessment of visual location: Theory and evidence. *Vision Research* **23**, 97 - 109.
- Watt, R. J. and Morgan, M. J. (1983b) The recognition and representation of edge blur: evidence for spatial primitives in human vision. *Vision Research* **23**, 1465 - 1477.
- Watt, R. J. and Morgan, M. J. (1985) A theory of the primitive spatial code in human vision. *Vision Research* **25**, 1661 - 1674.
- Watt, R. J., Morgan, M. J. and Ward, R. M. (1983) The use of different cues in vernier acuity. *Vision Research* **23**, 991 - 995.
- Weale, R. A. (1963) *The ageing eye*. Lewis, London.

- Weale, R. A. (1975) Senile changes in visual acuity. *Transactions of the Ophthalmological Society, U.K.* **95**, 36 - 38.
- Wehrhahn, C. and Westheimer, G. (1990) How vernier acuity depends on contrast. *Experimental Brain Research* **80**, 618 - 620.
- Westheimer, G. (1975) Visual acuity and hyperacuity. *Investigative Ophthalmology and Vision Science* **14**, 570 - 572.
- Westheimer, G. (1978) Spatial phase sensitivity for sinusoidal grating targets. *Vision Research* **18**, 1073 - 1074.
- Westheimer, G. (1979) The spatial sense of the eye. *Investigative Ophthalmology and Vision Science* **18**, 893 - 912.
- Westheimer, G. (1981) Visual hyperacuity. In *Progress in Sensory Physiology, Volume 1*, pp 1 - 30. Springer, Berlin.
- Westheimer, G. (1982) The spatial scale of the perifoveal visual field. *Vision Research* **22**, 157 - 162.
- Westheimer, G. and Campbell, F. W. (1962) Light distribution in the image formed by the living human eye. *Journal of the Optical Society of America* **52**, 1040 - 1045.
- Westheimer, G. and Hauske, G. (1975) Temporal and spatial interference with vernier acuity. *Vision Research* **15**, 1137 - 1141.
- Westheimer, G. and McKee, S. P. (1975) Visual acuity in the presence of retinal image motion. *Journal of the Optical Society of America* **65**, 847 - 850.
- Westheimer, G. and McKee, S. P. (1977a) Spatial configurations for visual hyperacuity. *Vision Research* **17**, 941 - 947.
- Westheimer, G. and McKee, S. P. (1977b) Integration regions for visual hyperacuity. *Vision Research* **17**, 89 - 93.
- Westheimer, G. and McKee, S. P. (1978) Stereoscopic acuity for moving retinal images. *Journal of the Optical Society of America* **68**, 450 - 455.
- Westheimer, G. and McKee, S. P. (1979) What prior uniocular processing is necessary for stereopsis? *Investigative Ophthalmology and Vision Science* **18**, 614 - 621.
- Westheimer, G. and Pettet, M. W. (1990) Contrast and duration of exposure differentially affect vernier and stereoscopic acuity. *Proceedings of the Royal Society of London, Series B* **241**, 42 - 46.
- Westheimer, G., Shimamura, K. and McKee, S. P. (1976) Interference with line orientation sensitivity. *Journal of the Optical Society of America* **66**, 332 - 338.
- Wetherill, G. B. and Levitt, H. (1965) Sequential estimation of points on a psychometric function. *British Journal of Mathematical and Statistical Psychology* **18**, 1 - 10.

- Weymouth, F. W. (1958) Visual sensory units and the minimal angle of resolution. *American Journal of Ophthalmology* **46**, 102 - 113.
- Whitaker, D. and Buckingham, T. (1987) Oscillatory movement displacement thresholds: resistance to optical image degradation. *Ophthalmic and Physiological Optics* **7**, 121 - 125.
- Whitaker, D. and Walker, H. (1988) Centroid evaluation in the vernier alignment of random dot clusters. *Vision Research* **28**, 777 - 784.
- Whitaker, D. and Deady, J. (1989) Prediction of visual function behind cataract using displacement threshold hyperacuity. *Ophthalmic and Physiological Optics* **9**, 20 - 24.
- Whitaker, D. and Elliott, D. B. (1989) Towards establishing a clinical displacement threshold technique to evaluate function behind cataract. *Clinical Vision Science* **4**, 61 - 69.
- Whitaker, D. and MacVeigh, D. (1990) Displacement thresholds for various types of movement: effect of spatial and temporal reference proximity. *Vision Research* **30**, 1499 - 1506.
- Whitaker, D. and MacVeigh, D. (1991) Interaction of spatial frequency and separation in vernier acuity. *Vision Research* **31**, 1205 - 1212.
- Williams, R. A., Enoch, J. M. and Essock, E. A. (1984) The resistance of selected hyperacuity configurations to retinal image degradation. *Investigative Ophthalmology and Vision Science* **25**, 389 - 399.
- Wilson, H. R. (1986) Responses of spatial mechanisms can explain hyperacuity. *Vision Research* **26**, 453 - 469.
- Wilson, H. R. (1991) Model of peripheral and amblyopic hyperacuity. *Vision Research* **31**, 967 - 982.
- Wilson, H. R. and Bergen, J. R. (1979) A four mechanism model for threshold spatial vision. *Vision Research* **19**, 19 - 32.
- Wilson, H. R. and Gelb, D. J. (1984) Modified line element theory for spatial-frequency and width discrimination. *Journal of the Optical Society of America A* **1**, 124 - 131.
- Wilson, H. R. and Regan, D. (1984) Spatial-frequency adaptation and grating discrimination: predictions of a line-element model. *Journal of the Optical Society of America A* **1**, 1091 - 1096.
- Wing, G. R., Blanchard, G. C. and Weiter, J. J. (1978) The topography and age relationship of lipofuscin concentration in the retinal pigment epithelium. *Investigative Ophthalmology and Vision Science* **17**, 601 - 619.
- Wong, E. and Weisstein, N. (1983) Sharp targets are detected better against a figure and blurred targets are detected better against a background. *Journal of Experimental Psychology* **9**, 194 - 202.

- Wright, M. J. and Johnston, A. (1985) The relationship of displacement thresholds for oscillating gratings to cortical magnification, spatiotemporal frequency and contrast. *Vision Research* **25**, 187 - 193.
- Wulfig, (1892) Über den kleinsten Gesichtswinkel. *Zeitschrift für Biologie* **29**, 199 - 202.
- Yap, Y. L., Levi, D. M. and Klein, S. A. (1987) Peripheral hyperacuity: Three-dot bisection scales to a single factor from 0 to 10 degrees. *Journal of the Optical Society of America A* **4**, 1554 - 1561.
- Yap, Y. L., Levi, D. M. and Klein, S. A. (1989) Peripheral positional acuity: Retinal and cortical constraints on 2-dot separation discrimination under photopic and scotopic conditions. *Vision Research* **29**, 789 - 802.
- Zeki, S. M. (1969) Representation of central visual fields in prestriate cortex of monkeys. *Brain Research* **14**, 271 - 291.
- Zeki, S. M. (1974) Cells responding to changing image size and disparity in cortex of the rhesus monkey. *Journal of Physiology, London* **242**, 827 - 841.
- Zeki, S. M. (1978) Functional specialization in the visual cortex of the rhesus monkey. *Nature* **274**, 423 - 428.
- Zeki, S. M. and Shipp, S. (1988) The functional logic of cortical connections. *Nature* **335**, 311 - 317.
- Foster, D. H., Thorson, J., McIlwain, J. T. and Biederman-Thorson, M. (1981) The fine-grain movement illusion: A perceptual probe of neuronal connectivity in the human visual system. *Vision Research* **21**, 1123 - 1128.
- Thorson, J., Lange, G. D. and Biederman-Thorson, M. (1969) Objective measure of the dynamics of a visual movement illusion. *Science, New York* **164**, 1087 - 1088.
- Van Santen, J. P. H. and Sperling, G. (1984) Temporal covariance model of human motion perception. *Journal of the Optical Society of America A* **1**, 451 - 473.
- Watson, A. B. and Ahumada, A. J. (1985) Model of human visual-motion sensing. *Journal of the Optical Society of America A* **2**, 322 - 341.